An Engineering Geomorphological

Investigation of Hillslope Stability

in the Peak District of Derbyshire

by

MARTIN CROSS, BA

Thesis submitted to the University of Nottingham for the degree of

Doctor of Philosophy, December 1987

ABSTRACT

Large-scale civil engineering works, planning and land-management in areas known to have a landslide problem require regional landslide susceptibility evaluation. The Matrix Assessment Approach (MAP) is introduced as a technique for establishing an index of slope stability over large areas. The method allows the relative landslide susceptibility to be computed over large areas using a discrete combination of geological/geomorphological parameters. MAP was applied to a region in the Peak District, Derbyshire. The model identified key geological/geomorphological parameters involved in deep-seated failures, provided an effective means of classifying the stability of slopes over a large area and successfully indicated sites of previously unmapped landslides. The resultant regional landslide susceptibility index provides useful preliminary information for use at the pre-site/reconnaissance stages of large-scale civil engineering works such as highway construction.

Unlike deep-seated failures, shallow translational slides usually do not prevent the use of areas above and below the failure, however, they can cause considerable inconvenience and expense when remedial engineering works are necessary. An investigation was undertaken in order to establish the precise critical state of geomorphological factors involved in shallow translational landsliding in the Peak District. Back calculations based on the Infinite Slope Stability Model showed how the factor of safety against shallow translational sliding changed as one geomorphological parameter varied. The value of the factor of safety was very sensitive to changes in the values of effective cohesion and piezometric height, moderately sensitive to changes in the values of regolith depth and the angle of slope

inclination and insensitive to changes in the values of angle of friction with respect to effective stresses and soil unit weight. The recognition of such meso/micro geomorphological thresholds is not only important for geomorphologists concerned with landform evolution, it is also fundamental to successful and safe engineering practices.

TABLE OF CONTENTS

Section I. Background Information

ACKNOWLEDGEMENTS

British Geological Survey, Engineering Geology Unit, Keyworth, Nottingham: Mr B Conway, Mr A Forester and Mr K Northmore.

Dr T P Burt, Department of Geography, University of Oxford.

Dr M P Chandler, Department of Civil Engineering, Imperial College, London.

Dr J D DeGraff, Department of Forestry & Outdoor Recreation, Utah State University, Logan, Utah.

Dr J Griffiths, Geomorphological Services Ltd., 1, Bassett Court, The Green, Newport Pagnell, Bucks

Dr R H Johnson, Department Geography, University of Manchester.

Dr R Jones, Department of Civil Engineering, University of Nottingham.

Mr A D Leadbeater, County Surveyor, Derbyshire County Council, Highway Engineering Department.

Mr M Reeve, Soil Survey of England and Wales, Shardlow Hall, Derbyshire.

Soil Instruments Ltd., Bell Lane, Uckfield, East Sussex.

Acknowledgements are also made to the following sources for figures and tables used in the text:

SECTION I

BACKGROUND INFORMATION

1.1 INTRODUCTION

Landslides continue to pose many engineering problems, from the immediate effect of physical damage, and in extreme cases the associate loss of life, to the costly stabilisation measures required. In recent years there has been an increasing number of reports relating slope stability to the disturbance of previously existing landslips. Pre-existing landslips in Great Britain are largely a product of slope processes which operated during the Late Devensian Glacial and early Flandrian. The displacement/ translocation of material during mass movements affected the geotechnical and geohydrological properties of the hillslope, markedly reducing the shear strength of the slope forming material to its residual or 'ultimate' strength. Such landslides often came to rest in a state of near limiting equilibrium which could be disturbed by engineering works undertaken at a much later date. The geomorphological expression of old and dormant landslides is frequently very subtle and easy detection is generally only possible on the completion of a thorough geomorphological/geological investigation, this fact is borne out by the number of old landslides that have not been discovered until reactivated by engineering works. It is apparent, therefore, that site investigation in areas susceptible to landsliding should encompass techniques capable of identifying those features and structures indicative of instability, thereby enabling the delineation of both areas of hillslope instability and areas of potential instability, and to differentiate these from adjacent areas of stable ground before engineering works commence.

There is an increasing requirement for slope stability information in planning/engineering management decision-making as the demand for

roads, structures, recreational facilities etc grows. Large-scale/extensive civil engineering works, planning and land-management in areas known to have a landslide problem require large area or regional landslide susceptibility (threshold) evaluation. Mass movements are the result of an interplay of a large number of interelated geological and geomorphological factors. The identification and measurement of mass movement in the field requires both surface and subsurface site investigations of the geotechnical, geomechanical and hydrogeological characteristics of the parent slope and the failed mass. However, an accurate stability analysis of natural slopes by means of intensively applied geotechnical techniques cannot be carried out at reasonable cost over large areas. In such cases an alternative approach is needed which is capable of identifying those sites most likely to be prone to instability. The procedure must of necessity be based on easily obtained parameters which can be readily collected over the whole of the investigated area and which are known to be directly or indirectly correlated with slope stability. A proven landslide susceptibility evaluation technique may provide a very useful source of information to planners who implement hazard-reduction programmes and to consulting engineers who serve as advisors to construction companies, local government or directly to government departments. Over the last three decades there has been an increasing interest by engineers and planners in establishing methods and techniques for more accurate terrain classification and land-use planning because of the mounting pressure imposed by developers in marginal areas (i.e. those areas originally left undeveloped because of their perceived engineering problems such as slope instability).

Engineering geological/geomorphological investigations have recently
contributed to the successful planning, design and construction of a
number of major civil engineering projects, particularly where
present-day processes can affect the planned design and/or actual
construction work. An important aspect of an engineering
geological/geomorphological investigation is the recognition of
'geological/geomorphological thresholds', especially those related to
slope stability (i.e. the recognition of those areas where there is a
potential for new/or renewed geological/geomorphological activity).
If the advent of a 'threshold condition' i.e. areas/slopes in a
'threshold state' can be determined and predicted, an important
service can be rendered to planners and engineers. Over the past
twenty years, or so, it has become common practice to use aerial
photograph interpretation and field based geomorphological mapping at
the reconnaissance stage of a project in order to identify those sites
where geotechnical investigations are most likely to be required.
Together these techniques normally provide a good basis for
recognising existing failures, including those of some antiquity.
However, most investigators are cautious of having to define 'slopes
potentially susceptible to failure'. Mapping in this manner tends to
identify landslides and leave the remaining slopes unclassified.
Although there is a clear distinction in terms of physical activity
between slopes which are undergoing movement and those which are
static, it over-siimplifies the issue to classify slopes as being
either 'stable' or 'unstable'. If a classification of slope
susceptibility/terrain sensitivity is required it is better to
envisage slopes as existing in a continuum of predisposition states
ranging from stable, through unstable (marginally stable) to an
actively unstable state. This continuum represents successively
smaller margins of stability culminating in the actively unstable

slope where the margin is zero. In deterministic terms, these stability states can be defined (at least theoretically) by the ability of transient forces to produce failure. Stable slopes are those where the margin of stability is sufficiently high to withstand all transient forces. Marginally stable slopes are those which will fail sometime in response to transient forces attaining a certain threshold level. Actively unstable slopes are those where the transient forces produce continuous or intermittent movement. The distinction between stable and marginally stable states in these terms is more easily made in theory than in practice.

Within the engineering geological/geotechnical professions there is at present an almost complete laissez faire system, with virtually complete freedom to solve slope instability problems, carry out investigations, conduct analyses and make predictions according to the inclinations of the practitioners or consultants concerned. Many situations arise in engineering geological/geotechnical consulting activities where there is no clear cut solution for an engineering problem, in addition data may be limited and therefore interpretive methods have been used to obtain the 'best result' for a particular situation. Equally, there are many routine situations for which the data is not in dispute, but for which there are numerous techniques available solutions for analyses, all leading to different answers. The first part of this thesis presents a supplementary technique to aerial photograph interpretation and geomorphological mapping called the Matrix Assessment Approach (DeGraff & Romesburg, 1980).The Matrix Assessment Approach is a quantitative method for establishing an index of instability states over large areas. The method allows the relative landslide potential/susceptibility to be evaluated over large areas using a few key measurable stability factors/parameters and

follows a well defined procedure. The standard procedure of the
Matrix Assessment Approach and the fact that results can be reproduced
and verified overcomes some of the problems of the laissez faire
system of investigations used by geological/geotechnical engineers
mentioned. The index of slope instability or landslide susceptibility
classes are defined by discrete combinations of measurable parameters.
The Matrix Assessment Approach which uses identified macro stability
factors (i.e. regional topographical/morphological and geological
controls on stability), was applied to a region of the Peak District,
of Derbyshire. A map of existing landslides served as the basic data
source for understanding the macro threshold conditions controlling
slope instability. Nine macro stability factors have been combined in
a computer data matrix in such a manner in order to create landslide
threshold/susceptibility values for a 1.5 ha grid network across the
study region. This regional landslide susceptibility index is
intended to provide a valuable additional source of information at the
pre-site investigation/reconnaissance stages of site investigation
procedures prior to large scale civil engineeriing works such as
highways.

The second part of this thesis examines the meso/micro stability
threshold conditions and considers whether specific geomorphological
threshold states can be identified within the superficial materials on
hillslopes, particularly with respect to shallow planar translational
slides in regolith. In order to monitor the present dynamics of the
threshold state of shallow planar sliding, a series of
geomorphological techniques were applied including a network of
instruments placed on the hillslopes of a small catchment (Callow
Bank). Using conventional 'Infinite slope stability Analysis', it was
possible to define the precise 'critical state' of a series of

geomorphological parameters (i.e. effective cohesion (c'),
piezometric head (h), depth of regolith (z), angle of internal
friction with respect to effective stresses ($\emptyset'$), pore water pressure
(u) etc) associated with the overall threshold instability state.
From such a threshold study (sometimes termed Sensitivity Analysis)
it is possible to show how a factor of safety against shallow planar
landsliding varies with changes in the value of the geomorphological
parameters. The effect on the factors of safety as a result of
variations in these parameters can then be assessed and, if
considered necessary, more or less conservative criteria may be
adopted for design based upon the frequency distribution of the
values of the parameters obtained during testing and observation.
The recognition of such meso/micro geomorphological thresholds is not
only important for geomorphologists concerned with landform
evolution, it is also fundamental to successful engineering. If the
threshold/sensitivity analysis shows that the stability of a slope on
an engineering site is inadequate, the designer should first
establish which particular geomorphological parameters have the most
important effect on the factor of safety and thus plan the design
criteria accordingly.

The format of this thesis is arranged in three sections. Section 1
provides the reader with a background to the factors causing
instability, with particular reference to the Peak District of
Derbyshire. The first part of Section 1 provides a brief resumé of
the geology, geomorphology and Quaternary history of the Peak
District with the intention of citing some of the most important
research relevant to the study area. The latter chapters of Section
1 consider the spatial distribution of landslides and the factors
initiating slope failure in the Peak District of Derbyshire.

Section 2 of the thesis emphasises the importance of identifying areas of slope instability and outlines techniques of landslide hazard mapping. The Matrix Assessment Approach for evaluating regional landslide susceptibility is introduced and applied to a region of the Peak District of Derbyshire.

Section 3 of the thesis deals with the most common type of present day landslide process in the Peak District, that of shallow translational landsliding. A detailed field investigation was carried out on the hillslopes of Callow Bank near Hathersage in the Peak District of Derbyshire in order to establish the precise critical state or threshold of a number of geomorphological factors involved in shallow planar translational landsliding. Five objectives were investigated:-

(1) To examine slope profiles in the Callow Bank study area in order to establish whether 'Characteristic slope angles' can be identified and whether these correspond to those found by other research workers (Carson & Petley, 1970; Carson & Kirkby, 1972).

(2) To examine changes in the piezometric surface within regolith material along slope profiles with respect to (i) rainfall, (ii) stream discharge, (iii) regolith characteristics, (iv) geology, and (v) hillslope morphology.

(3) To design and build an Open-sided Field Direct Shear Box. (Chandler et al., 1981).

(4) To examine the shear strength of regolith material at various positions along a slope profile using the Open-sided Field Direct

Shear Box and to compare the results with those obtained by other
research workers using more conventional shear box testing methods
(Carson & Petley, 1970; Carson & Kirkby, 1972; Rouse, 1975; Rouse &
Farhan, 1976).

(5) To apply Infinite Slope Stability Analyses in order to establish
critical parameter threshold values and to develop an index of
stability for shallow landslides under various conditions of slope
steepness and ground water conditions.

The concurrent theme throughout both Sections 2 and 3 is to develop
further the potential application and presentation of selected
geomorphological techniques to site investigation and construction
design procedures. A major advantage of geomorphological techniques
is that they can be applied cheaply and rapidly to many different
aspects of a large-scale engineering project and in a wide range of
environments, for example, in road alignment location and
construction. Such techniques can be applied by small teams/or
individuals and therefore, do not incur large support expenses.
Above all, the geomorphological survey techniques provide a spatial
and temporal perspective to the assessment of the overall 'ground
conditions'. Geotechnical engineers, engineering geologists and
other design engineers have traditionally been preoccupied with site
specific investigations, the geomorphologist perceives the landscape
within a much broader spatial and temporal framework compared to the
traditional approach of engineers. This intuitive awareness enables
the engineering geomorphologist to more fully understand the nature
of geomorphological processes which have operated or are actively
operating at the site of interest.

1.2 GEOGRAPHICAL SETTING

There is no single authoritive definition of the name 'The Peak
District'. Its main origins and use are in connection with
landscape appreciation and recreation. To most people it applies
as much to the high gritstone moors of the Dark Peak between
Sheffield and Manchester, as to the limestone plateau and dales of
the White Peak. It has statutory meaning in the formal designation
(1951) of the Peak District National Park. The Peak District is
situated at the southern end of the Pennines, a broad anticline of
carboniferous rocks with its crest eroded therefore exposing the
oldest rocks at the core of the range (Fig. 1.1.).
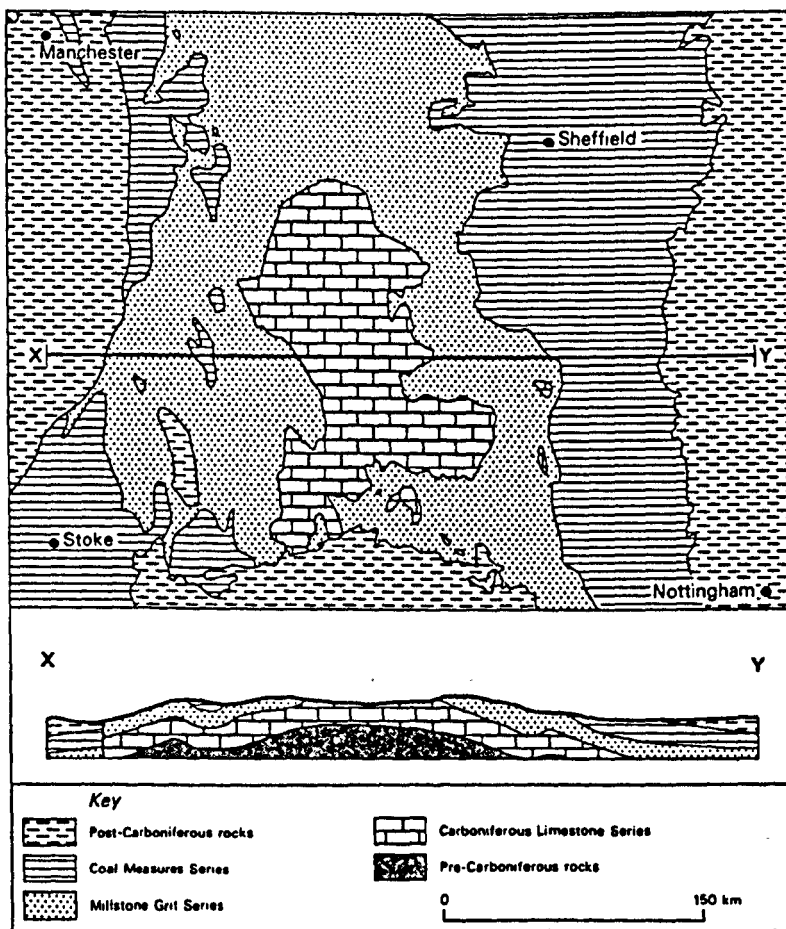
Fig. 1.1. Geological sketch-map of the Peak District and
adjoining areas, with diagrammatic cross-section to show
the structure (Simpson, 1982).
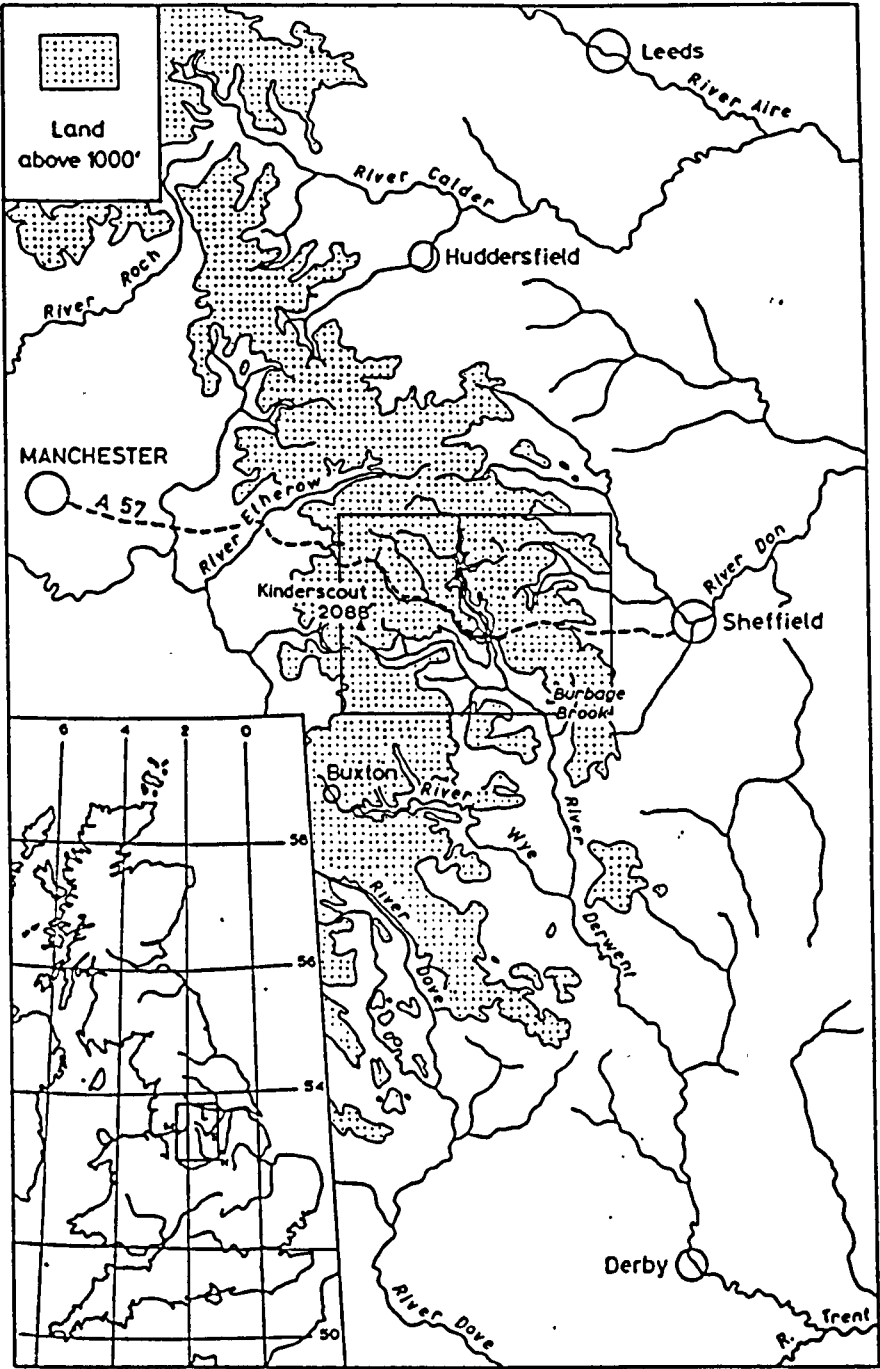
Fig. 1.2. Location map of the study region.

Although primarily an upland area (>275m above sea level) with a moderately uniform cool temperate maritime climate, there are marked contrasts between the landforms and drainage of the White Peak and Dark Peak.

The White Peak is essentially a gently undulating limestone plateau surface ranging in altitude from 275m to 450m and devoid of residual hills (Linton, 1963). In areas subjected to faulting or processes of erosion and weathering the limestone plateau margins are steep and scarplike (Parkinson, 1947; Stevenson & Gaunt, 1971). The plateau surface is dissected by a complex network of sinuous valleys most of which are permanently dry under present climatic conditions, few valleys carry perennial surface streams (except the Dove, Derwent, Manifold and Wye), (Warwick, 1964, Forde & Burek, 1977). The limestone plateau composed of thick soluble well-bedded and well-jointed limestone devoid of surface drainage and with a comparatively high effective precipitation (>800mm) suggests that extensive underground drainage systems exist; but to date only a few are known to any extent and most of these lie in small valleys contiguous to the limestone margin (Ford, 1966). Small surface streams occasionally emerge in areas where perched water tables have developed over impervious igneous rocks or clay bands within the limestone series. Karstic features such as potholes, sink holes, caves and limestone scars are common in the White Peak, though limestone pavements, typical of certain areas of the Yorkshire Craven area are poorly developed.

In contrast the High or Dark Peak is a region of high moorland plateau dissected by deep valleys eroded through a succession of Mid-Carboniferous sandstones, mudstones and shales. The higher relief of this area is dominated by a series of peat-covered structurally controlled plateaus which have been truncated by erosion to form extensive planation surfaces (Sissons, 1954; Linton, 1956; McArthur, 1977). These hills and plateau range in height from 400m to 610m above sea level. The geological

structure, i.e. the gentle easterly dip of the Namurian sandstones and shales, partly explains the general asymmetry of the valleys, the distribution of the escarpments and the susceptibility of the valley slopes to mass movement (Stevenson & Gaunt, 1971). Former glacial and periglacial processes have also effected the landforms and superficial deposits found within the Dark Peak (Johnson, 1967, 1979a; Wilson, 1981). Another major control on landform development has been the intermittently falling base-level that has successively rejuvenated the stream system (Waters & Johnson, 1958; Straw, 1968; Johnson, 1969b; Burek, 1977). The rivers draining the Dark Peak have cut through a complex succession of massive sandstones and incompetent shales, mudstones and thin sandstones, and have created stepped valley side profiles with prominent structural benches occurring wherever massive sandstone beds outcrop. Where Namurian sandstone and shale strata are inclined, a well developed scarp and dip slope cuesta topography has developed. Craggy escarpments or edges are conspicuous physiological features along the outcrops of the more massive and resistant Namurian sandstones. Valley side or summit tors have developed on valley and escarpment edges respectively; their location is largely controlled by the jointing pattern of the sandstones.

The alternating succession of Namurian sandstones and shale/mudstone have created inherently unstable valley sides particularly where competent massive sandstones have become exposed and overlie the weaker and incompetent shale/mudstone strata. Landslides are therefore a common feature in the Dark Peak.

Beneath the gritstone scarps of the Dark Peak, most stable hillslopes have either broadly concave or rectilinear profiles with

the steepest elements ranging from 17° to 25° (Carson & Petley,
1970; Carson & Kirkby, 1972; Johnson & Walthall, 1979). These
straight/rectilinear slopes have been interpreted to be a product
of slope wash and rill erosion processes which took place during
the late Devensian Glaciation (Rouse & Farhan, 1976). It has been
postulated that these characteristic straight hillslopes are a
product of the limiting angle of stability for superficial material
on the hillslopes (Rouse, 1969, 1975; Carson & Petley, 1970; Rouse
& Farhan, 1976).

The plateaus of the Dark Peak were covered by extensive snowfields
during the Devensian Glacial (Johnson, 1969a, Wilson, 1981). The
snowfields would have supplied sufficient meltwater both for ground
water storage and saturated throughflow. Permafrost must also have
been present at depth within the valleys, the presence of a
perenial permafrost table coupled with high snowmelt ensured a
series of high water tables in the area particularly during Spring
and Summer months. The development of high pore-water pressures in
the Namurian shales and mudstones at such times facilitated the
mass movement of debris by mudsliding, solifluction and creep
especially where weathered material could be easily transported to
form extensive spreads of head on the valley footslopes (Said,
1969; Wilson, 1981).

Fossil scree covers most of the steeper slopes particularly below
the gritstone edges. Boulders derived from former rockfalls from
the gritstone escarpments are now widely distributed over the
higher and middle slope sections of the valley sides, having been
transported principally by solifluction and landslide processes.

In areas where landsliding has taken place, clitter has been distributed on the outer slopes of rotated landslide blocks and in some places has been transported considerable distances downslope in secondary slip and mudslide movements. Frost shattered rock debris has also been redistributed by meltwater streams which carried the boulders down their channels, depositing them as boulder fans on the valley floors. Detailed accounts of the geomorphology of the Dark Peak are given by Johnson & Walthall, 1979; Johnson, 1980; Stevenson & Gaunt, 1971; McArthur, 1977, 1981 and Ford, 1977.

In historical and indeed prehistorical times human activity in the Peak District was primarily conditioned by the local geology and geomorphology (Hawke-Smith, 1981; Bradley & Hart, 1983). More recent human intervention, notably extractive industries and reservoir construction have had a large-scale impact on individual landforms and on the landscape as a whole.

1.3 LOCATION OF THE STUDY REGION

The inset in Figs. 1.3 shows the location of the study region. The region covers an area of 342 km^2 and is bounded by Bleaklow Hill in the north west, Broomhead reservoir in the north east, the Kinderscout plateau in the west, Dove Holes in the south west, Bradfield, Hallam and Burbage Moors in the east and extends to Nether Padley in the south east (National Grid Eastings 4080 to 4270 and Northings 3780 to 3960). The region incorporates the Alport, Ashop, Edale, Hope and Upper Derwent valleys, and the Derwent and Ladybower reservoirs. These valleys form the lowlands eroded in the basal Namurian shales. The gritstone plateaus of

Kinder, Bleaklow, Howden Moor and Hallam Moor and their associated gritstone edges including Blackden, Rushop, Bamford, Shatton and Stanage dominate the upland topography within the region. The uplands form part of the Dark Peak, whereas the southern part of the region contains the northern part of the Carboniferous limestone plateau which forms part of the White Peak.
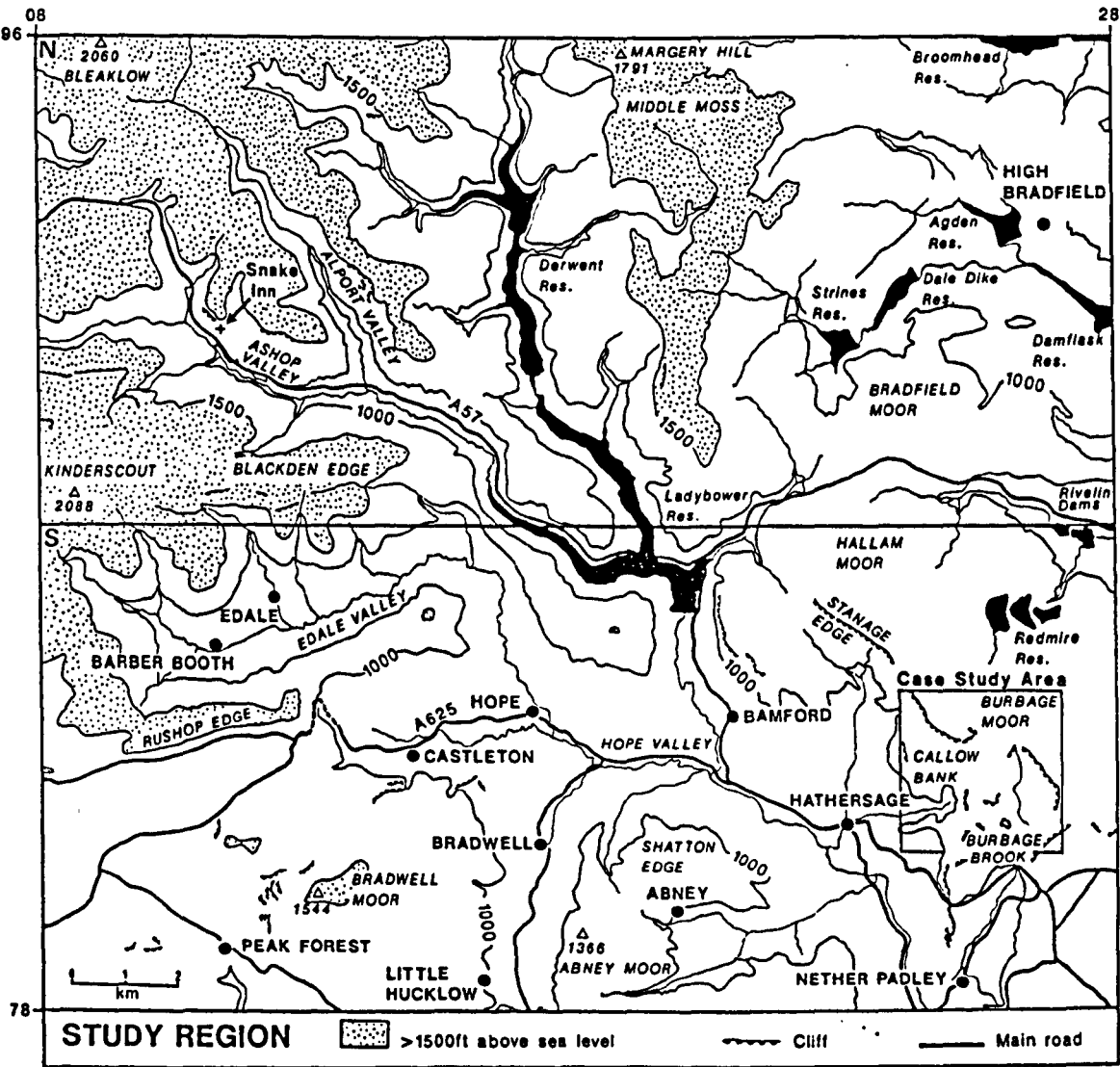
Fig. 1.3. Map of the study region, showing the northern and southern sections of the study region. The inset shows the location of Callow Bank Case study area.

Two principal roads cross the study region area, the A57 (Snake

Pass) between Manchester and Sheffield following the River Ashopton

and Holden Clough valley, and the A625 which forms a major Pennine

link from Sheffield, Bakewell, Matlock and Chesterfield in the east

to Buxton and Manchester. The A57 is frequently blocked by

snowdrifts in winter and the A625 is renowned for the Mam Tor

landslide which led to the closure of a section of the road in 1979

(Fig. 1.3).

1.4   GEOLOGICAL BACKGROUND

1.4.1   Introduction

Almost all the rocks in the Peak District belong to the
Carboniferous System and were formed between 280 and 345 million
years B.P.   Three of the major subdivisions of the system, the
Carboniferous Limestone (Dinantian) Series, the Millstone Grit
(Namurian) Series and the Coal Measures (Westphalian) Series are
represented in the study region (Fig. 1.4.).
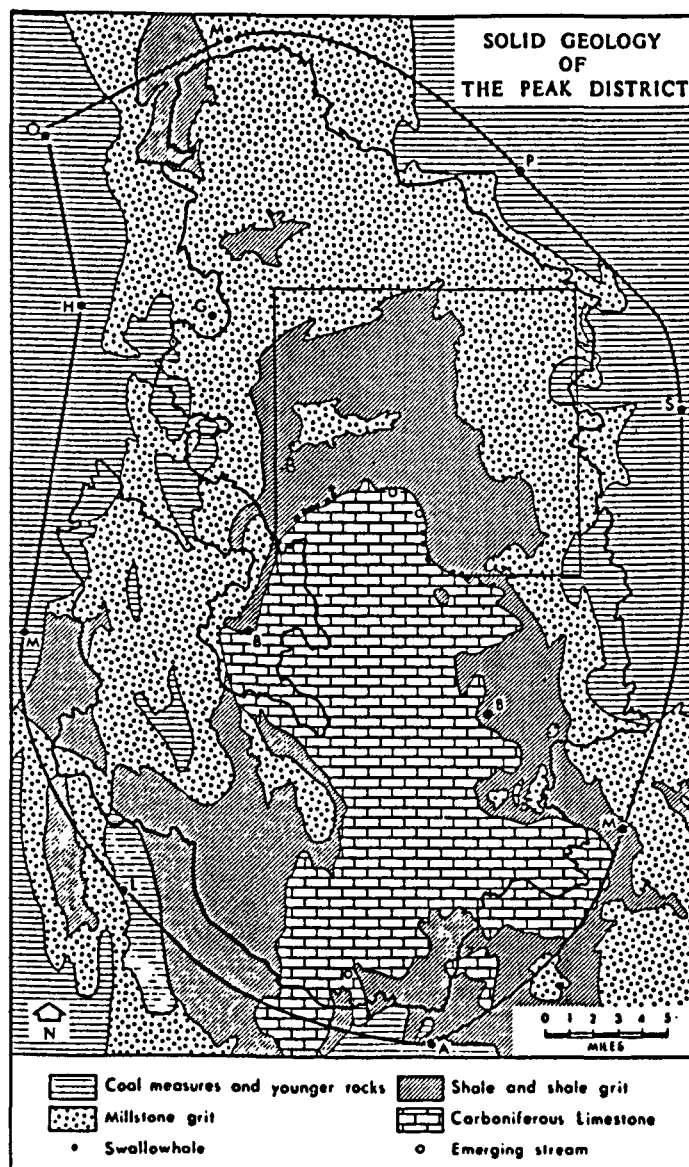
Fig. 1.4.   Solid Geology of the Peak District (Anderson & Shimwell, 1981)

Many exhaustive accounts of the stratigraphy of the limestone tract of the Peak District have been published (Rayner, 1953; Parkinson, 1957, 1965; Eden et al., 1964). Sedimentary petrologists have also paid considerable interest to the Namurian Series of the Upper Carboniferous (Hudson, 1943; Greensmith, 1956, 1960; Allen, 1960; Collinson, 1969). A number of geological memoirs have been published describing in detail the geology of the Peak District (Green et al., 1887; Gibson & Wedd, 1913; Eden et al., 1957; Sylvester-Bradley & Ford, 1968; Stevenson & Gaunt, 1971). A full account of the geology of the study region and surrounding area is given in the Chapel-en-le-Frith Geological Survey memoir (Stevenson & Gaunt, 1971). The study region is mainly covered by the 1:50 000 Chapel-en-le-Frith geological map sheet 99, but also extends into small sections of adjoining sheets 100, 86 and 87. Table 1.1. shows the geological sequence of the study region.

1.4.2. The Lower Carboniferous

The Dinantian rocks of the Peak District are a marine sequence composed mainly of limestones, but also contain some shales and standstone units. These rest unconformably on pre-Carboniferous rocks which are not exposed in the area but have been proved in three deep boreholes at Caldon Law, Woo Dale and Eyam (Cope, 1973; Dunham, 1973). During the early Dinantian, carbonates were probably deposited throughout the region but these beds are at present only exposed in the Dovedale - Ecton - Caldon Low area in the southwest of the region. During later Dinantian times shallow, well oxygenated seas were established in the northern and central parts of the region (the Derbyshire shelf) and also, on a smaller scale, in the extreme southwest (the Staffordshire shelf) while an

GEOLOGICAL SEQUENCE	
SUPERFICIAL FORMATIONS	
Recent and Pleistocene Hill Peat Alluvium River Terrace undifferentiated Head	
SOLID FORMATIONS	
UPPER CARBONIFEROUS	
COAL MEASURES (WESTPHALIAN)	Thickness(m) (generalised)
Lower Coal Measures Shales, mudstones and sandstones, including the Crawshaw sandstone with thin coals and seatearths and with the *Gastrioceras Subcrenatum* Marine Band at the base.	Up to 259m.
MILLSTONE GRIT SERIES (NAMURIAN)	
Rough Rock Group: Yeadonian (G₁) Shales and mudstones with Rough Rock at the top and the *Gastrioceras Cancellatum* Marine Band at the base.	Up to 131m.
Middle Grit Group: Marsdenian (R₂) Shales, mudstones and sandstones including Redmire Flags, Chatsworth Grit and Heydon Rock and with the *Reticulocerus gracile* Marine Band at the base.	Up to 546m.
Kinderscout Grit Group: Kinderscoutian (R₁) Shales, mudstones and sandstones including Kinderscout Grit, Shale Grit and Mam Tor Beds and including the upper part of the Edale Shales with *Homoceras Magistorum* Band at the base.	Up to 518m.
Beds below Kinderscout Grit Group: Pendleian, Arnsbergian, Chokerierian and Alportian (E1 to R2) Shales and mudstones with very thin ironstones, limestones, siltstones and 'Crowstones' (quartzite sandstones), consisting in the main part of the Edale Shales with *Cravenocerus leion* at the base.	Up to 301m.
LOWER CARBONIFEROUS LIMESTONE SERIES (DINANTIAN)	
VISÉAN	
Eyam Group (P₂) Dark thin bedded limestones; dark shales in upper part.	Up to 54m.
Monsal Dale Group (D₂) Grey and dark grey limestones with Litton Tuff and Upper Millers Dale Lava.	Up to 182m.
Bee Low Group (D₁) Pale grey massive limestones with Lower Millers Dale Lava.	Up to 167m.
Woo Dale Group (S₂) Dark grey and grey thin bedded limestones.	Up to 70m.

Table 1.1. Geological sequence of the study region (Stevenson &

Gaunt, 1971)

area of deeper water covered the intervening 'off-shelf' area

(Aitkenhead & Chisholm, 1982). On the shelves, pale-grey coloured

limestones were deposited (2000m in thickness) which are

distinctive for their lithological uniformity over wide areas, but

in the off-shelf province a more varied sequence of dark grey

coloured limestone with some shales and sandstones (1300m in

thickness) was laid down (Harrison & Adlam, 1984). In the closing

stages of the Dinantian a series of localised volcanic eruptions

occurred in both the shelf and off-shelf provinces and lavas and

tuffs were interbedded with the limestones. Walters and Ineson

(1981) give a comprehensive review of the Igneus rocks of

Derbyshire. Carbonate deposition diminished at the end of the

Dinantian and gave way to muds and sands during the Namurian.

Within the study region the Carboniferous Limestone Series outcrops

between Water Swallows, Castleton and Stoney Middleton; this area

is in the northern extremity of the 'Derbyshire Dome', slight earth

movements took place during deposition of the limestones but the

main phase of deformation took place at the end of the

Carboniferous period. The effect of the earth movement on the

shelf limestone was relatively minor but the rocks of the

intervening area were arched up into a series of north or north

westerly trending folds (Fig. 1.5). A long erosional interval

followed the earth movements. Alteration of the limestone to

dolomite occurred locally probably during Permian time, and

episodic mineralisation took place from the Carboniferous through

to Jurassic times, when fissures in the limestone were in places

infilled with calcite, baryte and fluorite locally containing lead,

zinc and copper ores.

Renewed uplift in the Tertiary led to the removal of post-Dinantian

cover rocks and the deposition on the limestone surface of the
sands and clays of fluvial and lacustrine origin. These are now
only preserved in steep-sided solution-pockets on the limestone and
are collectively termed Pocket Deposits.

In past years the geological literature of the region has produced
a lithostratigraphy of the Carboniferous Limestone Series
containing a large number of local rock names. With the completion
of the British Geological Survey's primary six-inch mapping of the
region, a stratigraphical scheme for the whole region has now been
formulated (Aitkenhead & Chisholm, 1982) (Table 1.2.) A useful
summary of the limestones of the Peak District is given by Harrison
& Adlam (1984).

CORAL-BRACHIO-POD ZONES	STAGES	DERBYSHIRE SHELF	OFF-SHELF PROVINCE	STAFFORDSHIRE SHELF
D_2	BRIGANTIAN	LONGSTONE MUDSTONES, EYAM LIMESTONES, MONSAL DALE LIMESTONES	MIXON LIMESTONE-SHALES AND WIDMERPOOL FORMATION	
D_1	ASBIAN	BEE LOW LIMESTONES	HOPEDALE AND ECTON LIMESTONES	KEVIN LIMESTONES
S_2	HOLKERIAN	WOO DALE LIMESTONES		
C_2S_1	ARUNDIAN		MILLDALE LIMESTONES	
C_1	CHADIAN			MILLDALE LIMESTONES
b	IVORIAN	Arundian at Eyam Borehole		
Z				RUE HILL DOLOMITES
K	HASTARIAN			REDHOUSE SANDSTONES

INCREASING AGE

Table 1.2. Limestones of the Peak District (Aitkenhead &
Chisholm, 1982)

1.4.3 Upper Carboniferous

The delta-swamps (paralic) facies ocurring in the lower half of the Upper Carboniferous of the Central Pennines has been termed the 'Millstone Grit', from the occurrence of coarse feldspathic sandstones which were until the last century used as a source for Millstones. The Millstone Grit Series was deposited during the Namurian, summaries of the Namurian have been written by Reading (1964) and Ramsbottom (1966). The alternating sandstones (grits) and shales of the Series extend along the Pennines between the Yorkshire and Lancashire coalfields, lying nearly horizontal but extensively faulted make a characteristic scarp and vale topography. With a slight reduction in thickness, the succession extends into North Derbyshire to overlap the eroded surface of the Carboniferous Limestone around Castleton (Jackson, 1927; Hudson & Cotton, 1945). Southwards from Castleton the Millstone Grit outcrops run either side of the Derbyshire limestone 'Dome' until they disappear beneath the Triassic unconformity, to the east of the Cheadle coalfield on the west, and to the west of the Derbyshire coalfield on the east. Detailed accounts of the Millstone Grit Series of the Peak District are given by Allen, 1960; Collinson, 1969; Walker, 1964, 1967 and Stevenson & Gaunt, 1971.

The Upper Carboniferous sequence is characterised by a repetitive succession of cyclothemic sedimentary units, which show corresponding developmental changes as the succession is ascended (Table 1.1). The Millstone Grit cyclothems of the Namurian are often very thick (60-150m); their coarse grained sandstones and grits are overlain by thick marine shales, which pass into thinner

non-marine shales and siltstones. Progressively the cyclothemic pattern changes to that of the Coal Measure type which averages 9-12m; the thin finer grained sandstones carry seat-earths or fireclays with thick coal seams. Both the rhythmic character of sedimentation in Upper Carboniferous and the lateral variations in the thickness and type of units are features which have an important bearing on the nature of the land surface which has developed on these strata.

The most complete representation of the lower members of the Millstone Grits occurs in the central area of the southern Pennine upfold in the Edale area (Hudson & Cotton, 1945). In this area the Edale Shales (E_1-R_1) at the foot of the succession are 210m thick (Jackson, 1925, 1927). They consist of dark marine mudstones, with calcareous layers and hard quartzose siltstones, and are succeeded by sooty shales containing fossil bullions (Ramsbottom et al., 1962). This part of the succession is dominantly marine and represents a facies of basinal shales with an abundant goniatite lamellibranch fauna. The upper part of the Edale Shales is marked by the appearance of the goniatite genus Reticuloceras which is used to define the base of the R_1 or Kinderscoutian stage. The overlying Mam Tor sandstone (120m) is recognised on a lithological basis by the appearance of well-bedded silty sandstones in the shale sequence. This series of closely spaced sandstones and shales represents east-west flowing turbidity-current deposits generated by the slumping of deltaic sediments on a higher submarine slope (Allen, 1960). Their distribution is restricted and their thickness varies rapidly from 90m at Mam Tor to less than 60m at Ashop Clough in the north (beyond which they die out) and become less than 30m thick in

Bretton Clough to the south east. Spectacular landslips are a characteristic feature where these beds outcrop.

The succeeding Shale Grit and Grindslow Shales contain sandstone bands, siltstone and shales. These in turn are overlain by the Kinderscout Grit (Jackson, 1927; Walker, 1967). This grit has an erosive base consisting of coarse pebbly sandstone intercalated with finer sandstones and shale. It is much thicker in the north (120-150m) and rapidly thins southwards passing into shales around Matlock. The Kinderscout Grit represents a southern advance of the delta front across underlying pro-delta sediments, the whole group suggests off-shore delta front sediments, followed by a thick accumulation of coastal plain and near shore pebbly sandstones and shales with rarer marine horizons (Allen, 1960).

This alternation between easily eroded shales and resistant gritstone and sandstone horizons becomes more marked and more frequent in the Middle Grits, where the individual units are often not more than 30m in thickness (Eden et al, 1957). The name given to the individual members of the Middle Grits varies from area to area (Table 1.3.) For instance, the sandstone known as the Halcombe Brook Grit or the Huddersfield White Rock on the northern edge of the Peak District becomes the Rivelin or Chatsworth Grit on the eastern flank of the area or the Shining Tor Grit on the west (Edwards, 1956, Edwards & Trotter, 1962). The name Rivelin Grit is used in this study. The Middle Grit Group contains the Rivelin Grit towards the top and the Ashover Grit below, these are coarse sandstones with pebbly seams decreasing upwards. The Ashover Grit thins out northwards, whilst the Rivelin Grit thins southwards.

SERIES	STAGES	CORAL/BRACHIOPOD ZONES			LITHOSTRATIGRAPHICAL UNITS					GONIATITE ZONES	MESOTHEMS (Ramsbottom 1977)
		Garwood 1913 Garwood & Goodyear 1924		Correlation with Vaughan (1905) zones (C₁-D₁) and coral zones (2 4) of Hill (1938-41)	Ravenstonedale area (based on Mitchell, 1978)	ASKRIGG BLOCK					
		ZONES	SUBZONES			N areas (and Stainmore Outlier)	S W area	S E area			
NAMURIAN	YEADONIAN							Laverton Sst / Laverton Shale		G₁	N11
	MARSDENIAN							Wensley Gill Sst		R₂	N10 / N9
								U. Brimham Grit			N8
	KINDERSCOUTIAN							L. Brimham Grit		R₁	N7
								Loadam Sst / Easton G'I Beds			N6 / N5
	ALPORTIAN / CHOKERIAN									H₂ / H₁	N4 / N3
	ARNSBERGIAN						Samson Tail M.B.			E₂	N2
	PENDLEIAN			Zone 4		Mirk Fell Transition / L Howgate Edge Grit	Grassington Grit	U Bowland Shales		E₁	N1
VISÉAN		Upper Dibunophyllum Zone	Dibunophyllum			Main Limestone					
	BRIGANTIAN		muirheedi	Zone 3	Upper Alston Group	Underset Lst / Five Yard Lst				P₂	D6B
				Zone 2		Middle Lst / Simonstone Limestone / Hardraw Scar Limestone / Gayle Limestone / Hawes Lst	Toft Gate Lst	Coldstones Lst		P₁	D6A
		Lonsdaleia floriformis								?———	
	ASBIAN	Lower Dibunophyllum Zone	Cyathophyllum murchisoni	D₁	Robinson Lst / Thorny Force Sst / Knipe Scar Lst	Danny Bridge Lst	Kingsdale Lst / Gordale Lst	Hargate End Lst / Greenhow Lst / Stump Cross Lst / Timpony Lst		B₂ / B₁	D5B
					Potts Beck Lst	Geredale Lst	Horton Lst / Cove Lst			?———	D5A
	HOLKERIAN	Productus corrugato- hemisphericus	Nematophyllum minus / ? Cyrtina carbonaria / Gastropod Beds	S₂ / S₁	Ashfell Lst / Ashfell Sst	Fawes Wood Lst / Ashfell Sst	Kilnsey Limestone			Pₑ	D4
	ARUNDIAN	Michelinia grandis	Chonetes carinata / Camarophoria isorhyncha	C₂	Michelinia grandis Beds / Brownber Pebble Bed / Scandal Beck Lst	Tom Croft Limestone					D3
	CHADIAN	Athyris glabristria	Seminula gregaria	C₁	Coldbeck Lst	Penny Farm Gill Dol / Marsett Sandstone / Raydale Dolomite					D2

Stage	Central Pennines	North Derby-shire	Matlock-Derby	North Stafford-shire
Yeadonian G₁	Rough Rock	Rough Rock	Rough Rock	Rough Rock or First Grit
Marsdenian R₂	Huddersfield White Rock	Chatsworth and Middle Grit Group	Chatsworth Grit Ashover Grit	Third (Roches) and Fourth Grits
Kinderscoutian R₁	Bramhope and Todmorden Grits	Kinderscout Grits Grindslow Shales Shale Grit Mam Tor Sandstones		Longnor Grit
Sabdenian H	Sabden Shales	Edale Shales	Edale Shales	Churnet Shales
Arnsbergian E₂				
Pendleian E₁	Skipton Moor Grits and Pendle Grit / Upper Bowland Shale			Crowstones and Morridge Grits

Table 1.3. Classification of the Viséan and Namurian with key giving local names of Stages.

The effect of the pronounced contrast between the main units of
sedimentation are the striking examples of differential erosion
which typify the land surface. The inclination of the strata is
also a fundamental factor in determining the landform expression
and the slope type which develops. The Kinderscout Grits give rise
to extensive level summits where their dip is nearly horizontal in
the central plateau area dominated by Kinderscout and Bleaklow, or
striking dip-slope ramps on the margins where the strata dip at
$5^{\circ}-10^{\circ}$, or prominent scarps where the underlying shale has been
eroded away.

Many members of the Millstone Grit Group are lenticular in
disposition, and attenuate at outcrop when followed over a distance
of some kilometres; this attenuation is particularly pronounced on
Bamford Edge. In addition to these changes in thickness of the
strata there are marked contrasts in the average size of the
constituent grains of the sandstones and variations in the
cementation or kaolinisation of the feldspars (Greensmith, 1957).
These variations in the lithological character of the Millstone
Grits provide marked contrasts in resistance to erosion between
the shale and grit units. The grits or sandstones themselves also
vary in resistance to weathering along their outcrop. The two
uppermost sandstone formations in the Millstone Grit series are the
Chatsworth Grit and the Rough Rock. Both are widespread over the
area but are thicker and coarser on the north-east, suggesting
derivation from that quarter.

A thin band of marine shale bearing the fossil goniatite,
gastrioceras subcrenatum , is the dividing line between the
Millstone Grit Series and the Coal Measures Series which follows

without a break. The rock in the Lower Coal Measures are very similar to those in the upper part of the Millstone Grit Series. Mudstones, shales, sandstones and thin coal seams predominate, but the sandstones are less coarse and coal seams more numerous than in the underlying series.

1.4.4 Geological Structure

The structures in the Carboniferous rocks of the study region are mainly of Hercynian age, although the prior existence of two structural units have affected sedimentation in both the Lower and to a lesser extent Upper Carboniferous. These pre-Carboniferous structures have affected the distribution and intensity of Hercynian folding and faulting during post-Carboniferous times. The most important of these Pre-Carboniferous units was the stable block of the Derbyshire Dome over which shelf sedimentation occurred in the Lower Carboniferous (Maroof, 1976). The other structural unit to affect Hercynian structural movements was the 'Edale Gulf' in the central part of the study region (Kent, 1966). This area functioned as a subsiding basin of sedimentation in the Late Viséan times.

During the Hercynian the carboniferous rocks of the Peak District were subjected to moderately strong folding and faulting. The axes of the folds trend in a NNW-SSE direction. The main effect of the folding was to cause the central part of the Peak District to arch upwards and form a broad anticline with gently dipping limbs on the eastern and western flanks. Minor folds, such as the Goyt Syncline in the west and the Ashover Anticline in the east, display much tighter folding.
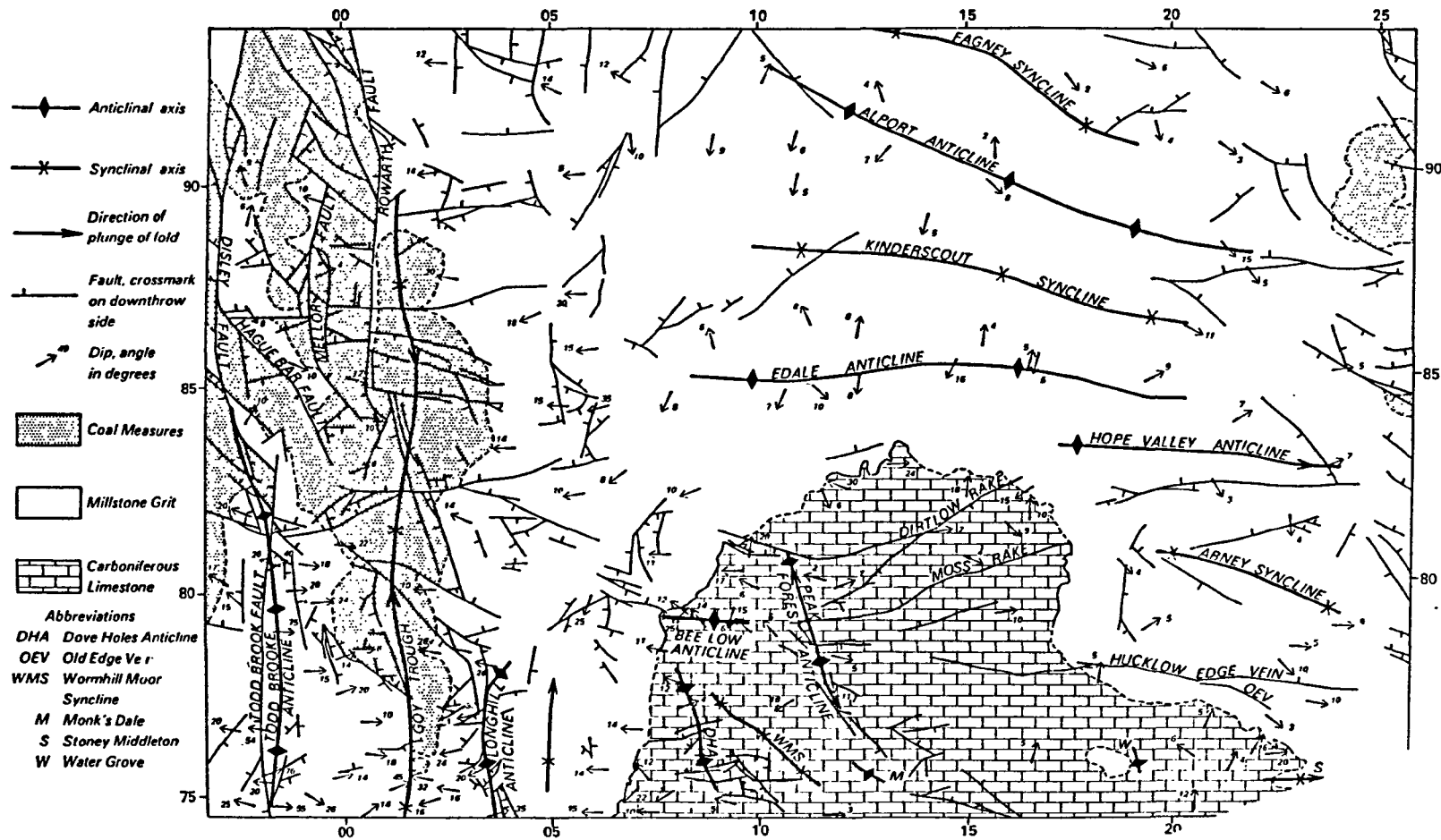
Fig. 1.5   Sketch map illustrating the geological structure (Stevenson & Gaunt, 1971)

The shelf limestones are characterised by gentle NNW - SSE folding and generally low dips. The traces of the main fold axes are shown in Fig. 1.5. In the off-shelf province the limestones are much more intensely folded. The axes of some of the main structures coincide with the lines of the main knoll-reefs. Dips commonly exceed 30°.

Faults occur in both shelf and off-shelf strata but in most cases their throw is only a few meters, the main faults are shown in Fig. 1.5. There is a tendency for the faults to be aligned in either a north-west to south-east or north-east to south-west direction. The faults subsequently played a major part in easing the passage of hot mineral bearing solutions through the rocks.

The outcrops of the Millstone Grit Series to the east of the Derbyshire 'Dome' show continuations of the easterly plunging folds seen in the limestone, though generally with less amplitude owing to the overlap-relationship of the Edale Shales on the folded limestone (Jones, 1942). Similarly the folds are continued on the overlying Coal Measures. The fold axes tend to swing to more south-southeasterly course away from the east-west folds in the limestone and at times become almost north-south. Dips are rarely more than 20° and usually much less.

1.4.5. Quaternary Deposits in the Peak District

The Quaternary history of the Peak District is still only poorly understood,. To a large extent this is because, in contrast to the lowland areas to the east and west, it contains only a sparse and scattered distribution of Quaternary deposits and, for the most

part lacks dateable materials (Straw & Lewis, 1962; Briggs et al, 1985). As a result, there has been little evidence on which to base a reconstruction of Quaternary events in the region, while correlations with surrounding areas is at best tentative.

Glacial tills are confined to two main areas, in the Manifold Valley around Butterton and the Wye-Derwent catchment around Bakewell. The lack of dateable materials beneath the tills makes it difficult to determine whether these deposits are a product of a single glacial episode or represent two (or more) distinct events. Striations, fabric analysis and stone counts all indicate an incursion from the NNW, and the implication is that the ice advanced into the Peak District across the Dove Holes Col, which lies at about 310m O.D.

Examination of the Bakewell Manifold tills on the one hand, and the sparse glacial deposits including erratic distribution at higher levels on the other, imply at least two separate glacial episodes were involved. This interpretation is tentatively suported by the occurrence of deeply weathered high level tills at a number of sites, most notably at Hope Quarry and Upper Town in the Southern Peak District (Briggs et al, 1985).

Evidence of periglacial activity during the Devensian is abundant and includes the process of freeze thaw, the presence of permafrost, wind action on unvegetated ground and solifluction of material above the permafrost table (Peltier, 1950; Palmer & Radley, 1961; Stevenson & Gaunt, 1971; Johnson, 1968). The formation of dry valleys (Warwick, 1964), solifluction deposits (Wilson, 1981), blockfields (Said, 1969), cemented screes (Prentice

& Morris, 1959) and other cryogenic features such as frost wedges and patterned ground attest that periglacial conditions prevailed at various times in the Peak District until about 10,000 years B.P.

A number of papers have been presented discussing the terrace sequence of the Derwent Valley (Linton, 1951; Waters & Johnson, 1958; Straw, 1968; Johnson, 1957, 1969b, Burek, 1977). These were originally interpreted as being the result of valley floor planation and aggradation during interglacial and interstadial periods, followed by degradation as the River Derwent incised to a lower base level and nick-points worked upstream in glacial episodes.

Comparable terrace sequences have not been found in other valleys of the area. Stevenson & Gaunt (1971) identified lower terraces in the Noe Valley, but from their relationship with Head and valley fill deposits all would appear to be relatively young features and probably relate entirely to the Devensian and later stages. This interpretation has recently been supported by evidence of radio-carbon dates derived from materials in the Highfield Terrace deposits in Edale (Redda, 1986). The Noe sequence, therefore, cannot be viewed as a direct correlative of the terrace sequence in the Middle and Lower Derwent.

Given the difficulties of reconstructing the Quaternary record from superficial deposits in the Peak District, attention is now being focussed on evidence collected from cave deposits in the area. A number of cave systems in the Carboniferous Limestone contain fills of gravel, sand and clay, together with speleothems. The clastic sediment fills probably represent phases of aggradation during cold

stages, when materials of glacial, glacial-fluvial or loessial
origin were washed into the cave systems. Speleothem formation was
likely to have been essentially a warm-stage phenomenon. Evidence
collected from speleothem dating has been summarised by Ford et al
(1983). A chronology of Quaternary events has been outlined by
Briggs & Burek (1985).

The late Devensian and Flandrian environments of the study region
as can be deduced from existing palynological and geological
evidence has been outlined by Conway, 1954; Tallis, 1964a, 1964b;
Said, 1969; Tallis & Switsur, 1974, 1983; Briggs,, et al 1985; and
Redda, 1986. A summary of the chronology of the vegetation,
geomorphological and land-use events in the study region compiled
by Said (1969) is given in Table 1.4. An understanding of the
bioclimatic environments of the late Devensian and Flandrian is
required since palynological methods have become standard and
frequently cited techniques to determine the terminal dates for the
cessation of landslide movements and to reconstruct the environment
in which mass movement occurred (Franks & Johnson, 1964; Johnson,
1965; Muller, 1979; Tallis & Johnson, 1980; Redda, 1986).

	Cultural Period	Climatic Phase	Pollen Zone	Climate	Vegetation	Geomorphological Events	Landuse Events
AD 1000		Sub-Atlantic	VIII	Colder and Wetter	Increased Podsolization & spread of heather. Increased Birch, Hazel & Pine. Decline in Lime. Growth of Peat in wetter periods. Initiation of Peat erosion.	(i) Deforestation, the deposition of wastes (ii) Deforestation, a short phase of Peat Erosion and the deposition of organic mud (iii) Deforestation, formation of gravel terraces	Continuous interference of natural vegetation, deforestation.
AD — Roman — Iron Age							
BC 1000 — Bronze Age	Neolithic Age	Sub-Boreal	VIIb	Drier more continental	Elm declines, appearances of first weeds. Expansion of Ash. Hazel, Birch, Pine woodlands in lowlands. Slow growing Peat in uplands.	(i) Brown earth soils developing (ii) Landsliding (iii) Weathering processes active	Deforestation, pastoralism, cultivation.
2000							
3000							
4000	Mesolithic Age	Atlantic	VIIa	Increased temperature and rainfall le Oceanis	English channel forms. Increased Alder, Birch, Oak, Elm, Hazel, Lime Deciduous woodland on lowlands. Peat formation begins on uplands.	(i) Rapid Peat growth (ii) Gully erosion (iii) Hill and sheet wash (iv) Landsliding (v) River erosion	
5000							
6000		Boreal	VI	Increased warmth, dry	Pine & Hazel replace Birch. Increase in Elm & Oak towards end. Small amounts of Alder.	(i) Development of soils (ii) Consolidation/stabilization of ground surface (iii) Moderate Hillwash and weathering (iv) Landsliding	Burning for improved grazing.
7000			V				
8000		Pre-Boreal	IV	Increased warmth Sub Arctic	Open Birch woodland, development of soils.	(i) Soil formation, (ii) Hillwash, (iii) stream incision, (iv) some landsliding	
		Upper Dryas	III	Return of cold Arctic	As Zone I	As Zone I	
9000		Allerød	II	Temperate, increased warmth	Open woodland, Birch, Pine and Herbs. Development of soil.	(i) Development of soil and vegetation (ii) Phase of erosion (iii) Hill wash (iv) Incision of gravel terraces (v) Mass movement processes	
10,000		Lower Dryas	I	Arctic Tundra	Arctic/Alpine Herbs e.g. Mountain Avens (Dryas)	(i) Periglacial processes, freeze-thaw, solifluction, cambering & valley bulging (ii) Deposition of head (iii) Terrace formation	

Table 1.4   Chronology of vegetation, geomorphological, and land use events in the study region (Said, 1969)

1.5 LANDSLIDE CLASSIFICATION

1.5.1 Introduction

This thesis is primarily concerned with the field recognition and identification of those relatively rapid mass movements generally referred to as landslides, as distinct from slow, long-term slope movements (e.g. creep). Many systems of classification have been established for mass movement based on criteria such as the mode of movement (Crozier, 1973; Hutchinson, 1968a), type of material (Hutchinson & Brunsden, 1974; Skempton & Hutchinson, 1979 Nemcok et al, 1972), causes of failure (Terzaghi, 1950; Varnes, 1958) etc. The proliferation of classifications in recent years however, has unintentionally defeated one of the principal purposes of the exercise, that is, the provision of a clear and unambiguous terminology. This has arisen because individual classifications have been developed for specific purposes or from observation in specific regions and their subsequent application has not always taken this into account.

1.5.2 Landslide Classification

The classification adopted here (Table 1.5) is similar to that used by the Institute of Geological Sciences for the South Wales Coalfield Landslip Survey (Conway et al. 1980) and is based on the classification systems of Hutchinson (1969) and Varnes (1978).

Table 1.5. Landslide Classification

Type of movement	Mass movement process		Minor mechanism
	Predominant mechanism		
R=Rotational slide	DR—Deep seated	>5m deep involving bedrock	r
	SR—Shallow	<5m Deep not involving bedrock	sr
	MR—Multiple	Retrogressive	mr
T=Translational slide	DT—Deep-seated	>5m Deep involving bedrock	t
	ST— Shallow	<5m deep not involving bedrock	st
	ST(h) With head slumping <5m deep not involving bedrock		st(h)
F=Mudslide/ Mudflow	F		f
X=Rockfall	X		x
Complex	Consisting of one or more of the above mechanisms		

This simple classification was selected in order to facilitate a rapid investigation of mass movements from readily observable surface morphological features which involved a programme of aerial photograph interpretation and 'walk over' surveys combined with a desk survey of published information in the form of geological maps and papers.

Two principal criteria were used to classify mass movement in the study area, (1) type of movement and (2) depth of failure.

1. Type of Movement

In categorising the various types of slope movement from aerial photograph interpretation and walk over surveys, emphasis was placed on the landslide morphology and arrangement of its constituent materials in the downslope longitudinal profile. Four main types of movement have been recognised in the study region, namely, rotational (R), translational (T), mudslides/mudflows (F) and falls (X). One particular type of rotational slide that may be recognised is the multiple retrogressive type (M). This type of slide is generally deep-seated and is thought to develop from single rotational failures which interact to form a common basal slip surface (Skempton & Hutchinson, 1969). This type of failure becomes more translational in character as the number of component slip units increases, although, in failing, each block itself rotates backwards. Descriptions of these types of movement are given by Skempton & Hutchinson (1969) and Varnes (1978) and therefore will not be repeated here.

Mass movements may be described as simple, comprising only one type of movement, or complex, comprising two or more types of movement. In complex slides, however, a dominant movement can generally be identified and the landslide classified accordingly. The term compound slide is used by Skempton & Hutchinson (1969) to describe the situation where a rotational failure is modified by an underlying lithological or structural discontinuity, which imparts a translational element into the slide movement. In the study region, the rotational components at the head of many of the slope failures comprise slumped and back-tilted masses of sandstone. In some instances this head slumping appears to have occurred after

initial translational movement had taken place, resulting in a subsequent slump failure of the unsupported sandstone scarp. At other localities, the morphology of some landslides indicates single non-circular shallow rotational failure, incorporating a well developed 'flat' or bench below the back scar. Complex mass movements showing evidence of a combination of both translational and rotational movement, therefore, may be represented in a gradation of type categories ranging from translational slides with subsequent head slumping; truly complex slides in which both types of movement share equal importance; through to rotational sliding on markedly non-circular slip surfaces.

Another common type of complex landslide in the study region occurs when the sliding mass breaks up and softens downslope to form mudslides/mudflows at its foot. The different types of complex landslide which occur in the Peak District have been described by Johnson (1980).

2. Depth of failure

An arbitary distinction has been made between deep-seated and shallow mass movements, based on a visual assessment and largely without recourse to subsurface information. A landslide has been designated as 'deep seated' (D) if the failure has involved bedrock to a depth estimated as being in excess of approximately five metres. Landslides designated as 'shallow' (S), typically involve weathered and superficial material with no significant part of the bedrock involved in the movement.

1.5.3 <u>Landslide classification type code</u>

Table Al in the Appendix gives the landslide number, the grid
reference and the landslide classification type code which
correspond to the landslide distribution maps for the northern and
southern sections of the study region. The landslide type codes
indicate the different types of movement or movements recognised for
each numbered landslide. The letter symbols used to identify the
type of movements are shown in Table 1.5.

In most complex landslides the main mode of failure is accompanied
by other less significant types of movement. Thus the type code for
each landslip (Table Al) which shows a combination of movements, the
major movement is indicated by the appropriate upper case symbol,
followed by the lower case symbol(s) indicating accompanying minor
movements. Deep-seated and shallow failures are represented by the
letters (D) and (S) respectively. For example, code DTRFx indicates
a deep-seated translational slide with a major rotational component
accompanied by large-scale mudsliding and minor rockfall failures.
It has been noted that mudslides/debris flows are frequently formed
at the foot of many of the slides. Where the mudslide/mudflow
component is on a minor scale compared to the dominant sliding
movement, a lower case 'f' is used in the type code. In some
instances, however, mudsliding has developed on a large-scale to
form an extensive debris apron covering the valley footslopes.
Where this is the case, the upper case 'F' has been used. The code
DMRTF therefore represents a deep-seated multiple rotational slide
with a major translational component, accompanied by large scale
mudsliding.

1.6   LANDSLIDE DISTRIBUTION

1.6.1   Introduction

Fig. 1.6 shows the spatial distribution of mapped landslides in the county of Derbyshire. The information was collected from 1:10,000 geological survey maps and plotted on a base map at the scale of 1:25,000. The inset on Fig. 1.6 bounds the regional study area used in the landslide susceptibility assessment discussed in Section 2. Fig. 1.6 shows that landsliding is a common feature of the southern Pennines within Derbyshire. A cursory comparison between Fig. 1.6 (the distribution of landslides in Derbyshire) and Fig. 1.4 (the solid geology of the Peak District) shows that their spatial distribution is largely restricted to the valley slopes eroded in the Namurian sandstones and shales. The rivers draining the high moors and plateaus have cut through a succession of Mid-Carboniferous sandstones, mudstones and shales and have created inherently unstable valley sides wherever competent massive sandstones overlie the exposed weak and incompetent series of strata. The instability of slopes resulting from incision under these conditions appears to have been relieved by mass movement.

1.6.2   Landslide Areas

Six major landslide areas can be recognised within the study region.

1.   Edale and Mam Tor

Present mapping has identified about 15 major and several minor landslides in Edale. Most of the major landslides in Edale occur on

north-facing slopes. Nearly all the landslides are of a deep-seated rotational type mainly involving the Mam Tor Beds and Edale Shales. The three largest landslides are Mam Nick (121), north west of Mam Tor, Back Tor (100), north west of Lose Hill and Mam Tor (137) situated to the west of Castleton at the head of Hope valley. Mam Tor landslide provides a very good example of a large rotational landslide, the slip plane is believed to have originated at the base of the Mam Tor Beds. The secondary slips of Mam Tor are still active, indeed the landslide is well known on account of the road stability problems it has posed. Continual collapse of part of the A625 road passing over the middle section of Mam Tor landslide led to its eventual closure in 1979.

2. Ashop and Alport valleys

Complex landslips are present along about half of the northern side of the Ashop valley, where the southerly dip has facilitated large scale translational down dip and deep-seated rotational sliding. In the Ashop valley the landslides cover an area of approximately 2000 hectares. At Cowms Rocks (25) a large deep-seated rotational slide has moved leaving an area of ground in the centre of the slip intact. The A57 which runs along the Ashop valley has been unstable in this area for a long time, Ashop (28), Cowms Rocks (25) and Dinis Sitch Tor (24) landslides in particular have caused continual damage to the A57 (Leadbeater, 1985). The most spectacular landslides in this area occur on the eastern slope of the Alport valley, where relatively large areas of ground have slipped without breaking up into smaller rotatated units. Alport Castles (18) is the largest individual landslide of this complex, it covers approximately 250 hectares. The distance from the dislodgement scar to the toe of this slide is about 2.5km and the width is approximately 1km across at its widest extent.

LANDSLIDE DISTRIBUTION IN DERBYSHIRE

Study Region

Legend:
— County boundary
······ Peak District National Park
Landslides:
> 0.25 km²
• < 0.25 km²

1 Holmfirth
2 Deepcar
3 Glossop
4 Sheffield
5 Castleton
6 Whaley Bridge
7 Chapel en le Frith
8 Hathersage
9 Macclesfield
10 Buxton
11 Chesterfield
12 Bakewell
13 Matlock
14 Leek
15 Alfreton
16 Ripley
17 Eastwood
18 Ashbourne
19 Heanor
20 Ilkeston
21 Nottingham

N

0   km   15

Fig. 1.6 The distribution of landslides in Derbyshire

3. Derwent valley

Small rotational slides with head slumping involving the Mam Tor Beds
and the lower part of the Shale Grit are present in a number of
places in the Derwent valley. Thornhill Carrs (129) landslide on the
eastern side of Win Hill is of considerable antiquity as its slipped
mass is greatly denuded and its dislodgement scar is virtually
overgrown. In contrast Ashopton (75) and Ladybower (76) landslides
adjacent to Ladybower reservoir possess sharper features and hence
are thought to be more recent scarp collapse landslides involving the
Kinderscout Grit. The dislodgement scars of both these slides are
bare; relatively recent large fissures opening to depths of up to
three metres are present in the Kinderscout Grit above the
dislodgement scar of Ladybower landslip (76). The landslipped masses
of both slides are boulder strewn and show a pronounced hummocky
morphology, with bare secondary scars.

4. Hucklow and Bretton

The Bretton Clough slide complex (221) lies within a broad gritstone
salient which stands prominently above the surrounding limestone in
the form of steep escarpments facing south (Hucklow-Eyam) and west
(Hucklow-Brough). The Bretton Clough landslide incorporates a large
number of intact slide blocks indicating many separate movements.
These are arranged in a series of approximately concentric shallow
arcs broadly in line with the course of the Bretton Brook, suggesting
major escarpment retreat by landsliding on the southern side of the
valley. The morphology of this area is dominated by these blocks
many of which have steep back and front slopes which meet in knife
edge ridges. The dominant geological unit involved is the Shale

Grit; at Bretton it is composed of thick sequences of coarse sandstones separated by thin shale beds. The main scarp face is formed by the lowest numbers of the Shale Grit. These lie conformably on the Man Tor Beds, which outcrop at the base of the main scar and in the rest of the slipped area in the form of a narrow inlier.

The striking Burrs Mount landslde (216) below the western face of Hucklow Edge originates from the lowest strata of the Shale Grit. A large number of smaller landslides have also occurred at a similar horizon on the western flanks of Abney Moor and the north facing slopes of Shatton Edge.

5. Bradfield and Broomhead Moor

The Broomhead landslide (2) on the southern edge of Broomhead reservoir is one of the largest landslide complexes in the study region. The landslide complex covers an area of over 2 km^2 on the north eastern flanks of Broomhead Moor from a series of rotated blocks at Canyards Hills in the west to the large deep-seated rotational movement at Rocher Bottom.

A number of deep-seated rotational slides have also developed on the north eastern edge of Bradfield Moor such as Rocher Top (13), Upper Thornseat (14) and Bradfield (15). These three landslips have an extensive mudslide component towards the foot of the landslide mass. The village of Bradfield lies on the mudslide/mudflow component of the Bradfield slide (15).

6. Limestone outcrop

Landsliding is not common in the limestone outcrop, but does occur on some slopes where masses of limestone are underlain by tuff or lava. The uppermost part of the lava tends to alter to soft impervious clay (toadstone clay) and the presence of a perched water-table also tends to favour slipping. Landslips of this type are, however, of very limited dimensions; an example of this type of slip is present above the Lower Lava at Cave Dale (149).

1.6.3 Shallow Planar Translational Slides

Shallow planar translational slides are common throughout the study region and occur in the mantle of superficial material (Head, colluvium, regolith) that covers the hillslopes virtually everywhere. The depth of superficial material controls the form of the failing mass which tends to slide along a shear surface running roughly parallel to the hillslope. Many of the smaller and degraded shallow planar slides are difficult to detect using panchromatic aerial photographs (1:12,000 scale) and many are too small to be mapped at the scale of 1:25,000, therefore many of these features have been omitted from the landslide distribution maps.

The indications are that the majority of slopes in the study region with a mantle of Head deposits are close to limiting equilibrium for such shallow movements. The recognition of these areas, which may be interpreted as relic features of periglacial mass movement, are of obvious importance in engineering and planning terms. Most of the slopes are currently stable, this is because of present low piezometric levels, although in the vicinity of some spring lines a

rise in groundwater level has resulted in renewed instability.

1.6.4 Parameter Base Maps and Landslide Distribution

A series of parameter base maps of the southern part of the regional study area were constructed at the scale of 1:25,000 for the landslide susceptibility assessment. The construction and use of the base maps for landslide susceptibility assessment is discussed in detail in Section 2. The base maps used for a regional assessment of landsliding included:-

1. Landslide distribution overlay maps for the northern and southern parts of the study region
2. Ordnance Survey/Topographic Map
3. Solid Geology Map
4. Pedology Map
5. Drainage Map
6. Morphological Map (showing individual slope angles)
7. Morphological Slope Classification Map

1.7 CAUSES OF INSTABILITY

1.7.1 Introduction

Occasionally a landslide occurs in a unique situation, but *landsliding usually takes place under geological (lithological, stratigraphical, structural), topographic and climatic conditions that are common to large areas*, Terzaghi (1950). The occurrence of landsliding in these areas is not a random process it is the result of the incidence of a number of identifiable factors which in combination give rise to an unstable situation.

The causes of landslides can be divided into two types (Terzaghi, 1950):

A. External causes that produce an increase in shear stress but no change in the shearing resistance of slope forming materials.

B. Internal changes in shearing resistance without change in shear stresses i.e. factors that contribute to low or reduced shear strength.

Possible causes and contributing factors are summarised in Table 1.6 overleaf. The table includes a selection of important references relevant to particular factors causing landsliding.

Table 1.6 Factors causing Landsliding

A. **FACTORS CONTRIBUTING TO HIGH SHEAR STRESS**

1. **Physical removal of lateral or underlying support**

(a) Undercutting by streams and rivers (Hutchinson, 1968).

(b) Squeezing out of underlying plastic material (Zaruba & Mencl, 1969).

(c) Washing out of granules and soluble material by seepage erosion and weathering (Ward, 1945; Terzaghi, 1931; Denness, 1972b).

(d) Excavation by man.

2. **Increased internal Pressure**

(a) Build-up of pore water pressure and intensification of its distribution system within jointed strata (Terzaghi, 1962; Hutchinson, 1969).

(b) Freezing of water in cracks.

(c) Cyclic loading and unloading and mobilisation of residual stress of slope forming materials through time (Bjerrum, 1967; Krinitsky & Kolb, 1969).

(d) Swelling as a result of hydration.

B. **FACTORS CONTRIBUTING TO LOW SHEAR STRENGTH**

1. **Materials, Composition and Texture**

(a) Composition: beds which decrease in shear strength if water content increases (shales, mudstones).

(b) Texture: low internal friction and cohesion of rocks involved in shearing in bedrock.

2. Gross structure and slope geometry

(a) Discontinuities, such as faults, bedding planes, cleavage planes and joints (Skempton & Petley, 1967; Fookes & Wilson, 1966; Bjerrum & Jorstad, 1968).

(b) Massive beds over weak or plastic material (Zaruba & Mencl, 1969).

(c) Strata inclined towards free face (Terzaghi, 1962; Selby, 1982b).

(d) Alternation of permeable beds (sandstone) and weak impermeable beds (shales) (Henkel, 1967).

(e) Slope orientation (Rice et al., 1969).

(f) Changes in structure may be caused by fissuring of shales and fracturing and loosening of rock slopes due to release of vertical or lateral restraints in valley walls caused by valley bulging and cambering (Kellaway & Taylor, 1968).

3. Changes due to weathering and other physico-chemical reactions

(a) Softening and reduction in cohesion resulting from the oxidation of Pyritic shale (Vear & Curtis, 1979).

(b) Hydration of clay minerals forming shales and mudstones. Softening, suffusion and slaking processes reducing cohesion (Ingold, 1975; Steward & Cripps, 1983; Cripps & Taylor, 1981).

(c) Removal of cement by solution.

(d) Drying of shales that creates cracks on bedding and shear planes and reduces shale to finely comminuted granules.

(e) Physical disintegration of granular rocks such as sandstone, through the action of thermal expansion and contraction (Rapp, 1960).

4. Pore-water pressure increase

(a) High ground water table levels in the past resulting from permafrost, the mantling of slopes with superficial debris or to increased precipitation due to changes in climate (Dennes, 1972a; Conway, 1974). Buoyancy in the saturated state decreases effective intergranular pressures and friction.

(b) Formation of cleft pore water pressure during glacial periods (Terzaghi, 1962).

5. Vegetation

(a) Removal of vegetation (Gray, 1970; O'Loughlin, 1974; Brown & Sheu, 1975).

It should be noted that the external changes are often closely associated with subsequent, autocatalytic, internal changes in shear strength. In addition long term changes occur and these cannot be related directly to any one external cause other than the processes that originally created the hillslope. These changes which involved a slow change in resistance included progressive failure by softening or stress concentration, weathering and seepage erosion. The development of factors favourable to landsliding may therefore be a long term process in which stream incision and progressive stratal weakening by ground water are important.

Although, instability may be modelled deterministically by stability analysis, it is a spatially stochastic phenomenon, in that, a probability distribution of factors of safety can be envisaged for the set of slopes in a given environment, since geotechnical

properties and ground-water conditions vary spatially. Separate
distributions may be defined for deep-seated and shallow mass
movements since each of these respond to different controls.
Similarly separate distributions may exist for a given type of
failure according to separate seasonal conditions of soil moisture
and ground-water levels. Such probability distributions represent
the spatial potential for instability, and cannot be assumed to
represent the probability of failure on any one slope.

Deep-seated and shallow mass movements reflect different controlling
conditions. The former occur in intact cohesive materials and
involve mobilisation of strengths in excess of residual. Slope
height and angle are both important influences, and instability
occurs if basal erosion either increases slope height beyond a
critical value at a given slope angle, or steepen the slope until the
actual height equals the limiting height. The Culmann Stability
Analysis defines the limiting height of vertical cliffs, which fail
on planar surfaces passing through the slope foot. Rotational slides
occur on slopes with angles less than 90°, and Taylor's (1937)
stability charts predict limiting heights for combinations of slope
angle, and material density, cohesion, and angle of shearing
resistance. These stability charts have been modified to incorporate
pore water pressure data (Chandler & Skempton, 1974).

Shallow translational slides generally occur in cohesionless regolith
at near residual strengths and are independent of slope height.
Slope angle is critical, and shallow failure restores stability on
over-steepened slopes by lowering the angle to approximately the
residual angle of friction ($\emptyset r'$) in the absence of positive pore
pressures which result in lower stable angles. Where basal erosion

is slow, progressive weathering gradually and discontinuously reduces Ør' as the clay content increases (Carson & Petley, 1970), and reduced permeability may eventually result in shallow slides which lower the slope angle to the semi-frictional angle, reflecting the worst ground-water conditions experienced.

Slope development by mass movement thus involves a range of processes, whose general effect is to lower the slope angle but whose balance varies according to the wider landform evolution processes including the effect of climatic change and the external effects (e.g. basal erosion). The need for 'Whole System' appraisal of controls is therefore necessary.

The general absence of detailed geotechnical and geological data on such matters as the position and character of failure surfaces; the pore water pressure distribution at the time of failure; and the real extent of the deterioration in rock strength of materials along the line of rupture at times when the slopes became critical in the Peak District, means that explanations for cause of failure can only be treated as incomplete and speculative.

The principal factors contributing to landsliding in the study region are outlined below.

1.7.2 The structural condition of massive Namurian sandstones overlying weak incompetent shales and mudstones

The common geological feature, within the study area, of massive competent beds of Kinderscout Grit or Shale Grit overlying the Edale Shales or mudstone strata whose total thickness is greater but whose

rock mass strength is markedly less, provides conditions conducive to mass movement. Below the gritstone 'cap rock' the hillslopes are eroded in a thick succession of alternating argillaceous beds of variable thickness and lithology. The mudstones, siltstones and shales differ in their degree of cohesion, their permeability and rock strength and since in some places the beds are only a few metres thick they provide many zones of weakness in which sliding or slip movements might commence.

Rock complexes with high strength overlying weaker rock units are subject to undermining or failure along deep failure planes. Rotational slides often retrogressive in type tend to occur in such conditions when maximum stress at the foot of the slope is transmitted by the processes of rock mass creep in the rocks within the slip zone. Creep of rock involves long term slow deformation in which the rock behaves plastically (Zischinsky, 1966; Scheidegger, 1970; Bruckle & Scheidegger, 1972; Radbruch-Hall, 1978; Radbruch-Hall et al., 1977). Some of the geological conditions under which rock mass creep may occur have been outlined by Selby, 1982a, 1982b.

It appears from field evidence in the Dark Peak that the first slip movement that took place for many of the large deep-seated rotational slides developed from outward bulging and deformation at the slope foot with retrogression taking place either where tensional stresses caused movement outwards and downwards from the original slope or where stream undercutting permitted further slip movement on the slide surface. Failure in the less competent shale strata depended upon the susceptibility of a particular bed to mechanical and chemical breakdown, but was also influenced by the thickness and weight of the load bearing down upon it. The presence of thick permeable sandstone

in the upper slope greatly increased the load that had to be supported. The well jointed overlying sandstones also enabled ground water to penetrate deep into the hillside. The alternating strata of sandstones and shales of the Middle Grits, possessing higher and lower mass strength characteristics respectively were particularly prone to failure because of deformation, chemical weathering and positive pore water pressure creating stress forces along the weaker beds.

1.7.3. The dip of the strata and the inclination of joints

Geological structure has been a key factor affecting slope stability. Both the Hercynian fold movements which took place after the deposition of the Carboniferous rocks and subsequent erosion have determined the general alignments of the plateaux, cuestas and edges and also the dip of the outcrops in the valleys of the Peak District.

The shear strength of a rock mass and its deformability are very much influenced by the nature and pattern of discontinuities within it (Terzaghi, 1962; Barton, 1973, 1976). As joints represent surfaces of weakness the larger and more closely spaced they are, the more influential they become in reducing the effective strength of the rock mass. The strength of bedded and jointed rocks is highly anisotropic therefore, unfavourable inclinations of either bedding planes or joints are a common cause of rock slope weakness Young, 1972; Barton & Choubey, 1977). In a rock slope in which structural surfaces dip outwards towards the free face at an angle less than the slope face, stability is much lower than for similar slopes with inward-dipping structures. Two examples of down-dip landslides are Cowms Rocks and Back Tor. At Cowms Rocks the Shale Grit which dips downslope at an

angle of 7° intersects the steep south facing slope of Ashop Valley.
At Back Tor the Mam Tor Beds which dip downslope at an angle of 4°
intersect with the very steep north facing slope at the eastern end of
Edale Valley.

The dip of the strata and cross joints together with the width and
spacing of the joints determines the rate at which water and
weathering processes can penetrate the joints. Joints can control the
morphology of both local and large-scale failures. Where suitably
inclined permeable beds permit water to enter discontinuities which
are closely spaced they allow deep and intense bedrock weathering to
occur, degrading the original bedrock strength, changing its
deformability properties and permeability characteristics, and
producing a complex of residual soil, weathered rock and unweathered
rock (Selby, 1980, 1982c; Moon & Selby, 1983; Moon, 1984). These
zones have a major influence on ground water flow and may cause
positive pore water pressures and even cleft water pressures to
develop, thus promoting instability. Once movement has taken place,
in any type of down dip or bedded failure, the residual strength will
be much lower than the initial resistance to shearing and subsequent
movements occur with less inducement. The recognition of an initial
small displacement is therefore critical in the assessment of bedrock
slope stability.

Movement down dip and along a potential slide plane is always likely
wherever a stream undercuts slopes in which the strata incline towards
the stream channel. Where strata dip into the hillslide,
undercutting, weathering or both may cause rock or soil falls and
slides if the stresses are increased sufficiently, but landsliding is

exceptional. Because of the effect of the overburden pressure exerted by the Millstone Grit the friction angle tends to decrease in the shales which have been undercut or weathered at the base, thus steepening the slope. The reduction of the angle of friction is probably because the increase in the normal stress with depth is associated with both an increase in the number of fractures across rock grains on opposite sides of a joint, and increased fracture intensities. Therefore, stable slope angles tend to decrease as the height of the slope in weathered and jointed rock increases. Where overburden pressures are lower weathering and pressure release by erosion results in the development of greater joint spaces within the outer parts of hillslopes compared with the interior part of the slope. Consequently the angle of internal friction as well as the normal stress, decreases towards the slope surface.

A characteristic feature of stratified sedimentary rocks such as the Mam Tor Beds and the alternating shales and sandstones of the Middle Grits is the presence of bedding planes, which provide surfaces of minimum resistance, separating rock layers of various thickness (Patton, 1966). Bedding planes may become preferred surfaces of shearing because internal erosion tends to occur along grit/shale or shale/mudstone junctions. Gravity induced bedding plane creep or sliding can produce residual stress condition and stress relief by erosion can also permit shear deformation.

1.7.4 The presence of sandstone aquifers at the footslope or midslope

Many of the landslips, irrespective of the scale of movement, can be shown to be related to the presence of naturally occurring reservoirs of ground water in the sandstones. The behaviour of reservoirs and their effect on slope instability have been described by (Denness, 1972a; Deere & Patton, 1967; Hodge & Freeze, 1977; Okimura, 1983; Harper, 1975). The Reservoir Principle (Denness, 1972a) was defined as the overall failure mechanism governing all types of landslip complex that degenerate more rapidly from their initial stages of failure in a relatively solid state to a more viscous or liquid state than would be the case if they were supplied only with run-off water. The necessary conditions are that a permeable stratum able to take in and discharge its water-store rapidly, overlies a relatively soft and impermeable stratum. Mass movements associated with the 'Reservoir Principle' are commonly of the mudsline/mudflow or degraded rotational, semi-rotational and slab slide types betraying the continuous softening influence of excess ground water.

The primary porosity and permeability of the well-cemented sandstones are very low. Their importance as aquifers, therefore, stems from the fact that they are well jointed giving the rock a secondary permeability, enabling it to both store and transmit water in well-developed planes. The argillaceous strata between the sandstone units are poor aquifers generally comprising shales and mudstones of low primary porosity and permeability. These strata are not well jointed and where secondary discontinuities have been developed they are often infilled by a self-derived clay.

Rain falling on outcrops of the sandstones therefore percolates downwards through the joints and fissures and along bedding planes until it reaches a layer of virtually impermeable mudstone or shale, above which it flows laterally to emerge on the valley slope as seepage and springs. Confined sandstone aquifers generally produce less water, but artesian conditions have been recorded at the outcrop of similar strata in the Pennant Sandstone of South Wales, particularly where they dip out of the hillslope, Daughton et al. (1977).

Springs and seepages may be regarded as 'safety valves' for the release of ground water pressure (Sowers & Royster, 1978). As long as springs can flow freely, an excessive build-up of ground water pressure in the aquifer that supports the spring is unlikely. Water concentrated or blocked at the interface of the sandstone aquifer and the underlying shales may provide a piezometric head capable of initiating slippage, particularly when bedding dips are downslope and major joint or fissure trends run sub-parallel to the slope crest. In any slope forming material there is a critical pore water pressure which, if exceeded may result in instability (Deere & Patton, 1967; Harper, 1975; Hodge & Freeze, 1977; Okimura, 1983). Confined aquifers were capable of generating high piezometric levels within the local geological succession and in certain circumstances strong hydrostatic (artesian) pressures in the sandstones may have raised the pore water pressure considerably. Such forces may have been directed upwards from a lower permeable sandstone member into overlying impermeable shale strata so helping to create conditions leading to slope failure.

Water naturally tends to accumulate in open joints and affects the stability of the mass directly in two ways. Firstly, water pressure

will reduce the effective stress along the sliding surface and thus reduce the friction between the sliding body and the base. Secondly, water in joints may exert an outward pressure on the sliding body, encouraging overturning. This direct action of water pressure is supplemented by the creation of rock fatigue through periodic variation in the water pressure in the joints. The fact that the rock mass does not behave completely elastically means that continual change in the water pressure in the joints is likely to lead to extension of the joint; this will be augmented by the wedging of crushed rock in the gaps, thus preventing the joints from returning to their original position after opening slightly under high water pressure.

During cold phases which prevailed during periglacial times (i.e. the Lower and Upper Dryas) exposed rock faces which became frozen inhibited the free egress of water through open joints to the slope surface causing the water table to rise within the rock masses forming the slopes. In the succeeding Spring and early Summer surface joints thawed out causing high seepage pressures acting towards the cliff face and thus reducing the strength within the joints (Bjerrum & Jørstad, 1968).

1.7.5 Valley Bulging and Cambering

Edale Valley contains numerous exposures of structures indicative of valley bulging and cambering. Around the margins of the valley floor the highest Edale shales and the lowest Mam Tor Beds exhibit sharp, almost symmetrical folds with straight limbs. At exposures nearer the middle of the valley floor the Lower Edale Shales devoid of thin sandstone bands, are irregularly crumpled, dislocations are at higher

angles and the overall intensity of deformation increases. Sharp, symmetrical, straight limbed folds are also present in the lower Mam Tor Beds and Upper Edale Shales in the lower Alport valley and adjacent parts of Ashop valley. Similar structures also occur in the Mam Tor Beds in the Derwent valley and its tributary valleys, particularly well developed cambering structures were exposed when the level of Ladybower Reservoir fell in 1976. Folding structures to a depth of almost 60m have been observed at the site of Ladybower dam (Hill, 1949).

Valley bulge structures are believed to have resulted from the pressure exerted on predominently argillaceous strata by superimposing beds that induced lateral pressure thus initiating movement or 'squeezing out' argillaceous strata into adjacent load-free valley areas, so producing convex bending compression folds and thrusts. Conditions favourable to such movements would occur wherever valley deepening exposed the surface of any substantial thickness of shale. Thermokarstic processes including the thawing of ground-ice leading to rapid erosion and downcutting in colder phases of the Late Devensian glacial would have facilitated these processes. Both cambering and valley bulging structures contribute to hillslope instability by attenuating the weaker shale strata at the base of a hillslope and by fracturing the more resistant beds in the hillslope wherever tensional stresses were increased (Hollingworth et al., 1944; Stevenson & Gaunt, 1971; Higginbottom & Fookes, 1971; Vaughan, 1976; Johnson, 1980).

Pleistocene valley overdeepening coupled with cambering and valley

bulging caused the rocks to move outwards from the hillside, thereby increasing the stresses on the rocks cropping out higher up the slopes. Widening of near surface bedding planes, joints and tension fissures, amounting in some instances almost to fragmentation was common in the valley side sandstone outcrops to depths of 1.5m. The fissures tend to run parallel to the valley and may be up to 250mm wide close to the valley side, but they became progressively narrower and finally disappear when traced back into the hillside (Johnson, 1980). Cambering and Valley Bulge processes may have played an important role in the development of these fissures, although subsequent cryostatic pressure initiated through freeze thaw processes along with other cryoturbation processes active during periglacial times would also have enlarged these joints and fissures. Examples of cryoturbation structures can be seen at a number of landslide scars where the upper beds have been folded and crumpled to a depth of 1.8m (Stevenson & Gaunt, 1971). Johnson & Walthall (1979) noted that ten landslides in the Longdendale valley just north west of the study region occurred at sites where cambering and valley floor bulging were present. At these ten sites other factors which may have caused a steepening of the hillslope and inducing failure (e.g. the direct undercutting or channel overdeepening by streams) were absent suggesting that cambering and valley floor bulging may have been an important prerequisite for instability at these sites.

1.7.6 <u>Ground water, saturated surface water flow and</u>
       <u>stream discharge</u>

Surface water, whether from springs, seepage or saturated surface runoff, is an important factor with regard to slope instability in that it contributes to fluctuations of the water table and to

increased pore water pressures that can result in reduced soil strength and to eventual soil movement. The high drainage densities which occur on the impervious shale strata or slowly permeable head, along with high rainfall and active stream incision assist present day mass movement processes.

Landslides can arise directly from stream incision, particularly when predominant forces are directed laterally rather than vertically downwards. The movement of surface and ground water in a valley slope is directed towards particular zones of water concentration determined by the morphological configuration of the hillside and the spacing and openness of joints. In seepage zones i.e. spring lines, saturated areas at the base of the slope or perched water tables on mid slope concavities, active processes of erosion and weathering take place. Springs and seepages on valley side slopes provide an indication of which aquifers contain water and could be involved in the build-up of pore water pressure.

Ground water, whilst maintaining a phreatic surface, is strongly concentrated within zones where the tensile strains have created an inter-connected system of voids, these may channel water preferentially to restricted points along a potential spring line. Internal forces holding rock masses intact may be substantially reduced by the addition of water to rocks which are not chemically altered in this process such as shales, mudstones and weakly cemented sandstones. The addition of water reduces the attractive forces holding rock together and increases the internal repulsive forces. The process involves cation exchange, hydration, the production of negative electrical force fields, the attraction of mineral surfaces for water and capillary tensions.

The swelling of rock and the opening of joints by weathering processes particularly when shale sediments become hydrated tends to occur in seepage hollows. Therefore, failure zones tend to occur close to the base of the slope and in weakened shale strata lying on sandstones that are much more resistant to solution and chemical change.

Many springs are responsible for raising pore water pressures causing shallow translational slides and mudslides/mudflows in superficial deposits. Water emerging above a slide or potential slide area may infiltrate and move downhill as saturated throughflow into the slide zone or superficial deposits below reactivating movement. Water spilling over a shale aquiclude onto the hillside has several effects which may directly affect hillslope stability: (a) by giving rise to saturation, (b) seepage forces, (c) downcutting and headward erosion, and (d) by accelerating degenerative weathering processes generally leading to a reduction in soil shear strength.

Mudsliding/mudflows have contributed substantially to the morphology of most of the landslides in the study region. Mudslides take place on discrete slip surfaces developed in the basal layers of rotated/slumped blocks which consist mostly of shales and mudstones. In such layers the slump debris is frequently strongly weathered, water saturated and subject to fluctuating perched water table levels. Under these conditions the shales and mudstones become 'sensitive' and can change from a weak solid to a viscous fluid capable of transporting sediment from the slump blocks onto valley slopes at the foot of the slide. Mudsliding/mudflows therefore, represented an important process of secondary mass movement, at times subsequent to the main translational or rotational slope failure.

Mudslides/mudflows have undoubtedly played a major role in transporting material from upper slump areas of the landslide, sometimes promoting instability in slump blocks by the removal of fines. Mudslides may have also undermined slump ridges causing them to fracture into large blocks which then moved independently downslope. Mudslides/mudflows may have also caused overburden pressure and blocked surface drainage thereby increasing pore water pressures. The efficacy of these mudslide mechanisms has been well documented by Brunsden, 1974; Brunsden & Jones, 1972, 1976.

Saturated seepage water from hillsides (e.g. along percolines) can lead to seepage erosion in fine sandy regolith firstly by a drag effect which transports individual soil particles, or secondly by seepage pressure which can move individual particles outwards from the slope. Eventually undermining can result and slope instability results (Terzaghi, 1950; Hutchinson, 1968a, 1970, 1971a). Seepage sites may be identified through the recognition of associated features such as belts of damp ground possessing characteristic marsh vegetation i.e. Juncus, Sphagnum), incipient gullies or rills, headward erosion, and spring-sapped hollows.

The water pressures within a soil or rock stratum, as reflected by the piezometric level, is a major factor influencing shear strength. A multiplicity of piezometric levels may be present in the hillslopes of the study region. Perched water tables are common (a perched water table being one that is sustained above an underlying independent body of water by an aquiclude). For example, where superficial deposits or shallow slide debris have a higher permeability than the underlying material, e.g. mudstones, there will be a tendency for a perched water table to be formed in the slip

debris. Normal aquifers may sometimes be converted to perched aquifers by the rotational movement associated with some types of landslides. The water table can change according to rainfall input, the influx of ground water from outside the area and landslip movement. The changing nature of perched water tables is one of the most important factors contributing to shallow planar translational slides.

Water, from saturated surface runoff, infiltration, or ground water originating elsewhere is a major factor involved in hillslope instability in the Peak District. The evaluation of ground water aquifers and changes in piezometric levels therefore plays a vital part in any detailed slope stability site investigation.

1.7.7. The weathering of shales and mudstones

The engineering properties of shales and mudstones are a product of a number of genetic factors, including mineralogical composition, degree of over-consolidation and diogenic changes (Mead, 1936; Casagrande, 1949; Badger et al., 1956). Consolidation with concomitant recrystallisation on the one hand and the parallel orientation of platy materials, notably micas, on the other, give rise to the fissility of shales. Moderate weathering can increase the fissility of shale by partially removing the cementing agents along the laminations or by expansion due to the hydration of clay particles (Taylor & Spears, 1970). The higher the degree of fissility possessed by a shale the greater the anistrophy with regard to strength, deformation and permeability (Chappel, 1974).

Casagrande (1949) noted that highly fissured over-consolidated shales have greater swelling tendencies than poorly fissured clay shales, the fissures providing access for water. The porosity of shale may range from slightly under 5% to just over 55% with natural moisture contents of 3% to 35%. The strength of compacted shales decreases exponentially with increasing void ratio and moisture content, whereas,in cemented shales the amount and strength of the cementing material are the important factors influencing its intact strength.

A feature of the breakdown of shales and musdstones is their disintegration to produce silty clays, Grice (1969). The disintegration of shales was studied by Badger et al., (1956), who concluded that their breakdown was due to the dispersion of colloidal material, which appeared to be a general cause of disintegration, and, to a lesser extent, due to air breakage, which only occur in mechanically weak shales. Disintegration was found to be controlled by the type of exchangeable cations associated with clay particles, and by the accessibility of the latter to hydration which in turn, depended upon the porosity of the shale. Air breakage could assist the process by presenting new surfaces of shale to water. The fracture pattern within mudstones and the lamination of shale therefore controls their disintegration.

Many shales slake almost immediately when exposed to air,depending on the relative humidity (Kennard et al., 1967). Dessication of shale, following exposure, leads to the creation of negative pore pressures and consequent tensile failure of the weak intercrystalline bonds. This in turn leads to the production of shale particles 0.6mm to 2.00mm in size. Alternate wetting and drying causes rapid breakdown of compaction shales. Low grade compaction shales undergo complete

disintegration after several cycles of drying and wetting, whilst well cemented shales tend to be resistant. Morgernstern & Eigenbrön (1974) used a water adsorption test (Slake Durability Test) to assess the amount of slaking undergone by shales and mudstones. This test measured the increase in water content of a sample in relation to the number of drying and wetting cycles it had undergone. They found that the maximum slaking water content increased linearly with increasing liquid limit and that during slaking all materials eventually reached a final water content equal to their liquid limit. Materials with medium to high liquid limits, in particular, exhibited very substantiated volume changes during each wetting stage, which caused large differential strains, resulting in complete destruction of the original structure. Thus shales with high liquid limits are more severely weakened during slaking than materials with low liquid limits. Franklin & Chandra (1972), found a general correlation between the Slake Durability Index, the rate of weathering and the stable slope angle. Mudstones tend to break down along irregular fracture planes, which when well developed, can result in their disintegration within one or two cycles of wetting and drying.

Removal of overburden through processes of erosion may have a significant influence on the engineering behaviour of shales and mudstones. Uplift frequently occurs where surface layers have been eroded, this is attributable to swelling and heave due to the release of stored strain energy. Swelling is attributable to the absorption of free water by certain clay minerals, notably montmorillonite, within the clay fraction of a shale. Sulphur compounds are frequently present in shales and mudstones. An expansion in volume can occur when sulphide minerals such as pyrite undergo oxidation to give anhydrous and hydrous sulphates (Fasiska et al., 1974). This

process is usually accompanied by vertical expansion of the formation which involves the development of joints and fissures together with softening. These changes are accompanied by a reduction in strength and an increase in deformability, water content and plasticity. When a load is applied to an essentially saturated shale the void ratio in shale decreases and the pore-water attempts to migrate to regions of lesser load. Because of the relative impermeability, water becomes trapped in the voids in the shale and can only migrate slowly. As the load is increased (e.g. removal of lateral support by undercutting or weathering) there comes a point when it is in part transferred to the pore water, resulting in a build-up of excess pore pressure. Depending on the permeability of the shale and the rate of loading, the pore-water pressure may increase to a point when it equals the pressure imposed by the load. This greatly reduces the shear strength of the shale and failure can eventually occur, especially in the weaker compaction shales.

Johnson & Walthall (1979) examined sections within shales and mudstone outcrops at the base of the Kinderscout Grit along the south side of Longdendale. They found that the uppermost shales in the Grindslow sequence have been weathered to a depth of 1m; in the upper 20cm the shales have weathered to a brown silt-clay, below this the weathered material consisted of brown, iron-stained, shaly-clay which had not quite lost its structure. They noted similar weathered horizons within a series of well jointed mudstones. The mudstones showed some indication of deformation, the bedding planes within the weathered horizon had in some cases been rotated throughout their exposure; open joints, which permit water movement, were also evident in the upper part of the exposure. These weathered rock horizons have been observed in other sections of shales and mudstones in the

study area and in some localities actual shear planes could be identified. The continued weathering of shale and mudstone has resulted in recent failures, at Torside Clough in Longdendale where deeply weathered and disturbed mudstones at the base of the fossil slide have slipped down onto valley gravels of recent age.

1.7.8. Weathering studies at Mam Tor

Instability of the slipped mass of Mam Tor landslide appears to be periodic, with relatively frequent small movements taking place on secondary slump blocks, especially during wet periods, separated by major failure events on a time-scale of several years. It may be assumed that the factor of safety against failure is permanently close to unity, so that a small reduction could initiate movement. Small failures could be triggered by increases in ground water level, but a less frequently occurring condition is required to explain the relatively occasional major movements.

It is generally accepted that chemical weathering processes can significantly modify the engineering properties of many natural materials. These processes tend to be thought of as progressive and unidirectional but in certain cases this view has been abandoned as a result of detailed analyses, in which several separate 'components' of the weathering processes have been distinguished. It should be possible to identify which specific reactions are the major control for bulk property modification and, particularly, the timescale upon which they are likely to be effective.

The Mam Tor landslide has cut through pyritic Edale Shale, the toe region of the slide is characterised by the emergence of acid-sulphate 'ochre' ground water attesting to pyrite oxidation within

the landslide. This reaction is known to cause physical disruption of pyritic shales by modifying both its mineralogical, and pore water composition. With fresh sulphuric acid these reactions can occur rapidly, certainly on timescales of days or weeks (Dougherty & Barsotti, 1972; Quigley & Vogan, 1970).

The sediments affected at Mam Tor are the Edale Shales, a dark grey, thinly bedded mudstone of Namurian age (Walker, 1967; Allen, 1960). A borehole drilled in the main unit of the Mam Tor landslide showed that the top 5m consisted of highly weathered Mam Tor Beds. These thinly bedded sandstones (distal turbidities) pass downwards into black pyritic shales which contained concretions and discontinuous bands of carbonate (Calcic Dolomite), Spears & Amin (1981). Edale Shales comprise abundant quartz with some feldspar, clay minerals and diagenetic pyrite (mixed layer clays – expandable component 50%; mixed layer clays – illite 21%, kaolinite 23%; chlorite 6%). Edale Shale appeared at 19m in a highly weathered state, becoming less disintegrated and iron-stained with depth. At approximately 26m there was a change to fresh Edale Shale with unweathered pyrite. This was accompanied by a change in dip of the bedding from 5° commensurate with the regional dip of Edale Shale, to steeper angles of $30^{\circ}-45^{\circ}$ indicative of back tilting. If, as seems likely, these changes occur at the slip zone, evidently oxygenated seepage water can penetrate deeply within the landslide and attack fresh rock. Continual decomposition of fresh shale along the slip zone may reduce the factor of safety of the landslide over a number of years to a critical failure condition.

Research by Vear & Curtis (1981) on the chemical composition, conductivity and temperature of seepage water in and around the site

of the landslip suggested that the weathering reactions occurred at depth within the slide. They sampled water emanating from springs in the landslide and surrounding area and found the hydrology of the slide area could be distinguished from that of its surroundings by the additional input of acid sulphate waters, presumably generated within the crush zone. In the case of most shales, unweathered material consists of a mineral assemblage which approached chemical equilibrium at considerable burial depths in contact with aqueous solutions of high ionic strength and under conditions of decreasing oxygen partial pressure. On exposure to the weathering zone chemical reactions take place in the presence of seepage waters of low ionic strength saturated with molecular oxygen. In fine grained sediments Fe, S, Mn and organic matter are reactive. Pyrite is particularly reactive, because both Fe and S are involved and because of its small grain size, Garrels & Thomson (1960). Vear & Curtis (1981) suggested that in surface and near surface shales this chemical weathering process is complemented by ferrous to ferric oxidation mediated by chemo-autotrophic bacteria (Thiabacillus ferrooxidans); however, no attempt has been made to enumerate this species at Mam Tor (Van Breeman, 1972). Clay minerals react on two timescales; interlayer cation exchange takes place rapidly, while a much slower process, brings clays into equilibrium with relatively low ionic strength solutions. The soluble products of rapidly occurring reactions will alter water composition (i.e. the addition of sulphuric acid) and as a result subsequent reactions with shale will be influenced. The ground water may become supersaturated with new minerals, which may be precipitated. More than 99% of sulphuric acid generated at depth is consumed by silicate and carbonate (clay mineral) reactions before reaching the surface as seepage.

The shales are subjected to significant volume changes during pyrite oxidation, carbonate dissolution and expansion of discontinuities due to the precipitation of geothite, limonite, jarosite and gypsum, all these processes facilitate breakdown of Edale Shale. Increases in porosity occur as a result of the destruction of pyrite and dolomite and reduction in aggregate size. Vears & Curtis (1981) showed that for each litre of water emanating from the most concentrated spring could be responsible for creating about 0.7ml of void space as a result of carbonate and sulphide dissolution. Since seepage water flow is concentrated along fracture surfaces deep within the landslide, the sulphide, carbonate and silicate decomposition reactions which create void space are also concentrated along these surfaces.

Steward & Cripps (1983) related changes caused by chemical weathering to modifications of the engineering properties of Edale Shale. They quantified the chemical weathering changes taking place in shale in terms of the residual shear strength of shale. A Bromhead Ring shear apparatus was modified so that the composition of pore solutions could be altered during shearing. The tests indicated that the residual shear strength of the shale is sensitive to modification of pore solution composition. The residual shear strength of shale appears to be modified during weathering because it is sensitive to pore water chemistry and mineralogical composition, both of which are altered by weathering reactions.

In conclusion the chemical weathering reactions which take place in the slip zones of Mam Tor enable oxygenated seepage waters to penetrate deep within the landslide and attack fresh rock. Continual decomposition of fresh shale along the slip zone may reduce the

factor of safety of the landslide over a number of years to a critical threshold condition. Other destabilising influences may then trigger movement, these may include loading of the main unit by material falling from the back scarp, removal of support to the rotational main unit after movements of the translational toe but probably most important of all a 'timely' rise in ground water level brought about by a period of heavy and intense rainfall.

1.7.9 Fluctuating Rates of Geomorphological Processes

1. Temporal Variation

At any one time most hillslopes will be in a stable state (factor of safety >1); a number of workers have envisaged failure conditions as occupying one tail of a probability distribution 'safety factor curve' (Brunsden, 1979; Bazynski, 1977). The overall shape of the curve varies according to a specific set of topographical, geological and geomorphological processes operating in a particular environment over a specified time period (Brunsden & Thornes, 1979. As the variables controlling the distributions of force and resistance change over time, a series of corresponding oscillations occur on the safety factor curve. The causes of variation in the safety factor can therefore be regarded as the fundamental causes of mass movement.

2. Fluctuating Processes

Many of the large landslides in the study region are fossil failures with only relatively shallow superficial movements occurring on them at the present time. Most of the slides are now in a quasi-equilibrium condition and there is little evidence for any

significant increase in shear stress within the slope forming materials that have not undergone mass movement. Peat development in many of the landslide slump depressions has been continuous indicating little or no movement since they were formed.

As discussed, slope failure has occurred where rocks forming a part of the hillside have been progressively reduced in strength to critical threshold levels of safety. The mechanism of lateral expansion, fissuring and progressive strain softening of clay shales and mudstone may lead to delayed failures that occur many years after stream undercutting (Skempton, 1970). The progressive failure of jointed rock has been discussed by Terzaghi (1950, 1962). This reduction in rock strength has taken place only after prolonged periods of denudation during which time the slopes endured a continued history of Pleistocene and Flandrian climatic fluctuations. Such changes caused marked variations in the ground water levels and controlled the rates at which weathering processes affected the hillslope. During certain times in the Pleistocene, conditions were often more extreme than those which eventually triggered the slide movements and former frost climates in particular were especially important in creating substantial talus and colluvial debris on valley slopes (Johnson, 1969a; Johnson & Walthall, 1979). By the end of the Late Devensian a precarious equilibrium became established on most Pennine slopes between the rates of debris supply and transportation and in consequence according to some authors long rectilinear slope profiles were established at this time (Summerfield, 1976; Rouse & Farhan, 1976). On many slopes however this equilibrium has been disturbed by increased rates of both runoff and mass movement, and such slopes are either convex-concave in profile or have been modified by considerable displacements of

material downslope in rock fall or large rotational/translational
slide movements.

1.7.10 Conditions favouring slope failure at the end of the Devensian glacial

Periglacial conditions prevailed for a period of 60,000 years in the
southern Pennines. Freeze thaw and dessication processes must have
been damaging to rock faces, particularly where joints and fissures
were opened in the sandstone. During cold phases permafrost would
have prevented sub-surface waterflow in regolith, the permafrost
table would have caused the maintenance of saturated soils on the
hillslopes. Under such conditions Terzaghi (1962) demonstrated the
importance of cleft pore water pressures in rock masses, and
demonstrated how the process may facilitate rockfalls and sliding
movements within jointed rock. The maintenance of a high water table
and a strong pore water pressure gradient in the hillslopes during
the Devensian glacial period inevitably must have caused a weakening
of rock strength, but the most extensive landslides appear to have
occurred after the return of the more temperate Boreal climatic
regimes. A number of workers have suggested that there was a time
lag in the fall of ground water level at the end of the Devensian
glacial firstly because the lower slopes would have been heavily
mantled with regolith and sometimes partly frozen preventing the free
egress of water from the slopes and secondly, that the rate of shear
stress would have progressively increased as the permafrost thawed
and the ground water was able to circulate more freely.

In the tributary valleys undercutting by melt-water streams would
have facilitated sliding or slip movements but once these slopes

became eroded by gullies the water table would have been lowered and effective shear stresses reduced. In such conditions shallow planar translational slides in regolith would commonly have taken place. Where increased ground water storage and pore water pressures became concentrated within particular zones on the hillslope the mass strength of the shale and mudstones would have deteriorated through the action of deep-seated creep and weathering processes to their threshold residual shear strengths and deeper slides would have resulted.

1.7.11 Climatic change and landsliding

The immediate cause of all landsliding appears, in all cases, to have involved slope failure resulting from a progressive weakening of the rocks at the base of the former hillslope. This can be seen as a natural process of hillslope evolution controlled by local geological conditions. There is a possibility, however, that environmental changes might also have been involved in actually triggering slide movements. For example, climatic change towards increased wetness, could perhaps be invoked as a trigger mechanism.

Until recently, little firm evidence was available to indicate the age of the landslides, though on the basis of their apparently degraded and subdued morphology many were thought to be relatively old. This interpretation appeared to be supported by results of pollen analysis from the Coombes Rocks landslide at Charlesworth which suggested initiation of activity in zone VI of the Flandrian (Late Boreal),(Franks & Johnson, 1964). Over the last few years, however, new research into the landslides of the study region and nearby areas has yielded a number of dates ranging from Late Devensian to Medieval (Redda, 1986) (Table 1.7).

Landslide & Location	Reference & Position of Sample	Pollen Zone	Date
Alport Castles, Alport Dale	Tallis (1983) Landslide toe	IV Pre-Boreal	8300-7600 BP
Buckstones Moss, Moss Moor	Muller (1979) Centre of landslide	VI-VIIa Boreal-Atlantic	7480 BP
Coombes Rocks, 1 & 2 Charlesworth	Franks & Johnson (1963) Slip depression within slumped ridge	VI-VIIa Boreal-Atlantic	7190 BP
Bradwell Sitch, A & B Longdendale	Tallis & Johnson (1980) Oldest part of the landslide middle of main slump unit. (altitude 295m)	VI-VIIa Boreal-Atlantic	7100 BP
Rakes Rocks Crowden Valley	Tallis & Johnson (1980) (altitude 330m)	VI-VIIa Boreal-Atlantic	7000 BP
Didsbury Intake, A Longdendale	Tallis & Johnson (1980) (altitude 235m)	VI-VIIa Boreal-Atlantic	7000 BP
Bradwell Sitch, C Longdendale	Tallis & Johnson (1980) (altitude 295m)	VIIa Atlantic	6500-7000 BP
Millstone Rocks Longdendale	Tallis & Johnson (1980)	VIIa Atlantic	6500 BP
Laddow Rocks Longdendale	Tallis & Johnson (1980) (altitude 405m)	VIIa-VIIb Atlantic-sub Boreal	4000-5000 BP
Long Gutter Edge Longdendale	Tallis & Johnson (1980) (altitude 400m)	VIIb Sub-Boreal	2200-4000 BP
Tintwistle Knarr Longdendale	Tallis & Johnson (1980) (altitude 330m)	VIIb Sub-Boreal	2200-4000 BP
Didsbury Intake B Longdendale	Tallis & Johnson (1980) (altitude 225m)	VIIb Sub-Boreal	2200-4000 BP
Upper Bradwell Sitch Longdendale	Tallis & Johnson (1980) (altitude 400m)	VIIb Sub-Boreal	2000-4000 BP
Edale End, Edale	Redda (1985)	VIIb Sub-Boreal	2560-2800 BP
Bradwell Sitch, D Longdendale	Johnson & Walthall (1979)	VIII Sub-Atlantic	1970 ± 100 yrs BP

Table 1.7. The age of landslides in the study region, from pollen
evidence of peat deposits found in landslide slump
depressions

At the termination of the Boreal period, and throughout the Atlantic
Period, climate became markedly maritime. Various workers have noted
the marked climatic shift at this time and was probably caused by the
continuing eustatic rise in ocean levels and the creation of both the
North Sea and Baltic Sea (Willet, 1950; Godwin et al., 1958; Zeuner,
1958; Manley, 1959; Lamb, 1966; West, 1977). This more oceanic
climate coupled with suggested more southerly tracking depressions,
would have brought increased precipitation and consequently must have
raised ground water tables. Investigations by Conway (1954) have
shown how, in the Pennines, this increase in both rainfall and ground
water during the Atlantic (Pollen Zone VIIa) allowed the expansion of
blanket peats at the expense of established wet alder and birch
woods. Müller (1979) has suggested that this increase in water may
have acted as a major participating factor in slope failure.

The basal dates for the biogenic slide deposits sampled do not all
support the hypothesis of climatic change to wetter conditions as a
landslide trigger mechanism. In some studies the earliest peats in
landslide depressions apparently started to accumulate under the
relatively dry Boreal (Zone VI) climate, whilst the peat infills in
the younger slides clearly are not related in their inception to
times of climatic wetness. A number of researchers have suggested
that landsliding might be more liable to occur under conditions of
reduced tree cover, none of the landslides in Longdendale have been
dated unequivocally to the Atlantic period (c. 5000-7000 Y.B.P.),
generally assumed to have been the period of maximum forest cover.

The basal peat deposits of the Longdendale landslides pre-dating
7000 Y.B.P. mark a time when expansion of forest was still occurring
and when the upper altitudinal limit of tree growth was well short of

its maximum; the possibility of anthropogenic disturbance by fire at the upper forest margins at this time, however, cannot be discounted (Jacobi et al., 1976). Most of the other landslide peat deposits post-date 4000 Y B.P. in their inception, and originated during a period of steadily increasing prehistoric forest clearance (Hicks, 1971; Tallis & Johnson, 1980; Said, 1969). The correlation may, however, be coincidental, and further evidence is required before any further conclusions can be drawn.

It is evident from studies undertaken in the Pennines (e.g. Franks & Johnson, 1964) and elsewhere (e.g. Gil et al., 1974; Hutchinson & Gostelow, 1976) that landsliding has occurred at times when geomorphological processes were less intensive than they had been during periods in the Pleistocene. The slopes clearly endured for long periods climatic vissitudes similar to and more severe than those of today and only failed when particular geological units became weakened to a point of critical 'threshold' stage. When this point was reached, the slope failed, regardless of climatic conditions, steepness of slope or any other factor.

The actual site of a landslide is therefore determined mostly by local conditions particularly, where structure and lithology especially favour the concentration of ground water into an area of steep surface slope. The condition of actual slope failure is only reached after a long period of time during which the cohesion of the rock material is slowly reduced. Thus, whilst it is probably true that most landslides in the study region occurred during climatic periods when the rate of weakening was accelerated, it would be wrong to conclude that all Pennine landslides took place during those periods. Table 1.6 shows that a number of landslides occurred at

times when the optimum climatic conditions discussed no longer prevailed. The apparent lack of evidence collected so far can only provide a somewhat speculative interpretation of the age of the landslides. Clearly more research is needed to investigate dateable deposits above and below landslide debris and also within river terrace gravels and solifluction deposits associated with the landslide debris, in order to reconstruct more exactly the time of inception of landslide events.

1.7.12 Superficial Material

The distribution of superficial deposits in the study region is largely a result of periglacial processes and their composition largely reflects the underlying bedrock. The principle process under periglacial conditions was frost shattering through joints and bedding planes of bare rock outcrops assisted by the permeability of the sandstones, producing angular and sub-angular rock fragments which mantled the slopes and the summits. These deposits are known as Head or 'scree associated deposits' and contain a sandy poorly sorted matrix and angular scree debris, the latter being replaced by stone flags at depth.

Head deposits cover most of the valley slopes in the study region, forming a variable thickness of rock debris derived from the alternating sandstone and shale sequences by the action of periglacial freeze thaw processes. They comprise such features as solifluction flows, screes, downwash and hill-creep which generally pass imperceptibly into one another, and in many cases into valley side accumulation of landslide deposits. Solifluction is the slow downslope movement, under the influence of gravity of water saturated

debris in the seasonally active layer above the permafrost table. Solifluction takes place when the downward percolation of water through the soil is impeded and where melting of segregated ice lenses provides excess water which reduces internal friction and cohesion in the soil. The Head deposits are heterogeneous, containing variable-sized rock fragments and numerous slip surfaces. Head deposits have variable permeabilities, although where the material has been derived from shale and mudstone strata the clay content of the Head can be high. Where a high clay content occurs the infiltration capacity of the Head will be lowered and surface runoff may result. When the base of a jointed sandstone aquifer is masked by a sufficient thickness of Head the release of water from the fissures may be impeded; under such conditions water builds up within the sandstone until it overspills the upper limit of the Head. This situation can produce artesian conditions in the aquifer at outcrop, leading to an increase in pore water pressures and consequently to instability of the overlying superficial deposits.

In frictionless, uncemented and weathered slope regolith usually derived from Head, the most common mode of failure is rapid translational sliding on a relatively shallow plane parallel to the ground surface. Shallow planar translational slides confined to soils are extremely common mass movement features, and occur throughout the study region. They are always shallow features and have essentially straight slide planes with some curvature towards the crown, and hence some rotational movement can occur. Some of the more complex forms disintegrate after their initial failure to form tongues of debris related to secondary mechanisms of mudsliding. The distinctions between debris slides, debris avalanches, and debris flows is based upon the degree of deformation of the soil material

and the water content of the sliding mass. As both deformation and water content frequently increase downslope what may be described as a debris slide at the crown of the landslide, with relatively large undeformed blocks of soil sliding down-hill, may become an avalanche of small blocks and wet debris in midslope to a thoroughly saturated mudslide/ mudflow at the base of the slope.

Unlike falls, slumps, and glides which may occur as a result of deep percolation of water, and hence at a considerable time after a heavy period of rain, translational slides nearly always occur during heavy (intense) rain. Rainfall with sufficient intensity and duration is required to raise the water table to near the soil surface or fill pre-existing tension cracks. In low intensity rainfalls the removal of water from the soil by throughflow can keep pace with infiltration, and in short-duration falls the field capacity of the soil may not be exceeded. Only when the field capacity of the soil is exceeded for long enough for water pressures to rise substantially can the soil lose sufficient strength to fail.

Conditions for failure are at an optimum when the soil is in a weathered or residual strength state, where the water table is at the surface and where water flow is parallel to the slope. Failure surfaces are concentrated at the soil/bedrock interface particularly soils which overlie argillaceous mudstones and shales.

There is a strong correlation between shallow planar slips and rainfall (Cambell, 1975; Nilsen et al., 1976a; Vargas, 1971; Canuti, 1985; Selby, 1976; Rogers & Selby, 1980). Many researchers have reported that these types of failure are associated with 'blow outs' of water under pressure and with secondary disintegration of the

failed mass into a debris flow (Kesseli, 1943). Many of these slips
are also located at gully heads. These observations confirm that the
initial failures occurred wherever suitable positive pore water
conditions developed in the soil mantle.

Shallow planar translational sliding remains an important process in
slope evolution where cohesionless regoliths occur on steep slopes.
Sliding occurs when weathering has proceeded far enough to reduce
soil strength towards a failure condition and where there is
sufficient thickness and water pressure. Generally short periods of
sliding are separated by long periods of weathering since the slide
movement usually removes all debris down to bedrock level. Erosion
rates are therefore limited by the rate of weathering and by the
frequency of occurrence of suitable pore pressure levels in the
regolith mantle. The spatial pattern of shallow slides seems to vary
randomly across a smooth rectilinear slope, although where valley
heads, gullies, percolines or other conditions cause water to
concentrate on steeper slopes, there may be preferred areas of
sliding.

1.7.13 Conclusions: The mechanisms causing slope failure and the
        location of the slip surface

The most important factors in Table 1.6 are those which have caused
variation in slope loading or have reduced rock strength directly.
Most of the larger slides in the study region tend to be deep-seated
with a strong translational displacement, with some backward rotation
at the head. The position of the slip surface is presumed to have
been strongly influenced by local variations in such characteristics

as the thickness, composition, permeability and inclination of the strata together with the texture of jointing or faulting within the beds. Because of the variable nature of the strata the failure surfaces are almost certainly irregular and can have only approximate regular geometric forms.

It would appear, however, that the failure path for the most part was in mudstone or shale strata. This is in the zone of contact between impermeable and permeable rocks and where the ground water flow is strongly anisotropic being determined by the dip of the beds. In such zones high pore water pressures can be generated with strong pressure gradients within the slopes. Equally important chemical and mechanical weathering in such zones reduces the rocks to very low strength levels. Denness (1972a) working on similar strata has observed that shales can be reduced to a 'clay-like' consistency by ground water erosion and weathering with only 5% of their original strength retained. Shales have been observed in stream sections weathered, buckled and attenuated and such deformations have undoubtedly contributed to the slumping and sliding of hillslope materials.

It is also probable that strong artesian and piezometric pressure gradients were formed in the past and contributed to the reduction of effective shear stress and the lowering with time of the effective angles of shear resistance of materials located on the potential slip surfaces. On stable slopes weathered sandstones and shale provides internal shearing resistance angles of c. $30^{\circ}-35^{\circ}$ and $27^{\circ}-45^{\circ}$ degrees respectively, but with a high clay content the residual angle can be lowered to $18^{\circ}-24^{\circ}$ degrees (Skempton, 1964). Frequent small shallow planar translational slides, cracks, and arcuate back

scars in Head material provide indications that many of the slopes with such superficial deposits are close to limiting equilibrium for shallow mass movement. The reason why many of the slopes which may be interpreted as relic features of periglacial mass movement are currently stable is due in part, to low piezometric levels, although in the vicinity of some spring lines a rise in ground water level has resulted in renewed instability particularly after heavy rain.

Initial sliding in the study area appears to have developed on shale slopes which failed with considerable dilation of the rotated slump blocks. The failures must have been attributed to general rock decay and to low effective resistance caused by high pore water pressures that prevailed at the base of the shales. Once sliding had taken place the residual strength of this already weakened material would be reduced to levels much lower than those prevailing initially and as a consequence later shearing and movement were achieved with smaller stress forces. As the stress conditions in the slope at the rear of the slump blocks increased and the frictional angle was lowered, the slopes became unable to support the now steep and heavier slope mass with its capping of sandstone. Subsequent slide movements therefore, took place along the same bedding planes as those movements which had controlled the initial sliding and facilitated the progressive displacement of slump blocks downslope onto the lower and older slide debris. The high pore water pressures which prevailed at the base of the shales and the lower residual strength of material at the landslide toe would also have facilitated further debris slide/mudslide movement.

1.7.14 Vulnerability of slopes

Johnson (1980) identified the most vulnerable slopes to landsling in Longdendale, in the Peak District. The most vulnerable slopes were identified as those situated in the main Longdendale valley, where 75% of the Grindslow Shale basal and mid slopes had already failed whereas only 10% of all the slopes developed on the Kinderscout Grit formation had become unstable. Johnson concluded that 'the presently stable slopes' of Longdendale are vulnerable to mass movement as they still possess characteristics conducive to failure. Johnson (1981) recognised two distinct types of slope which were vulnerable to deep-seated movements. The first type of slope is located in valleys where slope amplitude exceeds 220m and where the slopes are broadly concave. Failures on such slopes tend to be translational movements and take place along bedding-plane slip surfaces with rotational slide movements in the upper parts of the slide. Such slides take place in mid slope locations but debris sliding/mudsliding may later transfer weakened and saturated slope debris to the toe of the slope. The second type of slope where landsliding has taken place is where slope amplitudes are between 120-140m and where streams undercutting the base of the slopes have undermined their stability. The landslides on this type of slope tend to be rotational with slump debris extending over most parts of the slope below the landslide scar. Regolith movements on both these types of slopes and other slopes thought to be less vulnerable have also occurred. Although these shallow slides are more common they are much smaller in extent and are not likely to cause major problems to engineers unless they lie over seepage springs.

Johnson (1980) suggested a checklist of factors likely to influence

large scale slope instability based on his studies in Longdendale and Charlesworth, the checklist is equally applicable for the study region of this thesis (Table 1.8). The checklist can be applied to the study region using a method outlined by Cooke & Doornkamp (1974) and Crozier (1986). Each of the factors, is assigned a stability rating based on a scale varying from stable through degrees of potential instability to those slopes which have already failed. This method is best accomplished with the use of a morphological map whereby stability ratings can be assigned for each morphological hillslope unit. Although such an analysis cannot be a substitute for a full scale geotechnical investigation of particular slopes it provides a valid method of discrimination between slopes of varying stability. Such a map can be regarded as a simple form of relative-stability or slope susceptibility map. Section 2 of this thesis firstly outlines the principles and purposes of landslide hazard mapping with brief reference to recent landslide susceptibility studies, secondly, a regional landslide susceptibility study using the Matrix Assessment Approach (MAP) is described and is applied to the Peak District study region.

Table 1.8 A checklist for sites liable to large-scale instability

(Johnson, 1980).

A. Map Evidence

a) Local relief and slope height/length integral.

b) Slope gradient (mean and maximum valley side, slope angles).

c) Slope unit boundary limiting angle.

d) Degree of curvature along valley sides.

e) Drainage density within slope units. Ease of egress by
    ground water to surface channels.

B. Field Evidence

a) Thickness of valley-side cap rock and the ratio between its
    thickness and the valley side height.

b) Number of sandstone beds outcropping in valley sides, their
    thickness, inclination, orientation and permeability.

c) Structural conditions including texture of joints, faults and
    extent of valley side and floor bulging, cambering and
    attenuation of strata at the base of the slope.

d) Evidence of deep weathering.

e) Nature of superficial overburden; its texture and permeability.

f) Proximity of stream channels to base of slopes.

g) Evidence of past mass movements on slopes, degree of drainage
    integration where this has occurred.

SECTION II

REGIONAL SLOPE

SUSCEPTIBILITY MAPPING

2.1 LANDSLIDE HAZARD MAPPING

2.1.1 Introduction

The importance of accurately identifying areas of hillslope instability and areas of potential unstable ground, and to differentiate them from adjacent areas of stable ground before intended engineering or other development projects is now widely recognised by engineering geologists and civil engineers. The purpose of such an analysis is to convey information on ground stability to planners, engineers, and other concerned professionals. National programmes to reduce landslide losses have been implemented in a number of countries in the world these include: national landslide insurance in New Zealand, hazard zonation with land use controls in the U.S.A. and France, an extensive programme of research and stabilisation in Japan, and extensive programs of inventories and zonation in other European countries including Spain, Italy, Germany, Hungary and Czechoslavakia (Matula & Nemcok, 1965; Rybar et al., 1965; Pasek et al., 1977; Carrara & Merenda, 1976).

A study by Alfors et al. (1973) in California attempted to forecast the potential costs of natural hazards for the period 1970-2000, and of the possible effects of applying loss-reduction measures. Landsliding represented a major natural hazard; the projected $9580 million losses due to landsliding was estimated to be second to that of earthquake shaking in California. The study estimated 90 per cent damage loss savings if all feasible landslide loss-reduction measures were applied. Leighton (1976), said, 'This level of loss-reduction is possible because landslides are considered to be one of the most potentially predictable of geological hazards'.

Hansen (1984), suggested that, 'In general, the application of earth-science technology has a greater potential impact for the long-term reduction of natural hazards produced by surface and sub-surface phenomena than for meteorological processes such as hurricanes, because the latter are not site-discriminant in their distribution. Slope failure, although sometimes triggered by 'regional' hazards (e.g. earthquakes or intense precipitation), will tend to affect discrete parcels of land. As such, earth science technology particularly the spatial science of geomorphology can play a valuable role in determining these susceptible areas'.

Martin (1978), recognised two basic approaches to the assessment of potential instability, they are: (i) the Engineering Approach and (ii) the Geological/Geomorphological Approach.

The Engineering approach utilises rock or soil strength parameters in deriving the factor of safety of a slope. These parameters are derived either from laboratory analyses of slope-forming material, or by back analysis of failed slopes assuming a factor of safety of 1.0. The engineering approach is used mainly to assess instability arising within individual slopes. On the other hand the geological/ geomorphological approach to landslide hazard evaluation has concentrated mainly on regional assessments of landslide susceptibility, using essentially a derivative mapping procedure. The simplest means of constructing a regional landslide hazard map is to work on the assumption that the most hazardous areas are those containing the highest density of currently active landslides. The most widely used technique is to superimpose three basic maps ((a) a landslide distribution map, (b) geological map and (c) a slope distribution map) to develop a series of hazard zones or classes, the

boundaries of which are assigned either arbitrarily or by selected appropriate limiting values from the three component maps.

Landslide hazard mapping seeks to mitigate the danger to life, structure, land loss and social well being. As a general statement landslide hazard assessment may be achieved by: (i) historical methods using previously recorded data on the dates of occurrence and the magnitude and frequency of hazardous events (ii) by experimentation or the use of extrapolation and generalisation techniques, which may or may not be computer based. The general procedure for the assessment of landslide hazard and risk is set out in Table 2.1.

Table 2.1   General Procedure for the assessment of landslide hazard
and risk

1.   Identification of the nature, degree of activity and critical
levels of external destabilising factors;

2.   Identification of the physical responses of inherent factors to
the critical levels of activity of the external factors; that is,
a determination of terrain sensitivity;

3.   Investigation of both the frequency of occurrence of critical
levels of the external factors and terrain sensitivity to produce
a measure of the probability of landslide occurrence;

4.   Combination of the probability of the landslide occurrence with
mass movement characteristics, such as the rate, depth, volume,
and zone of influence to produce an assessment of potential
landslide hazard.   In effect, this is a statement of the
frequency/magnitude characteristics of the phenomenon (Landslide
Hazard Maps);

5.   Combination of potential landslide hazard with the potential
human, economic and environmental damage to produce a statement
on landslide hazard risk (Landslide Risk Maps).

In practice, however, there is often insufficient data to carry out all five phases. If only a small area is under consideration, phase 5 (evaluation of the risk) is likely to be considered early in the assessment. If potential risk is considered to be high, then both surface and sub-surface investigations may be carried out. A full stability analysis would ensue, combining phases 1 and 2 to achieve a statement on probability of occurrence. Knowledge of the morphology, material, volume, and site characteristics, combined with any preliminary assessment, would form the basis for a statement of the potential hazard.

On a regional scale, time and financial constraints usually prevent special sub-surface testing for all areas under consideration; instead use has to be made of existing information or data which can be rapidly obtained. The first decision to be made in a regional survey is the choice of the primary 'information unit' or mapping unit (Geological Society, 1983). The size and nature of this unit depends on the scale of the area under consideration, the time and financial resources available, the degree of detail of the existing information and the degree of terrain homogeneity. Subsequent mapping units, sub-division and hazard zones are then constructed solely on the basis of the acquired data. Generally, however, existing geological, soil, vegetation, slope or geomorphical units serve as the primary mapping units. Geomorphological units have been successfully employed in many hazard-evaluation schemes (Kienholtz, 1978; Ives & Bovis, 1978). Brabb (1982) for example, in preparing a map depicting landslide susceptibility for San Mateo County, California, used geological units as the primary map unit and sub-divided these on the basis of slope to form a geology/slope unit. This unit was then reclassified with respect to past landslide

behaviour to provide the ultimate units of landslide susceptibility. The method is simple, rapid and relatively successful in providing a regional assessment of the landslide hazard at a level suitable for basic planning decisions.

Having established the primary mapping unit, each one may be categorised on the basis of its current exposure to external destabilising factors (phase 1, Table 2.1). This can include such factors as presence and frequency of river or stream undercutting, efficiency of drainage or stormwater systems, and on a broader scale, frequency and magnitude of triggering factors, such as certain weather conditions, seismic activity or particular land use practices. This would allow each unit to be assigned a rating value representing the minimum return period of any potential destabilising activity. Phase 2 (Table 2.1), however, conventionally constitutes the principal basis for hazard assessment. Inherent stability factors are surveyed, numerically scaled, and recorded on the primary mapping unit to provide an assessment of 'terrain sensitivity'. An example of using a semi-quantitative scaling procedure of inherent factors to produce an overall measure of terrain or slope sensitivity, is shown by Selby's (1980) rock mass classification. In general, however, as many factors should be recorded as the constraints of the exercise allow. Examples of factor lists which may be ranked on a scale from 'potentially stable' to 'potentially unstable' can be found in Cooke & Doornkamp, 1974; Johnson, 1980; Crozier, 1986. Numerical rankings of individual factors may be weighted and summed to provide aggregate scores for each mapping unit which, in turn, can be ranked to provide an overall assessment of terrain sensitivity.

In phase 3 scores representing the incidence of triggering conditions (phase 1) are combined with those representing inherent stability conditions (phase 2) to provide a measure of probability of occurrence (Sheko, 1977; Kyunttsel et al., 1978). Thus, high inherent stability combined with low minimum return periods for the activity of external factors indicate high probability of landslide occurrence. It is also useful to record on the map the factors which are most influential in determining the overall probability of occurrence rating. This indicates not only those factors which might be effectively manipulated to improve stability, but also those which need to be preserved to maintain stability (Laird et al., 1979). A test of the validity of this method for determining the probability of occurrence can be carried out by correlating the classified units with the occurrence of pre-existing or new landslides.

Using phases 1, 2 and 3 of this procedure a probability of occurrence on the basis of pre-determined importance factors can be achieved. As such, this method can be employed where there is little evidence of landslide activity. If, however, landslide activity is prevalent in the area, then various forms of locational-factor-analysis and spatial and temporal correlation analysis can be carried out to determine the most influential stability factors within the region. For example, minimum and maximum threshold angles, landslide density/slope angle class and landslide density or landslide volume can be obtained for each geological unit. This information may be extrapolated to unaffected areas of the same mapping unit class. In the presence of landslides, terrain sensitivity can thus be assessed by post-event-determined importance of stability factors.

The results of the procedural phases of Table 2.1 and outlined above are usually summarised on hazard maps which portray existing or threatening processes or as risk maps which attempt to assess quantitatively or qualitatively, the likelihood of a landslide event occurring or the damage potential to the local population and structures. The maps may show various degrees of risk ranging from a statement of the hazards known to occur or to have occurred, through to estimates of relative risk (landslide susceptibility maps) and finally to probability maps, depending on the quality of data (Bolt et al., 1975; Scheidegger, 1975).

There are two approaches to landslide hazard mapping, direct and indirect mapping; both may be supplemented by geotechnical methodology at a later and more sophisticated stage. Direct hazard mapping techniques seek to identify the location and effects of natural and man induced processes in the landscape. Direct mapping includes landslide distribution maps, registers, inventories and geomorphological maps which seek to portray information as seen in the landscape, reported in the literature or derived from documentary sources. Indirect mapping is based on assumed or known causes and aims to identify the controlling parameters of the landslide system which could be used to construct models which predict favourable and unfavourable locations. The methods used for indirect mapping are to map or record digitally the distribution of such variables as slope angle, slope complexity, land use, geological parameters, drainage, mining, undercutting etc and to analyse the result to produce landslide isopleth maps or landslide susceptibility maps. The various techniques of landslide hazard mapping have been reviewed by a number of authors these include: Hansen, 1984; Brabb, 1984; Carrara & Merenda, 1976; Carrara et al., 1977a, 1977b, 1978; Cottecchia, 1978; Kienholz, 1978; Nilsen et al., 1979, Varnes et al., 1984.

2.1.2. The Matrix Assessment Approach

This thesis has examined one particular computer-assisted technique known as the Matrix Assessment Approach. This approach is a quantitative method for establishing an index of instability over a large area. The method uses existing or easily obtained geomorphological and geological data to define the tendency towards instability or the relative risk of instability of all slopes in a region. It lacks the ability to actually predict landslide susceptibility in terms of probability or confidence intervals. However, the Matrix Assessment Approach does allow relative instability to be evaluated over large areas using only a few key measurable factors. When this approach is used, the landslide susceptibility classes are defined by discrete combinations of measurable attributes. Matrix assessment reduces the subjective judgements in the evaluation process by using a simple objective procedure. Because very large data sets can be generated by this method, and because of the manipulations that are required a computer based approach is necessary. Management agencies in the U.S.A. such as the USDA Forest Service have instituted studies that incorporate landslide evaluation information into management decision-making. These studies usually attempt to evaluate stability for a particular project i.e. forest road building (Crockett, 1966) or for a management area (Bailey, 1971). Matrix assessment for landslide susceptibility is an outgrowth of the ECOSYM project. ECOSYM is a natural resources classification and data storage system developed by Utah State University for the Surface Environmental and Mining Task Force (SEAM) of the USDA Forest Service and the Office of Biological Services, USDI Fish and Wildlife Service. The Matrix Assessment

Approach has been applied to the 1036 km^2 Price Planning Unit of the Manti-Lasal National Forest (DeGraff, 1977) and a 1331 km^2 planning unit of the Fishlake National Forest in Central Utah (DeGraff, 1978; DeGraff & Romesburg, 1980). A more advanced Matrix Assessment Approach than that used by Degraff (1978) has been applied to a 360 km^2 case study region in the Derbyshire Peak District. The methodology of the Matrix Assessment Approach (MAP) to landslide susceptibility and its application is described in the following chapters of Section 2. However, it is pertinent at this point to briefly mention the landslide surveys which have been undertaken in the United Kingdom.

2.1.3 U.K. Landslide Surveys

With a few noteable exceptions landslides rarely cause severe loss of life in the United Kingdom but they do cause damage to property, disruption of highways, construction problems, loss of farmland and dangerous coastal cliffs. Until very recently there has been no formal systematic survey of landslides, either ancient or modern which covers the U.K. on a national scale. There has been no equivalent to the surveys of California by the USGS, the hazard surveys of the USDA. Forest Service, the studies of the Geotechnical Branch of the Canadian Geological Survey or the extensive national surveys of New Zealand, France, Poland and Czechoslovakia. The only published near national cover of the distribution of landslides in England and Wales is that shown on the 1:63,360 geological map sheets of the Geological Survey of England and Wales carried out by the Institute of Geological Science (The British Geological survey).

General studies of the stability of slopes in London Clay, particularly in the London Basin, have been carried out by many workers (Skempton & Hutchinson, 1976). Skempton (1964) reported the results of studies on the long-term stability of slopes, using examples from slopes on London Clay. Hutchinson (1965, 1968b,c,d) provided a major catalogue of landslides within the London Clay including the coastal landslides of Kent, Essex and the Isle of Wight. Skempton & La Rochelle (1965) reported the short-term failure of slopes in London Clay in the undrained condition at Bradwell in Essex. The Institute of Geological Sciences carried out a geological survey of South Essex for the Department of the Environment in 1977 (Northmore et al., 1977). The site investigation pertaining to the landslides of this area followed on from the general study carried out by Hutchinson, 1965, 1968a, b, 1969, 1973. The field investigation concentrated on those areas of South Essex with slope angles of greater than 7 ^{o}. A landslide map was constructed at the scale of 1:25,000 showing the location, direction of movement, type of movement, age and condition of each identified landslide and the location of springs that issue from the vicinity of the Claygate Beds/London Clay boundary. A similar study was also undertaken by the Institute of Geological Sciences at Milton Keynes (Cratchley & Denness, 1972).

Morphological mapping techniques using both aerial photography and field mapping have been successfully applied at the reconnaissance stage of the Taff Vale Trunk Road between Abercanaid and Merthyr in South Wales (Brunsden et al., 1975a,b). The mapping was used for identifying landslides along the proposed route and also provided useful information to highway engineers in the design of the engineering works. Applied geomorphological mapping techniques have

been used in the Char Valley, Dorset; Rutland Water, Leicestershire;
Hadleigh Cliff, Essex; Bath, South Cotswolds and the Killiecrankie
Pass, Scotland, to show areas of slope instability (Brunsden & Jones,
1972, 1976; Chandler, 1971, 1974; Hutchinson & Gostelow, 1976;
Hawkins & Privett, 1979; and Chaplow, 1983). Several large scale
engineering geological maps which include landslide data have been
produced, good examples of this type of mapping include the work
carried out by Dearman & Fookes, (1974) and Clarke & Johnson (1975).
Other localised landslide surveys in the U.K. of note include:
periglacial landslides in the East Midlands and Northamptonshire
(Chandler, 1970a, 1970b, 1971), parts of the Cotswolds (Kellaway &
Taylor, 1968), and the Lower Greensand escarpment near Sevenoaks
(Weeks, 1970; Skempton & Weeks, 1976).

Fahran (1976, 1978) developed a technique for an engineering terrain
classification in the Upper Lliw catchment (12 km^2) in South Wales.
The technique used a combination of both geomorphological and
engineering geological/geotechnical site investigation in order to
produce geomorphological maps indicating hazard areas for engineering
construction. Geomorphological site analysis was carried out on 54
geomorphologically identified units followed by a geotechnical site
investigation planned and guided within the geomorphological unit
framework (Rouse, 1975; Rouse & Fahran, 1976). A series of
engineering geomorphological (special and general) maps and plans and
a data matrix containing the differentiating characteristics of
surface form for each engineering site (site morphometric attributes)
was compiled along with a geotechnical survey map and a geotechnical
data matrix including the physical and mechanical differentiating
characteristics (grain size, in situ unit weight, dry unit weight,

saturated unit weight, liquid limit, the residual angle of shearing resistance, the predicted limiting angle and the comparison of the predicted limiting angles with mean slope angles) of the engineering sites. The data matrix of the site morphometric attributes was then combined with the geotechnical data matrix, and both employed as input for statistical classification using multivariate statistical techniques. Cluster analysis was used to produce several groups of engineering terrain classes based on similarity coefficients. The validity of the grouping was tested statistically using linear and multiple discriminant analysis.

Terrain zone maps have been prepared by the Institute of Geological Sciences (Conway, 1976) for a small area of the West Dorset Coast, in an area of intense landslide (especially mudslide) activity. The zones were defined on the basis of: slope steepness, slope drainage, instability potential, geological structure, and geotechnical properties of the rocks. The solid geology of the area surveyed consisted of Lower Jurassic Clays, mudstones and impure limestone overlain unconformably by Cretaceous clays, sands and chert. The boundaries of most terrain zones were found to be coincident with lithological boundaries. The 1:50,000 scale map shows active landslide areas, with the rest of the map being divided into six terrain zones. Each zone was classified according to its lithology and was identified from 1:4,000 scale aerial photographs. The terrain zones and slope instabilities were presented on 1:10,560 geological maps. An accompanying summary table gave information·on extended lithologies, slopes, and geotechnical conditions which existed within each unit. The purpose of the Dorset coast maps was fourfold: (i) to provide planners with a broad guidance on the possible use or uses to which coastal areas can be managed, (ii) to

provide a broad indication of likely instability and foundation conditions for the initial stages of planned engineering works, (iii) to pinpoint active or potential hazard areas and (iv) to provide the basis for the design of detailed site investigation procedures.

Chandler & Hutchinson (1984) have recently devised a scheme of assessing the relative degrees of landslide hazard in the Undercliff (large complex of old multiple rotational and translational coastal landslides) at Ventnor, Isle of Wight. The technique is based on consideration of the combined geological, geomorphological, historical, and instrument monitoring evidence, together with previously collected geotechnical data. Four ranked degrees of landslide hazard were identified based on the types of landslide movements currently occurring in the Ventnor area. The hazard zonation is not intended to be taken as a prediction of the occurrence of an actual landslide; the ranked categories merely identify areas which, according to the available evidence, have a designated probability of failure. This is seen as a useful preliminary guide to planners, local authorities and others concerned with the situation in Ventnor.

A regional landslide survey for the Department of the Environment was undertaken in the South Wales Coalfield between 1979 and 1981 following a preliminary limited regional survey in 1977 (Conway et al., 1980). The objectives of the extended survey were: (i) to identify and classify landslide types, (ii) to map the distribution of landslides in relation to slopes and the, solid and superficial geology, (iii) to indicate areas of present instability, and (iv) to prepare a report with data presented as a series of landslide distribution maps and a catalogue of all mapped landslides in the

coalfield area.

Two landslide susceptibility maps at the scale of 1:2,500 have been
constructed for two landslide areas at Tarren Pwllglo and Glynrhigos
in the South Wales Coalfield (Conway et al., 1983). A slope element
plot was superimposed on the solid geology map, two zones of high
landslide susceptibility were plotted, zone (A) the coincidence of
slopes greater than 25° and potential spring lines, and zone (B)
which showed the coincidence of 15° to 25° slopes, and potential
spring lines. A zone immediately downslope of the two previously
mapped zones (A & B) was delineated, this zone represented moderate
susceptibility, zone (C). Although zone (C) may not fail itself, it
may suffer from the resulting landslide debris and mudslides caused
by failures further up slope. Other areas with no identified
landslide causal factors operating were classed as zone (D).
Superimposition of a geomorphological map upon this zonal map allowed
slight modification of the four zones by showing where superficial
material was likely to be deep. It also introduced a sub-zonation of
areas which showed signs of previous movement thereby indicating
areas of residual strength which were, therefore, classed as more
susceptible to failure. The geomorphological map also showed zones
of high but localised slope susceptibility caused by bank
undercutting by stream erosion, zone (F). The final derivative map
established five zones of varying susceptibility to landslide
movement.

The work of Johnson (1980) provided one of the few examples of
landslide susceptibility mapping undertaken in northern Britain.
Johnson used a similar technique to that employed by Brabb et al.
(1972) to construct a landslide susceptibility map for an area of

72 km^2 in Longdendale, Derbyshire. Instead of using a generalised slope gradient map with slope classes determined arbitrarily as used by Brabb et al. (1972), the Longdendale map was compiled by examining each slope profile in terms of its individual geological and hydrological conditions as well as its gradient. A geomorphological/ geotechnical investigation of selected slopes was also undertaken in order to determine the following parameters: slope angle, slope height, cohesion, bulk density, angle of internal friction, and ground water levels. Slope stability charts (Hoeck & Bray, 1977) were then used to determine the factor of safety for different slope units, assuming a factor of safety of 1.0 when it became critical to failure. Critical slope gradients from actual valley side profiles were then compared with theoretical values and by using this comparison five slope susceptibility units could be recognised. The base map used for the landslide susceptibility mapping was a slope classification map: whereby each morphological slope unit was classified according to Dalrymple's nine unit land surface model (Dalrymple et al., 1968).

A landslide survey of the U.K. sponsored by the Department of the Environment has recently been completed by Geomorphological Services Ltd. The survey involved the creation of a large data bank of landslide information gathered on a standard proforma. Information was collected from published geological maps, landslide reports, documents and various academic journals on a county basis. Each type of landslide was then plotted on a base map (scale 1:250,000) by a representative symbol and classified according to whether the slide was active or fossil.

The application of the Matrix assessment approach to landslide susceptibility in the Derbyshire Peak District case study that follows thus represents one of the few attempts in northern Britain to define the slopes of a large area in terms of relative risk of instability.

2.2 Landslide Susceptibility Mapping using the Matrix Assessment Approach (MAP)

2.2.1 Introduction

Over the past 20 years, it has become common practice to use aerial photograph interpretation and field-based geomorphological mapping at the reconnaissance stage of civil engineering projects in order to identify those sites where geotechnical investigations are most likely to be required. Such an approach normally provides a good basis for recognising existing failures, including those of some antiquity. However, most investigators are nervous of having to define 'slopes potentially susceptible to failure'. Mapping of this style therefore tends to identify landslides and leave the remaining slopes unclassified. Much more difficult is the task of identifying sites which are close to instability or even where instability may exist, but has not been recognised either in past records, by aerial photograph interpretation, or by reconnaissance mapping. In order to assist in this task a technique of slope susceptibility assesssment known as the Matrix Assessment Approach (MAP) is outlined. This approach uses existing or easily obtained geomorphological and geological data to define the tendency towards instability or the relative risk of instability of all slopes in a region. The matrix

assessment approach can be regarded as a supplementary technique to aerial photograph interpretation and geomorphological mapping. It provides a classification of all slopes in a manner which indicates the relative risk of slope failure in each case.

The Matrix Assessment Approach (MAP) has been applied to the 1036 km^2 Price planning unit of the Manti-Lasal National Forest, U.S.A.

(DeGraff, 1977) and a 1331 km^2 planning unit of the Fishlake National Forest in Central Utal (DeGraff, 1978; DeGraff & Romesburg, 1980). Section two of this thesis sets out to examine the following questions:-

1. Can the MAP technique proposed by DeGraff, (1978) be improved in order to provide a more detailed landslide susceptibility assessment.

2. Can MAP be applied satisfactorily to terrains other than those described by DeGraff & Romesburg, (1980) to provide an accurate assessment of landslide susceptibility.

3. How successful is the MAP technique for establishing an index of relative stability over large areas in a selected case study area in the U.K.

The technique uses a square grid-based digital model for landslide susceptibility and has been implemented and tested on a sample area in the Peak District of Derbyshire. The techniques used to collect, encode, store and process the parameters used in the MAP approach are described below.

2.2.2 The aims and application of the Matrix Assessment Approach

The aims and application of MAP can be discussed by reference to seven main points:

1. Regional survey economics

2. Classification of instability

3. Temporal change

4. Identification of undetected instability for highway engineering

5. Hazard assessment subjectivism

6. The end user

7. Rapid and cost effective technique

1. Regional Survey Economics

Mass movements are the result of an interplay of a large number of interrelated geological and geomorphological factors. Their identification and measurement in the field would need both surface and sub-surface site investigation regarding geotechnical, geomechanical and hydrogeological characteristics of the parent slope and of the failed mass. However, as pointed out by Bjerrum (1967), accurate stability analysis of natural slopes by means of intensively applied geotechnical techniques cannot be carried out at reasonable cost and relatively rapidly over large areas. Site accessibility may also be a problem in remote areas, either for transporting large boring machinery, or the removal of suitable material samples. In such cases an alternative cost effective approach is needed at very least to identify those sites most likely to be prone to instability. Such an approach must of necessity be based on easily obtained parameters which can be readily collected over the whole of the

investigated area and which are known to be directly or indirectly correlated with slope instability. Such parameters will therefore tend to be those related to relief (morphology and geomorphology) and materials (geology and soils).

2. Classification of Instability

Although there is a clear distinction in terms of activity between slopes which are undergoing movement and those which are static, it oversimplifies the issue to classify slopes as being either 'stable' or 'unstable'. If a classification of slope instability is required, it is better to envisage slopes as existing in a continuum of states, from stable, unstable (marginally stable) to an actively unstable state (Crozier, 1985). This continuum represents successively smaller margins of stability, culminating in the actively unstable slope where the factor of safety is zero. In deterministic terms, these stability states can be defined (at least theoretically) by the ability of transient forces to produce failure. Stable slopes are those where the margin of stability is sufficiently high to withstand all transient forces. Marginally stable slopes are those which will fail at sometime in response to transient forces attaining a certain threshold level. Actively unstable slopes are those where transient forces produce continuous or intermittent movement. The distinction between stable and marginally stable states in these terms is more easily made in theory than in practice. Besides the problem of establishing accurately the stress conditions within the slope, the main difficulty lies in determining the full range of stress changes that can be brought about by transient factors. All forces determining stability are controlled or influenced by identifiable phenomena which are referred to as stability factors. When these

operate to induce instability they are referred to as destabilising or causative factors. The Matrix Assessment Approach (MAP) is a quantitative method for establishing an index of instability states over large areas. The method allows the relative landslide potential/susceptibility to be evaluated over large areas using a few key measureable stability factors/parameters. The index of slope instability or landslide susceptibility classes are defined by discrete combinations of measureable parameters. MAP is therefore based on the assumption that the factors causing instability are known, therefore, the determination of the terrain thresholds (i.e. ground conditions conducive to mass movements) is a prerequisite to the assessment. The provision of a classification of instability over large areas other than being of academic interest may also provide a useful application for planning large scale engineering projects or land use management decisions; the application of MAP is outlined in point 4.

3. Temporal change

Transient factors, such as climate vary greatly with time and thus a long record is required in order to predict confidently their full range of activity. Without such a record, the rigid deterministic definitions of stability states discussed in point 2 cannot be applied and it may be necessary to use a more approximate probabilistic statement of slope stability. In any accurate assessment of long-term stability of a slope, changes in the factor of safety over time must be accounted for. In practice this is extremely difficult and as far as the notion of 'landslide hazard' is concerned in this study, it is more useful to use a loose definition (i.e. the potential instability of a slope) rather than resort to the

more rigid quantitative notion of probability.

By definition, marginally stable slopes can be predicted to fail at some time within a given period under the prevailing regime of transient forces. The frequencies with which critical failure conditions are reached obviously becomes an important consideration. If there is no evidence of past or present movement (for example, cracks, scars, landslide deposits) the slopes can be considered to have withstood the activity of transient factors for a long period, at least long enough for any evidence of previous failure to have been obliterated by other slope processes. In the absence of stress analysis (often the case in large-scale regional surveys), such evidence is generally accepted as indicating a stable slope. The problem of this kind of evidence is its inability to reveal deterioration in the margin of stability over time. Certain slopes may become weaker with time and their margin of stability may decrease sufficiently to allow a 'first time' failure to occur. Slope deterioration, therefore, also affects the long-term validity of stability assessment by stress analysis. In marginally stable slopes, however, the history of slope movement may offer a better approach to determining frequency of failure than does inference by stress analysis because the geological record of critical conditions is invariably much longer than instrument monitoring records. Establishment of historical records requires the application of dating techniques and sometimes drill-core sampling and therefore can be as costly to implement as stress analysis. Bearing these points in mind MAP may provide a useful alternative technique for slope susceptibility assessment over large areas.

In addition to the geological deterioration of the margin of

stability with time, any survey of slope stability must also take into account regime changes within the transient factors. For example climatic changes, shifts of tectonic activity and human modification of slopes, may all affect both the inherent margin of stability as well as the frequency and magnitude of transient activity. Designation of instability therefore requires qualification by time and space. Many of the large deep-seated rotational slides in the study region took place shortly after the Devensian (Pollen zone VI); during this time the climatic conditions and processes were different from those currently operating. There are few cases of present large-scale deep-seated instability in the study area except the continuing instability at Mam Tor and Snake Pass. When an area of high instability potential has been determined only on the existence of a hazardous event in the past (e.g. based on the existence of old or undated landslide deposits which may have been formed under different environmental conditions) without any estimate of present stability conditions or frequency of event; problems may exist through ill-advised extrapolation. The final susceptibility map is aimed to show those areas which appear to be pre-disposed to instability by correlating some of the principal factors that contribute to landslide movements, such as steep slopes and weak geological units, with the past distribution of landslides. This important point has been taken into consideration in the appliction of MAP and can be explained by reference to the type of destabilising factors responsible for causing slope instability. The concept of a continuum of stability states as previously discussed offers a useful framework for understanding the causes of instability, in this context three groups of destabilising factors can be identified on the basis of 'function' (Crozier, 1986).

(a) Preparatory factors:- which dispose the slope to movement, that is factors which make the slope susceptible to movement without actually initiating it, thereby tending to place the slope in a marginally stable state.

(b) Triggering factors:- which initiate movement, that is, those factors which shift the slope from a marginally stable state to an actively unstable state.

(c) Controlling (perpetuating) factors:- which dictate the condition of movement as it takes place, that is, factors which control the form, rate and duration of movement.

MAP concentrates essentially on preparatory factors which dispose the slope to movement. It should be stressed that the purpose of such an assessment is not to estimate the degree of potential losses (i.e. the risk), but to identify the geological and geomorphological nature of the landslide hazard. Therefore, the technique can be seen as a means of only identifying potential or vulnerable areas where caution is required when planning engineering structures which may activate sliding. The application of the Matrix Assessment Approach to the Derbyshire study area should be regarded as a hypothetical and essentially academic test case; since it is widely perceived that there is not a present day threat posed by deep-seated rotational type mass movement processes in this area. Most of the present day major instability problems have taken place on former landslip areas such as at Mam Tor and Woodhouses at Snake Pass. Shallow planar translational slips are still a common mass movement process today particularly after heavy and prolonged rainfall, however, such small-scale shallow sliding, though a nuisance, is not considered to be a

major problem to engineers and planners. In this context MAP provides a useful supplementary technique for locating and delineating undetected landslide areas in areas like the Derbyshire case study area where most of the large landslides are of some antiquity. It should be emphasised that susceptibility mapping should be regarded as a preliminary ground investigation technique providing only a guide to slope instability, not an absolute indicator of instability, more detailed geotechnical investigations are required to determine local variation.

4. Identification of undetected instability for highway engineering

Landslides are one of the most serious ground problems faced during road construction in areas of moderate to high relief; they are encountered more frequently in highway engineering than any other type of natural hazard. In recent years there have been an increasing number of reports relating slope stability to the disturbance of pre-existing dormant or fossil landslips. In Britain pre-existing landslips are generally attributable to events in the recent geological past, particularly the Late Devensian and early Flandrian periods. The geomorphological expression of some old and dormant landslides is often very subtle as is borne out by the number of old landslides that have not been discovered until reactivated by engineering works. The recognition of these areas, which may be interpreted as relic features of periglacial mass movement are obviously important in engineering and planning projects.

It is apparent, therefore, that prior to site investigation in areas susceptible to landsliding, a technique is required that is capable of identifying slopes prone to instability and even fossil landslides

which have remained undetected by aerial photograph interpretation and field checking, possibly because they have been masked by superficial material, vegetation or by agricultural practice. Such a technique should be capable of being used during the desk study and reconnaissance stages of engineering projects and should be used to guide the eventual site investigation programme. For highway reconnaissance surveys one is seldom in a position to pre-judge the effect of engineering construction. Therefore, the hazard assessment of slopes discussed in this project refers only to natural controls of the landslide potential. The final susceptibility map provides a useful guide to help the highway engineer choose a number of potentially suitable routes, or provides assistance in the choice of one route from a number of alternatives previously identified. The technique provides a spatial perspective to the assessment of ground conditions, enabling an engineering site to be placed within a geomorphological context, (i.e. the position of the site in relation to slopes above and below it; and how the site may be influenced by processes operating outside the zone of immediate engineering interest).

No large-scale highway engineering projects are currently planned for the study region in Derbyshire. The situation in Derbyshire is very different to that occurring in places such as California, Calabria and regions of Czechoslovakia where present day instability still poses a serious and costly environmental hazard affecting large areas, sometimes densely populated. Although the Derbyshire case study area does have some landsliding problems it cannot be compared and considered in the same manner as the case examples mentioned above. Therefore, the application of the Matrix Assessment Approach to the Derbyshire study area should be regarded as a hypothetical

case study in order to test the MAP model of DeGraff (1978). The technique may well provide an extremely useful preliminary guide for environmental planning in places like California, Calabria and Czechoslovakia which have continual large-scale mass movement problems.

5. Hazard assessment subjectivism

There is often a subjective element in landslide hazard assssments, this may be partly dependant upon the experience of the individual researcher involved (Kienholz, 1978). For example, a great deal of experience and professionalism is required in the compilation of engineering geomorphological hazard maps and therefore these maps tend to be highly subjective depending on the style and precision of the individual involved. In order to reduce the level of subjectivity, techniques should be used which are as objective as possible, given the financial, time and policy restraints which are imposed on the hazard evaluation project. Some investigations have used a standard inventory/proforma to collect information for data storage. Such schemes are still prone to subjective error and usually require large numbers of workers either collecting information in the field or by desk investigation.

The standardised and objective procedure of MAP overcomes this subjectivism. Although the technique is based on the intuitive processes by which an investigator perceives the controls on or determinants of slope stability in an area which inevitably means some degree of subjectivity, MAP systematises this intuitive process by relating causal factors which are widely accepted to be conducive to landsliding to a few basic measurable attributes/parameters, and

by employing an objective numerical procedure. The technique follows a simple and easily understood methodology where results can be substantiated and clearly reproduced. This is important for the reason that many hazard judgements are likely to meet opposition from parties with interests at stake.

6. The End User

The concept of a map and the manner in which it is displayed is controlled by the purpose to which it is to be used and the experience and knowledge which is possessed by the user. The intended purpose of a map will control the scale at which it is drawn, in that the scale must allow for the representation of the smallest significant detail for the purpose in hand. Under normal circumstances where the map purpose defines scale, the scale then defines the density of information to be obtained to achieve the required information coverage on the map. The available information used in the MAP case study was considered in the light of its density, accuracy and original scale. The resultant landslide susceptibility map was produced at a scale of 1:25,000 as the best balance of available accurate information which would be meaningful at a scale useful at the regional planning level, reconnaissance stage of a large scale engineering project (e.g. road construction, pipelines, railways, canals, pylons, etc.) and environmental land use/management projects (forestry, agricultural practices, building developments, recreation, etc.).

The way in which the landslide susceptibility map is presented is controlled by the end users experience and expertise. It is reasonable to assume that the end user will not necessarily be

familiar with geological, geomorphological, or geotechnical terms and that these should, therefore, be simplified or avoided. The final graphic output of the susceptibility maps in this study has been displayed in a manner allowing easy comprehension and interpretation by various types of end user.

7. Rapid and Cost Effective Technique

The underlying concept behind MAP lies in its ability to be applied relatively rapidly and cheaply to large areas. It can be applied using a small team of individuals and does not incur large support expenses in terms of manpower and materials (i.e. field work, geotechnical investigation equipment, expensive computer facilities, etc.).

By taking into consideration factors such as the time needed for data acquisition, limited financial constraints, the purposes of the project (i.e. to provide a preliminary assessment of instability for engineers and planners) and the quality of the existing information used in the assessment (for example, 1:25,000 topographical and geological maps) the technique should of necessity be cheaply and rapidly applied (Newman et al., 1978).

The advantage of a grid-based digital model such as MAP lies in the fact that each terrain attribute/parameter can be represented by data matrices which are easily handled by computer (data storage, retrieval and processing) and information is in a suitable form for statistical treatment. The design of the grid cell sample size has been carefully selected in order to economise on costs but still

produce as accurate assessment as possible. Although a smaller grid size will produce a more accurate map it will be more expensive to produce in terms of factor map production time, computer time and in terms of the data storage space required. The benefits of using a reduced grid size will only extend to the limits of accuracy of the original data source.

MAP has been designed so that it can be carried out on a micro-computer. The benefit of using computers for hazard mapping rather than manual calculation and cartography lies in being able to experiment with different classifications and associations of the variables and data sources involved. Computers make possible the testing, discarding, and refinement of hypotheses regarding the inter-relationships between the variables being studied. Computer analysis using MAP as well as allowing large numbers of variables to be considered also identifies the best combination of parameters and their relative sub-classification for slope stability assessment. The use of a computerised graphics facility enables output of the final susceptibility maps to be handled easily and accurately without manual intervention. A computer/data base approach is also useful since the final hazard zonation can be quickly updated if new data is added, either in the form of additions to existing factor maps (for example, as new landslide deposits are recognised) or even as new factor maps are produced.

Recent technological developments in the field of automatic data acquisition by means of highly sophisticated digitiser instruments, scanners or through pattern recognition methods, will allow in the future significant economics in cost and time involved in data acquisition and encoding for any terrain attribute. Therefore, MAP

should become even more accurate, efficient and cost effective.

2.2.3 Basic Principles

The whole of this approach is based on a grid which is created across the area of concern. The area to be investigated must be defined and boundaries established. Values are assigned to each cell of the grid based on selected geomorphological and geological parameters chosen because they are believed to have a contributing influence on slope stability, and because they can be obtained from existing sources. A map of existing landslides in the case study area was created from information provided on geological maps (1:10,000 geological survey sheets) and 1:12,000 panchromatic aerial-photographs combined with a programme of field checking.

The next stage of the procedure was to calculate both the landslide area factor (LAF) and the corresponding regional area factor (RAF). A landslide area factor (LAF) is defined as the total area occupied by landslides possessing a particular combination of hillslope attributes. A regional area factor (RAF) is the total area within the region, occupied by a particular combination of hillslope attributes. Each unique set of attributes therefore has its own RAF. For each set of combinations a landslide susceptibility index (LSI) can be calculated from:

$$LSI = \frac{LAF}{RAF}$$

The closer the LSI approaches unity the more susceptible that particular combination of attributes is to slope failure. The index values can then be used to produce a new map showing both the existing landslides and the LSI value by an appropriate shade class in each cell for the particular combination of attributes found in that cell. Fig. 2.1 shows a schematic diagram of MAP for a case using seven environmental attributes; where:

$$\frac{\text{LAF (98 ha)}}{\text{RAF (141 ha)}} = \text{LSI (0.695 ha)}$$

This particular combination of environmental attributes can be regarded as having a high susceptibility to failure according to the susceptibility in the schematic diagram.

Compilation of base maps

A Landslide matrix (LAF)

Sum of landslide matrix cell areas with the same attribute combination

```
a Bedrock class 2
b Superficial deposits class 4
c Slope class 3
d Slope aspect class 1
e Relative relief class 4
f Height above valley class 4
g Altitude class 3

A Landslide area = 98 ha.
```

Attributes

Landslide distribution

g Altitude

f Height above valley

e Relative relief

d Aspect

c Slope

b Superficial deposits

a Bedrock

B Regional matrix (RAF)

Sum of regional matrix cell areas including landslide matrix cell areas with the same attribute combination

```
a Bedrock class 2
b Superficial deposits class 4
c Slope class 3
d Slope aspect class 1
e Relative relief class 4
f Height above valley class 4
g Altitude class 3

B Regional area = 141 ha.
```

C Landslide susceptibility matrix (LSI)

Landslide susceptibility value for cells with combination

```
a Bedrock class 2
b Superficial deposits class 4
c Slope class 3
d Slope aspect class 1
e Relative relief class 4
f Height above valley class 4
g Altitude class 3
C Landslide
  susceptibility = 0.675
```

Susceptibility index

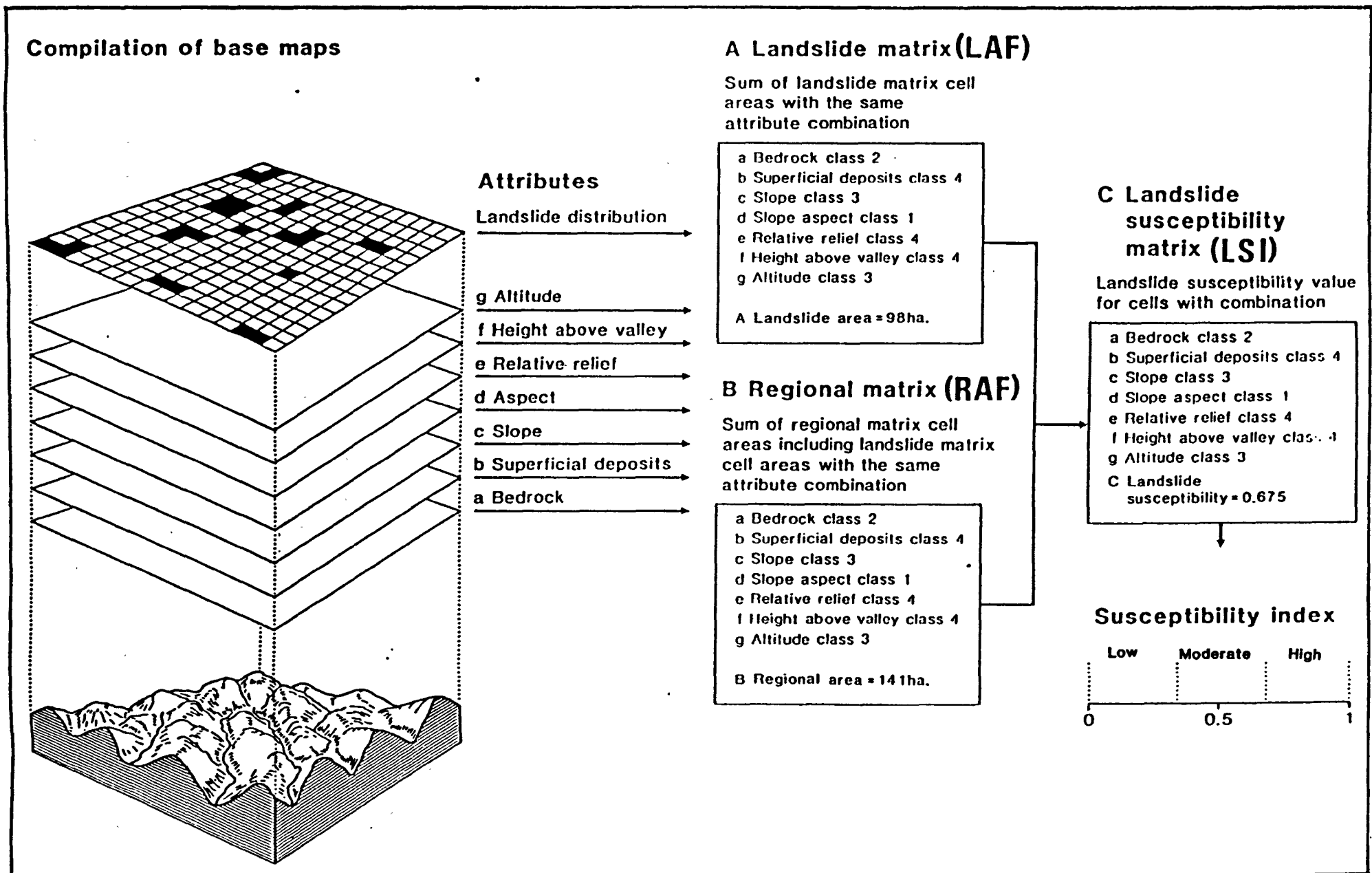| Low	Moderate	High

```
0          0.5          1
```

Fig. 2.1. Schematic diagram of the Matrix Assessment Approach for a case using seven geomorphological/geological attributes

2.2.4 Slope Susceptibility Attributes

An awareness of the local conditions which may lead to a situation of instability is required in order to select the slope susceptibility attributes for a particular area. Recognition of the potential for instability can be achieved from a preliminary assessment of the expected landforms and the materials, together with the processes and timescales at which they are evolving.

Whilst it is possible in theory to imagine a long list of contributing factors, experience elsewhere has shown that relatively few parameters, when taken in combination, can go a long way towards making a meaningful regional assessment (Brabb, 1982; Crozier, 1982; Nilsen et al., 1976b; Varnes, 1984). Where landslide activity is prevalent in an area, then various forms of locational-factor analysis and spatial and temporal correlation analysis can be carried out to determine the most influential stability factors within the region. For example, minimum and maximum threshold angles, landslide density/slope angle class, and the landslide density can be obtained for each geological unit. A practical limit on the number of attributes/parameters used is set by the ability of the compiler to acquire the appropriate data during a desk study. Costs tend to increase when more parameters are used, so in regional investigations the number of variables should be constrained to avoid prohibitive costs. The number of possible combinations of variables produced by combining a set of different parameters will be equal to the product of the number of variable classes of each parameter used in the assessment. Thus, even if three parameters containing two to three class combinations there will be 2 x 3 x 4 = 24 eventual factor combinations; some possible outcomes will not exist because of

autocorrelation between variables.

MAP uses a maximum of nine geological/geomorphological attributes for slope susceptibility assessment, these are:

1. Bedrock geology

2. Superficial materials

3. Slope steepness

4. Slope aspect

5. Relative relief

6. Height above valley floor

7. Height above sea level

8. Bedrock combination

9. Soils

1. Bedrock

Particular bedrock units may be more susceptible to landsliding than others. Greater susceptibility may result from a unit's physical and chemical characteristics including its permeability, fracture spacing and cementation. Inherent structural weaknesses in a bedrock unit may result from circumstances involving bedding, joint or fault plane characteristics. Bedrock used as a matrix attribute is, therefore, assumed to incorporate lithological, structural and stratigraphic conditions into the landslide susceptibility assessment.

2. Superficial Materials

Slope susceptibility may be a function of landslide-prone regolith or Head derived from a particular bedrock unit. For example, a feature of the breakdown of shales and mudstones is their disintegration to produce silty clays (Grice, 1969; Taylor & Spears, 1970; Badger et al., 1956). Superficial materials occur as an infinite variety of potentially mobile heterogenous masses which tend to attain the lowest energy state available to them. Solifluction materials in particular usually have been reduced to their residual shear strength and often come to rest on slopes at their angle of limiting stability. Fine-grained solifluction and landslide material in the case study area frequently consists of a clay or shale breccia within a remoulded clay matrix. Shear surfaces are widespread in such solifluction materials. The presence of a permeable superficial material overlying a more impermeable bedrock unit often leads to high positive pore-water pressures (perched water table conditions) which trigger shallow slope instability. Therefore, the combination of bedrock unit and type of overlying superficial material is an important factor of slope stability.

3. Slope Steepness

Slope supplies the potential energy gradient on which a landslide moves to attain a more stable lowered energy state. The steeper the slope the more liable it is to be unstable. Slope is employed as a measurable parameter regardless of the geological/geomorphological factors responsible for the measured inclination.

4. Slope Aspect

Aspect is the compass direction in which a slope faces. It can be expressed as eight directional classes, (N, NE, W, SW, etc.) defined by degree of azimuth. Aspect is used to identify any significant slope orientation and steepness of the ground surface that may coincide with structural conditions (i.e. joint directions and incliations, bedding planes and fault planes, etc.) that may enhance slope failure.

5. Relative Relief

Relative relief provides information on the gravitational forces existing in an area. Steep slopes and free faces tend to predominate where deep valleys have developed particularly where the more resistant gritstone has been exposed on the valley sides.

6. Height above valley floor

Height above the valley floor provides information on the potential energy available for landslides.

7. Height above sea level

Height above sea level provides information on elevation effects on landsliding such as the altitudinal position of structural weaknesses or seepage areas (e.g. spring lines) on the valley sides.

8. Bedrock combination

Critical areas of instability tend to occur where a particular stratigraphical combination of rock types occur. For example, where a massive well jointed sandstone overlies a relatively impermeable shale strata, slope instability may result because of increased pore-water pressures ('Reservoir Principle').

9. Soils

The soil type (Soil Associations) provides information on the soil water regime (Avery, 1980; Clayden & Hollis, 1984). The soil water regime is the cyclical seasonal variation of wet, moist or dry soil states. The duration and degree of waterlogging are described by the system of wetness classes, grading from wetness class I, well drained, to wetness class VI, almost permanently waterlogged within 40cm depth (see Table 2.3). The incidence of waterlogging depends on soil and site properties, underdrainage and climate. For example, surface water gley soils (seasonally waterlogged slowly permeable soils) and ground water gley soils (seasonally waterlogged soils affected by a shallow fluctuating ground water table) are identified. Such information provides an indication of ground water levels particularly the presence of perched water tables which are often associated with areas of instability (see Table 2.4).

TABLE 2.3 SOIL WETNESS CLASSIFICATION.

WETNESS CLASS	DURATION OF WATERLOGGING
I	The soil profile is not waterlogged within 70cm depth for more than 30 days[1] in most years[2].
II	The soil profile is waterlogged within 70cm depth for 30-90 days in most years.
III	The soil profile is waterlogged within 70cm depth for 90-180 days in most years.
IV	The soil profile is waterlogged within 70cm depth for more than 180 days, but not waterlogged within 40cm depth for more than 180 days in most years.
V	The soil profile is waterlogged within 40cm depth for more than 335 days in most years.
VI	The soil profile is waterlogged within 40cm depth for more than 335 days in most years.

1 The number of days specified is not necessarily a continuous period.
2 'In most years' is defined as more than 10 out of 20 years.

TABLE 2.4 WETNESS CLASSIFICATION ACCORDING TO SOIL TYPE.

SOIL TYPE	WETNESS CLASS
Typical Brown Earth	I
Raw Oligo fibrous Peat Soils	VI
Cambic Stagnogley Soils	IV
Iron Pan Stagnopodzols	III/IV
Cambic Stagnohumic Gley Soils	V
Humo Ferric Podzols	I
Typical Brown Podzolic Soils	I
Brown Rankers	I
Typical Brown Alluvial Soils	I

2.2.5 Using the Matrix Assessment Approach

The initial aim in data collection is to arrive at a value in each grid cell (1.56 ha) for each of the nine attributes thought to influence landsliding. This will lead to nine separate maps (one for each attribute) whose data will then be compared and combined to provide a landslide susceptibility classification and a susceptibility index (LSI) for each cell.

The first step, therefore, is to establish a basis for sub-dividing each attribute group into a sensible classification. In the approach suggested here it is not necessary to seek an absolute value to represent a physical state. For example, in the case of bedrock geology, superficial deposits, soils and bedrock combination it is only necessary to identify the lithological types involved, place these into suitable groups, and assign a code number to each group. Aspect directions acquire their classes naturally (i.e. N, NE, E, etc.); and each can be awarded a code number. Relative relief and heights, can be grouped into classes such that, in the first instance, the complete range is covered by 8 to 10 classes. Slope steepness, once measured (e.g. by applying the indicator charts, based on contour interval, published in Thrower & Cooke, 1968), can also be assigned to one of (up to) six classes devised to cover the full range of slope angles measured. At this stage, therefore, each cell on each attribute map shows by a numerical indicator, the appropriate classification for the area covered by that cell.

If the landslide map is used as a basis for comparison it is now possible to identify the combinations of parameters (and there may be more than one combination) which occur within the cells, which have

been classified as landslides. From this it is an easy step to
calculate the area of landsliding associated with each identified
combination. The immediate response at this stage is to search for
all other cells which possess the same identified combinations of
attributes which have not been classified as landslide cells. It
might be assumed that such sites are close to failure or carry
undetected (perhaps old or masked) landslides. To carry out such a
search manually is very time-consuming. If possible it is advisable
to use a computerised approach, for, not only will this enable the
task to be carried out efficiently it will also make relatively
simple the search for those cells which nearly achieve the
(apparently) critical combinations.

2.2.6 Computer Software

The benefit of using computers for hazard mapping rather than manual
calculation and cartography lies in being able to experiment with
different classifications and associations of the variables and data
sources involved. Computers make possible the testing, discarding,
and refinement of hypotheses regarding the inter-relationships
between the variables being studied. Output of final susceptibility
maps can then be handled easily and accurately without manual
intervention.

Software to perform the necessary operations becomes the limiting
factor in such investigations. The software required for these
operations involves (i) topographic model creation, (ii) derivative
mapping, (iii) image processing, and (iv) final map output. The

problem is that such systems are available separately but rarely in an integrated form except at large institutions with large computing centres, whereas the day to day work in hazard mapping tends to be undertaken by relatively small engineering consulting companies without adequate access in terms of either distance or cost to the dedicated software and hardware systems that are centrally available. As prices of hardware have fallen, and micro computing systems have become more complex and reliable, many small companies are prepared to use whatever computer they can afford to perform these tasks. This often has to be in addition to their standard computing requirements (e.g. word processing, mail addressing, accounting, etc.) as they cannot justify a super-micro computer on the basis of an image-processing facility alone.

2.2.7 Software Systems

Three computer software systems have been used (PANACEA, DERIVATIVE and MIRAGE), these have been developed for use on Super-Micro Computers and written in Fortran 77 to be compatible with and transferrable to other computers (all of the programs described here and used in the MAP procedure were written and made available by Dr. M.J. McCullagh whose help is gratefully acknowledged).

PANACEA: The PANACEA system is a surface generation system typically taking in contour strings, spot heights, cliff and river lines, and producing as output high accuracy grid digital terrain models (DTM's) with associated block diagram and contour output. The complete system contains seven modules (PAN, PANIC, PANDEMON, PANDORA, PANARAMA, PANACHE, PANEL) arranged to perform six logical functions.

(1) String preprocessor (PAN) to reduce string complexity and size
to a level consistent with the final display cell resolution.

(2) Spatial structure generation program (PANIC) that defines the
inter-node relationships.

(3) Graphic editor (PANDEMON), including structure display and
contouring, to adjust automatically derived relationships to suit
special purposes and to allow insertion of extra special purpose
strings.

(4) Grid generation program (PANDORA), operating on the data
structures created by PANIC and PANDEMON.

(5) Display suite to permit direct checking of the grid by sampling,
using isometric views (PANARAMA) and contouring (PANACHE).

(6) Amalgamation module (PANEL) that takes grids generated by the
system (possibly at differing resolutions and possibly covering
overlapping areas) and combines them into one grid (McCullagh
personal communication).

DERIVATIVE: DERIVATIVE is a sub-system which uses a collection of
derived mapping programs based on PANACEA or other DTM's as input.
These are used in order to generate grids representing slope
steepness, slope aspect, height above sea level, and other
information that can be derived from the DTM. The DERIVATIVE system
also allows an interface to be created between the topographic DTM
and any areally associated imagery such as LANDSAT images in
classified, level-sliced, or raw-mode, and cartographic line/area

data.

MIRAGE: The MIRAGE system, currently under development, consists of a set of programs to perform a wide range of functions in the acquisition, registration, display, enhancement and analysis of monochrome or false-colour digital images. There are three basic types of module in this system:

(1) Operations initiated by the user to enter and format imagery from outside the system via magnetic tape.

(2) Image merging, combination, geometric rectification and registration processes.

(3) Real-time manipulation, classification and display.

All operations are menu-driven from a fully interactive question/ answer sequence. A series of utility programs also allows the user to read directly a range of satellite computer compatible tapes, such as LANDSAT, TIROS-NOAA, CZCS and HCMM.

Interaction is the most important underlying requirement of an image processing system. All image display functions are performed in real-time and involve no disk input/output delay as the images are stored in main memory or graphic memory if space permits. Thus the only limitation on update speed for this fully interactive phase is that imposed by the processor and memory and the parallel link to the colour hardware. The following basic operations are available:

(a) Windows are implemented whereby the user can allocate different parts of the monitor screen to hold different images, and hence operate on several images at one time.

(b) The images may be displayed either in monochrome or in false colour.

(c) Full incremental zoom and unzoom facilities are provided with automatic windowing.

(d) If the image in the memory is larger than the displayed image it is possible to 'roam' the image as required. If the image is in zoom mode then the roaming will maintain the zoom, thus allowing detailed inspection of the complete memory-held image. Any other images on display will remain 'locked' to the present focus of attention.

Arithmetic facilities include:

(a) Linear or histogram based contrast stretch methods using a Gaussian, uniform, or user supplied step function.

(b) Standard spatial convolution techniques are available using either a fast median filtering algorithm where the high-pass filtered image is formed as the subtraction of the low-pass filtered image, or by incorporating user defined filter weights such as the filter function (e.g. Robert's gradient, Laplacian).

(c) Edge detection options enable the user to define edge detection criteria adaptively over the image area.

(d) Frequency domain filtering using the Fast Fourier Transform can be undertaken. A range of bandpass and directional filters can also be used, and provision is made for user defined filter functions.

(e) Arithmetical facilities include addition, subtraction, functional transformations, multiplication and division (ratioing).

(f) Principal Components Analysis can be undertaken (Karhunen-Loeve) to replace the original images with the component score images. Alternatively, canonical transforms can be performed.

(g) A fast classifier is included as an option, based on either the parallelipiped method or a one-pass K- means algorithm. This is particularly useful for initial observation and exploratory studies, as it operates in near real-time. Alternative, but slower methods are also available. These include ISODATA, and maximum likelihood algorithms, and contain options to allow the user specification of class prior probabilities.

Various parts of these software systems, written in Fortran 77 for a Unix 68000 super-micro computer have been used for map analysis and output in the Derbyshire slope susceptibility mapping project. The large memory size that can be addressed by the Unix 68000 enables a fast response despite the system's slow disc transfers.

2.3 PEAK DISTRICT CASE STUDY

2.3.1 Introduction

Fig. 2.2 shows the study region (32.2 km by 29.0 km) used for the application of the Matrix Assessment Approach. The region (932 km^2) is divided into northern and southern sectors. MAP was initially applied to the southern sector and tested for its predictive accuracy in the northern sector. Details of the study area including its geomorphology, geology and Quaternary history have been discussed in Section 1. The distribution of landslides in the study region and the causes of instability have also been outlined in Section 1.
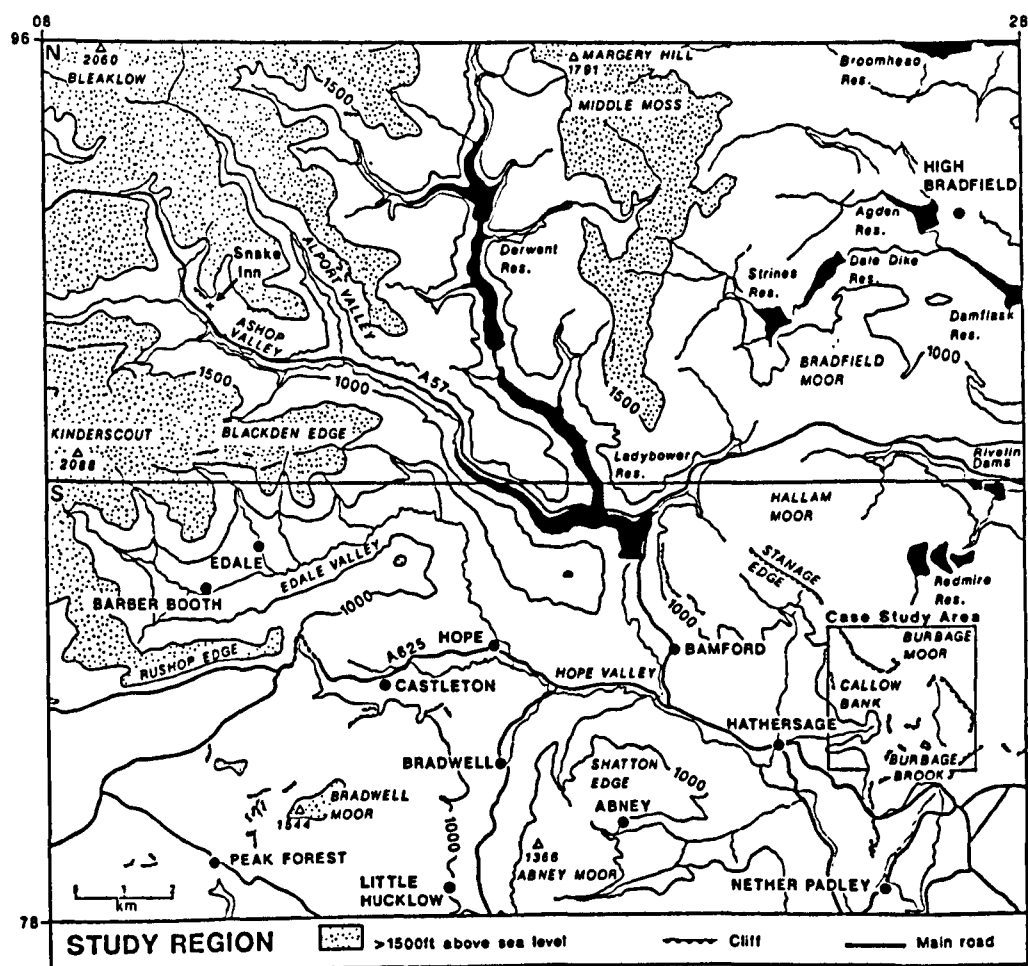

Fig.2.2 Map showing the study region used for the Matrix Assessment Approach.

2.3.2 Compilation of Base Maps

The compilation of base maps is discussed under three main headings:

(a) Base map extrapolation

(b) Grid cell sampling scheme

(c) Automated data acquisition

(a) Base Map Extrapolation

Just as the quality of hazard evaluation is improved by the use of more than one method of data collection, so further improvements can be made using more parameters, and more exact parameter determination. Data can usually be collected at a variety of levels, and this should be considered in relation to the constraints imposed by the project. Since natural ground conditions are subject to variability (Lumb, 1966, 1972), this must also apply to many of the parameters which control the mass movement system. Thus, where parameters are evaluated from extrapolation from maps, the degree of accuracy of the final susceptibility assessment must decrease because of the increased probability of local variation, with greater changes being expected if larger areas are to be investigated. This factor precludes the application of MAP for detailed site investigations, the technique is designed to be used for preliminary regional landslide assessment. Care should be exercised in interpreting data derived from an existing source. For example, geological maps are usually based on stratigraphical considerations and may conceal a large amount of internal lithological variability, both vertically

within a sequence and laterally within a geological unit.

(b) Grid Cell Sampling Scheme

The susceptibility assessment parameters differ in their spatial distributions, therefore, the measurement and cartographic representation can present problems. An ideal sampling unit to measure environmental parameters is the geomorphological unit (Geological Society, 1983) which contains a set of 'ground conditions' which differ from adjacent units across definable boundaries. Factors can be represented either within geomorphological units, if these have already been mapped; or alternatively, the unit can be derived from the superimposition of several factor-maps. However, the problem in using this approach is that the boundaries on the factor-maps do not usually coincide spatially. Also the fact that the maps may be derived from different sources coupled with errors resulting from operator variability will account for boundary discrepancies, even in high contrast landscapes. It is the intention of MAP to avoid as much subjective interpretation as possible.

One method of collecting data across the region is to use a grid cell sampling scheme. Although the use of such a scheme may result in the loss of some detail and boundary definition it does provide an approximate location of parameter boundaries depending upon the size of the grid unit used. The use of regular grid cells has several advantages, these include:

(i) Since all factor-maps used in MAP have common dimensions, the problem of parameter boundary variability does not arise.

(ii) A grid-based model in which terrain attributes are represented by data matrices is readily amenable to computation (data storage, retrieval and processing) and information is in a suitable form for statistical analysis.

(iii) By combining the information of the same grid cell on each factor-map final susceptibility classes can be rapidly evaluated objectively.

The assigned value of each parameter can be derived either by noting the value at the mid-point (or some other fixed point) of the cell, or by determining the largest area contained within the cell. In both cases, data relating to small (but perhaps critical) areas within each cell may be lost, therefore the problem of grid size and spacing is very important (Stevanovic et al., 1977) since the size of the grid mesh used controls the reliability of the parameter map produced; investigators should carefully select the size of the grid cell according to the physiographic characteristics of the study area and the scale of the original mapping (Tilmann et al., 1975). A smaller grid size will produce a more accurate map, but will be more expensive to produce in terms of factor-map production time, computer time and the data storage system. Taking into consideration the time needed for the data acquisition, the purposes of the project (i.e. preliminary assessment) and the quality and detail of the existing information such as topographic and geological maps, a grid cell size of 1.56ha has been selected to collect the environmental parameter data. Hence, a $15.6m^2$ grid network, referencing to the Ordnance Survey National Grid, has been superimposed on 1:25,000 scale base maps.

(c) Automated Data Acquisition

When computer programs are clearly set up, data acquisition is by far the most time-consuming and costly phase of the total process, and it may constitute a serious limitation to the application of MAP. There are, however, a number of simple techniques to automatically or semi-automatically obtain certain surface geometric attributes such as slope angle (Evans, 1972, 1979). Evans (1972) outlines a geomorphometric model based on five surface geometric attributes, altitude, gradient, aspect, vertical and horizontal convexity. These five attributes may be generated by an altitude matrix, which can in turn be obtained from topographic maps or aerial-photographs by various automated techniques such as a computer-supported stereoplotter (Anselmo & Godone, 1976). Data acquisition can be achieved through digitisation of contour lines, or sampling along regular profiles or grid points on topographic maps. In the absence of digitiser instruments and the necessary software to carry out automatic encoding of altitudinal data, terrain attributes were collected manually. A slope indicator chart was used for the interpolation of slope steepness from contour lines (Thrower & Cooke, 1968).

There are techniques commercially available to obtain digitised contour lines from topographic maps automatically through electronic scanners, lasers and pattern recognition methods (Fu, 1974), however, these tend to be very expensive. Perhaps in the future, the work involved in digitising a contour map may become unnecessary, since cartographic automation is already taking place at the survey stage of some U.K. mapping projects. As the technology for automatic data acquisition improves, and becomes commercially available at

competitive rates, it will allow in the future a significant

reduction in the time involved in data acquisition and encoding for

any terrain attribute. This trend will also be supplemented by the

use of higher resolution satellite imagery which is soon to become

more readily available. However, in view of the limited financial

and hardware resources available for this project the parameters used

in MAP were collected and encoded manually.

2.3.3 Application of the Matrix Assessment Approach

The Matrix Assessment Approach was applied to the southern sector as

shown in Fig. 2.2. Ordnance Survey 1:25,000 map sheets were used to

construct the base maps. A grid was placed over the O.S. maps, with

each grid square covering 1.56 ha ($15.6m^2$) of land. Corresponding

geological, superficial deposit and soil maps were also constructed

at the same scale. Information was then transferred from the base

maps onto the grid. Landslides were identified initially from

1:10,000 geological maps, and then boundaries were modified and

previously unmapped landslides were added to the base map through

aerial-photograph interpretation (1:12,000 panchromatic aerial-

photographs) and field mapping (Norman, 1970; Norman et al., 1975;

Carney, 1974). All classes of instability were included (see Table

1.4).

The geological and geomorphological attributes were collected, for

each cell, as follows:

1. Bedrock Geology: The largest area of bedrock type (>50%)

contained within the cell was assigned to that particular type using

7:50,000 and 1:25,000 Solid Geology maps.

2. Superficial Materials: The largest area of superficial material type (>50%) contained within the cell was assigned to that particular type using a combination of 1:25,000 Drift Geology maps and the 1:250,000 Soil Map of England and Wales.

3. Soils: The largest area of soil type (>50%) contained within the cell was assigned to that particular type using the original 1:25,000 map sheets used to compile the 1:250,000 Soil Map of England and Wales.

4. Bedrock Combination: The cell was classified according to whether it contained one particular bedrock type or a combination of two bedrock types using 1:50,000 and 1:25,000 Solid Geology maps.

5. Height above sea level: The height value (in feet) at the mid-point of the cell was recorded using 1:25,000 Ordnance Survey maps.

6. Relative Relief: The height difference (in feet) between the highest and lowest contours within the cell was recorded using 1:25,000 Ordnance Survey maps.

7. Height above the valley floor: The difference in height (in feet) between the elevation recorded at the mid-point of the cell and the elevation of the valley floor perpendicular to successively lower intervening contours using 1:25,000 Ordnance Survey maps.

8. Aspect: The compass direction (degrees of azimuth) of a line drawn perpendicular to the contour lines within the cell using 1:25,000 Ordnance Survey maps.

Table 2.5   Slope Aspect Classification

Fine Classification	Coarse Classification
1. N (1)	1. N,NE
2. NE (1)	2. E,SE
3. E (2)	3. S,SW
4. SE (2)	4. W,NW
5. S (3)	
6. SW (3)	
7. W (4)	
8. NW (4)	

Table 2.6   Relative Relief Classification

Fine Classification	Coarse Classification
1. 0 - 25 (1)	1. 0 - 25
2. 25 - 50 (2)	2. 25 - 75
3. 50 - 75 (2)	3. 75 - 125
4. 75 - 100 (3)	4. 125 +
5. 100 - 125 (3)	
6. 125 - 150 (4)	
7. 150 + (4)	

Table 2.7   Height above the Valley floor Classification (ft)

Fine Classification	Coarse Classification
1. 0 - 100 (1)	1. 0 - 200
2. 100 - 200 (1)	2. 200 - 400
3. 200 - 300 (2)	3. 400 - 600
4. 300 - 400 (2)	4. 600 - 700
5. 400 - 500 (3)	5. 700 +
6. 500 - 600 (3)	
7. 600 - 700 (4)	
8. 700 - 800 (5)	
9. 800 + (5)	

Table 2.8   Height above sea level Classification (ft)

Fine Classification	Coarse Classification
1. 0 - 250 (1)	1. 0 - 500
2. 250 - 500 (1)	2. 500 - 1000
3. 500 - 750 (2)	3. 1000 - 1500
4. 750 - 1000 (2)	4. 1500 +
5. 1000 - 1250 (3)	
6. 1250 - 1500 (3)	
7. 1500 - 1750 (4)	
8. 1750 + (4)	

Table 2.9   Superficial Deposits Classification

Fine Classification

1. Head (1)
2. Hill Peat (2)
3. River Terraces (3)
4. Brown Earths (4)
5. Iron Pan Stagnopodzols (5)
6. Brown Podzolic Soils (5)
7. Cambic Stagnohumic Gley Soils (6)
8. Humic Rankers (7)
9. Brown Rankers (7)
10. Cambic Stagnogley Soils (6)
11. Humic Ferric Podzols (5)

Coarse Classification

1. Head
2. Hill Peat
3. River Terraces
4. Brown Earths
5. Brown Podzolic Soils
6. Stagnogley Soils
7. Rankers

Table 2.10   Soils Classification

Fine Classification

1. Typical Brown Earths (5.41) (Trusham, Bearstead 1, Malham 1 & 2, Rivington 2, Crediton) (4)
2. Raw Oligo-fibrous Peat Soils (10.11) (Winter Hill) (1)
3. Cambic Stagnogley Soils (7.13) (Brickfield 3, Bardsey, Dale) (3)
4. Iron Pan Stagnopodzols (6.51) (Newport 1) (2)
5. Cambic Stagnohumic Gley Soils (7.21) (Wilcocks 1) (3)
6. Humo Ferric Podzols (6.31) (Angelzark) (2)
7. Typical Brown Podzolic Soils (Withnell 1) (2)
8. Rankers (3.13) (Crwbin, Vetton 1) (5)
9. Typical Brown Alluvial Soils (5.61) (6)

Coarse Classification

1. Raw Peat Soils (10.1)
2. Brown Podzolic Soils (6.1)
3. Stagnogley Soils (7.1)
4. Brown Earths (5.4)
5. Rankers (3.1)
6. Brown Alluvial Soils (5.5)

Table 2.11   Bedrock Geology Classification

Fine Classification

1. Edale Shale (d_4) (Namurian Millstone Grit Series). (1)
2. Kinderscout Grit (KG) (Kinderscoutian R_1). (2)
3. Shale Grit (SG) (Kinderscoutian R_1). (2)
4. Mam Tor Beds (MT) (Kinderscoutian R_1). (3)
5. Monsal Dale Beds (Mo), Knoll Reefs (K), Flat Reefs (Kf), Litton Tuff (Z),
   Lower Millers Dale Lava (B_{11}), (Monsal Dale Group d_{3b}). (4)
6. Bee Low Limestones (BL), Apron Reefs (Rap), Woo Dale (W), Dolerite
   (Igneous Intrusives) (D), Volcanic Tuff (V), (Bee Low Group d_{3b}). (4)
7. Rivelin Grit (RG), Redmire Flags (RE), Heydon Rock (HR), (Marsdenian
   R_2). (5)
8. Crawshaw Sandstone (CRS) (Lower Coal Measures d_{6a}). (5)
9. Rough Rock (R) (Rough Rock Group). (6)
10. Lower Coal Measures (d_{6a}) (Lower Coal Measures d_{6a}). (6)
11. Eyam Limestones (EM), Longstone Mudstone (LSM) (Eyam Group). (4)

Coarse Classification

1. Edale Shales (d_4) (Namurian Millstone Grit Series)
2. Kinderscout Grit (KG), Shale Grit (SG), (Kinderscoutian R_1)
3. Mam Tor Beds (MT), (Kinderscoutian R_1)
4. Dinantian (Carboniferous Limestone Series d^{2-3})
5. Marsdenian R_2 and Yeadonian R_2
6. Lower Coal Measures (d_{6a})

Table 2.12   Slope Steepness Classification (Percentage)

Fine Classification	Coarse Classification
1. 0 - 10	1. 0 - 15
2. 10 - 20	2. 15 - 35
3. 20 - 40	3. 35 - 70
4. 40 - 50	4. 70 +
5. 50 - 75	
6. 75 +	

Table 2.13 Bedrock Combination Classification

Fine Classification

1. Edale Shale (d_4). (1)
2. Shale Grit (SG), Kinderscout Grit (KG).(Kinderscoutian R_1). (2)
3. Mam Tor Beds (MT). (Kinderscoutian R_1). (3)
4. Dinantian. (Carboniferous Limestone Series d^{2-3}). (4)
5. Rivelin Grit (RG), Redmire Flags (RE), Heydon Rock (HR) (Kinderscoutian R_1), Crawshaw Sandstone (CRS) (Lower Coal Measures). (5)
6. Lower Coal Measures (ds_a). (7)
7. Edale Shale/Kinder Scout Grit Group combinations (SG/d_4, KG/d_4) (Kinderscoutian R_1) (8)
8. Mam Tor Beds/Edale Shale (MT/d_4) (Kinderscoutian R_1) (2)
9. Mam Tor Beds/Kinderscout Grit Group combinations (MT/SG,MT/KG) (Kinderscoutian R_1) (2)
10. Edale Shale/Middle Grit Group combinations (d_4/HR,d_4/RG,d_4/RE) and Edale Shale/Rough Rock Group combinations (d_4/R) (Marsdeian R_2, Yeadonian G_1) (5)

Coarse Classification

1. Edale Shale (d_4).
2. Kinderscout Grit, Shale Grit, Mam Tor Beds/Kinderscout Grit, Mam Tor Beds/Shale Grit.
3. Mam Tor Beds, Edale Shales/Mam Tor Beds.
4. Dinantian (Carboniferous Limestone Series d^{2-3}).
5. Middle Grit Group, Rough Rock Group, Edale Shale/Middle Grit Group, Edale Shale/Rough Rock Group.
6. Lower Coal Measures.
7. Edale Shale/Kinderscout Grit, Edale Shale/Shale Grit.

9. Slope Steepness: The slope was derived from the 1:25,000 Ordnance Survey map, by converting the contour intervals within each cell by means of a slope indicator chart mounted on stable acetate film into percentage of slope (Thrower & Cooke, 1968).

Each susceptibility attribute along with its class sub-division are shown in Tables 2.5 to 2.13. The attributes are classified in two ways; firstly a fine classification to obtain maximum information by sub-division into as large a set as could easily be discriminated, and secondly a coarse classification using fewer sub-divisions. As will be shown, the consequence of having a fine classification involving a large number of classes (which satisfies the natural desire to have as much detail retained as possible) increases the ultimate load in terms of data analysis. The greater the sub-division for each attribute the greater will be the possible number of combinations of attributes that have to be examined. Tables 2.5 to 2.13 include (by numbers in parenthesis) the way in which the attributes can be combined in a coarse classification in order to reduce the total number of combinations that have to be considered.

2.3.4 Computer Analysis and Mapping

The process of creating the landslide susceptibility grid from the nine terrain attributes has been described theoretically above. The practical problem lies in handling the total possible combinations ($>4 \times 10^6$) when using the fine sub-division of all nine attributes. However, the maximum possible number of combinations for the Derbyshire case study area is 11,520,(the grid consists of 72 rows and 160 columns, 72 x 160 = 11,520 possible unique combinations). The number of zero entries in a table of all possible combinations

will therefore be high, because of this fact the data storage and
retrieval system is designed so that only those combinations actually
in use are retained for the rest of the analysis. This means that
data storage for all 4 million combinations is unnecessary, and when
a susceptibility ratio has been calculated for each cell a vast
search is not required to find any given combination.

Rather than creating an actual nine dimensional matrix in the
computer memory, a data base structure has been implemented to index
only those combinations that exist. This approach has to maintain
rapid access to the data and should know unequivocally when a given
combination has not been accessed, firstly, the use of a disc based
linked direct access hierarchical file structure, and secondly, the
use of a memory held hash table. Both methods were tried; the first
method had the advantage of smaller process size, but an inversely
large number of input/output disk operations; whereas the second
method was very rapid, but also could occupy a large process space.
Both algorithms could be used for query response situations where the
user wanted a single answer to a specific question rather than a
continuous stream of random data. Input/output overheads are such
that the hash table approach was considered to be much more
appropriate for a super-micro system, such as that used for this
study, which had in the region of 1mb of memory available for any
given process. The hash table approach was therefore used. The
operation of such data structure systems is outlined in Pfaltz
(1977).

2.3.5 Program Details

The computer program used to calculate the landslide susceptibility index is given in the Appendix (see Table A2). Fig. 2.3 shows a flow diagram of the various steps involved in the program for a case using seven attributes.

A level structure was used as an efficient way of processing and storing the grid cell data. On the first level, seven records exist, one for each class interval of that attribute. In each of these records there are eleven pointers relating to the eleven categories of the second attribute (superficial deposits). These pointers point to level 2 i.e. the first pointer on the fourth record on level 1 will relate to a grid square which involves the fourth class sub-division (Mam Tor Beds) for the first attribute (bedrock) and the first class sub-division (Head) for the second attribute (superficial deposits). Similarly, there will be a pointer from level 2 to level 3 and so on until level 7 is reached. As the level increases there will be a corresponding increase in the number of records, since the number of combinations will increase. In the seventh level a count of grid cells (grid cells = 1.56 ha) with particular combinations within landslide areas (LAF) and those cells devoid of landslides is kept using a memory held hash table in order to calculate the (RAF). When a new grid cell is accessed a certain pathway is followed through the appropriate levels depending upon the combination of attribute sub-classes until the seventh level is attained, or the pathway terminates in which case a new path is created linking the terminating point to the seventh level. The landslide susceptibility index (LSI) can be calculated for every grid square in turn once all the combinations that exist have been determined, and a tally kept of
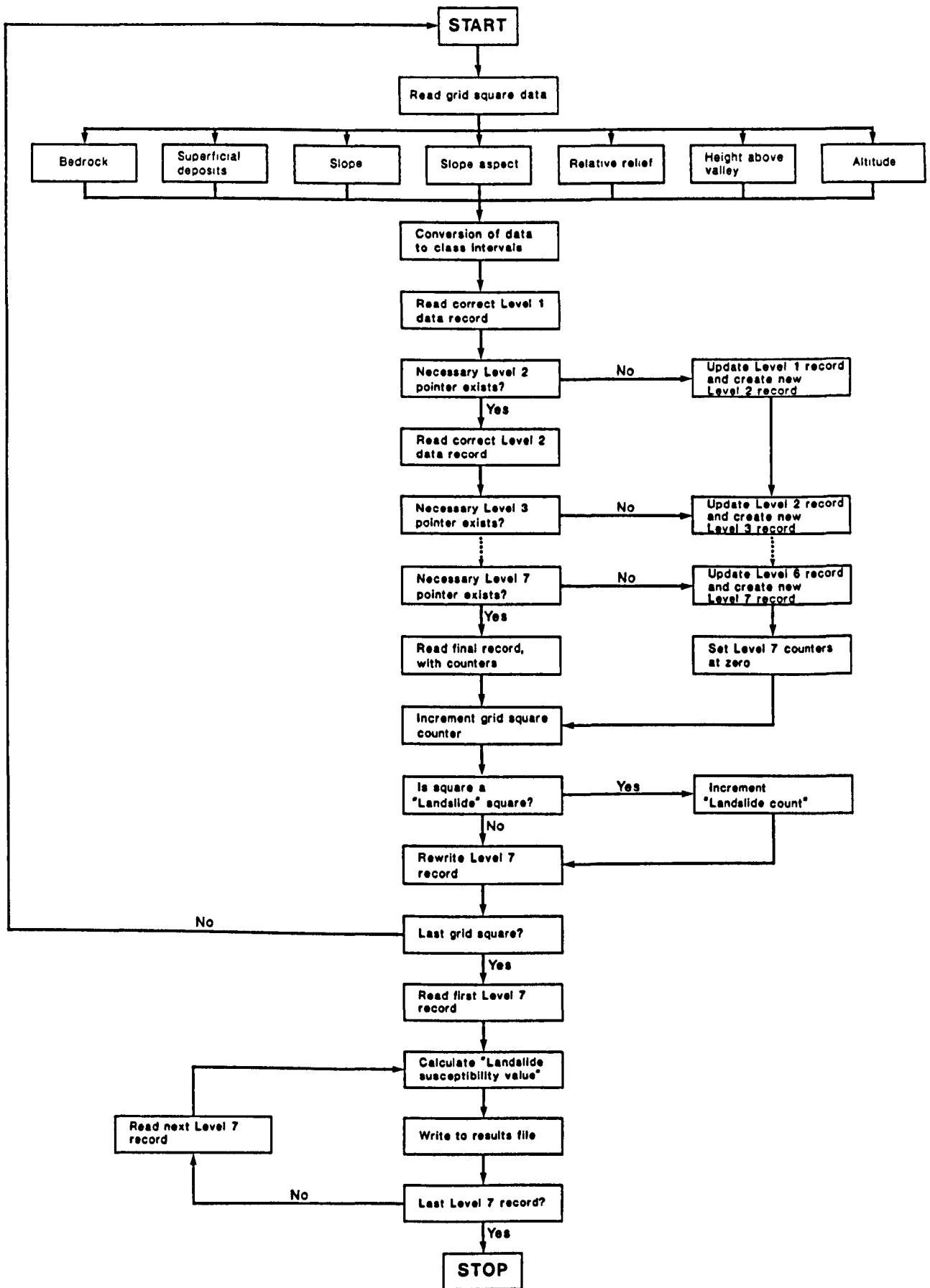
Fig.2.3 Flow diagram to show the various steps involved in the program for the Matrix Assessment Approach for a case using seven geological/geomorphelogical parameters.

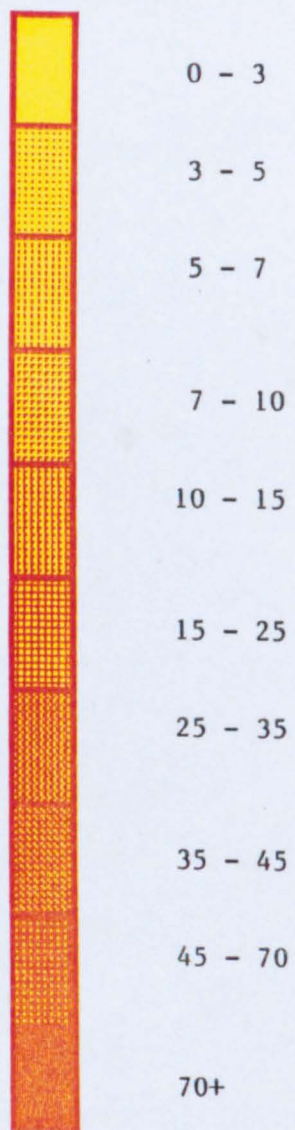the number of (RAF) cells containing that combination and the number of (LAF) cells with that combination.

The landslide susceptibility index (LSI) have been computed for the detailed nine attribute full class sub-division, and also for a limited number of attributes and reduced class sub-divisions in order to compare the (LSI) ratios obtained and to study the sensitivity of the (LSI) ratios to altered classification systems. The reason why this has been done is a practical one. If it is possible ultimately to obtain an acceptable answer to landslide susceptibility by using either fewer (than nine) attributes and/or a coarser class sub-division (of the selected attributes) then the amount of data acquisition and handling is greatly reduced. This in turn, has the advantageous implications in respect to the computer memory size required for the susceptibility assessment.

The nine variables used in the Matrix Assessment Approach along with landslide location are shown in Figs. 2.4 to 2.12. The PANTONE halftone mapping output system (one of the units of the PANACEA Digital Terrain Model system) was used to produce variable maps of slope steepness, relative relief, height above sea level and height above valley floor, these are shown in Figs. 2.4, 2.5, 2.6 and 2.7 respectively. The grids have been output on an inkjet printer with each grid cell being a single 3 by 3 halftone unit. The MIRAGE mapping system was used to produce the coloured maps of bedrock geology, bedrock combination, slope aspect, superficial deposits and soils, these are shown in Figs. 2.8, 2.9, 2.10, 2.11 and 2.12 respectively.

Figs. 2.13(S) & 2.13(N) show the critical constraining gradients for various land uses including road building as classified by Goudie (1981).

Fig. 2.4S   Southern Sector of the study region
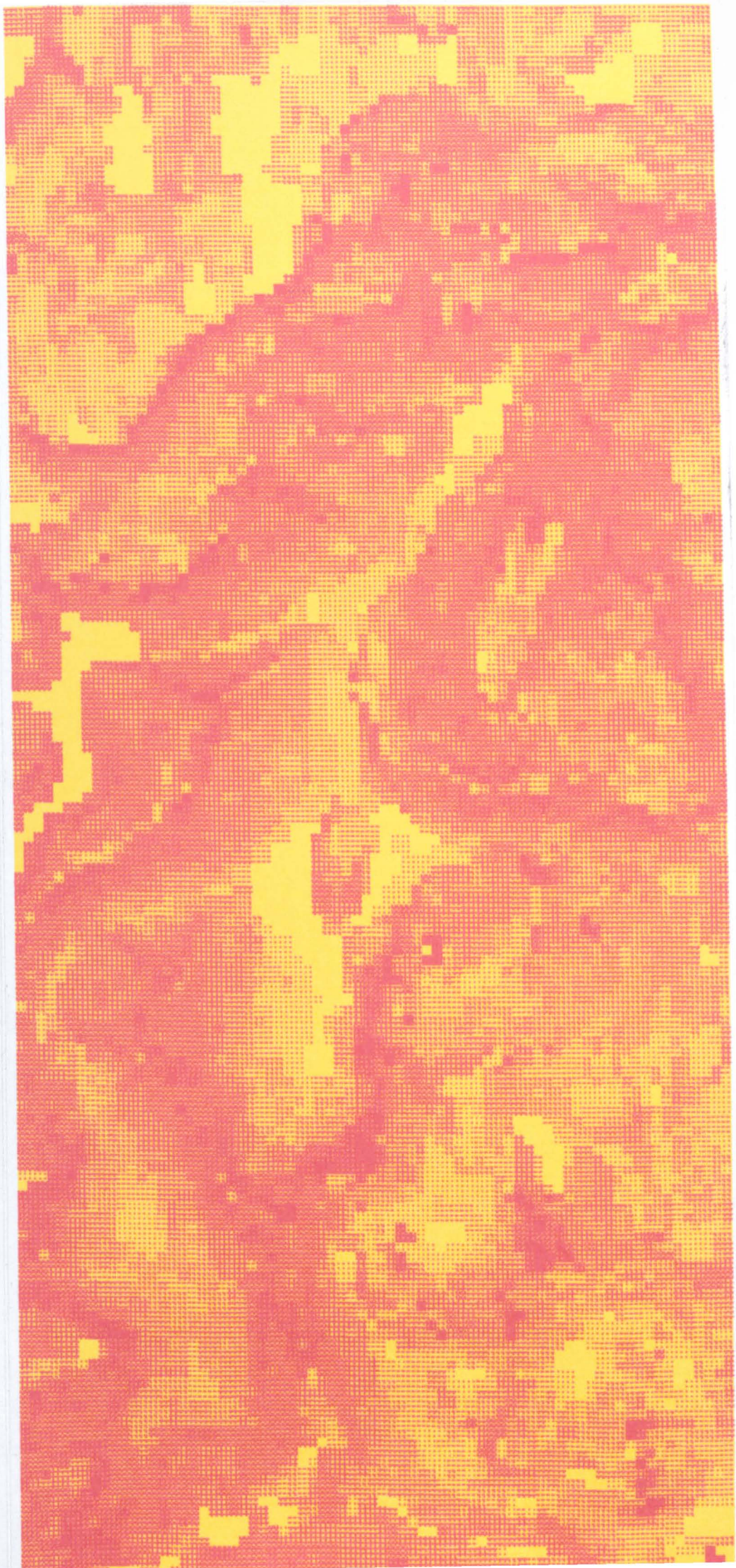
Slope Steepness (Percentage)

0 - 3

3 - 5

5 - 7

7 - 10

10 - 15

15 - 25

25 - 35

35 - 45

45 - 70

70+

Fig. 2.4N   Northern Sector of the study region

Slope Steepness (Percentage)

0 - 3

3 - 5

5 - 7

7 - 10

10 - 15

15 - 25

25 - 35

35 - 45

45 - 70

70+

Fig. 2.5S   Southern Sector of the study region

Relative relief (feet)

Reservoirs

0 - 20

20 - 40

40 - 60

60 - 80

80 - 100

100 - 120

120 - 140

140 - 160

160+

Fig. 2.5N   Northern Sector of the study region

Relative relief (feet)

Reservoirs

0 - 20

20 - 40

40 - 60

60 - 80

80 - 100

100 - 120

120 - 140

140 - 160

160+

Fig. 2.6S   Southern Sector of the study region

Height above sea level (feet)

Reservoirs

400 - 600

600 - 800

800 - 1000

1000 - 1200

1200 - 1400

1400 - 1600

1600 - 1800

1800 - 2000

2000+

Fig. 2.6N   Northern Sector of the study region

Height above sea level (feet)

Reservoirs

400 - 600

600 - 800

800 - 1000

1000 - 1200

1200 - 1400

1400 - 1600

1600 - 1800

1800 - 2000

2000+
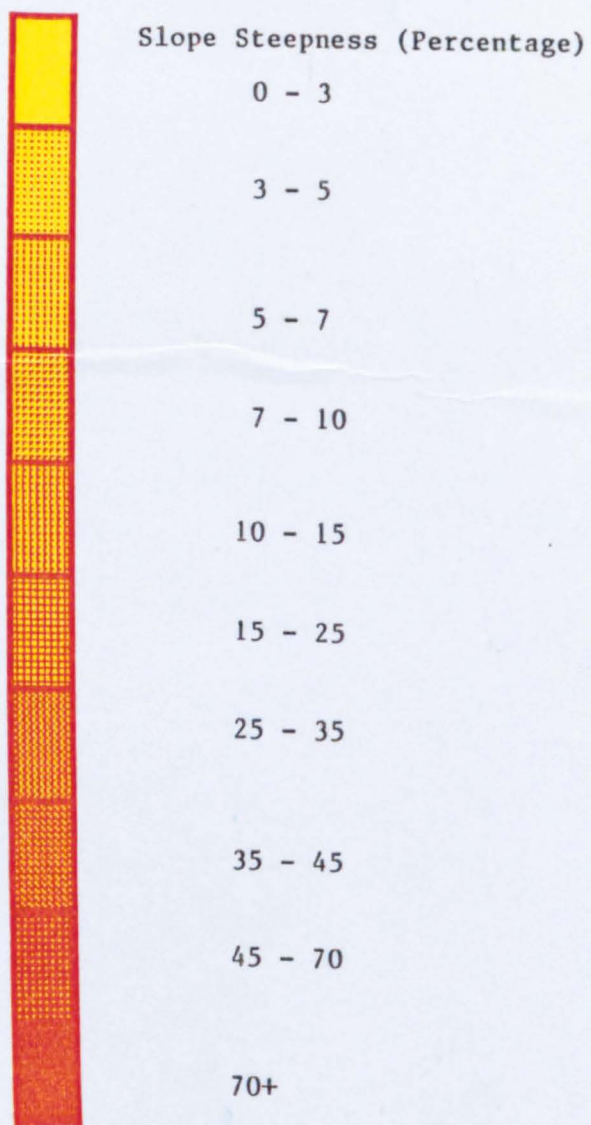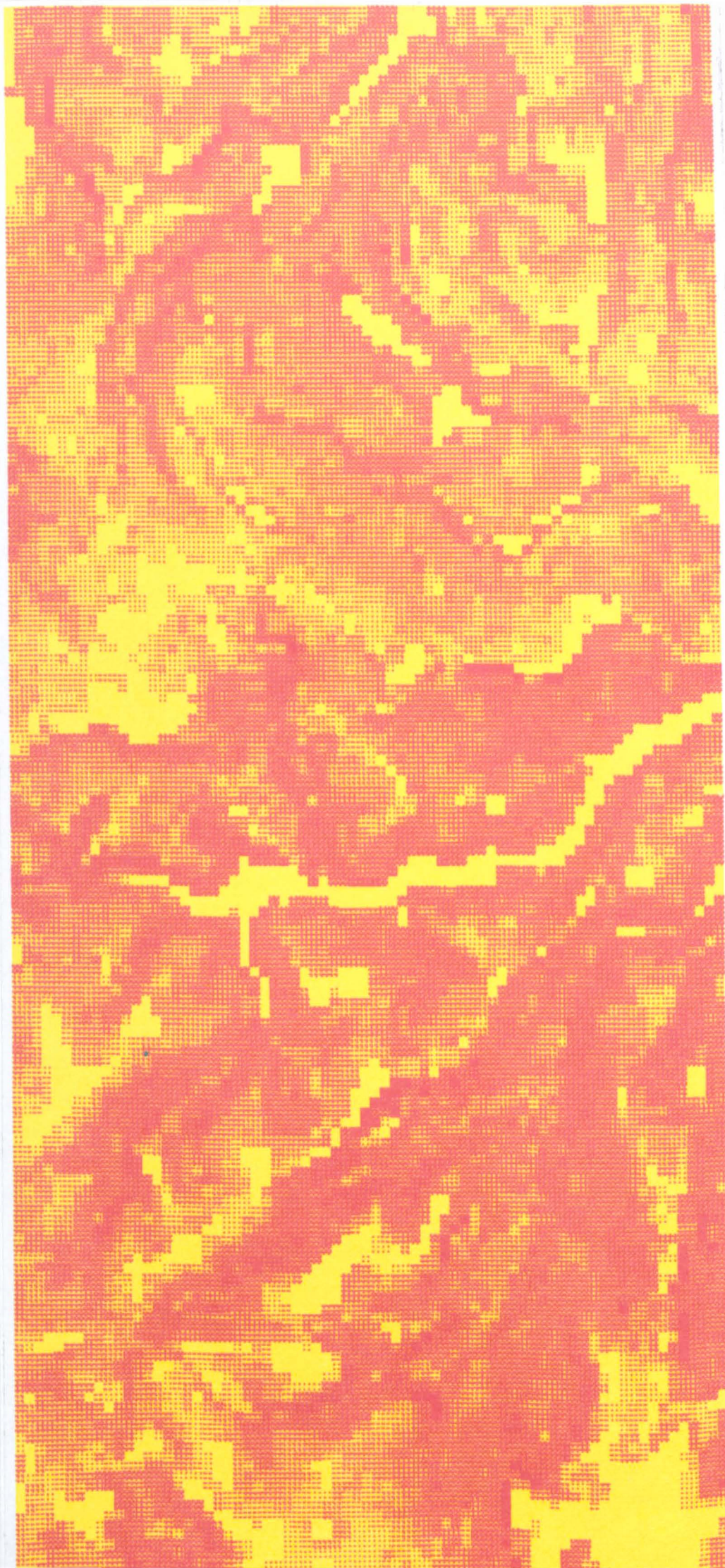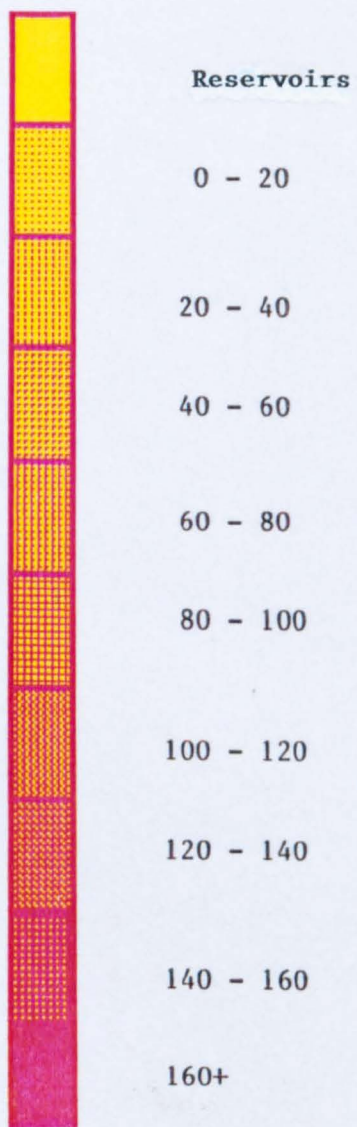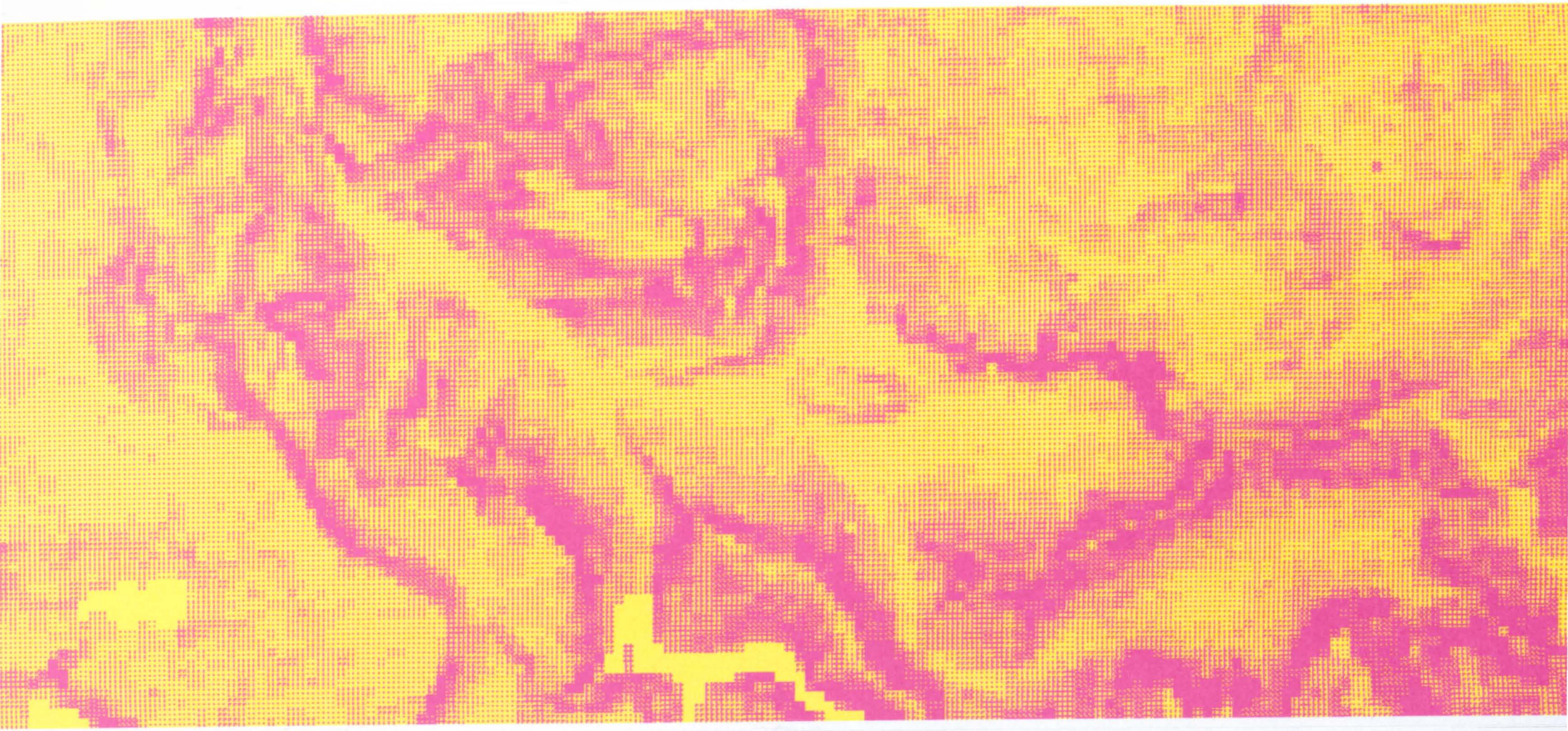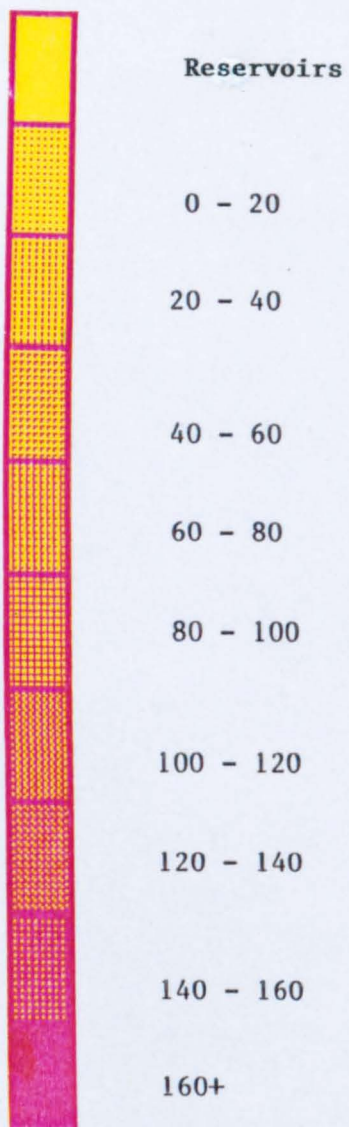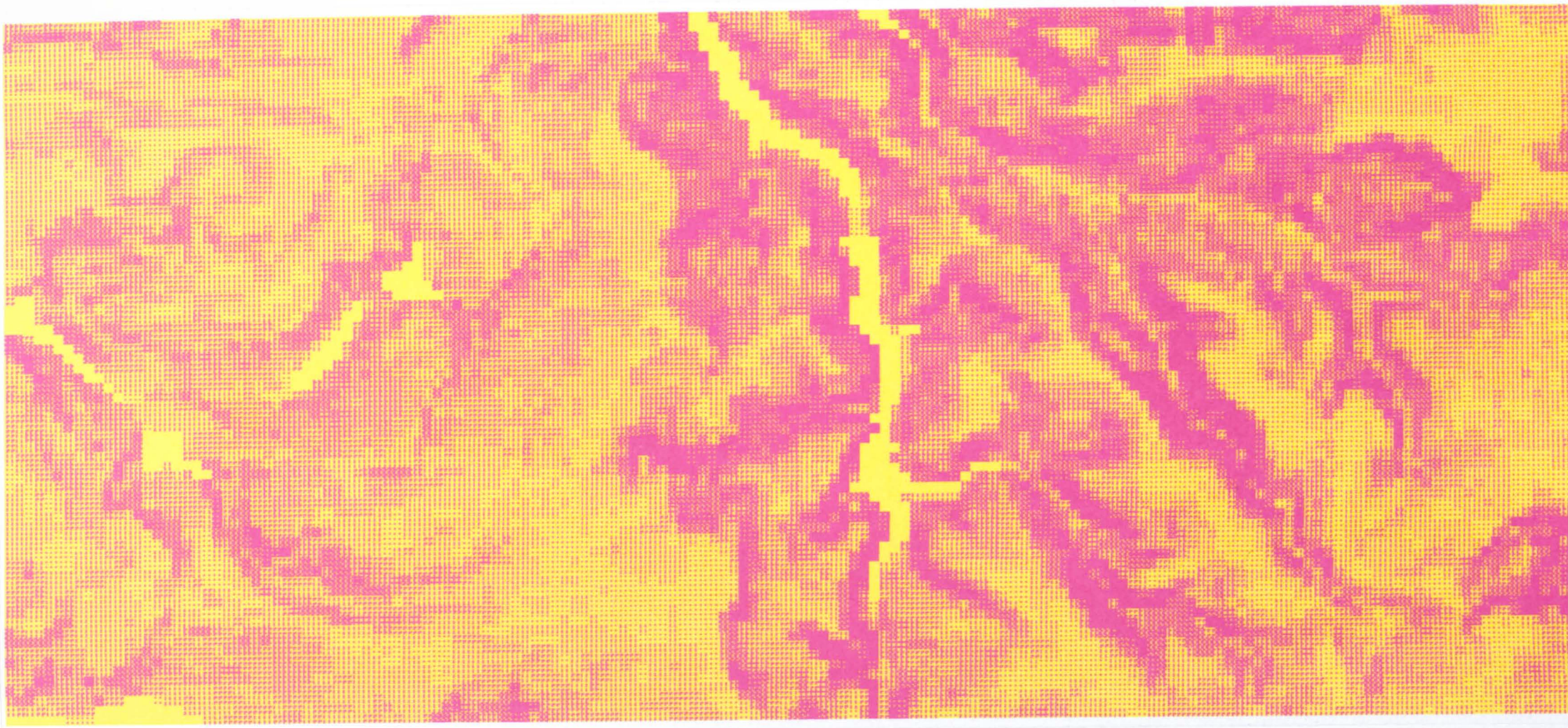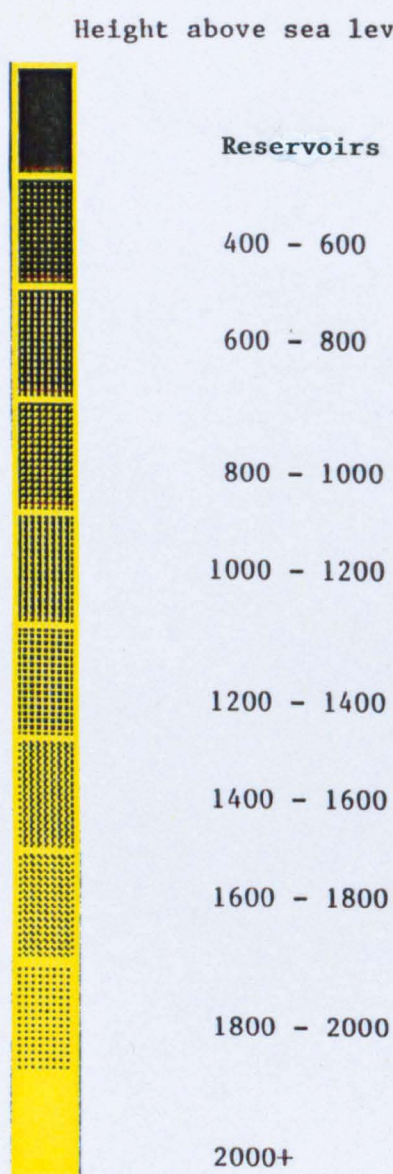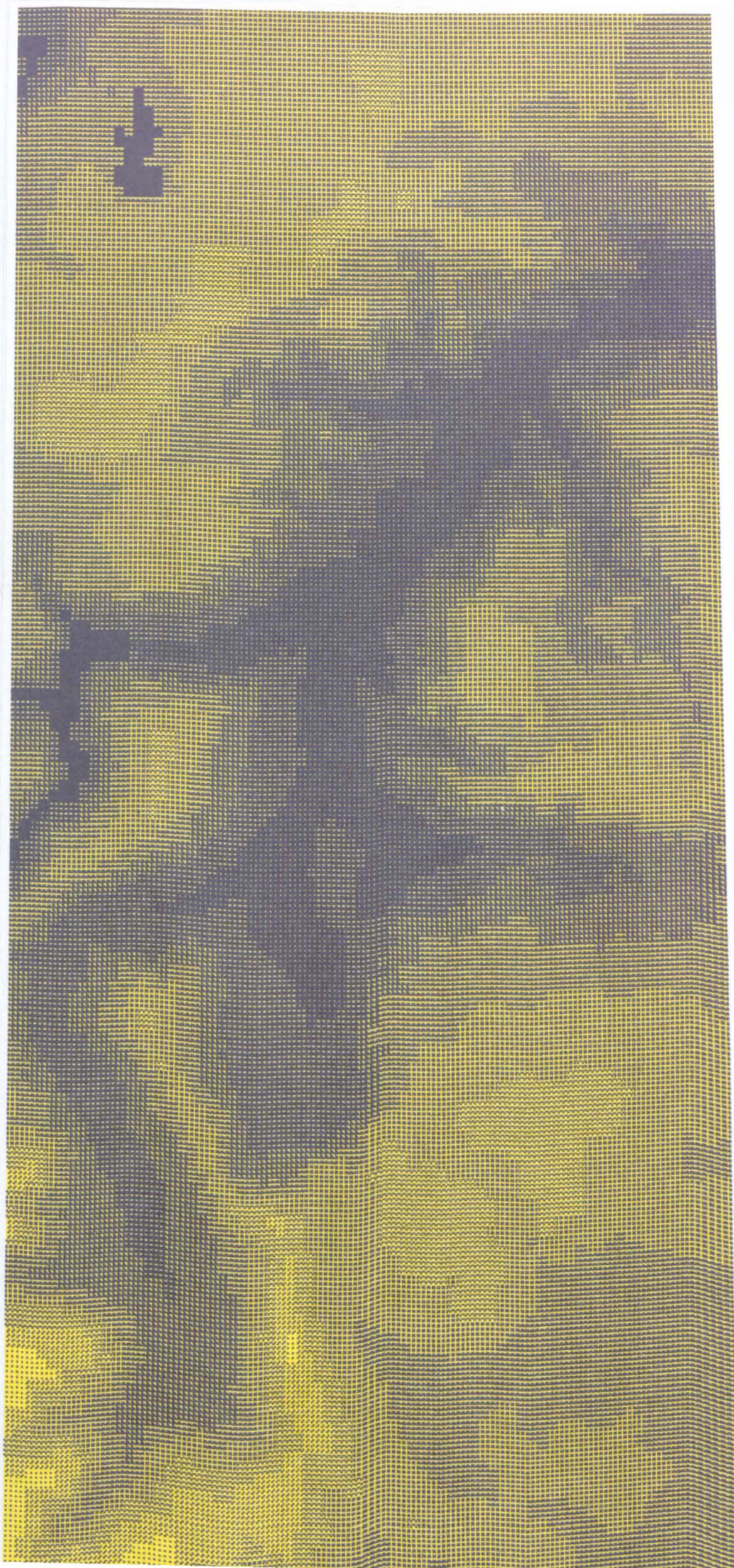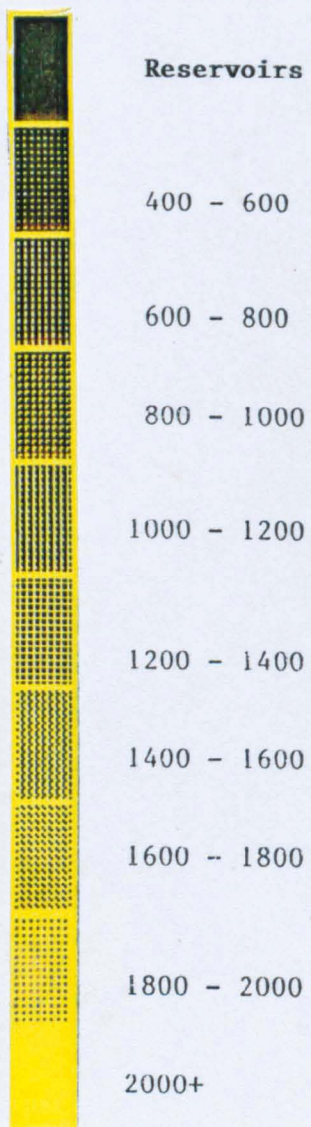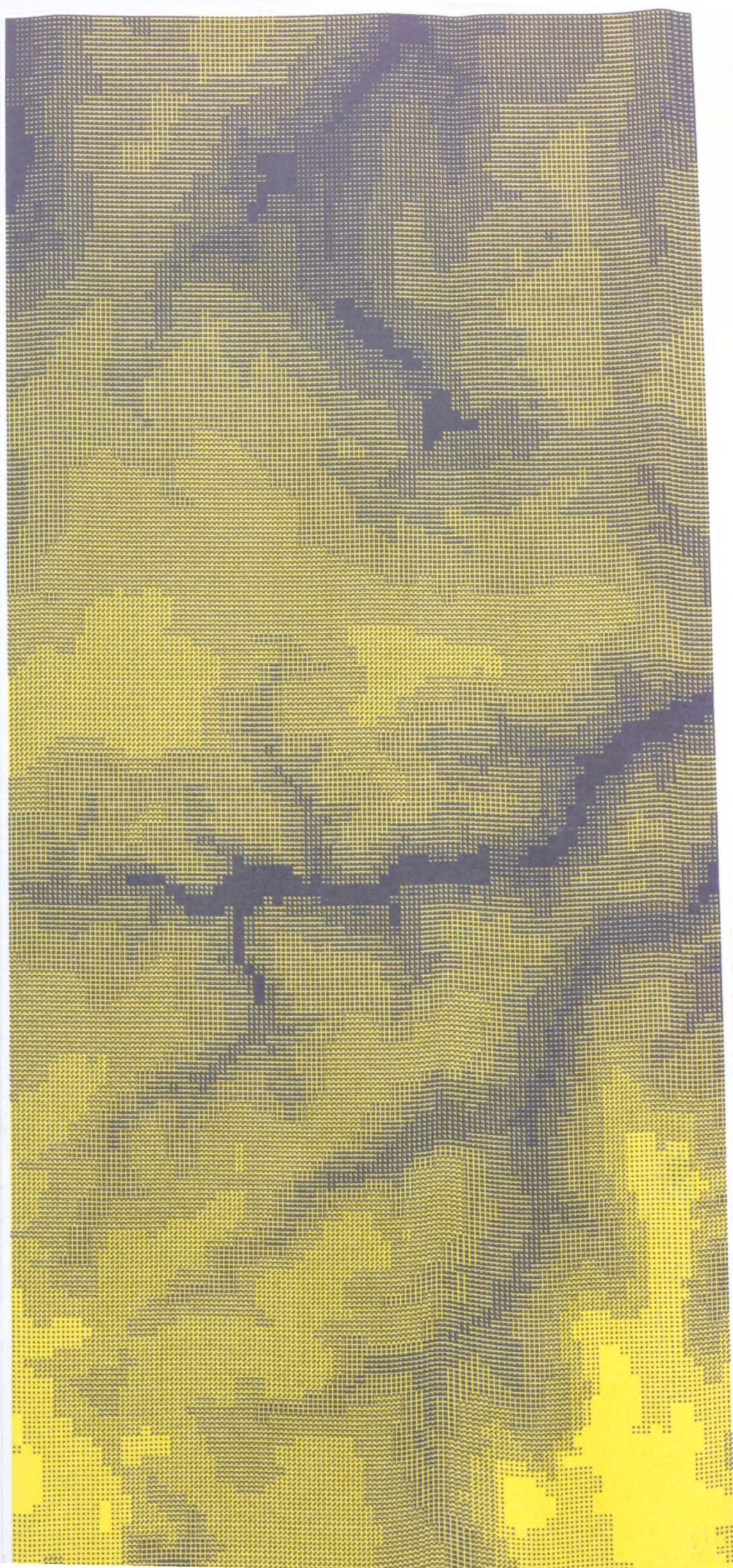
Fig. 2.7S   Southern Sector of the study region

Height above valley floor (feet)

0 - 20

20 - 40

40 - 60

60 - 90

90 - 120

120 - 160

160 - 220

220 - 300

300 - 450

450+
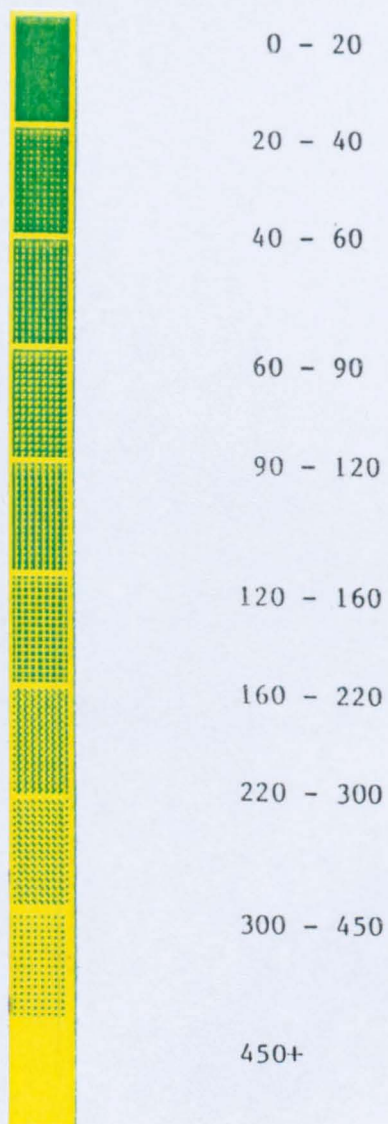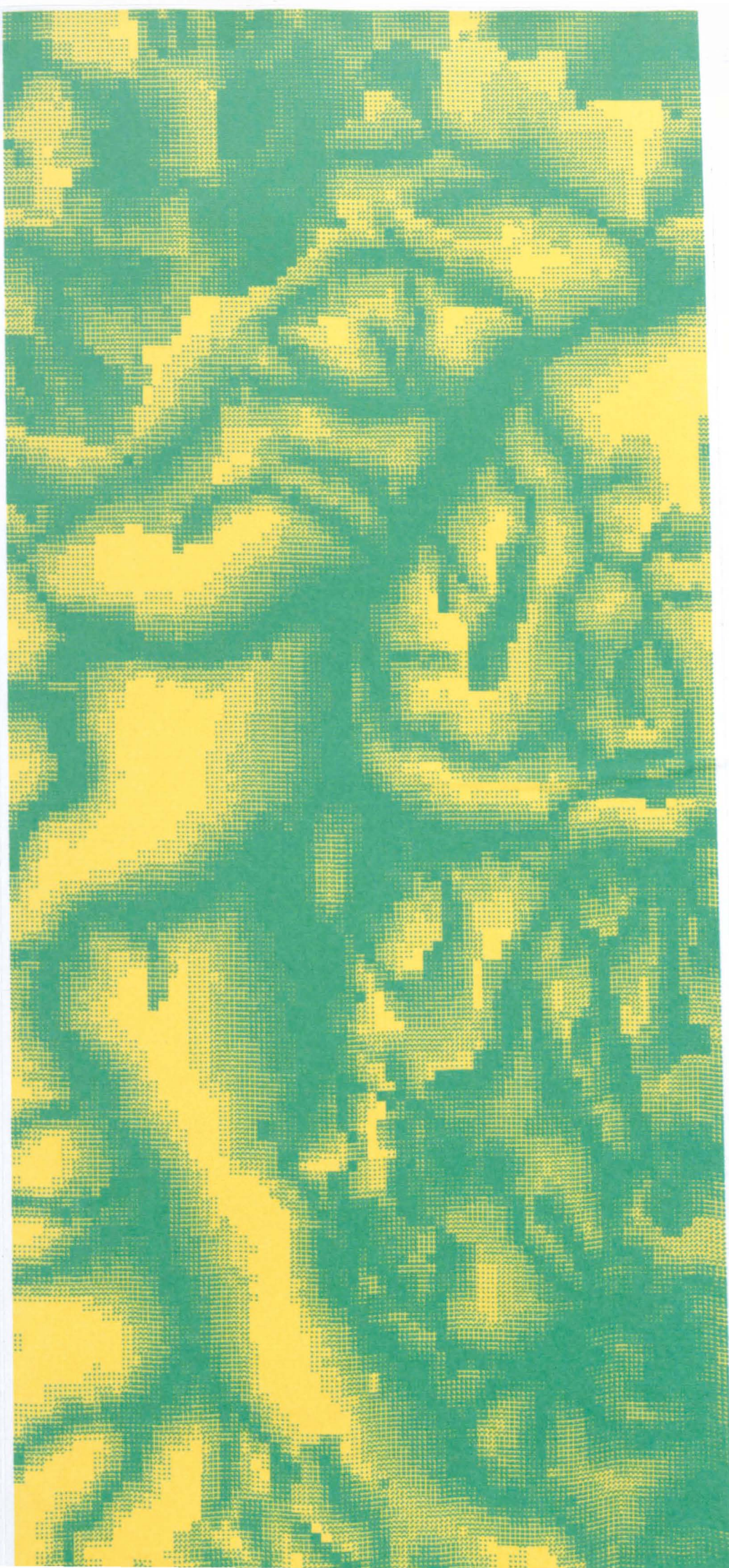
Fig. 2.8S   Southern Sector of the study region

Bedrock Geology

Edale Shales (d4) (Namurian Millstone Grit series)

Kinderscout Grit (KG), Shale Grit (SG) (Kinderscoutian R1)

Mam Tor Beds (MT) (Kinderscoutian.R1)

Dinantian (Carboniferous Limestone Series d^{2-3})

Marsdenian R_2 and Yeadonian R_2

Lower Coal Measures d^{sa}

Reservoirs

Fig. 2.8N   Northern Sector of the study region

Bedrock Geology

Edale shales (d4) (Namurian Millstone Grit series)

Kinderscout Grit (KG), Shale Grit (SG) (Kinderscoutian Rl)

Mam Tor Beds (MT) (Kinderscoutian Rl)

Dinantian (Carboniferous Limestone Series d^{2-3})

Marsdenian R_2 and Yeadonian R_2

Lower Coal Measures d^{sa}

Reservoirs
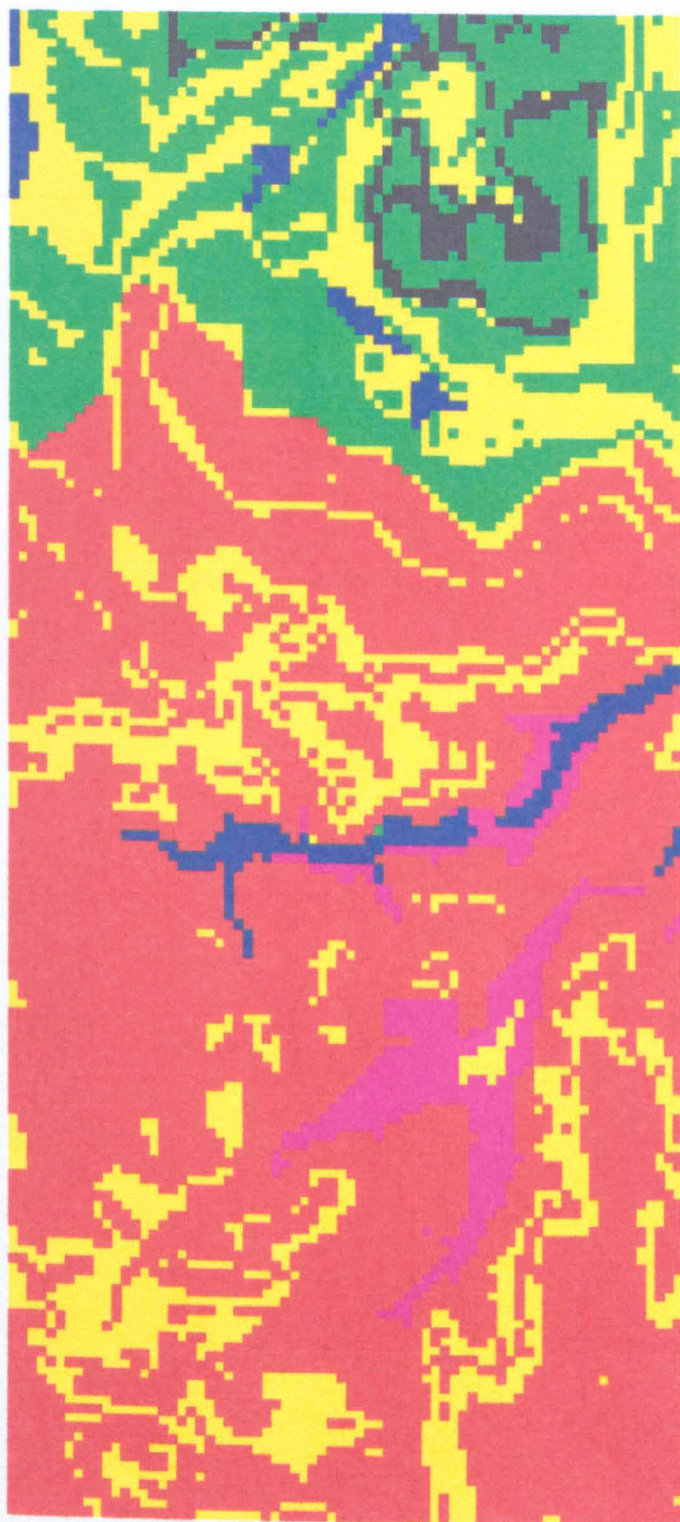
Fig. 2.9S   Southern Sector of the study region

Bedrock Combination

○ Edale Shale (d4)

● Kinderscout Grit, Shale Grit, Mam Tor Beds/Kinderscout

    Grit, Mam Tor Beds/Shale Grit

● Mam Tor Beds, Edale Shales/Mam Tor Beds

● Dinantian (Carboniferous Limestone Series d2-3)

● Middle Grit Group, Rough rock Group, Edale

    Shale/Middle Grit Group, Edale Shale, Rough

    Rock Group

● Lower Coal Measures

● Edale Shale/Shale Grit, Edale Shale/Kinderscout Grit

● Reservoir

Fig. 2.10S Southern Sector of the study region

Slope Aspect

●   N, NE

●   E, SE

●   S, SW

●   W, NW

●   Reservoirs
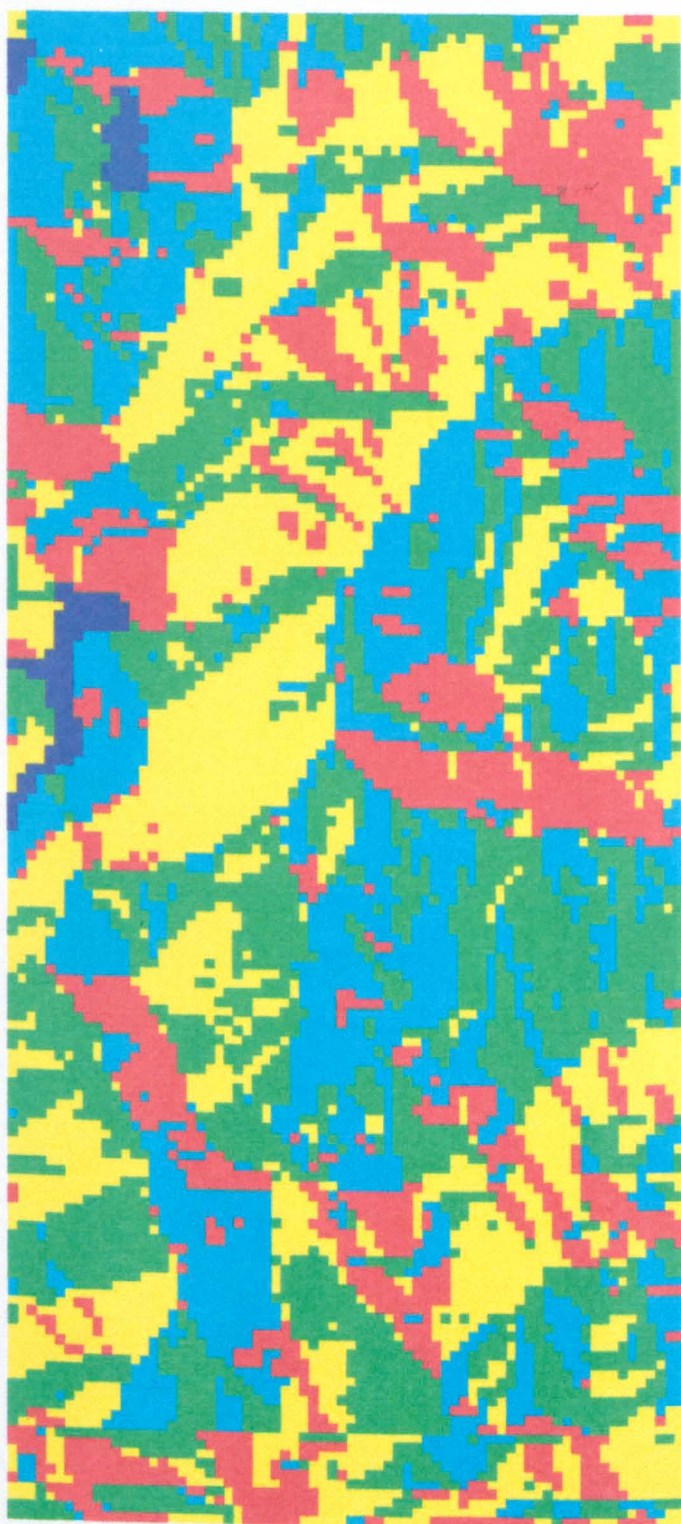
Fig. 2.11S Southern Sector of the study region

Soils

●   Raw Peat soils (10.1)

●   Brown Podzolic soils (6.1)

●   Stagnogley soils (7.1)

●   Brown Earths (5.4)

●   Rankers (3.1)

●   Reservoirs

See Table A3 in the Appendix for the
Classification of Major Soil Groups
and Subgroups in the study region.

Fig. 2.12S Southern Sector of the study region

Superficial Deposits

Head

Hill Peat

River Terraces

Brown Earths

Brown Podzolic soils

Stagnogley soils

Rankers

Reservoirs

Fig. 2.13S   Southern Sector

Critical Gradients for Road Construction

(Percentage), (Goudie, 1981)

0 - 2

2 - 4.5

4.5 - 12

12 - 19

19 - 36

36+
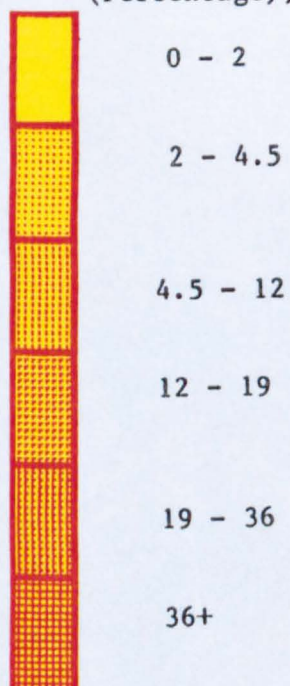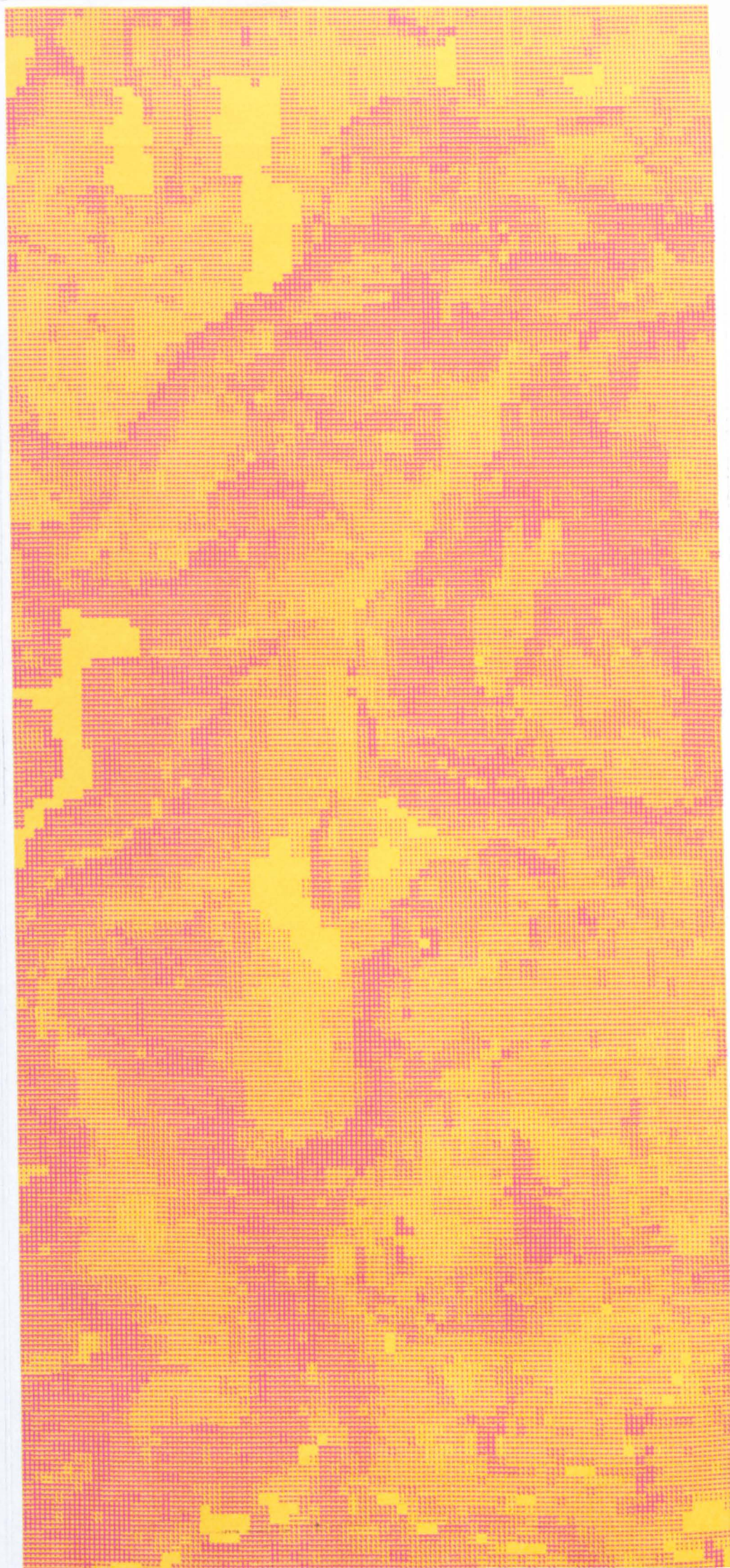
Fig. 2.13N   Northern Sector

Critical Gradients for Road Construction

(Percentage), (Goudie, 1981)

    0 - 2

    2 - 4.5

4.5 - 12

12 - 19

19 - 36

36+
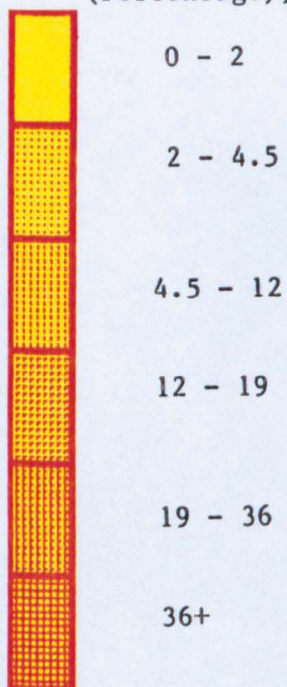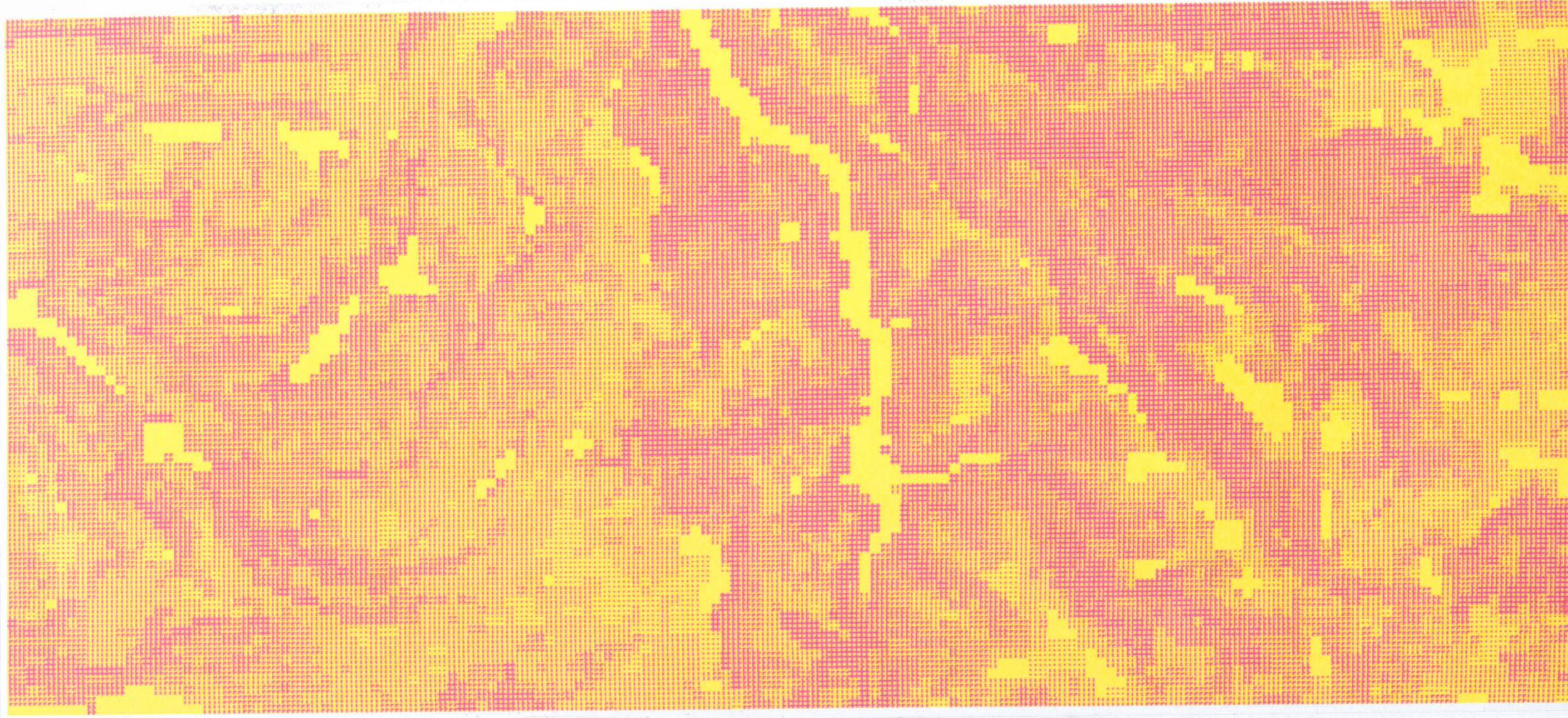
Fig.2.14S   Southern Sector of the study region
Landslide Distribution.
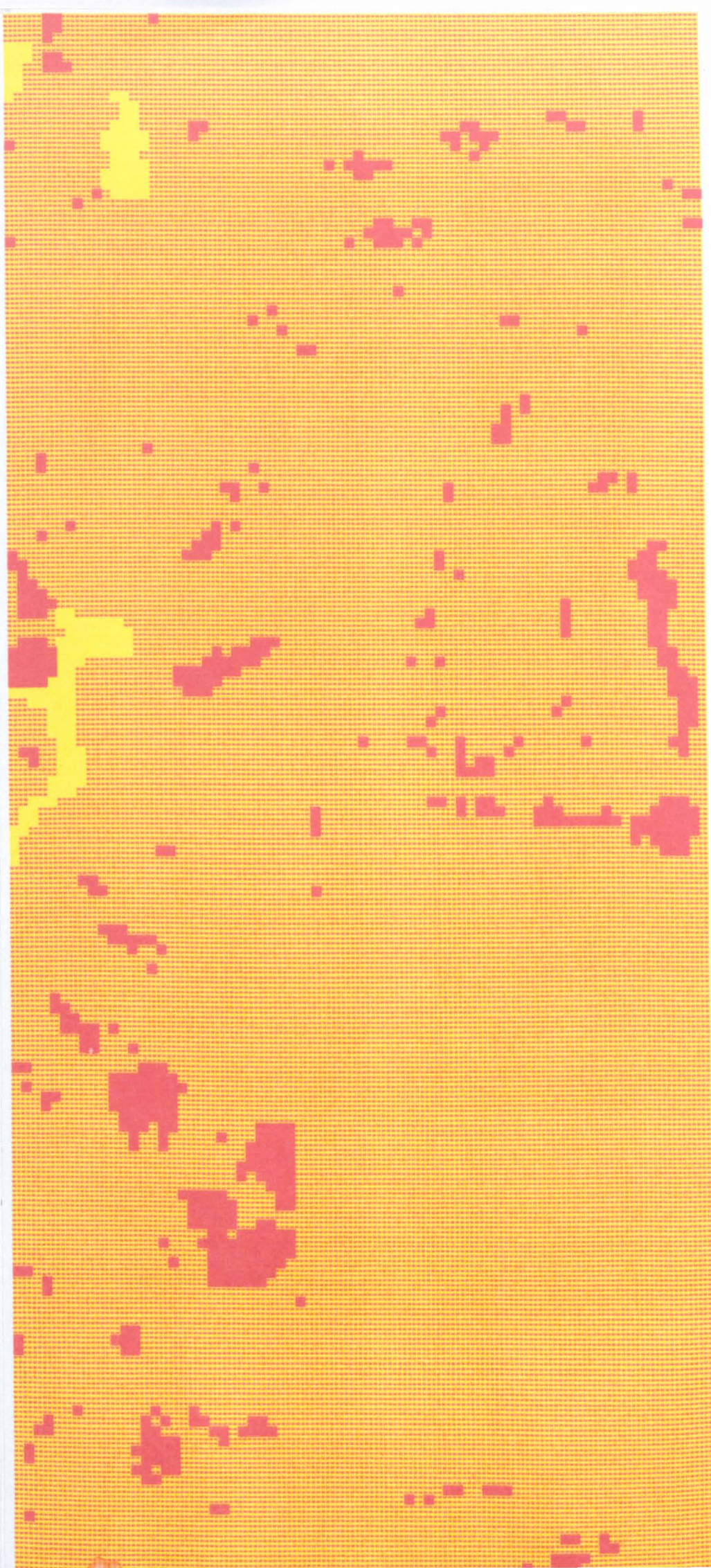
Fig.2.14N   Northern Sector of the study region
Landslide Distribution.
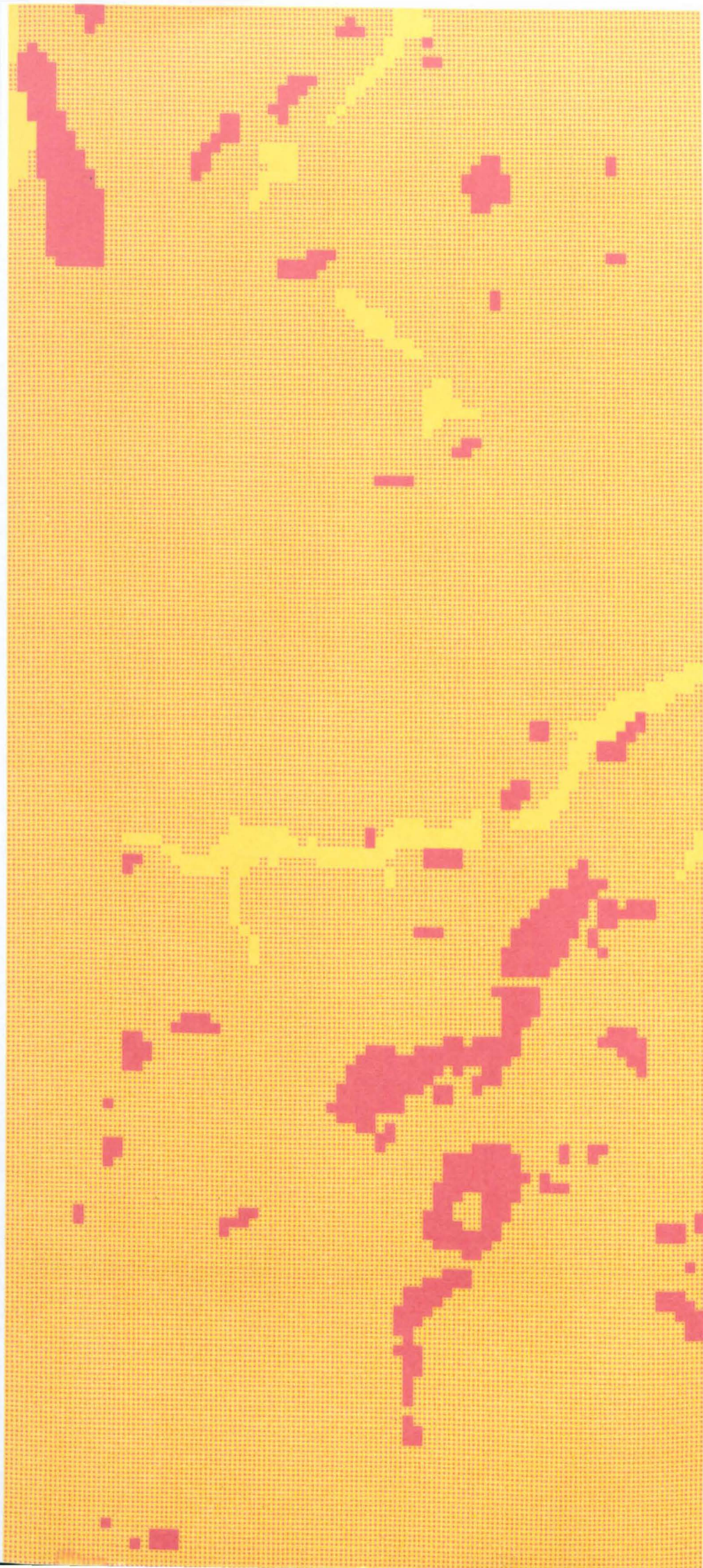
2.4 RESULTS

Fig. 2.15(S) shows the spatial distribution of landslide susceptibility index ratios (LSI) for all nine attributes using the full class sub-division. The rigid classification used in this case tended to give either a high LSI ratio or a low one with few intervening values. As the number of attributes was reduced but still retaining the fine class sub-division the LSI ratios decreased in magnitude, but tended to cover a larger area of the total study area (see Figs. 2.17(S), 2.19(S), 2.20(S), 2.21(S), 2.22(s), 2.23(S), 2.24(N), 2.28(S), 2.29(S), 2.30(S), 2.31(N)). Figs. 2.16(S), 2.18(S), 2.23(S), 2.26(N), 2.27(N), 2.32(S), 2.33(N), 2.34(N), show the effects of reducing the class set for varying attribute combinations. The Figures with a reduced class set show that LSI ratios tended to decrease in magnitude when fewer attributes were involved and covered a larger area when compared with their attribute combination counter-part using the fine classification.

The Matrix Assessment Approach requires to be considered in two ways:

1. Does the reduction in data (i.e. reducing the number of attributes and the class set) used in the case study degrade the results to an unacceptable point?

2. Has the technique successfully identified a classification of slope susceptibility to landsliding?

Landslide Susceptibility Index Classes

Fine Classification   Coarse Classification
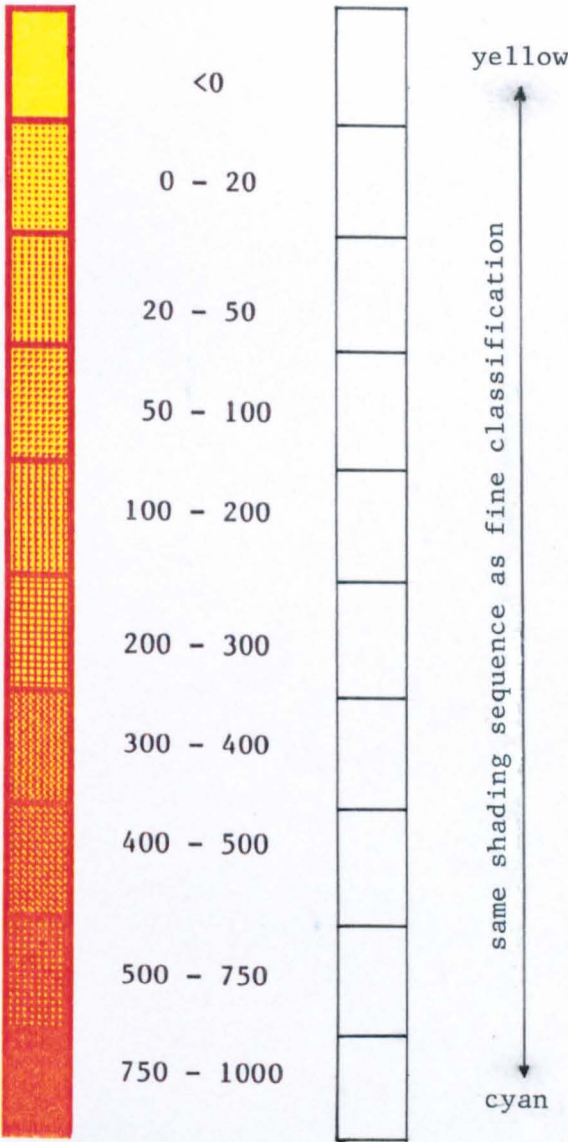
Fig. 2.15 S   Southern Sector of the study region

Nine Attributes, fine classification

1. Slope Aspect

2. Superficial Deposits

3. Bedrock Geology

4. Relative Relief

5. Height above valley floor

6. Slope steepness

7. Height above sea level

8. Bedrock Combination

9. Soils
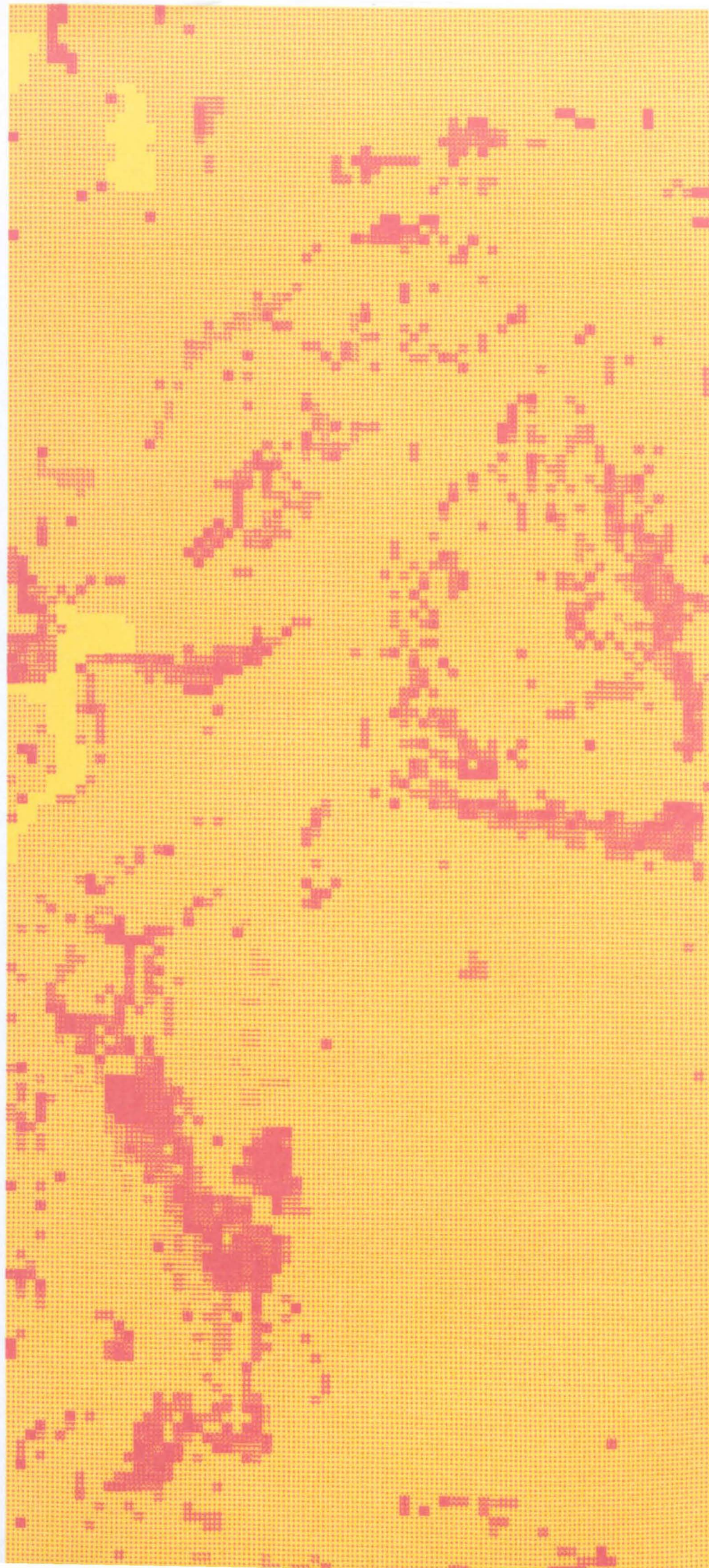
Fig. 2.16S   Southern Sector of the study region

Nine Attributes, reduced classification

1. Slope Aspect

2. Superficial Deposits

3. Bedrock Geology

4. Relative Relief

5. Height above valley floor

6. Slope steepness

7. Height above sea level

8. Bedrock Combination

9. Soils
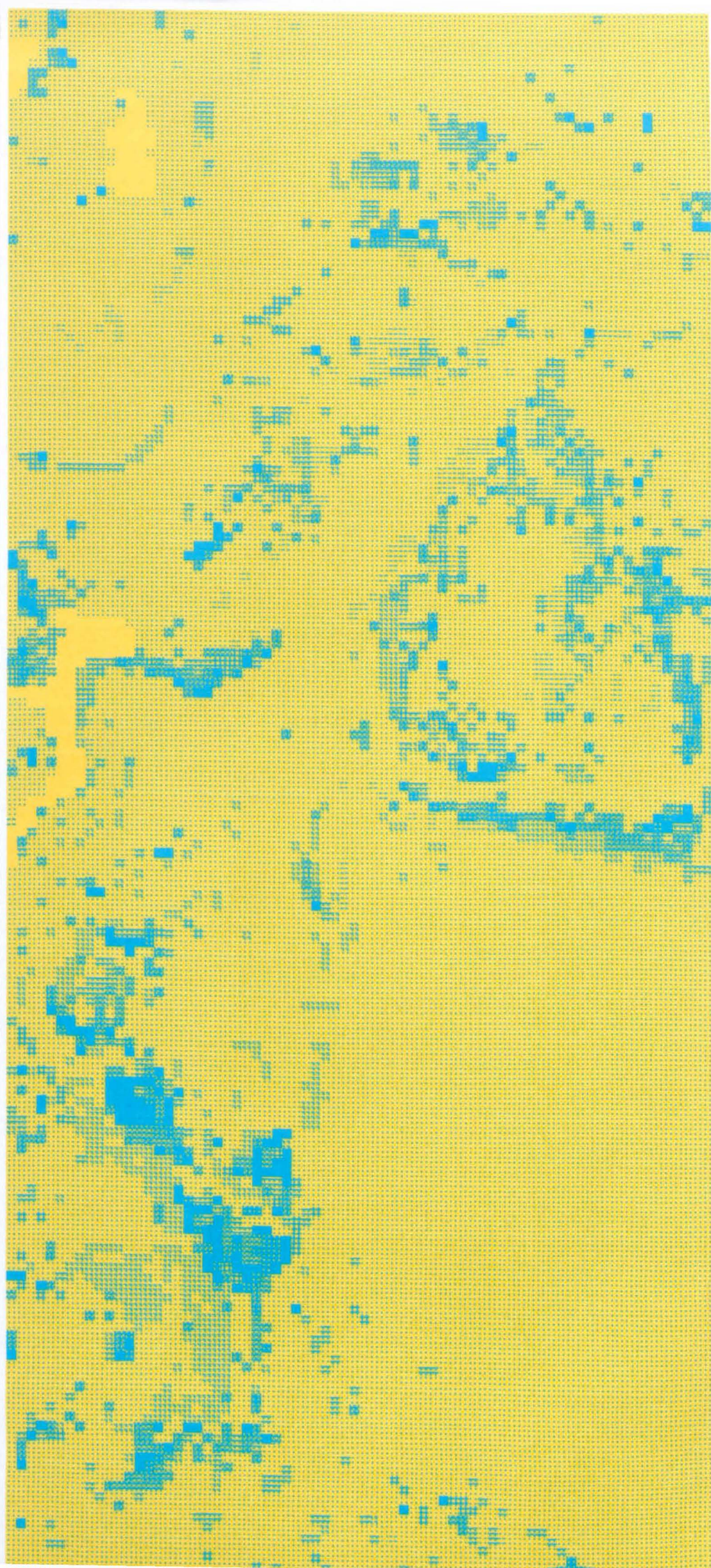
Fig. 2.17S   Southern Sector of the study region

Seven Attributes, fine classification

1. Slope Aspect

2. Superficial deposits

3. Bedrock Geology

4. Relative Relief

5. Height above valley floor

6. Slope steepness

7. Height above sea level

Fig. 2.18S   Southern Sector of the study region

Seven Attributes, reduced classification

1. Slope Aspect

2. Superficial Deposits

3. Bedrock Geology

4. Relative Relief

5. Height above valley floor

6. Slope steepness

7. Height above sea level

Fig. 2.19S   Southern Sector of the study region

Five Attributes, fine classification

1. Slope Aspect

2. Bedrock Geology

3. Relative Relief

4. Height above valley floor

5. Slope steepness
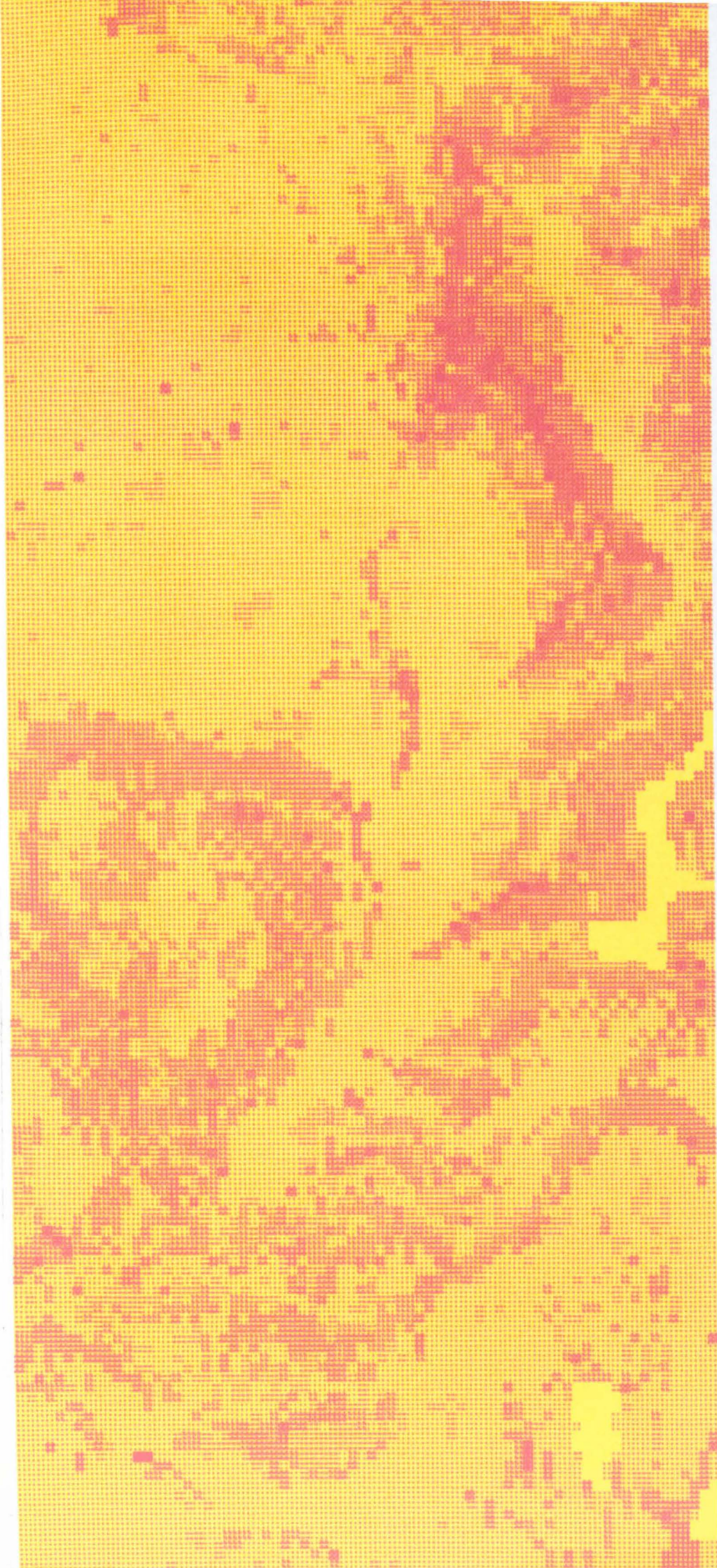
Fig. 2.20S   Southern Sector of the study region

Four Attributes, fine classification

3. Bedrock Geology

4. Relative Relief

5. Height above valley floor
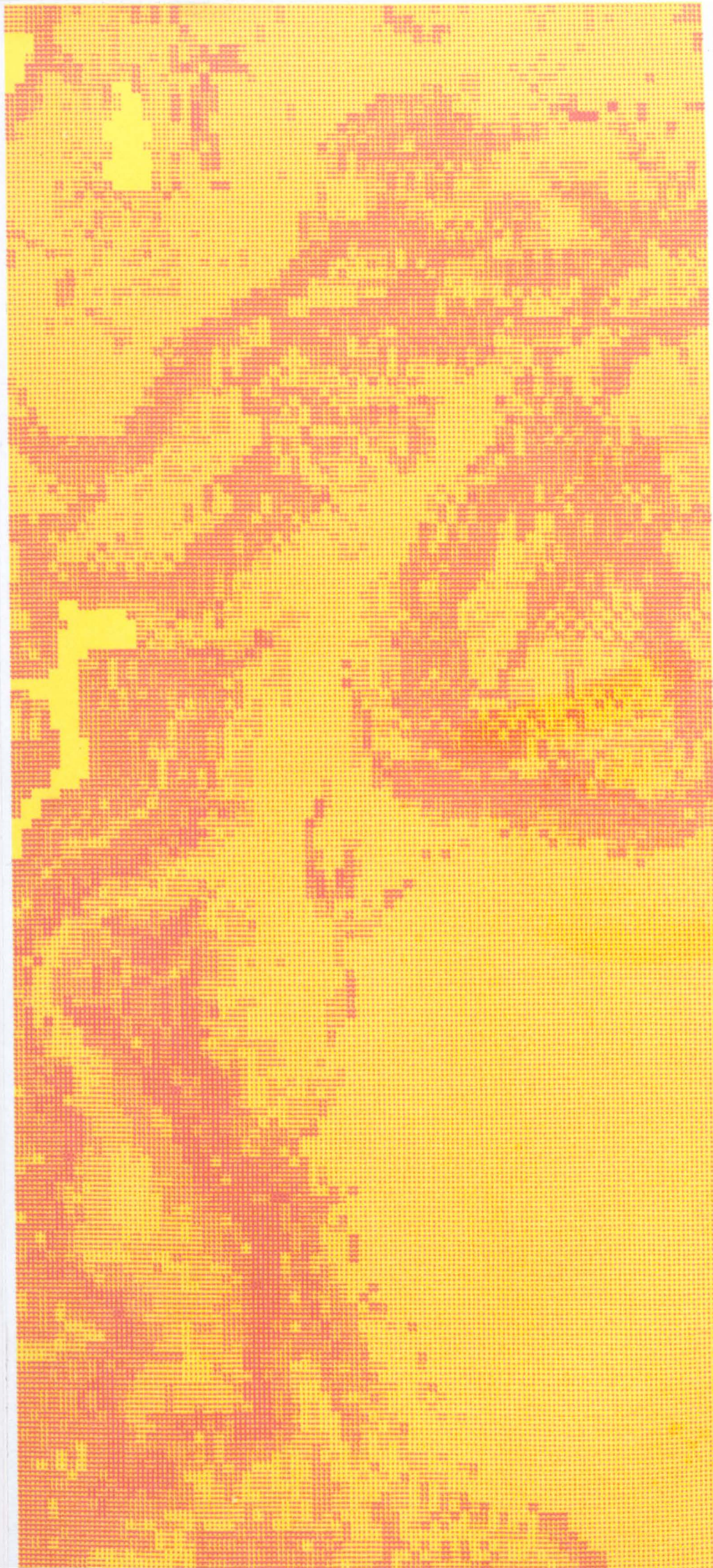
6. Slope steepness

Fig. 2.21S   Southern Sector of the study region

Four Attributes, fine classification

1. Slope Aspect

4. Relative Relief

6. Slope steepness

8. Bedrock Combination

Fig. 2.22S   Southern Sector of the study region

Four Attributes, fine classification

1. Slope Aspect

3. Bedrock Geology

4. Relative Relief
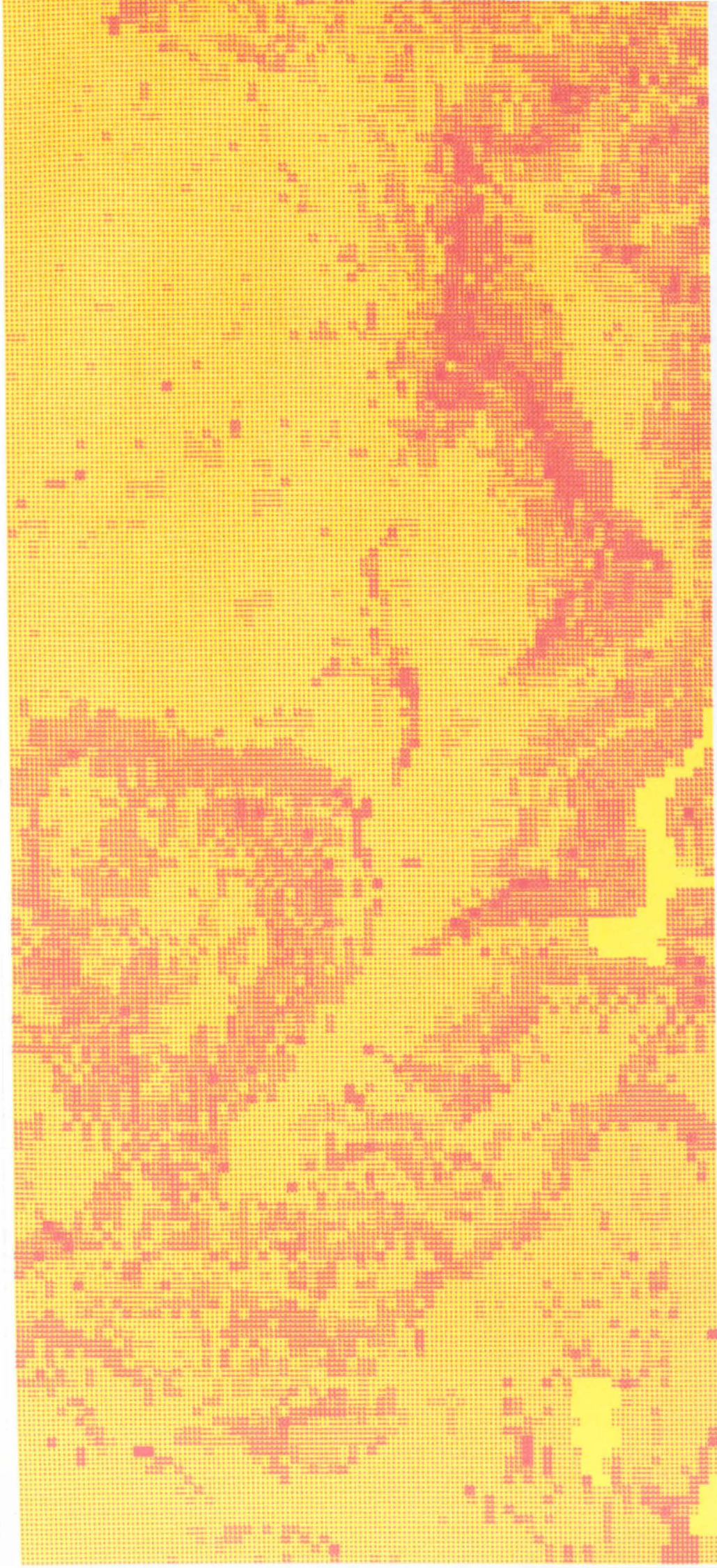
6. Slope steepness

Fig. 2.23S   Southern Sector of the study region

Four Attributes, fine classification

3. Bedrock Geology

4. Relative Relief

6. Slope steepness

7. Height above sea level
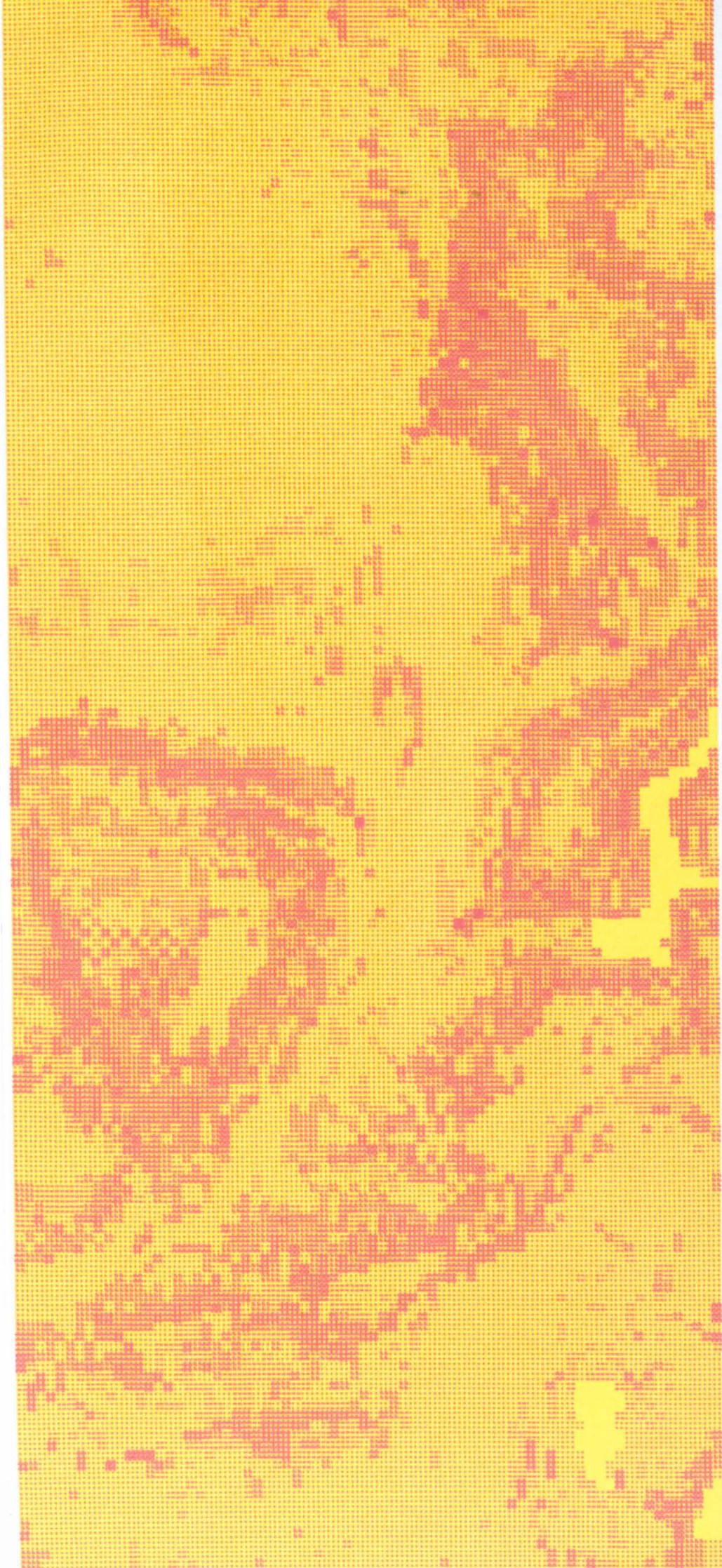
Fig. 2.24N   Northern Sector of the study region

Four Attributes, fine classification, using LAF combination of the Southern Sector in order to predict landslide areas in the Northern Sector.

3.   Bedrock Geology

4.   Relative Relief

6.   Slope steepness

7.   Height above sea level

Fig. 2.25S   Southern Sector of the study region

Four Attributes, reduced classification

3. Bedrock Geology

4. Relative Relief

6. Slope steepness

7. Height above sea level
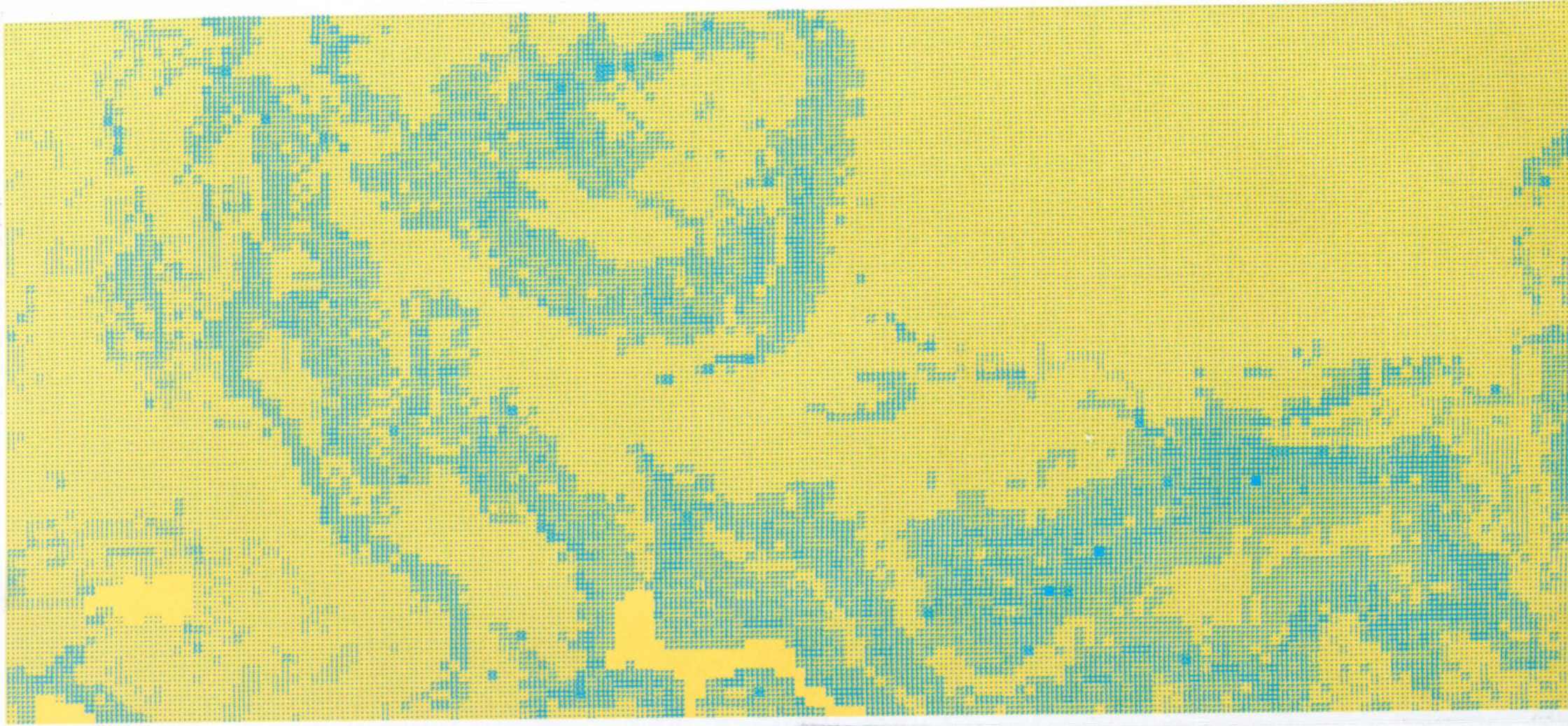
Fig.   2.26N   Northern Sector of the study region

Four Attributes, reduced classification, using LAF
combinations of the Southern Sector to predict land-
slide areas in the Northern Sector.

3.   Bedrock Geology

4.   Relative Relief

6.   Slope steepness

7.   Height above sea level
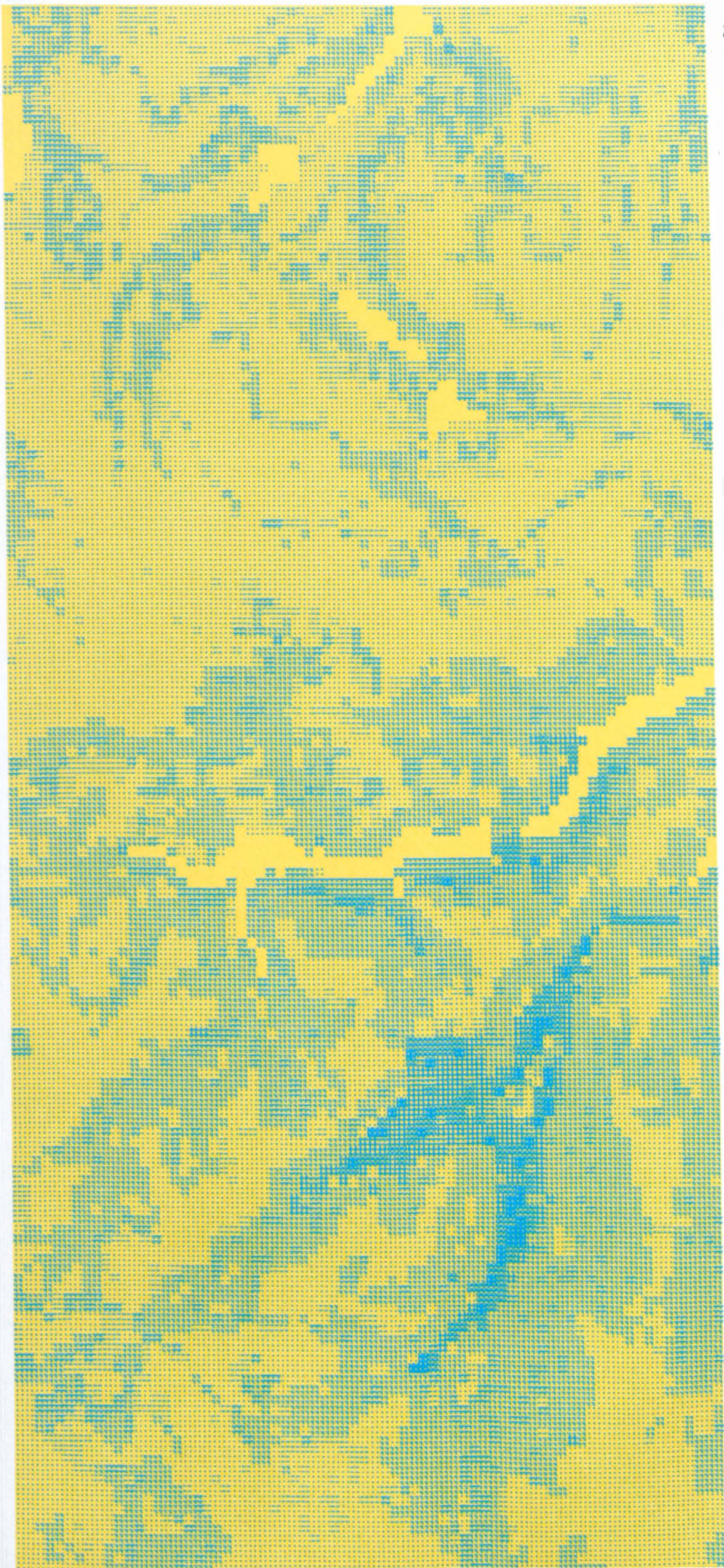
Fig. 2.27N Northern Sector of the study region

Four Attributes, reduced classification, using LAF
combinations of the Northern Sector landslides.

3. Bedrock Geology

4. Relative Relief

6. Slope steepness

7. Height above sea level
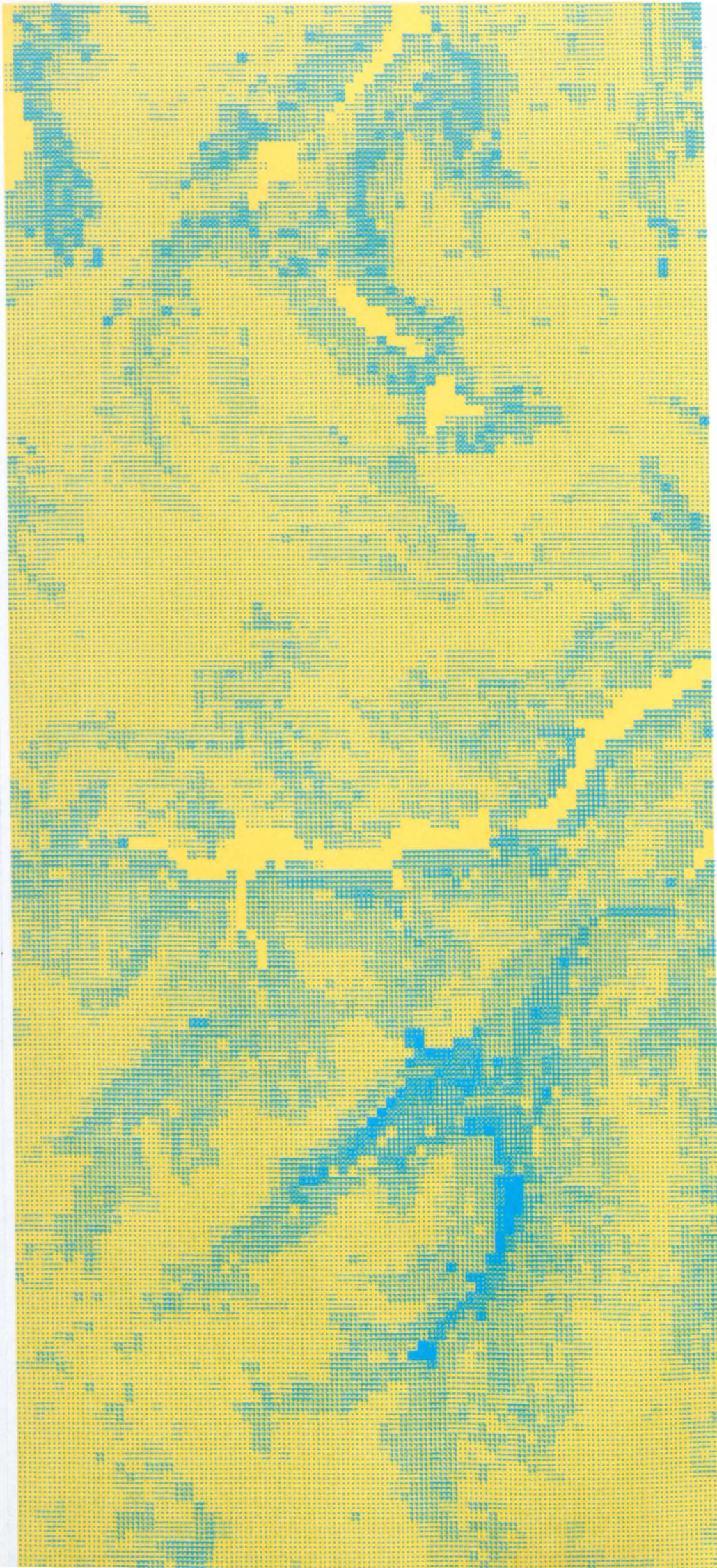
Fig. 2.28S   Southern Sector of the study region

Three Attributes, fine classification

1.   Slope Aspect

3.   Bedrock Geology

6.   Slope steepness
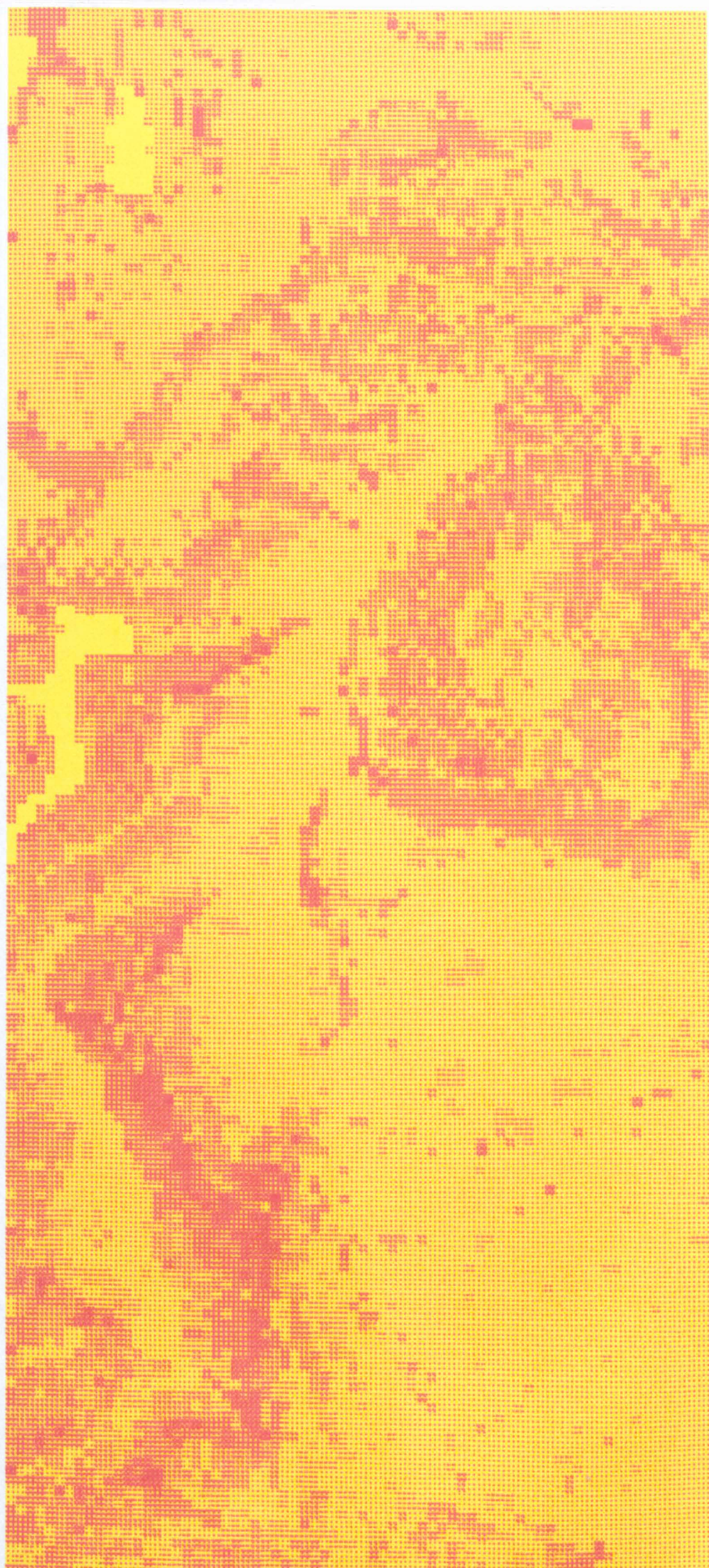
Fig. 2.29S   Southern Sector of the study region

Three Attributes, fine classification

1. Slope Aspect

6. Slope steepness

8. Bedrock combination
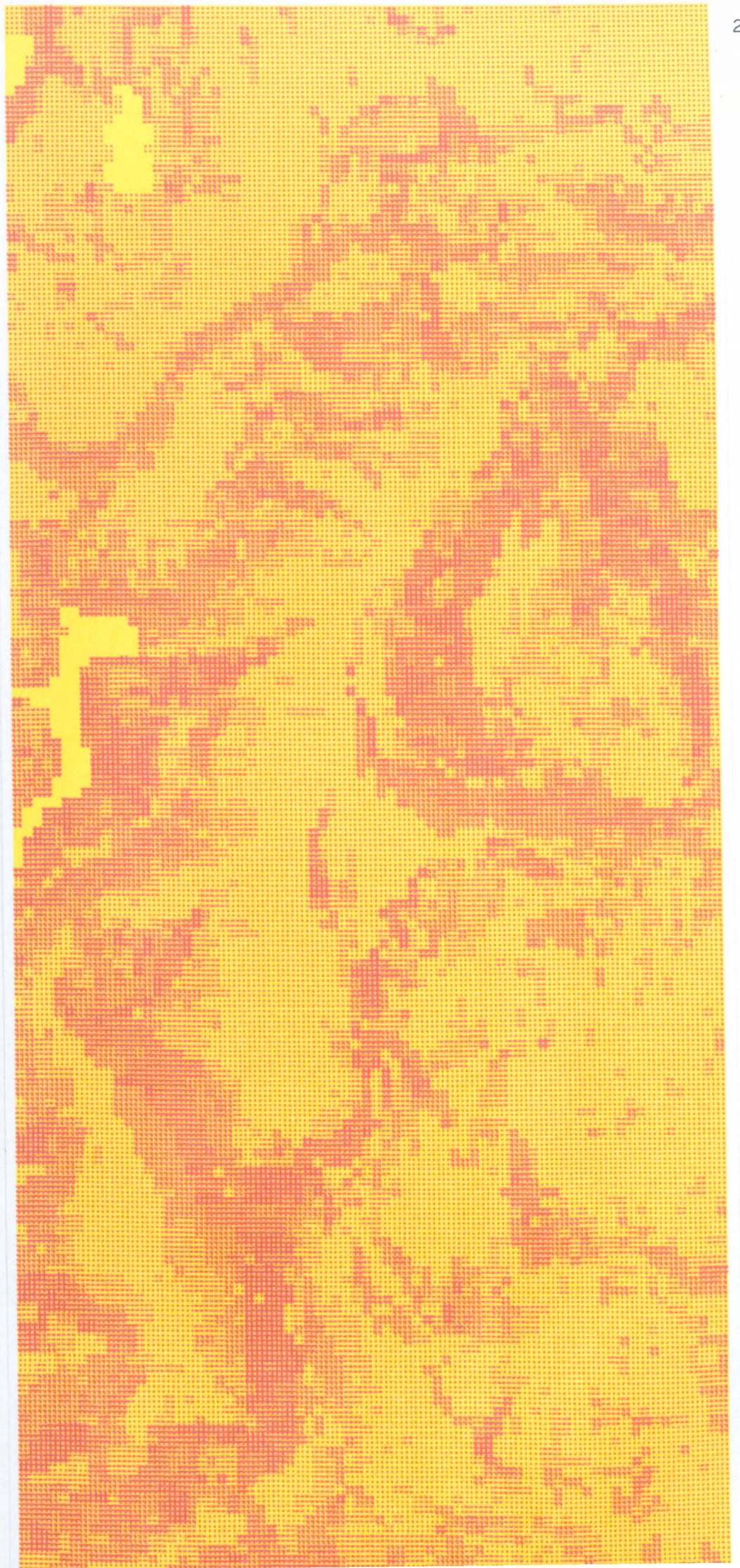
Fig. 2.30S   Southern Sector of the study region

Three Attributes, fine classification

3. Bedrock Geology

4. Relative Relief
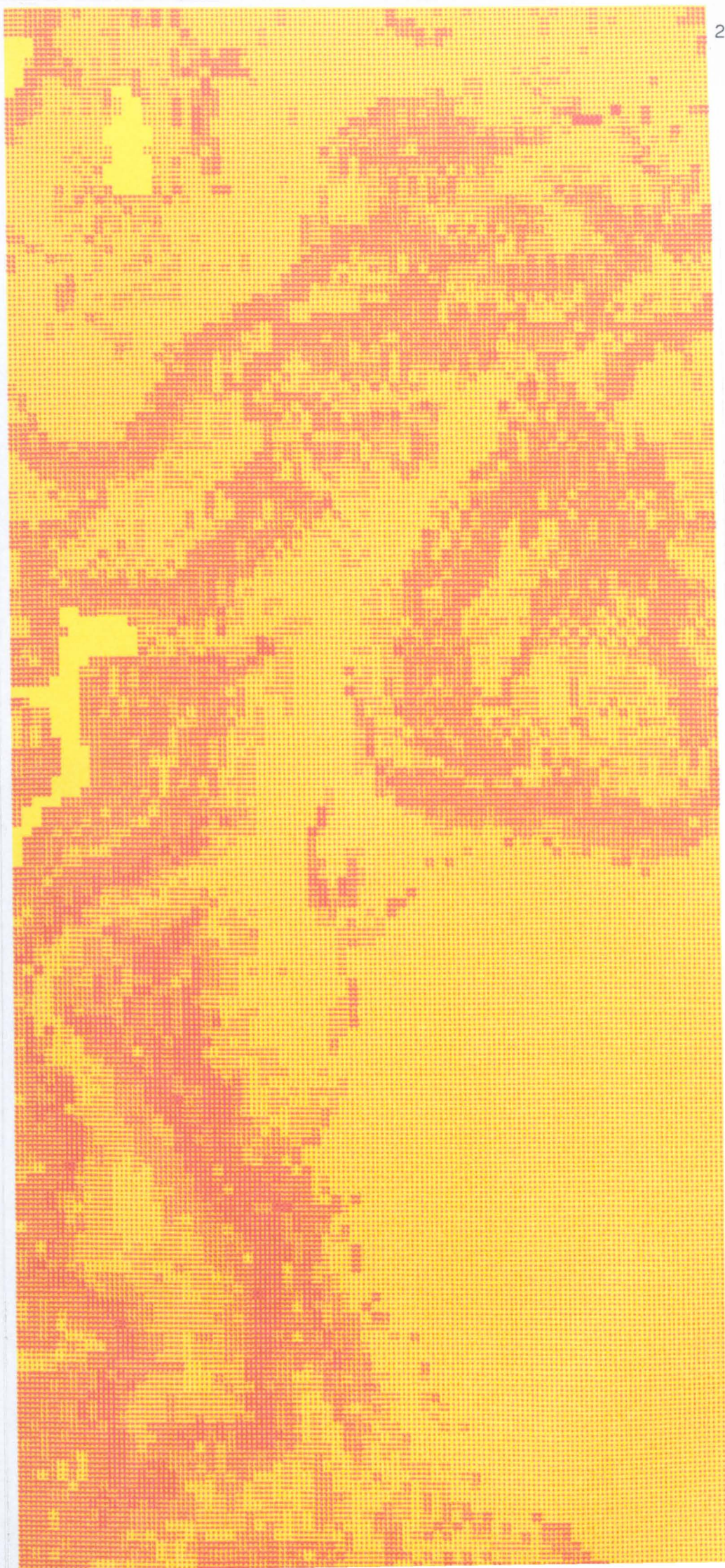
6. Slope steepness

Fig. 2.31N Northern Sector of the study region

Three Attributes, fine classification, using LAF

combinations of the Northern Sector landslides

3. Bedrock Geology

4. Relative Relief
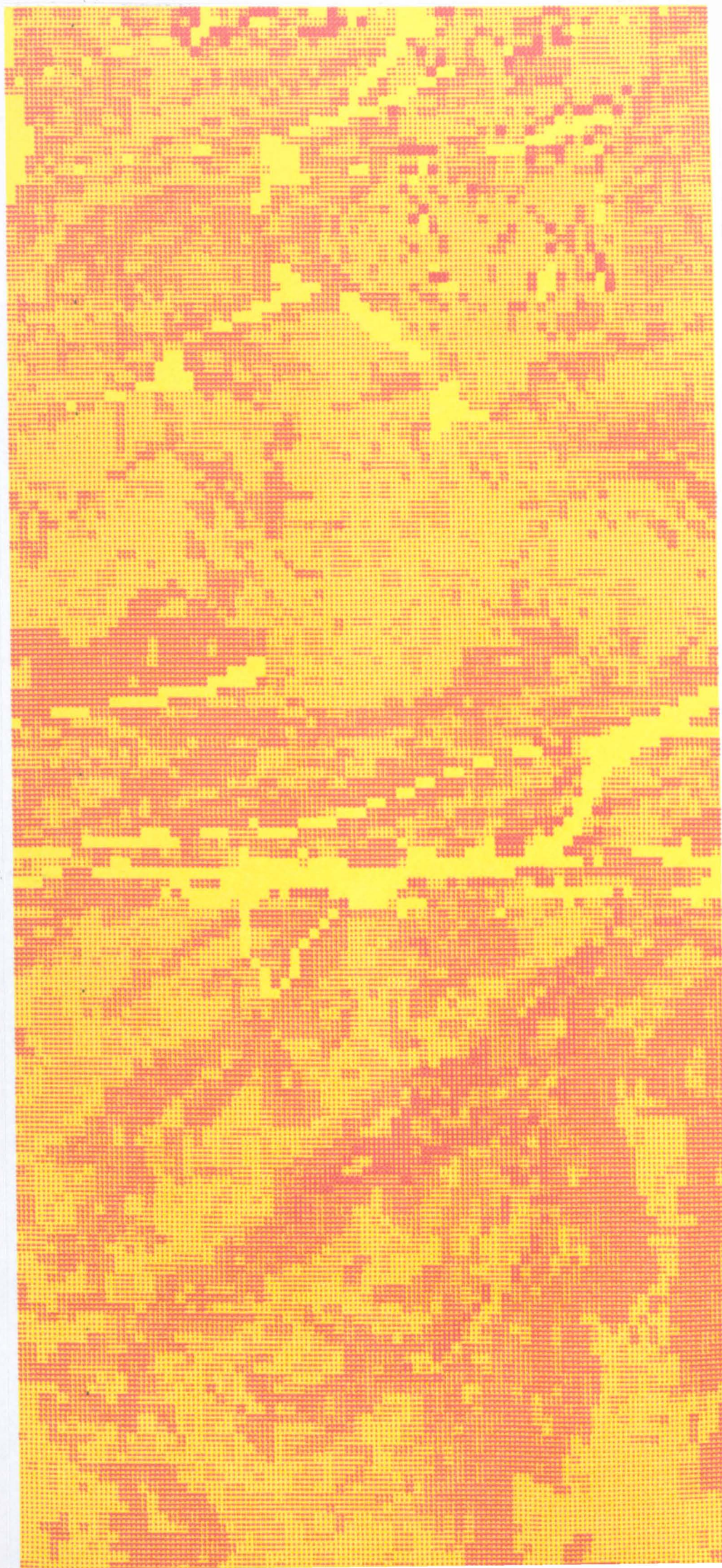
6. Slope steepness

Fig. 2.32S   Southern Sector of the study region

Three Attributes, reduced classification

3. Bedrock Geology

4. Relative Relief

6. Slope steepness
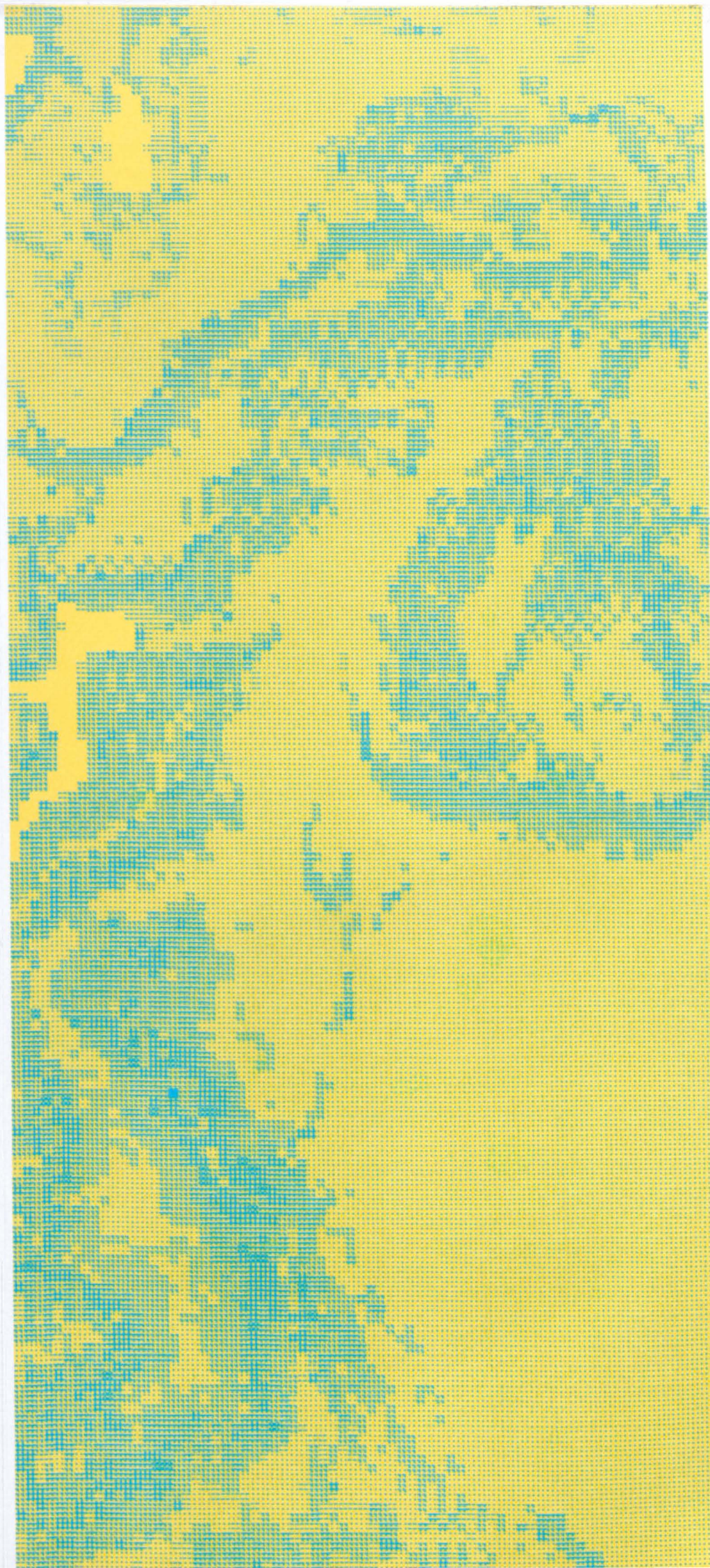
Fig. 2.33N   Northern Sector of the study region

Three Attributes, reduced classification, using LAF
combinations of the Southern Sector in order to predict
landslide areas in the Northern Sector.

3.   Bedrock Geology

4.   Relative Relief
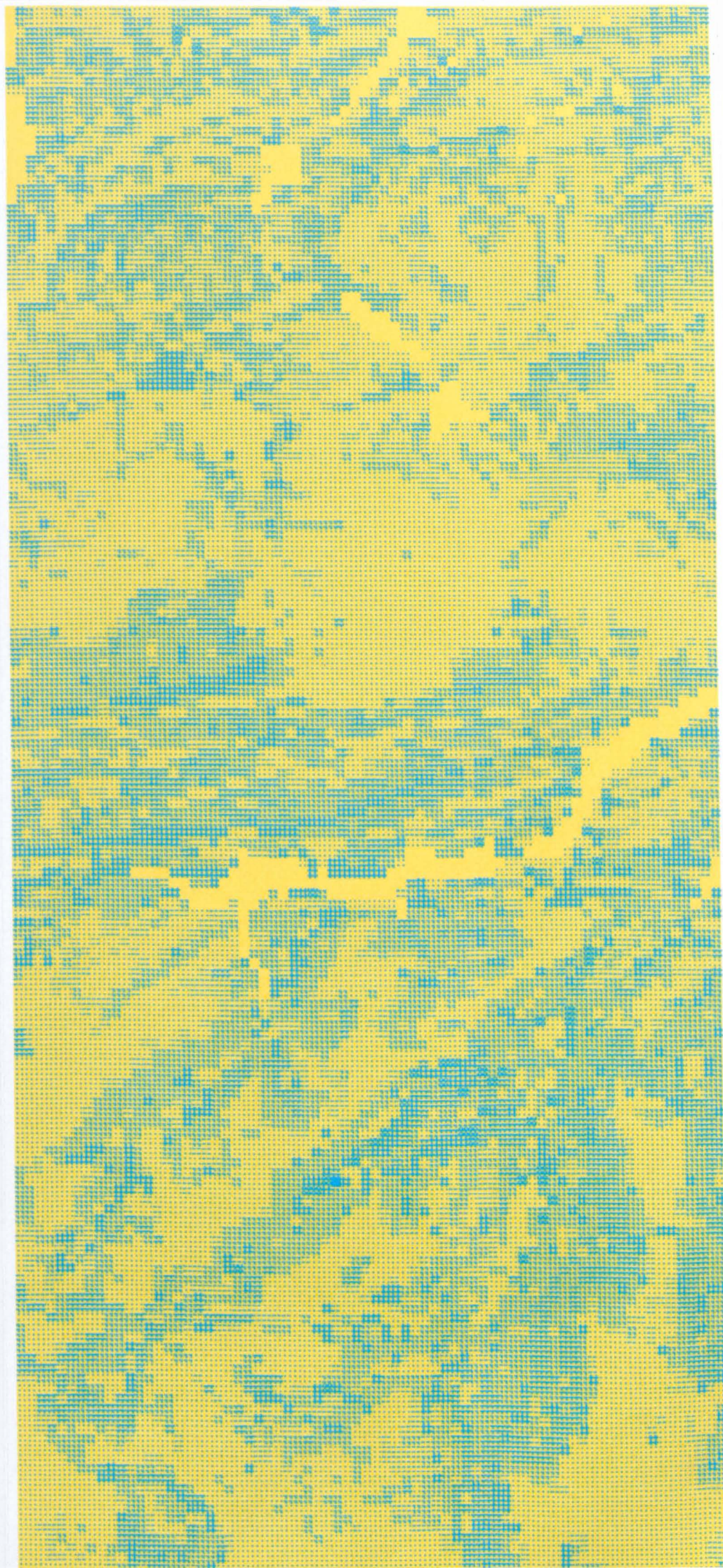
6.   Slope steepness

Fig. 2.34N Northern Sector of the study region

Three Attributes, reduced classification, using LAF
combinations of the Northern Sector landslides

3. Bedrock Geology

4. Relative Relief

6. Slope steepness
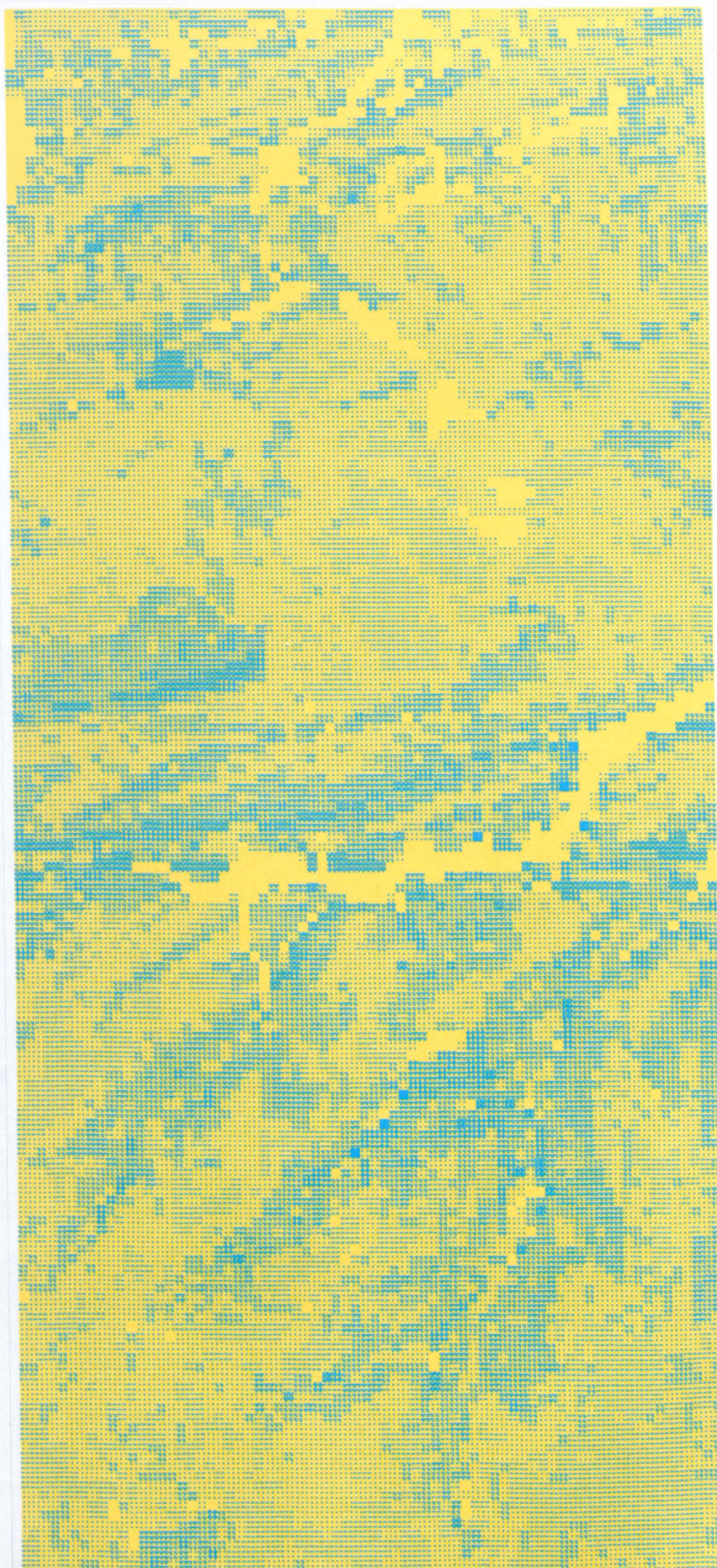
1. Does the reduction in data used in the case study degrade the results to an unacceptable point?

An easy test to answer this question is to compare the effects of a reduction in the number of attributes used and the coincidence of a high susceptibility rating within actual landslide areas. Figs. 2.14(S) and 2.14(N) show the spatial distribution of landslides for southern and northern areas.

Table 2.15 shows the frequency of landslide susceptibility values for each landslide susceptibility class using 7, 4, and 3 attributes for both fine and reduced class sets. The Landslide Susceptibility Index (LSI) classification in this case was user determined (see Table 1.5). The first class contained 144 LSI values in each case, these represented water areas (reservoirs). The landslide susceptibility classes then increase by steps of 0.1 to a top class covering the range of 0.8-1.0. In the case of the 7 variable full class set the number of combinations actually used was 6560 out of a maximum of 11520. This indicated that most combinations only contained on average fewer than two cells. Thus in the 7 variable fine classification, cells tended to have either a high LSI ratio or a low one with few intervening values. This is demonstrated in Fig. 2.17(S) and more so in Fig. 2.15(S) which show the area distribution of susceptibility indices for the 7 variable full class set case. Both Fig. 2.17(S) and Fig. 2.15(S) compare favourably with Fig. 2.14(S) which show the actual landslide distribution in the southern sector.

As the number of variables was reduced the LSI ratios tended to decrease in magnitude, but covered a larger area. Fig. 2.20(S) shows

Table 2.15   Frequency of landslide susceptibility index values for each landslide susceptibility class
using 7, 4 and 3 variables for both fine and reduced class sets

Landslide susceptibility classification (LSI)	Class Frequency					
	7 variable (fine class set) Fig. 2.17(S)	7 variable (reduced class set) Fig. 2.18(S)	4 variable (fine class set) Fig. 2.20(S)	4 variable (reduced class set) Fig.	3 variable (fine class set) Fig. 2.28(S)	3 variable (reduced class set) Fig. 2.29(S)
Reservoirs	144	144	144	144	144	144
0 - 0.1	10533	9522	9200	8702	9326	8601
0.1 - 0.2	70	841	1240	2068	1234	2449
0.2 - 0.3	63	435	499	537	450	316
0.3 - 0.4	63	281	249	43	176	6
0.4 - 0.5	5	77	52	10	140	0
0.5 - 0.6	174	87	84	10	36	4
0.6 - 0.7	36	53	6	3	6	0
0.7 - 0.8	0	26	0	0	0	0
0.8 - 1.0	432	54	46	3	8	0
No. of combinations	6560	1617	1228	192	516	74

Footnote: variable combinations used in Table 2.15:

7. Variable Case: Bedrock geology, slope steepness, slope aspect, height above sea level, height above valley floor, relative relief, superficial deposits.

4. Variable Case: Bedrock geology, slope steepness, height above valley floor, relative relief.

3. Variable Case: Bedrock geology, slope steepness, slope aspect.

the 4 variable situation (bedrock geology, slope steepness, relative relief and height above the valley floor), and Fig. 2.28(S) the 3 variable case (bedrock geology, slope steepness and slope aspect). Note that locationally the spatial distribution of the susceptibility index values are very similar, although the number of combinations observed was 1228 for the 4 variable case, and 516 for the 3 variable case. There was almost a 13:1 drop in the number of combinations between the 7 variable and 3 variable full class sets. The ratio level for the 3 variable case had fallen owing to averaging effects but the values covered a wider area of the study region than the LSI ratios in the 7 variable case. Comparisons between Figs. 2.15(S) and 2.16(S) and between Figs. 2.17(S) and 2.18(S) show the effects of a reduced class set are minimal despite the lower number of combinations involved, this pattern is also apparent for the 3 and 4 variable cases as shown in Table 2.15.

Figs. S1 to S4 show computer printouts of the Landslide Susceptibility Index (LSI) values used to construct the PANTONE landslide susceptibility maps. Figures S1 to S4 show LSI values for the southern area and Fig. S5 for the northern area. The LSI values have been printed out in the range between 0 and 1000 rather than 0 and 1.0 previously given in Fig 2.1. The value -1 represents reservoir areas. The ratio values highlighted in pink represent the mapped landslide areas. As can be expected a casual inspection reveals that the LSI ratios produced by the four different attribute combinations are greater in those cells corresponding to mapped landslide areas (pink cells) compared to none-landslide cells. The LSI ratios for mapped landslide areas (pink shaded areas) were summed and the mean LSI ratio was calculated for each of the four different attribute combinations, represented by Figs S1 to S4. Table 2.16

Fig. S1 Print-out of landslide susceptibility

index values, 9 attributes, fine

classification, southern section.

(Fig. 2.15(S) (see Table 2.16

for variables)

Fig. S2   Print-out of landslide susceptibility
          index values, 7 attributes, fine
          classification, southern area.
          (Fig. 2.17(S)) (see Table 2.16 for
          variables)

Fig. S3 Print-out of landslide susceptibility

index values, 4 attributes, fine

classification, southern area.

(Fig. 2.22(S)) (see Table 2.16 for

variables)

Fig. S4   Print-out of landslide susceptibility

index values, 4 attributes, fine

classification, southern area.

(Fig. 2.21(S)) (see Table 2.16 for

variables)

```
  0   0  21   7   9   9   9   9   9   0   0   0   9  10  10  21   0  10   9  10   9  63  95  95  95
  9  21  21   7   7  10   7   7   7   9   7   9  21   0   0  16   9  10   9   0 125 101  95  95
178 125   9  10   7  10  63   7   7   7   7   9   7   9   9   7  16  63  95 101  10 125 101  10  10
125  21   9  63  63 125 125   9   9   7  21  21  21   7  10  95  95  63  95  95  10 125 151  63  10
  7  21   7  10  10 125  63  63   0   0   0   7   7   7  23  95  10  95 101  10 151 151 125 101 125
  9   7   9  10  10   9   9   7   0   0   9   9   9  95  95  95  23  23  95  95  63  63  23  95 151
 10  63  10  10   9   7  95   2   0   0  95   7  95  23   8  95  10  95  95 101  95  95  28  95  95
178  10   7  10  23  10   0   0   2   0   2  10  95   0   0  28  10  95 101 101   2  95  28  95 101
  0   2   0   9  10  21  21  21   0   0   2  63 151   0  16   0  31 151  95  95  28   2  23  95  95
174 101 125  10 125   7 178 178   7   0   2 178 174  33  33  16  16 101  95   2   8  28  23  95  23
173 113 178  10 151 174 174 178   9 178 178 174 151   0  78  78 151 101 101 101   0   8 151 151  23
173 113 151 123 123 174 174 154 178 178 125  95 125  33  25  16 101 101 151 101 174 113  78 113 113
173 173 125 174 151 174 125 125  63  63  10  95 125  33  25  25   0  10  95  23  95  95 101 101 151
173 173 174 151 151 174   7  10  10  10  63 151 125  31  33  25   0   7  95  23  95  95  28  95  95
 78 151 174 113 174 178   7   7 179 125 125 151 125  31   0   2  21 125  95  23  23  23   2   2  95
 78  23  78 113 174 125   9  95 125 125 178 174  63  16  33   9 151  95  95   8  28   8   8   2 101
113 174  31 123 101 125  21 151 125 178 151   7  21  16  31  78  19  16   0   0   8  28  28   8 151
 78 113 113 113 123 174 151  95 178 174   2  21  19  16  16  33  33   0  19  23  19  33  95  28
113 113 173  31  78  78  78 173 174 151  25   2   8  33   0   0   0   0   0   8   2  16  19   8  28
113 113 173 173  78 173 173 173  95   2   2  33  28   8   8  25  33  33  33  19 101  23  25   8  33
 95  16  16 113 151 113  78  23   2  19  19  28   2   2   2  25  19  28  23  78   8   2  25  23  16
 23  25   0  16  78  31   0  25  25  28  28   2   2  25  25  16  19  23  23  28  28   0  23  16
  2  25  33  33  16  33  25  25  28  23  28  16  19  19  19  16  95  31 151   8   8   8  95  23  19
  2  25  25  25   0   0  25  25  28  28  16  16  31  33  16 151  78 113  16   8 101 151  95  95  33
  2  25  25  25  25  25  25  33  28  33  16  33  16  31  78  78  78 113  16 174 151 151  16 101  33
 23  33  16   0  25  25  25  25  28  33  16  16  16  78  78  78  79 113 113 113  95  95  16  95  33
 95  19  33   0  25  25  25   2  28  19  16  16  16  16   6  78  16 113  19  95  19   2  25
 25  25  16   0   0   0   0   8  28  23  19  19  16  23  23  23  16  78  31 113  33  33  19   2   2
 95  16   0   0   0   0   8  28  29  28  28  23  16  23  95  23  16  78 113 173  31   0  25   2   2
 19  28   0   0   0  33  28  23  28  28  28  28  23  28  95  95  16 113 113 173  78   0  25  25   2
 25   2  25  25   0  23   2   2  28  28   8  28  28   2  95  95  31  78  78 173 173   0  25  25  25
 25   2  25  25   8  23   2   2  95  23   8   2   2   2  28  95 113  78  31  31 173  78   0  25  25
 25  23   0   0   0  19  95  95  23  23  95  23  28  28  28  23 113  78  78  78 173 173   0   0  33
 33  95   0   0   0   0  19  23  28  28  28  95  28  23  95  23  78 113 113 113  78 173 173 173 113
 95  19   0   0   0   0   0   0  28  28  19  95  95  23  95  23  33  31 113 113 113  78 113 113  78
 19  33  33   0   0   0   0   0  28  23  33  28  29  95  95  16  19  16 113  78  78  78  78  78 113
 16  33  25   0   0   0  33  29  95  33  23  16  16  16  19  19  33   0  78  78 113  33  78 113
 16  25   0  33  16   0   0  33  16  95  23  28  16  16  31  16  19  33  33  16  78 113 173  78 113
 33  19  33   0  33  33  33  23  31  19  23  16  31  31  78  16  16  19  33  19 113 113 173 113 113
 33   0  25  19  33  33  19  23  31  16 101  78  31  31  78  31  31  19  19  19  78 113 223  31 173
 33  33   0   0   0  16  16  31  78  31  16  31  31  31  31  78  31  31  31  31  79 113   0  16 113
  0   0   0   0  16  16  31  31  78  78  79  78  31  78  31  78 113  78 113 113  78 113  49   0  79
 16  16  16  16  33  33  78  78  78 113  78 173 113 113  78  78  78 113  78  78  78 228  18 228 228
 16  16  16  16  79  31  31  33  78 113  78  78  79  31  31  78  78  78 113 113  78  78 113  31 228
 16  16  16  16  31  78 101 174 174 151 151  78  78  78  78 151  31 101 101 101 151  78 113  78  16
 95  95 101 101 101  28  28  28  95 123 151 151 151 151 151 151 174  78 101  16  16 101 101 113 113
 78  78  78 151 151 151 174 151 101 101 174  78  78 151  78  78  78  78  31  95  19  95  95  19  78
151 151 174 151 174 151 174 151 151 151 151 101 151 151  78  78 151 101  95 101  31  16  78
174 151 151 101 174 174 174 151 178 178 178 178 174 174 101 151 151  78 151 151  78  78  78  78 113
151 151 151 151 125 125 178 125 125 125 125 125 125 125 151 174 174 173 174 113  78 113 113  78  78
  0   0  63 125  10  10  63   0   0   0   0  10 125 151 151 151 113 123 123  78  31  78  78  78  79
  0   0   0  10  63  10  10   0   0   0   0  10 125 174 174 151 113 174 151 101 113  78  78  78 151
  0   0   0   0   0   0  21  21   0   0  10 125 100 174 151  78 113  31  31  16 151 101 151 151 151
  0   0   0   0   0   0   0   0   0   0  10 178 178 174 174 174   8  31 101  95 101 101 151 101 101
  7   7   7   0   0   0   0   0   0   7 125 178 125 178 174 174 174 174 113  78  31 101  78  78  78
125 178 178 178 178   0   0   0   0   0  63   9   7   7 100 100 174 151  78 151 101  78 101 101 151
125 125 125 125 125 125   0   0   0   0  10  21  10  21  10  10 100 123 174 174 151 151 151 151 123
174 125 125   7  63 125   0   0   0   0  21  21  10   9   0  63 178 178 178 100 100 100 178 178 178
174 125 125   9   0   0   0   0   0   7   9   9   9   7   0  10  10   9  63 178 178 178 178 178   7
178 125 125   0   0   0   0   0   0   0   7  10   0   0   0   0   0   7   7   7   0   9  21   0   0
125 125  21   0   0   0   0   0   0   0   0   0   0   7   7   0   0  21  21   0   0   0   0   0
125 125   9   0   0   0   0   0   0   0   0   0   0  10   9   9  21   7  21  21  21  21  21  21
125 125  10   0   0   0   0   0   0   0   0   0   0  10  21  10   7   7   7  21  21  21   7   7
125 125  10   0   0   0   0   0   0   0   0   0   0   7  28   0   0   7   7   7   7  21   7   9
125 125  21   0   0   0   0   0   0   0   0   0   0  63  10  21   0   0  21  21   0  21   9
 63  10   7   0   0   0   0   0   0   0   0   0   0   0  10  63   7  10  21   0   0  21  63
  7  21  21   0   0   0   0   0   0   0   0   0   0   0  10   9  21  63  10  10  10 125
  0   0   0   0   0   0   0   0   0  21  21  21  21   0  21   0   0  10  21 125  63  63 125 125
  0   0   0   0   0   0   0   0   0  21  21  21  21   7   7  63  63 125   7   7  63  63 101 174 174
  0   0   0   7  21  21   0   0   0  21 125 125 125 125 178  10   7   7  21  21 178 151 151 151  78
 21  10  10  63  10  10   0   0   0   7 125 125 178 125 125 125   9   7   7   0 178 174 101 101 151
 21  10 101  63  10  10   7  10   0  21  63 125 125 178 178 178 125 178 125   0   0 178 151 174 174
```

Fig. S5   Print-out of landslide susceptibility
index values, 3 attributes,
fine classification, northern
area.
(Fig. 2.34(N)) (see Table 2.34(N)
for variables)

Table 2.16 The mean LSI ratio values calculated for mapped land-
slide areas for four different attribute combinations
and the frequency of none land-slide cells possessing
an LSI value greater than the calculated mean

Attribute Combination (see key below)	Mean LSI Ratio for Landslide areas (Landslide cells – Pink)	Number of none landslide cells > mean LSI ratio value (Orange cells)
1. Fig. S1	583	51
2. Fig. S2	479	136
3. Fig. S3	208	449
4. Fig. S4	127	1317

Footnote: Attribute combinations for Table 2.16:

1. 9 variable, southern sector (fine class set): slope aspect, superficial deposits, bedrock geology, relative relief, height above the valley floor, slope steepness, height above sea level, bedrock combination, soils.

2. 7 variable, southern sector (fine class set): slope aspect, superficial deposits, bedrock geology, relative relief, height above the valley floor, slope steepness, height above sea level.

3. 4 variable, southern sector (fine class set): slope aspect, relative relief, slope steepness, bedrock geology.

4. 4 variable, southern sector (fine class set): slope aspect, relative relief, slope steepness, bedrock combination.

shows the mean LSI ratio values for mapped landslide areas for four different attribute combinations and the frequency of non-landslide cells possessing an LSI value greater than the calculated mean.

The intention of calculating this mean LSI value was to indicate by orange shading the number of none landslide cells which possessed LSI ratios greater than the mean LSI value; these locations are considered to have a high degree of susceptibility to landsliding.

All cells possessing a susceptibility Index ratio greater than the mean value calculated for each attribute combination 1-4 in Table 2.16 have been shaded orange, the frequency of orange cells for each attribute combination is given in Table 2.16. The 51 (orange cells) with LSI ratios greater than the mean in the 9 variable (fine class set) see Fig. S1 are also identified by shading LSI ratio values greater than the mean for attribute combinations 2, 3 and 4 (see Figs. S2, S3 and S4). Since the LSI ratios for the 9 variable full class sub-division tended to give either a high LSI ratio or a low one with few intervening values; the 51 cells shaded orange in Fig. S1 are therefore considered to represent the most susceptible areas for instability in the southern sector of the study region.

The seven variable (fine class set), Fig. S2 shows a further 85 orange cells other than the 51 cells already predicted using the 7 variable (fine class set) as having a high susceptibility to failure. By comparing Fig. S1 with Fig. S2 the distribution of LSI ratios is very similar particularly with respect to the most vulnerable areas. Thus, it seems that the addition of the two extra variables (bedrock combination and soils) in the 7 variable full class set Fig. S1 has had little effect on the overall distribution of LSI ratio values. The 7 variable (fine class set) included the variables bedrock

geology and superficial deposits, these are very similar with respect
to their spatial distribution to the variables bedrock combination
and soil respectively, therefore one might expect little change in
the LSI ratio distribution with the omission of bedrock combination
and soil variables in the 7 variable case.

Figs. 2.16(S) and 2.18(S) show the LSI distributions for the 9
variable reduced class set and 7 variable reduced class set, both the
reduced class set LSI ratio distributions are very similar to each
other and are not very different from the fine class set
distributions. Thus, the seven variable reduced classification
appears to provide a reasonably accurate and acceptable level for
landslide susceptibility classification.

Fig. 2.19(S) which uses five variable combinations (bedrock geology,
slope steepness, slope aspect, relative relief, and height above the
valley floor) is very similar to Fig. 2.20(S) (slope aspect, bedrock
geology, relative relief, slope steepness), which includes the same
variables used to produce Fig. 2.19(S) but excludes one variable,
height above valley floor. Therefore, it appears that this variable
(height above the valley floor) has a minimal effect on the final LSI
ratios produced using this particular combination of variables.

A comparison between Figs. 2.22(S) and 2.21(S) shows that the
combination of variables used to produce Fig. 2.22(S) provides a
better landslide susceptibility classification than those used to
produce Fig. 2.21(S). The LSI ratios used to produce Fig. 2.22(S)
are shown in Fig. S3, this shows there are 449 cells greater than the
mean LSI ratio for landslide areas opposed to 1317 in Fig. S4 which
shows the LSI ratios used to produce Fig. 2.21(S). Table 2.16 shows
that the mean LSI ratio (208) for landslide cells in Fig. S3 is much
greater than the mean LSI ratio (127) used in Fig. S4. This again

appears to confirm the contention that bedrock combination is not as effective as bedrock geology, as a predictive attribute.

A comparison between Figs. 2.23(S) and 2.25(S) shows the effect of reducing the class set, this has its limitations, in that a certain level of detail has been lost in Fig. 2.25(S) particularly higher LSI ratios.

A comparison between Figs. 2.29(S), 2.30(S) and 2.28(S) (i.e. combinations using only 3 variables), shows that the variable combination used in Fig. 2.28(S) is the most effective variable combination of the three. This particular attribute combination (Fig. 2.28(S): bedrock geology, slope steepness and slope aspect) was used by DeGraff & Romesburg (1980), in their susceptibility mapping for the U.S.D.A. Forest Service. A comparison between Figs. 2.28(S) and 2.30(S), demonstrates the importance of slope aspect as a combinatoral variable. The attribute combination used to produce Fig. 2.30(S) is better than that used to produce Fig. 2.29(S), again suggesting that bedrock combination is a poor choice of attribute for landslide susceptibility assessment in this case. By using only three variables one is still able to observe a general pattern of landslide susceptibility in the study area. As slope steepness and bedrock geology were the only variables not changed in the various trials including Figs. 2.29(S), 2.30(S) and 2.28(S) (three variable cases) these two variables were considered to have the most dominating effect on the landslide susceptibility assessment model.

By systematically comparing the resultant changes caused by altering the number and combination of slope susceptibility variables as shown one can begin to establish which variables appear to be the most important for landslide susceptibility assessment. The evidence gained from comparing the LSI value in each Fig. suggests that the

following variables appear to be the most important: bedrock geology, slope steepness, slope aspect, relative relief and soil. Unfortunately, in the time available for computer analysis on the UNIX Super-Micro computer I did not try this particular combination of variables.

The reason why the use of the soil variable is here considered to be better than the use of superficial deposits data is due to two main factors:

(a) The classification used and the scale of mapping (1:25,000) carried out by the Soil Survey of England and Wales was such that it provided far more accurate and detailed information on the distribution of different soil groups.

(b) The soil classification provided a useful source of information regarding ground moisture conditions i.e. through the soil wetness classification (see Tables 2.3 and 2.4). The superficial deposits classification did not take into account ground moisture conditions.

2. Has the technique successfully identified a classification of slope susceptibility to landsliding?

In order to determine whether the technique successfully identified a classification of slope susceptibility a test was conducted to establish whether the LAI (Landslide area index combinations) in the southern sector could be used to predict the position of known landslides in the northern sector. Because of the limited time and available computer storage space only four variables (bedrock geology, slope steepness, relative relief and height above sea level, see Figs. 2.8(N), 2.4(N), 2.5(N) and 2.6(N) respectively) were

collected for the northern area (RAF cells) using exactly the same
procedure as that used for the southern sector landslide
susceptibility mapping. Fig. 2.24(N) shows the result of using all
four variables and a full class set to predict landslide areas using
the southern sector LAF in the northern section. The problem of
using the full class set was that many of the cells in the northern
sector were left unclassified because they contained a variable not
identified in the LAF combinations of the southern sector, therefore,
producing a very poor indication of landslide susceptibility. These
unclassified cells were undoubtedly those RAF cells of the northern
sector which contained values for height above sea level that were
much greater than those of the southern sector, and therefore were
not included in the LAF combinations of the southern sector. Fig.
2.31(N) shows the situation when three variables, full class set
(bedrock geology, slope steepness and relative relief) were used
excluding height above sea level; one can see that very few cells
remained unclassified. However, by reducing the class set for these
four variables as shown in Fig. 2.26(N) one can see that this problem
was partly resolved and a reasonable prediction of known landslides
in the northern sector was achieved (comparison between Figs. 2.26(N)
and 2.14(N)). This demonstrated that the technique was successful in
identifying a classification of slope susceptibility to landsliding.
Fig. 2.27(N) shows the landslide susceptibility classification
produced when the LAF combinations obtained from the northern sector
are used in MAP rather than the southern sector attributes (Fig.
2.26(N)). A comparison between the distribution of Landslide
Susceptibility Index (LSI) values of Figs. 2.26(N) and 2.27(N) shows
that they are very similar although the LSI ratios in Fig. 2.27(N)
have a slightly greater magnitude particularly in known landslide
areas. This demonstrates that the four variables (bedrock geology,

slope steepness, relative relief and height above sea level) used in MAP have a similar importance for both the northern and southern sectors of the study area.

Fig. 2.33(N) shows the landslide susceptibility classification for the 3 variable case, reduced class set, using LAF combinations of the southern sector in order to predict landslide areas in the northern sector. Fig. 2.34(N) shows the landslide susceptibility classification for the same three variables as used in Fig. 2.33(N) but using the LAF combinations of the northern sector landslides. A similar pattern to that identified in Figs. 2.26(N) and 2.27(N) emerged whereby the LSI ratios produced by using the northern sector LAF combinations as shown in Fig. 2.33(N) are slightly higher in magnitude than corresponding LSI ratios in Fig. 2.34(N).

Fig. S5 shows the actual LSI ratios used to produce Fig. 2.33(N) in the northern sector. All LSI ratios greater than 200 were shaded pink. Actual landslide areas are bounded by the red lines. The technique of shading higher LSI values has been reasonably sucessful for the identification of large multiple rotational landslide complexes along Snake Pass and Alport Dale. However, the technique has not been very successful in locating landslides in other areas.

By comparing Figs. 2.27(N) and 2.34(N) one can see that by removing the variable height above sea level a significant decrease in detail has resulted. The landslide areas in the Snake Pass and Alport Dale area are not as conspicuous in terms of their LSI classifications in Fig. 2.34N as compared to those in Fig. 2.27(N).

The ultimate test to see whether the technique had successfully identified a classification of slope susceptibility to landsliding was to establish by using a quick walk-over survey in the field to see whether areas represented by high LSI ratio cells other than mapped landslide areas showed any evidence of instability. A number of cells containing high LSI ratio values from both northern (15 cells) and southern sectors (9 cells) were selected at random. These areas were visited and their degree of instability was noted (see Tables 2.17 and 2.18).

The results of the field survey are shown in Tables 2.17 and 2.18 which gives the grid reference for each site along with a description of instability found at that site. The evidence gained from the field survey provided ample support that the matrix assessment model was indeed providing a useful model for classifying slope stability in both northern and southern sectors. None of the landslide sites given in Tables 2.17 and 2.18 had previously been mapped on the 1:50,000 geological map sheets or had been recognised through aerial photograph interpretation as landslide areas. These identified landslide sites can then be added to the landslide distribution maps used in MAP and the landslide area factor (LAF) can be amended so that a more precise landslide susceptibility assessment of the study region can be undertaken.

An interesting exercise given further time would have been to use MAP on a specific type of landslide only rather than for all types of landslide as in the case discussed here. By operating MAP for each type of landslide it may be possible to establish which variables are more important for specific landslide types. Separate landslide susceptibility maps could be created for each identified landslide

Table 2.17 Field investigation in the northern area

No.	Grid Ref	Name	Degree of instability
1.	(130 925)	Hope Woodlands	Rotational slipping
2.	(135 897)	Hayridge Farm	Rotational slip
3.	(145 907)	Hucklow Lees Barn	Rotational slip and mudflow
4.	(153 889)	Woodlands	Rotational slip
5.	(166 923)	Marebottom	Small rotational slip
6.	(170 897)	Nabs Wood	Small rotational slip stabilised by batter wall
7.	(175 897)	Pike Low	Small rotational slip
8.	(179 885)	Hag side	No evidence of instability, but much of the lower section of slope had been removed for a car park
9.	(182 891)	Old House	Rotational slip
10.	(245 881)	Hollow Meadows	Rotational slip
11.	(262 891)	Load Brook	Small translational debris slide
12.	(273 931)	High Bradfield	Rotational slip
13.	(280 919)	Cliffe House	Rotational slip
14.	(280 939)	Bent Hills	Rotational slip
15.	(285 904)	Stacey Bank	Earth Embankment stabilised above Damflask reservoir outflow

Table 2.18 Field investigation in the southern area

No.	Grid Ref	Name	Degree of instability
1.	(086 869)	Edale Head	Shallow debris slide
2.	(093 855)	Lee House	Rotational slip
3.	(105 839)	Chapel Gate	Rotational slip
4.	(131 853)	Hollins (1)	Rotational slip
5.	(135 851)	Hollins (2)	Rotational slip
6.	(193 819)	Shatton Edge	Rotational slip
7.	(200 820)	Westfield	Rotational slip
8.	(195 860)	Ashop Farm	Rotational slip
9.	(196 853)	Win Hill	Rotational slip

type in the study region. The spatial distribution of high susceptibility index values for each type of landslide could then be compared and vulnerable areas for specific types of landslide could be recognised and delineated. Such an investigation would be very useful in planning the position and type of monitoring instrumentation or the appropriate type of remedial engineering measures necessary to prevent a specific type of failure from occurring in predicted high susceptible areas.

2.5 Conclusions

The landslide combination matrix technique coupled with an on-line interactive graphics facility enabled the user to test hypotheses concerning:-

(a) The necessary set of attributes to help explain slope failures, and

(b) The spatial pattern of slope susceptibility for large areas.

The study has also shown that the matrix combinatorial model is

(i) sensitive to changes in the combination of variables used.

(ii) only somewhat sensitive to changes in the classification.

(iii) bedrock geology and slope steepness are the most important variables used, but relative relief, slope aspect and soils also appear to be important susceptibility variables.

The matrix assessment approach therefore provides a useful preliminary technique which could be implemented during the reconnaisance stage of a proposed engineering project. The landslide

susceptibility map produced using this technique should be considered primarily as a guide to slope instability and not an absolute indicator of landslides. At the construction stage more detailed site geotechnical investigations are required in the indicated areas (i.e. those cells containing high LSI values) to determine precise local variation. The basic data collected for the landslide susceptibility assessment could also be used by other specialists to carry out a variety of environmental investigations as part of a single multidisciplinary and multipurpose project for land resource evaluation and planning. The application of the Matrix Assessment Approach in the study area has provided a useful example of how techniques in automated cartography and numerical analysis can be integrated not only to provide a better understanding of the landslide susceptibility problem, but also to the development of interactive display software systems of use to both researchers, planners and engineers.

SECTION III

CALLOW BANK CASE STUDY

3.1 INTRODUCTION TO CALLOW BANK

3.1.1 Introduction

Section 2 of this thesis concentrated on producing a regional landslide susceptibility model for mainly large deep-seated rotational landslides. This next section deals with the most common form of landslide process, that of shallow translational landsliding, which has affected regolith material largely composed of head which mantles virtually all the valley slopes of the study region. They are always shallow features and have essentially straight failure planes with some curvature towards the crown, and hence some rotational movement can occur. The distinction between debris slides, debris avalanches, and debris flows is based upon the degree of deformation of the soil material and the water content of the sliding mass. As both deformation and water content frequently increase downslope, what may be a debris slide at the crown of the landslide with relatively large undeformed blocks of soil sliding downhill may become an avalanche of small blocks and wet debris in midslope and a thoroughly liquefied flow at the base of the slope.

The slopes of the study region have undergone periodic degradation by periglacial processes and continue to degrade under present climatic conditions. The valley sides according to Carson & Petley, 1970, show a distinct morphological profile with straight mid-slope segments. The frequency of shallow instability indicates that mass movements are an important process by which hillsides are currently adjusting to changing conditions (including climate). A number of authors have interpreted the occurrence of 'characteristic slope angles' as 'limiting angles' or 'threshold angles' for various types of mass movement, and have recognised that many areas may be interpreted as relic features of periglacial mass movements,

(Hutchinson, 1968a, 1971a; Weeks, 1969; Carson & Petley, 1970; Chandler, 1970b,c, 1972a,b, 1973, 1982; Early & Skempton, 1972; Rouse, 1975; Rouse & Farhan, 1976). The indications are that the head-covered slopes rest in a quasi-equilibrium state at angles near to limiting equilibrium. Under such conditions the widespread occurrence of shallow mass movements in these materials particularly in conjunction with water issuing from the base of the sandstone cap-rock and springs within the hillside successions, is to be expected. Unlike falls, slumps, and glides which may occur as a result of deep percolation of water, and hence at a considerable time after a rainfall, shallow translational slides nearly always occur in response to heavy rain and with a short time lag. Rain storms of sufficient intensity or duration are required in such cases to raise the water table to near the soil surface or fill pre-existing tension cracks. In low-intensity rainfalls the removal of water from the soil by interflow can usually keep pace with infiltration, and in short-duration rainfalls the field capacity of the soil may not be exceeded. The soil will lose sufficient strength to fail when the field capacity of the soil is exceeded for a time period long enough for pore-water pressures to rise substantially.

Frequent signs of current instability in the form of fresh landslide scars and tension cracks can be observed on slopes throughout the study region. The recognition of these landslide prone areas, is obviously important in an engineering or planning context. Road or building construction is likely to reactivate movement at such sites since the failure criteria affecting the slope are at a minimum. The reason why many slopes are currently stable appears to be due to present low piezometric levels, although in the vicinity of some spring lines a rise in ground water level may result in the

development of perched water tables which can initiate renewed
instability. In attempting stability analyses at specific sites, it
is essential that efforts are made to locate and define any pre-
existing slip-planes and that the pore water distribution on the slip
surface is determined as accurately as possible. Assuming residual
shear strengths the hillslope material will be mobilised more easily
on such surfaces and the relevant soil parameters at each site should
be evaluated accordingly. Prediction of the angle of ultimate
stability is a difficult matter, as it depends on a detailed
knowledge of piezometric conditions and soil properties at shallow
depth. As a first approximation, however, the stability of the
natural hillslopes with regard to shallow, largely planar, mass
movements may be assessed by 'Infinite Slope Analysis' (Skempton &
DeLory, 1957).

The Callow Bank study area was chosen for the following reasons:

1. Easily accessible by road along with the permission of the
   landowner to carry out the fieldwork.

2. Compact drainage basin of manageable size.

3. Geomorphology, geology and hydrology typical of the Dark Peak.

4. Example of large rotational failure within the study area.

5. Shallow planar translational sliding active within the study
   area.

3.1.2 Objectives of field investigation at Callow Bank

The objectives of the detailed field investigation carried out on hillslopes at Callow Bank are listed as follows:

(a) To examine slope profiles in the study area in order to establish whether 'characteristic slope angles' can be identified and whether these correspond to those found by Carson & Petley (1970).

(b) To examine changes in the piezometric surface within regolith material along slope profiles with respect to (i) rainfall, (ii) stream discharge, (iii) regolith characteristics, (iv) geology and (v) hillslope morphology.

(c) To design and build an open-sided direct shear box to be used in the field.

(d) To examine the shear strength of regolith material at various positions along a slope profile using the open-sided field direct shear box and to compare the results with those obtained by Carson & Petley, 1970; Carson & Kirby, 1972; and others using conventional laboratory shear box testing methods.

(e) To apply Infinite Slope Stability Analyses (Skempton & DeLory, 1957; Skempton & Weeks, 1976; Rouse & Farhan, 1976) in order to establish critical parameter threshold values and to develop an index of stability for shallow landsliding under various conditions of slope steepness and ground water conditions.

These objectives were achieved by employing standard geomorphological

techniques which included surface and sub-surface investigation, instrumentation of hillslope profiles, *in situ* and laboratory geotechnical testing of regolith materials and computer analyses. These techniques were implemented at specific sites along selected hillslope profiles which included areas which had undergone shallow translational landsliding and areas which appeared to be relatively stable.

Before each technique is described there follows a brief description of the geology and geomorphology of the Callow Bank study area and a review of previous work undertaken by various authors on characteristic slopes and limiting/threshold slopes. The location of the Callow Bank study area in the context of the regional study area is shown in Fig. 1.3. (see photographs of the Callow Bank study area).

3.2   GEOLOGY AND GEOMORPHOLOGY OF CALLOW BANK

3.2.1   Geology of Callow Bank

The geology of the Callow Bank study area is shown in Fig. 3.1.
Within the case study area there is a close relationship between
lithology and structure of the rocks and the morphology of slopes,
character of blockfield material, and the distribution of
gritstone/sandstone edges and tors (compare Figs. 3.1 and 3.2). All
the rocks within the study area belong to the Millstone Grit Series
of the Namurian System. This comprises beds of gritstone, sandstone,
shale and mudstone that total about 610m in thickness. The grit
varies from fine grained often flaggy beds to coarse pebbly
gritstone, the pebbles are composed mainly of quartz and feldspar.

The shales form more than half of the total thickness of the
formation. They contain Goniatites in marine bands, which because of
their short vertical ranges have been used to establish an effective
system of stratigraphic zones.

In the Callow Bank area the succession of the Millstone Grit Series
is extremely complicated since multiplication of grit beds occurs; in
particular the Kinderscout Grit varies by splitting or possesses
additional lenticular beds of grit. The second and third grit bands
in the succession also consist of multiple beds; causing further
problems of discrimination. The total sequence of these grit bands
are referred to as the Middle Grit Group.

Fig. 3.1 Callow Bank Geological Map

Legend:
- Shale d.
- KG Kinderscout Grit
- SG Shale Grit
- RG Rivelin Grit
- RF Redmire Flags
- R Rough Rock
- H Head
- — Alluvium
- M..M Marine Band
- ★ Geological section
- ⫶⎮⎮⫶ Landslide

0 100 200 300 400 Metres

In this case study the following classification of Millstone Grit beds has been adopted (Edwards, 1956; Eden et al., 1957).

Rough Rock Group:	Thickness (m)
Pot clay	1.5
Rough Rock and Rough Rock Flags	18.3
Mudstones	42.7

Middle Grit Group:	
Redmire Flags	9.1
Mudstones	30.5
Rivelin Grit	30.5
Mudstone with Marine bands	61
Heydon Rock	24.4
Mudstone	21.3

Kinderscout Grit Group:	
Kinderscout Grit	152.4
Grindslow shales	91.4
Shale Grit with Mam Tor sandstone	213.4
Mudstones	45.7

Edale Shales:	
Mudstones	219.4

Kinderscout Grit: The chief component of this group is from 121.9m
to 243.8m thick. It consists of coarse, massive, and current-bedded
beds of grit with a number of thin shale partings and is highly
jointed. The Kinderscout Grit is exposed at Carhead Rocks
(SK 241 828) and the north facing scarp slope of Dale Bottom (SK 245
816).

Rivelin Grit: Most of the Callow Bank case study area is underlain
by Rivelin Grit; it contains beds of coarse grit, thin-bedded fine
sandstone, and shales and mudstone. Grit and sandstone form 80% of
the Rivelin Grit Group; the rest is shale and mudstone.

A clear division of the Rivelin Grit into its upper and lower leaves
is seen on a line of section running from Callow Bank (SK 252 824) to
the trigonometrical point at the southern tip of Stanage Edge (SK 252
830). The upper leaf of the Rivelin Grit is about 45.7m thick, the
lower leaf exceeds 30.5m in thickness. About 24.4m of the upper leaf
are well exposed on Stanage Edge (SK 240 843) and its southerly
extension towards Cowper Stone (SK 255 832). The upper leaf of the
Rivelin Grit is a coarse grained sandstone and contains scattered
quartz pebbles. Apart from local bodies of massive bedded sandstones
the upper leaf is dominated by planar sets of cross strata. The
upper leaf forms Burbage Edge which is about 2.5km long. Rivelin
Grit is the major tor forming rock, and is also the major component
of scree, clitter and rafted boulders extending below its cliff
exposures. Rivelin Grit outliers occur at Higger Tor (SK 256 819)
and Carl Wark (SK 259 814).

Approximately 9m of siltstone are present below the Rivelin Grit
lower leaf in Callow Bank and these are underlain by the Reticulocera

<u>superbilingue</u> marine band. Alternations of sandstones and sandy siltstones make up the lowest 18.3m of the lower leaf and these are exposed in the upper part of the slip face of Callow Bank (see Fig. 3.1 and geological section description below).

Callow Bank Geological Section 1 (SK 2519 8229)

4.6m   sandstone, massive medium grained (Rivelin Grit, main bed).

1.8m   shale, dark, poorly exposed.

0.3m   sandstone.

3.6m   mudstone, grey silty, poorly exposed.

3.0m   sandstone, massive, lower leaf of Rivelin Grit.

1.2m   mudstone, grey silty.

0.6m   sandstone, soft, fine grained.

1.7m   shale, dark, fossiliferrous.

2.4m   shale, dark.

The sandstones of the lower leaf are fine grained and have sharp slightly transgressive bases. The tops of the sandstone beds usually exhibit aggregates of flattened siltstone fragments and surfaces of scour are discernible within some beds. The sandy siltstone horizons show current-ripple lamination. The upper 18.3m of the lower leaf are poorly exposed in the study area.

The lowest strata in the Millstone Grit Series at Callow Bank can be seen in a stream section at Mitchell Field (see Fig. 3.1 and geological section description below).

Mitchell Field Geological Section 2 (SK 2487 8192)

0.9m   shale, black.

0.3m   seatearth, sandy.

>1.2m sandstone, hard top of Kinderscout Grit.

A topographic shoulder marks the position of a siltstone band between the upper and lower leaves, this is particularly well developed at 400m O.D. in the area between Callow Bank (SK 252 824) and Overstones Farm (SK 249 829). The thin-bedded, fine sandstone of the lower leaf forms a prominent bench along the foot of Burbage Edge. In some cases this sandstone band creates only a minor break in slope (see Fig. 3.1 and geological section description given below).

Burbage Brook Geological Section 3 (2375, 8162)

       sandstone (lower leaf of the Rivelin Grit)

9.1m   not exposed.

2.7m   shale, dark, fossiliferrous.

4.6m   not exposed.

3.8m   shale, grey.

0.4m   shale, soft grey, sulphurous.

Redmire Flags: These are composed of yellow flaggy sandstone and fine gritstones. They are exposed in two localities, Ringinglow Bog in the north, and Stoney Ridge in the north-east. The Redmire Flags form a narrow band, at most not more than 15.2m thick. There are no good exposures available as in both places it is buried under thick peat.

Rough Rock: Rough Rock forms the upper divisions of the Millstone Grit Series and falls into two major lithological divisions; the lower division consists of shale and mudstone containing at its base the Concellatum marine band, and the upper division is sandstone which includes the Rough Rock Flags and Rough Rock. The Rough Rock is covered almost everywhere by deep-peat deposits.

Head

Over the greater part of the case study area most shale outcrops are buried under head, varying in thickness from 1.2m to 3.0m. The head contains material derived from the alternating sandstone and shale sequences by the action of periglacial freeze/thaw processes and modified by solifluction flow and multiple sliding. As a result the head deposits are heterogeneous, containing an ill-sorted and variably-sized material and often possessing numerous discontinuous slip surfaces. Ideally head may be defined as the material produced by freeze/thaw and moved by solifluction. Solifluction material may not be a product of frost action alone, it may incorporate a variety of readily available material, e.g. pre-existing regolith and head, glacial till, and vegetation matter. In most head deposits rock fragments tend to be angular, the material lacks sorting and shows little sign of bedding (Dines et al, 1940). It usually includes a large proportion of fines, but the coarse fraction may include very large boulders. They are particularly prone to landslipping, and in north Derbyshire the great majority of observed shallow landslips have occurred in these materials. Chronological distinction between head materials of different age, is very difficult. This is because each new cold phase may not necessarily produce fresh congelifractate; in many cases the older head is merely reworked.

Even in cases where the head is not reworked all evidence of previous bedding of a weathered profile may be destroyed by frost heaving.

Within the Callow Bank area there is no evidence of bedding within the head. However, Said (1969) identified two different types of head in the adjacent Burbage Brook catchment area. An older head was identified below a well marked soil horizon (Allerød layer) which was highly weathered, and incorporated little clay and no vegetation content. The younger head situated above the Allerød soil layer contained a relatively large proportion of fine clayey material and vegetation fragments. The lower head, organic soil, and upper head corresponded to the Lower Dryas (Pollen Zone 1), Allerød (Pollen Zone II) and the Upper Dryas (Pollen Zone III) respectively.

In the Callow Bank study area the prominent lithology of the head is a matrix of sandy-clay with rubbly sand lenses, and containing cobbles, boulders and flaggy blocks of sandstone. The deposits form subdued hummocky boulder strewn slopes with irregularly located springs particularly where the shales outcrop beneath the Rivelin Grit. Scarp-slope head deposits are common below the scarp slopes and edges of the Rivelin Grit. These head deposits consist of a heterogeneous matrix, varying from grey clay to rubbly sand, and contain a variable proportion of angular and sub-angular sandstone fragments. Many of these deposits merge up-slope into, or may underlie, boulder screes or block fields below Rivelin Grit edges.

Extensive Block Fields can be seen below Stanage Edge particularly on the slopes near Overstones Farm (SK 249 829), on the slopes below Higger Tor where the Block Field extends some way down the north western scarp slope of Callow Bank and below Carhead Rocks,

(SK 241 828). The scarp-slope head deposits tend to thin out laterally against spurs and slopes of increasing steepness. Downslope the matrix tends to become more clayey and there are fewer cobbles and boulders, particularly where the slope levels out on the argillaceous strata below the Rivelin Grits. In some places on the upper slopes the scarp slope head deposits are overlain by peat.

3.2.2 The Morphology of Callow Bank

Figure 3.2 shows the morphology of the case study area. The morphology and interpreted geomorphology of the Burbage catchment has been described in detail by Said (1969) and therefore will not be described here. The Callow Bank catchment and adjoining Overstones catchment are situated between Higger Tor and Stanage Edge in the south-west quarter of Fig. 3.2.

The name Callow is Anglo-Saxon in origin, meaning Cold Hill. Callow Bank has a long history of lead smelting; in the 16th century Callow Bank was known as 'The Bole Hill' which meant a westward facing slope having a strong persistent updraught. Lead ore was transported via pack horses from the Castleton area to Callow Bank in order to be smelted in the cupola. The hillsides around Callow Bank soon became denuded of trees used to fuel the lead smelters, this may have affected the stability of slopes and possibly accounts for the absence of trees is a characteristic of the area today. Evidence of the cupola and an early 19th century reverbatory tunnel used for lead smelting can be seen in the form of a 1.5m high ridge running 19m upslope on the south eastern flank of the main landslide mass of

MORPHOLOGICAL MAP OF THE
CASE STUDY AREA

Stanage Edge

Burbage Brook
Catchment

Overstones
Catchment

Callow Bank

P1

V8

V7

P2

P3

3

P4

Higger Tor

V3 V4

y5

V2

P5

V1

Dale Bottom

P6

Carl Wark

0 100 200 300 400

Metres
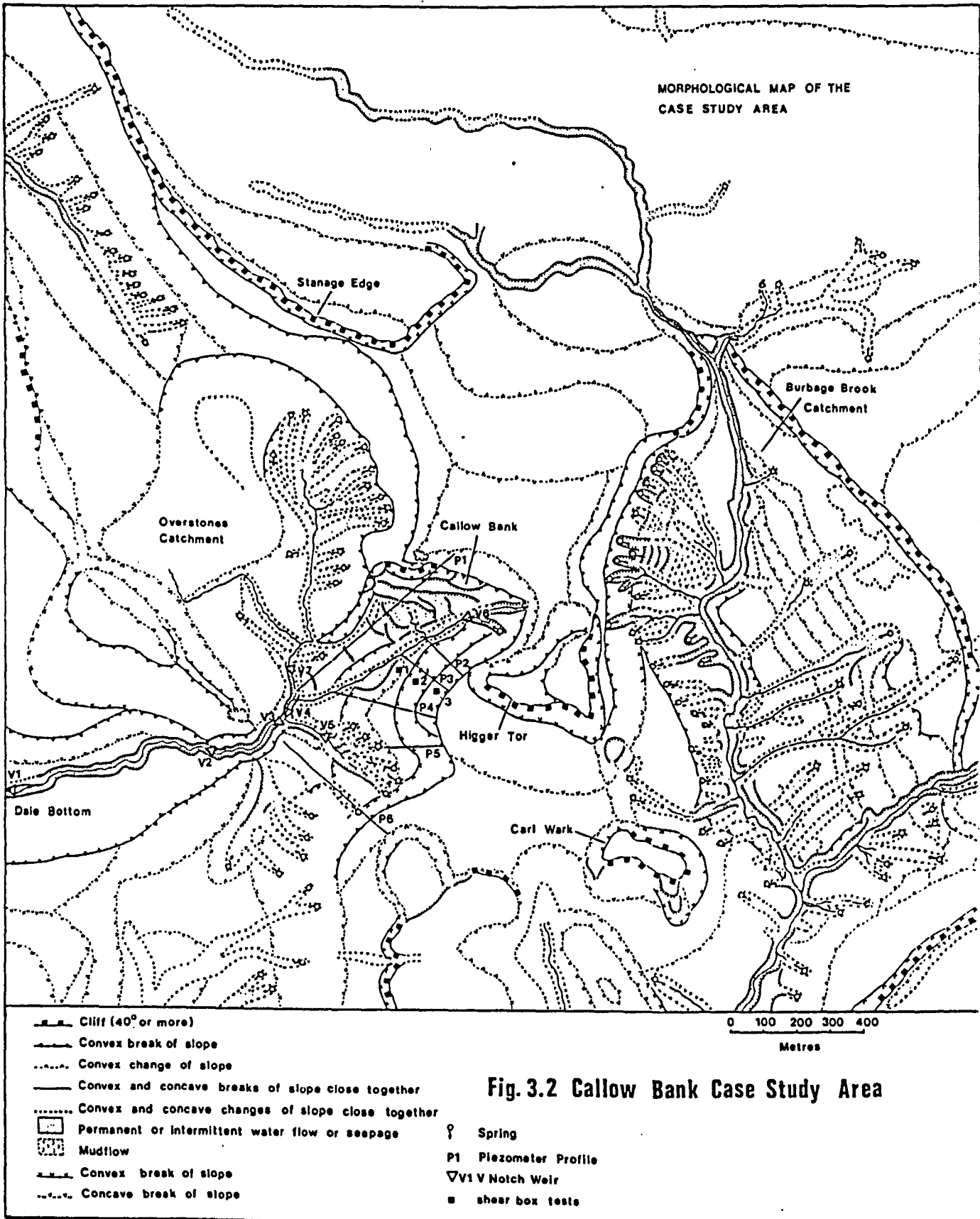
Fig. 3.2 Callow Bank Case Study Area

Cliff (40° or more)

Convex break of slope

Convex change of slope

Convex and concave breaks of slope close together

Convex and concave changes of slope close together

Permanent or intermittent water flow or seepage

Mudflow

Convex break of slope

Concave break of slope

⚲ Spring

P1 Piezometer Profile

∇V1 V Notch Weir

■ shear box tests

Callow Bank, (see Geomorphological Map on page 263).

The geomorphology of Callow Bank is dominated by the presence of a multiple retrogressive landslide. This landslide is shown in section in Fig. 3.3. The landslide has involved a series of mudstones, siltstones, shales, sandy-shales and thin sandstones, known collectively as the Middle Grits. These strata are very variable and alternate rapidly so that the uppermost sandstone members provide little protection to the intermediate underlying formations. The Callow Bank landslide is a multiple retrogressive type of landslide, where the rotational movements were deep-seated with moderate/weak backward rotation of separate blocks. Fig. 3.3 shows that possibly four major successive rotational movements may have taken place within the main slide mass. The heterogeneous character of the Middle Grit Series suggests that secondary movements took place at times subsequent to the period of main slope-failure on more than one non-circular slip surface. The deepest and predominant failure probably occurred on the black shales and seatearths which lie immediately above the Kinderscout Grit sandstone which outcrops in the stream bed at Mitchell Field, (see geological section 2 and Fig. 3.1). Weathering of the marine shales at the base of the Middle Grits may have induced deep-seated creep in the failure zone. The main landslide scar is about 25m high, the exposed section (geological section 1) has been described in the preceding section on Geology (see Fig. 3.1), see Plates 1 - 6 on pages 268 - 270.

At the foot of the landslide scar the main slide mass is character-ised by a sequence of topographic benches and depressions. The first two rotated blocks beneath the main scar show some back tilting and are covered by Rivelin Grit boulders and scree derived from the
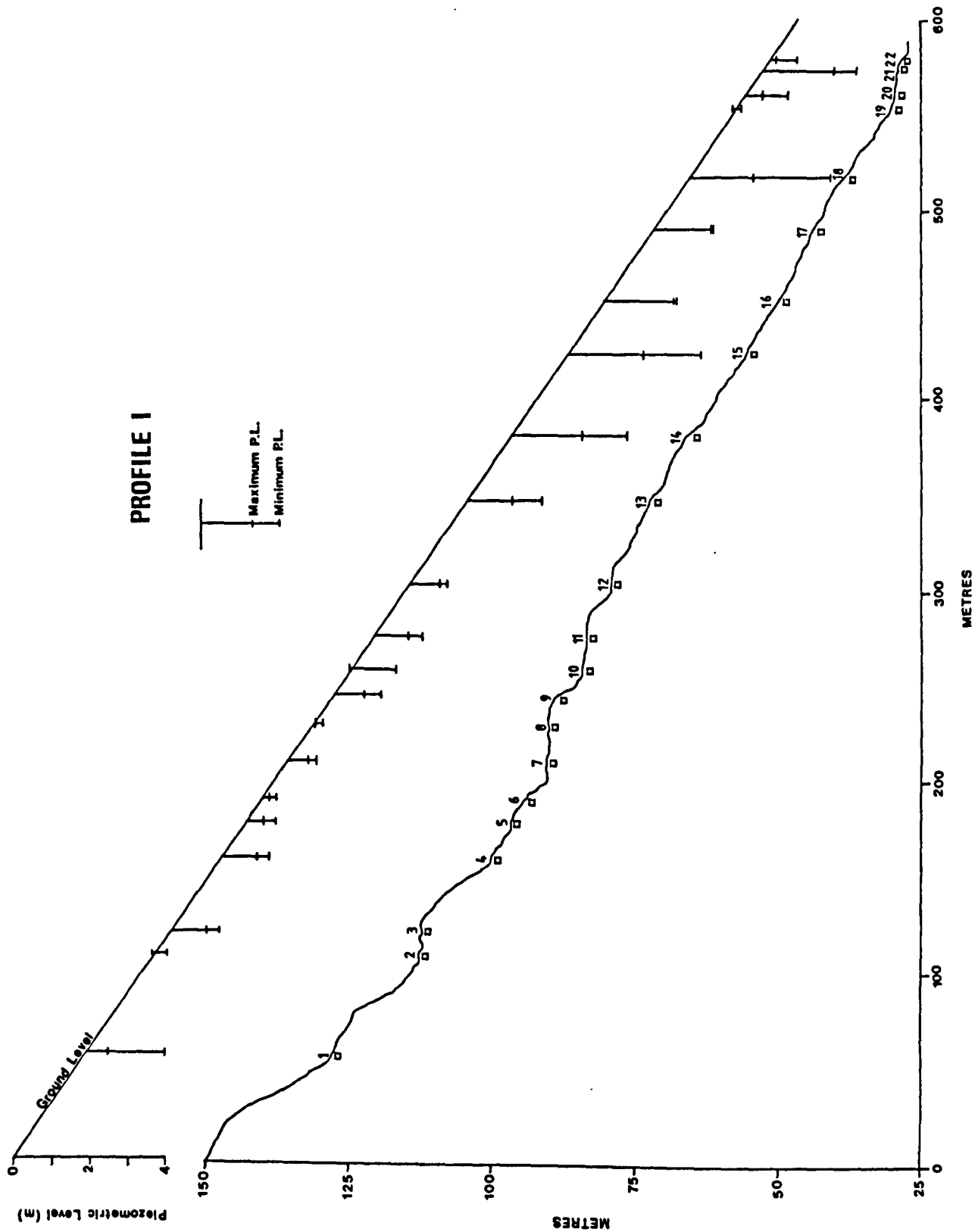
Fig. 3.3   Slope Profile 1, Callow Bank multiple retrogressive landslide

Geomorphological Map of Callow Bank Landslide

Scale – 1:260

N

Legend:

- Cliffs (bedrock standing in excess of 45°)
- Convex break of slope, sharp
- Concave break of slope, sharp
- Ridge, sharp
- Valley or depression, sharp
- Convex change of slope, rounded
- Concave change of slope, rounded
- Ridge, rounded
- Valley or depression, rounded
- Scarp or bluff, sharp (convex and concave) breaks of slope in close association)
- General direction of slope
- Drainage lines (may emerge or disappear suddenly)
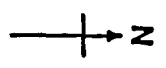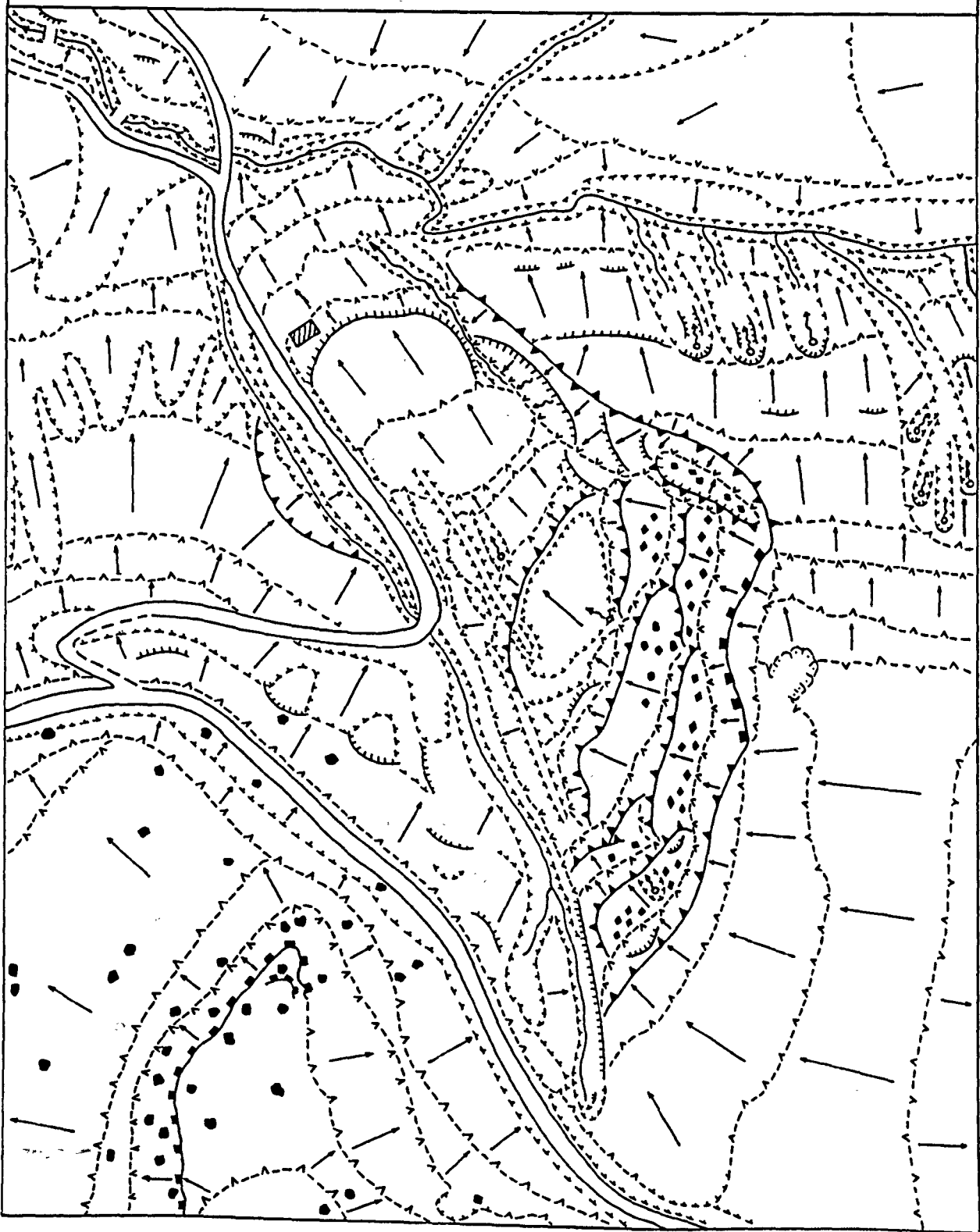
sandstone cliff above. A number of the lower rotated blocks have formed a sequence of terraces, these have developed perched water tables. However, on one particular rotated block situated 210m downslope from the main landslip scar a spring has been dammed along the downslope edge of the block leading to the development of a small pond. The dam may have been constructed by lead miners in order to wash the lead ore and for cooling the molten lead. The dam has been breached and water seeps beneath the base of the clay core used to construct the dam. This has led to the formation of a marshy area with free standing water on the next downslope rotated block immediately below the position of the dam.

The main displacement at Callow Bank created additional stress on the adjacent north western slope of the main interlocking spur between the Callow Bank landslide and the Overstones catchment. Two back-tilted rotational blocks have developed on the spur and have come to rest on the main landslide mass.

The lower section of the slide, i.e. the area beyond 300m below the landslide scar, can be interpreted as debris-slide/mudslide. In this section the debris appears to have been more mobile and moved by sliding outwards from the rotated units to create a low but uneven morphology as far as the stream which drains the Overstones catchment. Callow Bank Farm was built in 1720 and is situated on the debris-slide/mudslide apron 450m below the landslide scar. Since its construction the farmhouse has been subject to major structural damage. Material derived from mudsliding and soil creep has progressively built up behind a retaining wall at the back of the farmhouse and despite the addition of buttress supports on the rear wall of the farmhouse the wall has buckled causing the roof to

collapse. The front wall of the farmhouse showed extensive tension cracking and displacement in a number of places. A more recent brick outbuilding adjacent to Callow Farm had also suffered partial collapse; the remaining standing wall of this building collapsed during a wet spell in November 1985. In the toe area of the slide in the field below Callow Bank Farm a break in slope is located parallel to the contours and the stream draining the Overstones catchment area. The farmer reported that the break in slope had only become noticeable since 1982. During the period of field investigation the break in slope became more pronounced and a prominent soil scar became established. The farmer first allowed cattle into the field in 1980 after which the cattle had trampled and puddled the stream banks affecting the water course, partially blocking some areas and eventually creating a marshy area. The partial blockage of the stream preventing free drainage of water may have caused an increase in the pore water pressure in the toe area thereby reactivating pre-existing shear surfaces in the mudslide. The renewed instability was probably responsible for the development of the soil ridge running parallel to the stream.

To summarise, the slide in its upper zone has an irregular form that can be attributed to pre-existing planes of discontinuity in the strata. Slip movements have taken place along such bedding plane failure surfaces. From morphological evidence these failure surfaces appear to correspond to silty mudstone strata within the sequence. Some slight rotation of the blocks nearest the main back scar occurred, but the whole initial landslide mass has been substantially modified by the continued duration of the lower rotated blocks and displacement of material from their distant slope. These later secondary movements have greatly extended the length of the slide to

a point well beyond the limit of the initial failure zone. This elongation was probably controlled by the steepness of the slope (20°), the configuration of the narrow Callow Bank catchment and springs seeping from beneath the Rivelin Grit sandstone in the scarp face of Callow Bank. The unstable nature of the debris-slide/mudflow section of the main slide is attested by structural damage to Callow Bank Farm and renewed instability at the toe caused by recent blockage of the stream.

The alignment of the prominent gritstone edges of Stanage, Burbage and Carhead is shown in Fig. 3.2, these edges along with Higger and Carl Wark tors have been affected by ancient rockfall and topple failures. Some of the detached gritstone blocks have been rafted downslope beyond the foot of the cliff on solifluction sheets. Millstone Grit blocks derived from the south western free face of Higger Tor were moved during periglacial times within a gully in the upper part of the Callow Bank catchment area and now remain as a fossil boulder stream.

The mid-slope/transportational slopes (20° or more) of the east facing slope of the Burbage Brook catchment and the west facing slope of the Overstones catchment have been incised by numerous gullies and rills which have developed along former seepage percolines. Active gully-head erosion, as evidenced by the formation of fresh soil scars is presently occurring, particularly where springs emerge at the sandstone/shale interface on the west facing slope of the Overstones catchment. A number of shallow rotational and translational failures involving regolith materials have also occurred on these slope units, particularly where seepage water becomes localised or where springs emanate from beneath the Rivelin Grit and meet the relatively

impermeable shales. Similar failures have also occurred in a number of places on the north west facing slopes of Callow Bank. The road which runs along the foot slope of Higger Tor has been repaired in a number of places where rotational slides have occurred. At one point along this section of road the back scar of an old rotational slide has exposed 5m of shale. Derbyshire County Council highway maintenance engineers have installed a slit trench infilled with limestone packing in order to drain water issuing from a spring in the shale back scar of the slide and to channel the water beneath the road. On the slope directly beneath the back scar and road, the rotational slide has developed into a small mudslide. This material remains very wet throughout the year due to the drainage water and high pore water pressures are maintained in the area immediately below the road. Fines continue to be removed in this mudslide, this is consequentially causing subsidence of the road surface on its downslope edge.

A number of relatively fresh back scars and tension cracks running parallel to the contours on the north west facing slopes of Callow Bank have been observed during field investigations, indicating that the materials forming these slopes are close to limiting equilibrium for shallow planar translational movements. Terracettes, soil falls and micro-soil slumping tend to occur on the steeper convex creep slopes (15-19°). The streams draining the Callow Bank and Overstones catchments have cut the steep sided almost V shaped Dale Bottom valley. The uppermost section of the north facing slopes of Dale Bottom are littered with Kinderscout Grit boulders and scree; many springs emerge near the foot of these slopes causing small rotational failures and shallow translational slides.

Plate 1. Callow Bank landslide, Callow Farm is situated in the centre of the photograph.

Plate 2. Showing the back Sear and toe of a small translational landslide on the South west facing slope below Higger Tor, Callow Bank.

Plate 3. Debris apron of Callow Bank landslide, consisting of a series of benches and waterlogged slump depressions. Area of translational sliding and stream undercutting in the top right of the photograph.

Plate 4. Landslide damage to a minor road passing below Higger Tor, Callow Bank.

Plate 5.

Plate 6

Plates 5 and 6 show landslide damage to Callow Farm,
Callow Bank.

3.3 CHARACTERISTIC AND LIMITING OR THRESHOLD SLOPES

3.3.1 Characteristic slope angles

Strahler (1950) introduced the use of statistical analysis of slope profile data generated in profile surveys. A technique frequently used in the analysis of slope form has been the examination of the frequency distribution of slope angles. Studies in various parts of Britain have used this technique to demonstrate the existence of characteristic angles. Young (1961) defined characteristic angles as "those which most frequently occur, either in all slopes, under particular conditions of rock or climate, or in a local area. They appear as modes on a graph of angle frequency distribution". Examination of the occurrence of characteristic angles has shown that certain groups of angles have a higher than average frequency of occurrence in a number of areas studied within the British Isles. Young (1972) recognised 5 recurrent groups, of which 3 were important in the areas studied in Britain. These were:

1. $30^{\circ} - 38^{\circ}$ typically $33^{\circ} - 35^{\circ}$
2. $25^{\circ} - 29^{\circ}$ typically $25^{\circ} - 26^{\circ}$
3. $5^{\circ} - 9^{\circ}$

Studies have shown that two or three characteristic slope angle groups could occur on any particular rock type. A study of slopes on shale and Millstone Grit rocks in the south Pennines by Carson & Petley (1970) showed three modal values (20°, 26° and 33°) in the frequency distribution.

A number of explanations have been proposed for the occurrence of characteristic slope angles. Young (1972) identified five main explanations. These may be summarised as:

1. The angle frequency peaks are the result of random variation (statistical testing of this hypothesis is difficult due to the lack of knowledge of the distribution pattern of angles to be taken as the null hypothesis).

2. Particular conditions of structure produce characteristic angles. This is suggested by the association of different characteristic angles on different geological strata as cited above.

3. Certain angles are intrinsic features of slope evolution, irrespective of rock type and climate. Young (1972) considered that this can only be supported for the $33^{\circ} - 35^{\circ}$ group of angles.

4. Characteristic angles reflect local morphological evolution. Young (1972) cites the example of Exmoor where, assuming the hypothesis of slopes becoming gentler with time and using Davisian terminology, two successive rejuvenations may be considered to have produced a polycyclic landscape of a relict peneplain dissected by valley-in-valley forms. The three sets of charcteristic angles suggested a correspondence to the stages of the cyclic development on each of the main rock types:

shales: $3^{\circ} - 4^{\circ}$, $9^{\circ} - 10^{\circ}$, $23^{\circ} - 25^{\circ}$.
sandstones: $4^{\circ} - 5^{\circ}$, $13^{\circ} - 15^{\circ}$, $28^{\circ} - 29^{\circ}$

These characteristic angles are thus time dependent features related to stages of morphological evolution.

5. Characteristic angles are related to limiting or threshold angles for processes. Young (1972) states that slopes above 45° undergo rapid retreat and that $33^\circ-35^\circ$ slopes develop from these. This slope angle range ($33^\circ-35^\circ$) is close to the limiting angle for a continuous regolith cover and the angle of repose of scree. The $25^\circ-29^\circ$ slope angle group also occurs on predominantly rectilinear slopes and this was considered to replace the steeper slopes ($33^\circ-35^\circ$) by relatively rapid slope retreat where rapid basal erosion was absent. This lower slope angle was considered by Carson & Petley (1970) to correspond to the stability angle of the reduced or weathered regolith material on the slope i.e. the threshold angle. The lower angle slopes of $5^\circ-9^\circ$ were considered to be associated with the limiting angle for relatively rapid solifluction (Young, 1972) or as a further application of the concept of threshold angles (Carson & Kirkby, 1972). These hypotheses explain characteristic angles in terms of time independent forms related to specific processes.

3.3.2 Limiting or Threshold slopes

Many engineering geomorphological studies have been conducted on slides which have taken place on slopes consisting of cohesive material such as clay where the morphology of the failure plane is sufficiently well preserved for stability back analysis (i.e. to model closely the depth, shear surface curvature, and lateral extent of failure), Chandler (1971, 1982). However, where direct evidence of past failure is tenuous (e.g. in less cohesive material) back

analysis may be impossible. In such cases the interpretation of limiting or threshold slope angles identified as modal peaks in frequency distributions of the angles of straight slope segments has been used as an alternative geomorphological technique.

In their study of slopes on Exmoor and the Pennines, Carson & Petley (1970) proposed that straight segments on hillslopes at about 25° represented the angle of long term stability for non-clay regolith material. Their work was developed and extended into a broader explanation of the development of hillslope form. This 'threshold slope' concept attempted to explain the relationship between the weathering and reduction of the slope mantle material and the angle of stability of the slope. The mechanics of the instability process in soil mantles on hillslopes was further examined by Carson & Kirkby (1972). Their conclusions were based on the work of Henkel & Skempton (1954) on the Jackfield landslide in Shropshire and the work of Skempton (1964), Carson (1969), Carson & Petley (1970) on the Gritstones and shales of the Pennines and Exmoor. They considered that most slopes in temperate areas are debris mantled slopes composed of the products of weathering with the underlying hillmass being of strong rock. Normally such mantles are 1-2m thick so that instability causes shallow slides to occur rather than deep-seated slides. See Figure 3.4 which shows the relationship of the forces involved for stability analysis of a shallow planar translational slide (Carson & Kirkby, 1972).
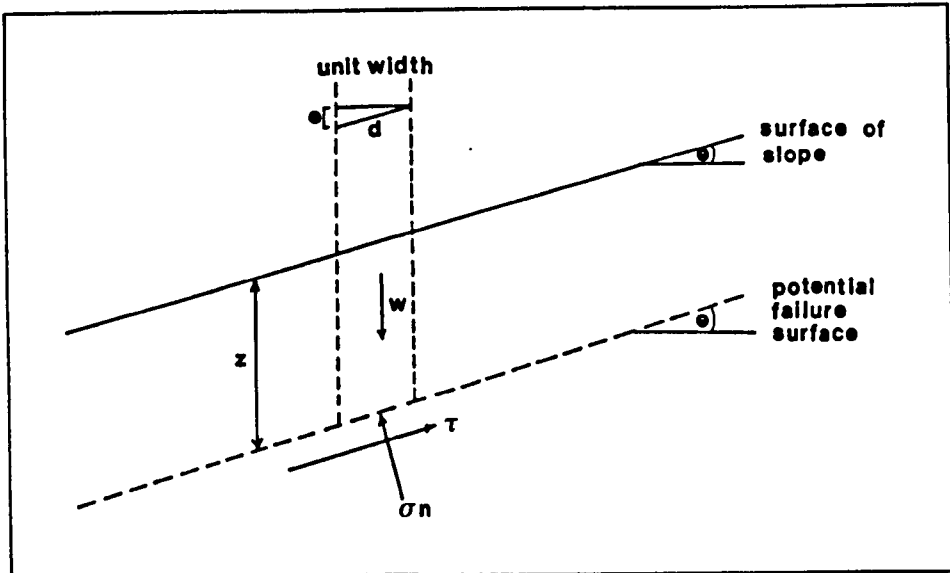
Fig. 3.4   Relationship of forces for stability analysis of an
           infinite slope subject to shallow sliding (based on
           Carson & Kirkby, 1972).

where:

Vertical stress = w/d = $\gamma.z.\cos\theta$ (1)

Shear stress   = τ = $\gamma.z.\cos\theta.\sin\theta$ (2)

Normal stress   = σn = $\gamma.z.\cos^2\theta$ (3)

Shear strength = s = $c + \sigma.\tan\phi$ (Coulomb, 1966) (4)

c = cohesion, $\emptyset$ is the angle of shearing resistance, and z is the
depth to potential failure surface.

The factor of safety (Fs) of a hillslope is given by: Fs = $\frac{s}{\tau}$ (5)

The effective normal stress ($\sigma n'$) on the potential failure surface
will vary according to changes in the pore water pressure (u)

Thus: $\sigma n' = \sigma n - u$ (6)

For long term stability of a slope it is necessary to assume the
maximum pore water pressure that is likely to occur in the mantle
debris (Skempton & DeLory, 1957). They suggested that this condition

would occur when the water table was at the ground surface and sub-surface flow of water was parallel to the slope of the ground. The relationship of pore water pressure (u) and soil depth (z) is given by:

$$u = \gamma_w . z . \cos^2 \beta$$

(7)

where γw is the unit weight of water (9.81 kN/m^3)

Carson (1971) stated that the maximum stability angle of a hillslope (β_l) depended on the effective shear stress and the geometry of the incipient failure surface. Or a straight hillslope, the failure surface would be confined to the slope mantle debris and would be almost a plane parallel to the slope.

The condition of limiting stability on an infinite plane failure surface would occur when:

Fs = 1 and τ = s   (8)

Thus from equations 2, 3, 4 and 6 the condition of limiting stability can be expressed by:

(9)

$$\gamma . z . \cos\beta \; \sin\beta \; = \; c' + (\gamma . z \cos^2 \beta - u) \tan \phi'$$

Under maximum pore water pressure cohesion would become zero so that the maximum slope β_l would occur when:

(10)

$$\gamma . z \; \tan\beta = (\gamma . z - u / \cos^2 \beta) \tan \phi'$$

substituting for equation (7):

$$\gamma . z \; \tan\beta = \left[\gamma . z - \gamma_w \frac{z . \cos^2 \beta}{\cos^2 \beta} \right] \tan \phi'$$

Thus:

$$\beta_l = \text{arc } \tan\left[\frac{\gamma - \gamma_w}{\gamma}\right] \tan \phi^{\cdot}$$

On the assumption that the mean value of (γ) is approximately $2 \gamma_w$

Then:

$$\tan \beta_l = \tfrac{1}{2} \tan \phi^{\cdot}$$

(11)

That is the maximum slope angle β_l depends on the angle of shearing resistance ($\emptyset'$).

In analysing the behaviour of residual soil mantles, Carson & Kirkby (1972) considered that if the mantle debris was composed of talus with large voids the condition of maximum pore water pressure would not occur and pore water pressure would be equal to atmospheric pressure (u = o). In this case equation (9) becomes:

$$\tan \beta_l = \tan \emptyset'.$$

so that the slope angle is equal to the angle of repose of the debris and would normally be about 35°.

With continuous weathering Carson & Kirkby (1972), considered that the mantle debris would progressively change, breaking down through a sequence of talus, mixed talus and colluvium (taluvium) eventually to form soil. The production of a mixture of rock rubble and finer particles would produce greater interlocking than in talus and this would give higher angles of repose, $43^\circ-45^\circ$. However, pore spaces would become smaller and for long term stability the assumption must be made that pore water pressure would reach a maximum so that the slope angle depended on the condition of equation

(11). Thus, for taluvial mantles the angle of maximum slope stability (β_l) would be about $25^{\circ}-26^{\circ}$.

Carson & Kirkby (1972) cited evidence from a number of studies (Savigear, 1956; Young, 1961; Melton, 1965; Robinson, 1966) indicating that in a range of climatic conditions rocks weathered to produce taluvium mantles which resulted in slope angles of $25^{\circ}-27^{\circ}$. This evidence led to the recognition that a number of angles of limiting stability exist on a slope each associated with a stage in the breakdown of the mantle. The slope analysis of the southern Pennines of Derbyshire by Carson & Petley (1970) showed a trimodal distribution of straight slopes (20°, 26° and 33°) associated with three stages of breakdown of mantle material. Carson (1969) considered that there were strong grounds for suspecting that such a pattern was very common and that all rocks in all climates should pass through these three stages of disintegration. This recognition led to the development of a general model of slope development under mass failure.

The main slopes were:

1. Instability on a slope caused a steeper slope to be replaced by a gentler slope. Different landscapes would experience more than one such phase of instability and the nature of the rock, its history of disintegration and the climate would determine the number of these phases. Thus in a well jointed rock mass three phases would be likely to occur. In phase one a cliff would be replaced by a scree slope. In phase two the scree slope would be replaced by a taluvial slope and finally in phase three this would be replaced by a soil slope.

2. The phases of instability would be separated by threshold slopes. Under the prevailing conditions of mantle character and pore water pressure the mantle would be in a state of temporary stability. Due to the great variety of such conditions a whole range of threshold slope angles would exist. However, Carson & Kirkby (1972) suggested that certain threshold slopes were common. They were:

$43^{\circ}-45^{\circ}$: slopes on fractured and jointed rock with high density packing, large voids and pore pressure limited to atmospheric.

$33^{\circ}-38^{\circ}$: slopes on the same material with a looser state of packing.

$25^{\circ}-28^{\circ}$: slopes on taluvial material.

$19^{\circ}-21^{\circ}$: slopes on sandy material where the pore water pressure corresponds to that in equation (7).

$8^{\circ}-11^{\circ}$: slopes in clay.

Thus, Carson & Kirkby (1972) proposed that the pattern of slope development depended on the number of phases of instability and the steepness of the threshold slopes.

Kirkby (1973) examined further the manner of breakdown of slope mantle material during weathering, to analyse the pattern of continuous and discontinuous reduction in the angle of internal friction ($\emptyset'$), affecting the shear strength and so causing changes in the angle of slope stability. The composition of slope mantle material may be represented as a three component mixture of gravel,

sand and clay as shown in Fig. 3.5. In each corner of the triangle there is a zone where a single component forms the fabric of the material and in the centre the fabric combination of all three components. Using the same triangular graph base, Fig. 3.6 gives an interpretation of values of stable slope angles (β_i) in the field and their corresponding ($\emptyset'$) values devised by Kirkby (1973), and based on data from Skempton (1964) for clay soils, Carson & Petley (1970) for coarse debris and Holtz (1960) and Vucetic (1958) for soils of moderate gravel content. Fig. 3.6 shows that mixtures of coarse and fine material have higher values of ($\emptyset'$) than single component soils. In Fig. 3.7 the percentages show the theoretical variations of porosity for a three component mixture. Changes in particle size composition will affect the pore water pressure characteristics and consequentially alter the values of ($\emptyset'$). As non-clay parent material weathers mechanically and chemically so the composition of the slope material will alter and may follow various routes across the composition triangular graph.

Kirkby (1973) suggested two possible routes shown in Fig. 3.7 as 1 and 2. A rock which weathered and followed route 1 would show a rise of ($\emptyset'$) with a reduction in gravel content and then a fall in ($\emptyset'$) would occur at a late stage in weathering. A rock weathering along route 2 showed the same pattern of change of ($\emptyset'$) but at significantly different rates and times in the weathering process. Kirkby considered there was some reason to suggest a step-like fall in ($\emptyset'$) as had been observed at about 20% gravel for the weathering of rock following route 2 whereas for route 1 there seemed to be a steady fall in ($\emptyset'$). Kirkby loosely associated these two routes with two different types of rock breakdown. Rocks such as sandstone, limestone or granite would undergo discontinuous breakdown. They
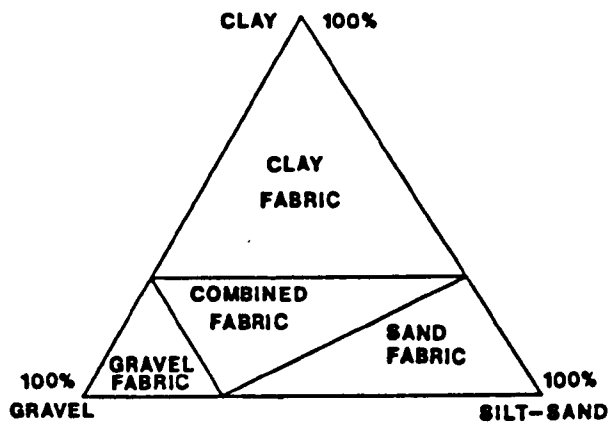
Fig. 3.5   A three component mixture of gravel, silt-sand and

clay (based on Kirkby, 1973).
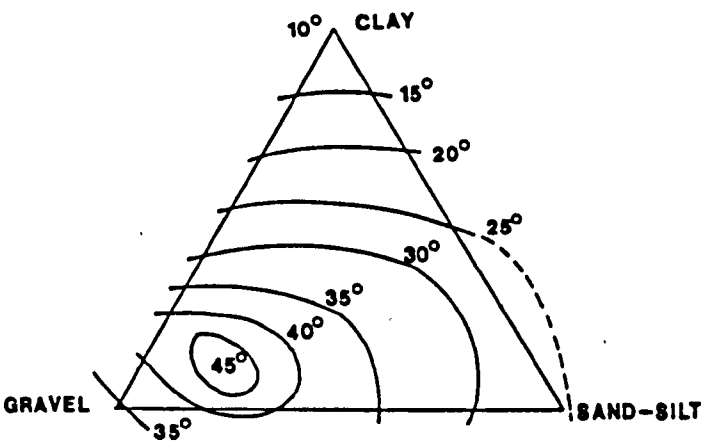
Fig. 3.6   Relationship between the grain size composition and

angle of internal friction (∅') (Kirkby, 1973).
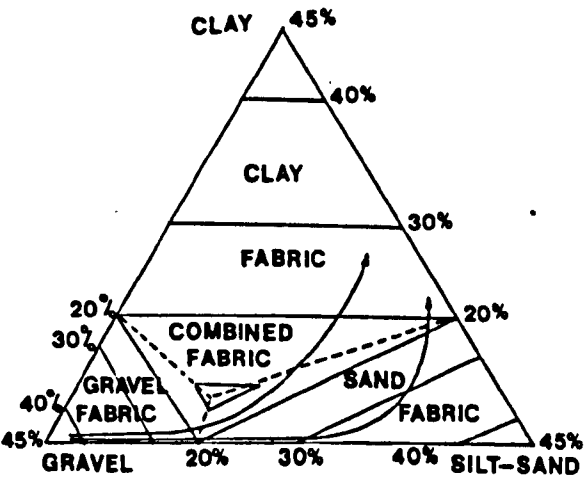
Fig. 3.7   Theoretical variations of porosity for a three-component

mixture. The routes 1 and 2 refer to different paths

followed during weathering (Kirkby, 1973).

would produce sand or finer grains from the joint blocks. Their material would be like a sand and gravel mixture with sand being produced at a constant rate and clays would appear only as the smaller grains weathered; this pattern of breakdown corresponds to route 1. In rocks such as schist, shale and basalt a continuous pattern of breakdown would occur with all sizes of material tending to breakdown together so that initially hardly any sand sized material would be produced, but after a time large amounts would be produced rather quickly; this pattern corresponds to route 2.

Kirkby (1973) indicated that the presence of sand or finer material determined the critical water holding property of the slope material so that the rate of production of sand determined the switch in stable slope conditions from tan β_l = tan $\emptyset'$ to tan β_l = ½ tan $\emptyset'$. This would mean that if there were a rather rapid appearance of sand during the early stages of weathering then there would be an abrupt change from the dry to the wet stable angle. Thus he argued that rocks which broke down continuously tended to have two stepped reductions in stable angle, and rock which broke down discontinuously tended to have a steady unstepped reduction in stable angle.

Kirkby (1973) compared this dichotomy of breakdown types to the observed dichotomy between slopes with thick soils of more than 30cm and slopes with thinner soils. In the first case the slopes with thick soils showed landslide scars and bi- and tri-modal slope angle distributions as described by Carson & Kirkby (1972) on shale and Shale Grit in Derbyshire, South Pennines. This suggested that

landslide slopes were those with continuous rock breakdown where an abrupt fall in the stable angle (β_ι) would cause large slides to occur. In the second case, slopes with thinner soils (<30cm) would tend to have terracettes and a continuous slope angle distribution and would be associated with grits, sandstones and limestones. These rock types tend to break down discontinuously and small amounts of weathering would produce small reductions in the angle of stability (β_ι). Only very small slides would be required to restore equilibrium.

When material underwent mass movement it came to rest at a lower slope angle at which it remained stable. Further weathering would eventually produce instability and so slopes would develop with two or more straight segments each being replaced by the one below it in a sequence of parallel retreat. Kirkby (1973) indicated that when there was a continuous change of stable angle two possible slope forms result. Either there would be the replacement of each entire straight slope for every small adjustment of angle producing straight slopes over a wide range of slope angles as in the 25°–35° range for talus to taluvium, or there would be an indefinite number of short straight segments each replacing the one above and effectively producing a concave slope. Thus Kirkby indicated that heterogeneous mixtures and different weathering sequences would produce variations in ($\emptyset'$) and stable slope angles during the course of weathering.

Among more recent studies investigating threshold slopes those of Rouse (1975) and Rouse & Farhan (1976) may be cited. These further

demonstrate the interpretation of modes of frequency distribution of straight slope angles in terms of the threshold values for mass movement processes. The uniformity of the valley side slopes of South Wales were found to be associated with rapid mass movement processes related to the engineering properties of the regolith. The important process in slope denudation was found to be the repeated operation of micro-slides leading to an irregular surface. The application of the limiting equilibrium model for shallow sliding gave threshold angles in two case study areas of 35° and 36° (dry state) and 17° and 22° (saturated state) and these corresponded closely to the 'characteristic angles' of the valley side slopes.

British Geological Survey, in their South Wales Coalfield Landslip Survey (Conway et al 1980), found that for slopes showing clear evidence of planar (translational) failures within superficial material, the frequency distribution plot of slope angles gave a population mean of 17.4°–18.6° (95%-confidence). The predicted mean limiting angle (β_l), for the head materials tested was 17°, which lies close to the confidence interval of the slopes with identified shallow planar failures. It was also near to, or slightly lower than, the mean angle of all the measured slopes that showed evidence of all types of shallow failures 18.1°–19.3°, (95%-confidence) and compares closely with the predicted limiting angle of 17.2° for slopes in the Upper Lliw Valley determined by Rouse & Farhan (1976).

Rouse & Farhan (1976) identified the following slope types:-

Slope Angle	Slope Type
36°	Upper limit for valley side slopes
$36^{\circ} - 34^{\circ}$	Dry scree accumulation at the foot of free faces
$30^{\circ} - 28^{\circ}$	Fossil scree on sandstones
$22^{\circ} - 18^{\circ}$	Fossil scree on shales
$10^{\circ} - 8^{\circ}$	Solifluction slopes on valley floors and on escarpment crests
$6^{\circ} - 2^{\circ}$	Flat areas of valley floors

Rouse (1975) has shown that processes of rapid mass movement can be used to interpret most of the valley side slopes in the British landscape where the slopes are largely a relict feature of a periglacial environment. Glacial action created free faces which under periglacial conditions developed large scree slopes. Weathering and lateral eluviation created an increase in fines downslope so that the footslope conditions possessed different ground

water regimes and therefore limiting angles compared to the dry scree slopes. Rapid mass movement particularly small scale planar slides continue to affect these slopes.

3.4 TECHNIQUES

3.4.1 Slope Profile Survey

In order to establish whether the hillslopes have characteristic angles and that these correspond to the occurrence of slope segments, a slope profile survey was carried out. Identification of relevant modal slopes in the landscape presents a sampling problem. The aim of the slope profile survey techniques should be that they provide an accurate portrayal of the true slope profiles and avoid any purposive sampling so that a true random sample is selected. The techniques proposed by Pitty (1966, 1967, 1968) and Young (1961, 1964, 1971, 1972) aim to achieve these objectives and were used in the case study area. The method of sampling of slope profiles is that outlined by Young (1972). The interfluves and talwegs are marked on the base map of the study area. The midslope line is then drawn midway between talweg and interfluve. Twenty four sample points were then marked off at equal distances along this profile sampling line starting from a randomly selected point. The slope profile lines are then drawn up and down the true slope from these points. The ends of the profile at the interfluves and talwegs always follow the true slope as indicated by Pitty (1967) terminating at the point where the slope profile angle equals that measured longitudinally down the interfluve or talweg. The selection of positions along the profile for the measurement of slope angle must also be objective and in this study a standard measured length avoided any prejudging of position of change

or break of slope and places the entire analysis of the slope profile
to statistical methods. Gerrard & Robinson (1971) investigated the
variability of slope measurements and demonstrated the effects of
selecting different measured lengths on the frequency distribution of
slope angles and of micro-relief features on slope angles. A
pantometer based on the design of Pitty (1968) was used.

3.4.2 Presentation and Analysis of slope Angle Data

The slope data for each slope profile was recorded starting from the
top of the profile. A micro-computer program (SAVE DATA) was used
for storing the data on a disc file system using a BBC micro-
computer; other programs were then used to present and analyse the
slope data. The program (PLOTPROF) converted the data for each
profile into a profile graph of slope angle against measured length.
These were drawn for each profile. The program (HISTGRM) was used to
plot slope frequency histograms for any selected group of data files
of slope profiles. The program (SLOPVAR) was used in order to
determine the coefficient of variation of slope angle between
successive measured lengths. The coefficient of variation was
calculated using the following equation:

$$Va = 100 \times \frac{\sqrt{\frac{\Sigma \ell \theta^2}{\Sigma \ell} - \bar{\theta}^2}}{\bar{\theta}} \tag{1}$$

where: Va = variability of slope angle

θ = slope angle of each unit

$\bar{\theta}$ = mean slope angle of each unit

ℓ = measured length along the slope profile

The print-out from the slope variation analysis was used for the selection of the longest slope segments; these were then compared in order to determine the 'Best Segment Units' using the method proposed by Young (1971).

'Best Element Units' which are based on the angle measurements of successive measured slope angles were also determined. The curvature (cq) of a measured slope length q was determined by comparison with adjacent slope angles θp and θr of lengths p and r. The curvature is then given by:

$$cq = 100 \times \frac{\theta p - \theta r}{0.5\ell p + \ell q + \ell r} \text{ degrees/100 m} \tag{2}$$

where: cq = the curvature of a measured slope length

ℓq = measured slope length

ℓp & ℓr = adjacent slope lengths to q

θp & θr = adjacent slope angles to q

The mean curvature can be obtained and the coefficient of variation Vc is obtained from equations (1) and (2) by substituting the curvature c for angle θ .

Young (1971) proposed that it was desirable to specify maximum percentage values of variation of angle for segments and curvature for elements, normally these would be, Va max = 10% and Vc max = 25%. Young (1971) found that these maximum percentage limits provided a good standard of internal uniformity in slope units and avoided the excessive fragmentation of slopes into short units. Each slope unit was therefore tested to determine in the case of segments whether the coefficient of variation of angle was above 10% and in the case of

elements whether the coefficient of variation of curvature was above 25%. If they exceeded these limits then the program returned to the beginning of the slope profile again and started from the second measured length. In this way a succession of overlapping segments and elements were identified. Young (1971) recognised that a method of discrimination had to be adopted to identify the 'Best Units'. Where a measured slope length occurred in two segments or elements it was allocated to the longer unit; if both units were of the same length it was allocated to the unit with the lower coefficient of variation, if the coefficients were equal it was allocated to a segment in preference to an element. This method of 'Best Unit Analysis' was defined by Young (1971) as the "partitioning of a slope profile into segments and elements in such a manner that the coefficients of variation (Va, Vc) of angle and curvature respectively did not exceed specified maximum values, and each measured length was allocated to the longest acceptable unit of which it is a part". A lower limit on the number of measured lengths acceptable in a 'Best Unit' was also set, it was decided that 6 measured lengths (9m) was the shortest acceptable 'Best Unit' for the hillslope at Callow Bank.

3.4.3 Piezometric Survey

Climatic parameters, ground water levels, basal undercutting, channelling, undrained loading, and reduction in shear strength properties have all been proposed as factors accounting for shallow planar translational failures. Variations in ground water levels, in particular, have been widely recognised to be critical factors involved in failure due to changes in strength properties and stability conditions which this variable may produce. Carson (1971)

has postulated that many shallow planar landslips are caused by a reduction in shear strength along a potential failure plane brought about by a rapid rise in pore water levels due to periods of heavy and prolonged rainfall. Intergranular pressure and friction is due to capillary tension in a moist soil, these are destroyed on saturation as a result of bouyancy effects.

Fluctuations in the level of the water table (i.e. phreatic surface) or the creation of temporary perched water systems, will markedly affect the factor of safety of a hillslope. Indeed, after heavy rainfall it is highly probable that the piezometric level may be higher in tension cracks and fissures, small topographic hollows, or in sites immediately above rills and gullies, than the general ground water table level. There is increasing evidence that water moves rapidly through well structured soils along preferred flow paths when they are not water saturated (Germann, 1986). Soil structural elements allowing for rapid flow are referred to as macropores; they comprise voids, root channels, animal burrows, desiccation cracks and fissures. Studies by Germann (1986) and Germann & Beven (1986) have shown that macropores which are active during the infiltration process may enhance the soils infiltrability by one to two orders of magnitude. This suggests a relationship between failure, heavy rainfall conditions, and locally high pore water pressures, with mean ground water conditions lagging somewhat behind. In engineering geomorphological analyses of shallow planar slide stability, the factor of safety should be considered in relation to the maximum pore water pressures likely to occur in our present climate. Skempton & DeLory (1957) suggested that this condition is attained when the phreatic surface coincides with the ground surface and when sub-surface flow is parallel to the ground slope (e.g. the slide at

Uppingham, Chandler, 1970c). This condition need not imply that the regional ground flow net extends to the surface of the slope; 'throughflow' has been found to provide the main element of discharge in channel sections (Wilson, 1971; Kirkby & Chorley, 1967; Weyman, 1970; Whipkey, 1965a,b; Carson & Petley, 1970).

3.4.4 The Nature of Pore-pressures in the Superficial material

In the study area the hillslopes for the most part are steep sided, the regolith materials tend to have a high sand/gravel fraction and the true ground water table generally occurs well below the surface. It seems unlikely that the true water table ever rises to the surface even during the most prolonged rainstorms. It may thus seem surprising that meaningful results have been obtained using Infinite Stability Analyses in this type of terrain and using the assumption of a water table at the surface during critical conditions (Carson & Petley, 1970; Vargas & Pichler, 1957).

Carson & Petley (1970) described the pattern of development of the pore-water pressure during prolonged rainstorms. Most shallow planar translational slides in the study region involve the slipping of the whole regolith mantle over the bedrock. The regolith mantle tends to overlie a zone of weathered bedrock consisting of fragments of sandstone where joints have been opened by frost action and solution. The joints within the true bedrock situated beneath the weathering front are largely unopened and therefore are not as permeable as the weathered zone. This abrupt change in hydraulic conductivity at the junction between weathered and unweathered bedrock can create a perched water table. In most rain storms little water would reach this junction but, occasionally, in a very prolonged rainstorm,

downward seeping water will reach this transition area, and the impeded permeation of water will result in a perched ground water system above the true water table, this may in time build up to reach the surface. The Middle Grits comprise a series of alternating sandstones and shales and it is well established that the presence of the shale bands has led to many perched water systems within the regolith mantle, and that these water systems seep out into the regolith at many points on the valley side. The development of positive pore water pressures in the regolith mantle therefore owe much to the presence of many thin shale bands within the Middle Grit Series. Taking into consideration this mechanism of permeability impedance at the weathered/unweathered bedrock transition area and the position of thin shale laminae, preferred points along the hillslope profile may attain perched ground water tables at or near the ground surface more rapidly than others. Shallow planar translational slips may be more inclined to develop at such locations.

Two simple techniques which are commonly used to study ground water fluctuations are well levels (Hutchinson, 1971b) and Casagrande standpipe piezometers (Hutchinson, 1970). These methods are of limited accuracy, however, because of the uncertainty of measuring the specific ground water conditions on the failure plane. Continual (i.e. weekly) observations of ground water levels at potential failure sites in coarse regolith over extended time periods are few. Consequently, little published information is available relating the pattern of mass-movement on natural slopes composed of granular soils to ground water fluctuations. There is a requirement for detailed monitoring of ground water conditions, particularly along hillslopes which have experienced shallow slope failures, in order to assess the

pore water pressure. In particular the relationships between the trend in pore water pressure values and stability, on the one hand, and between pore water pressure values and the mode of failure with subsequent movement, on the other, required detailed investigation.

3.4.5 Technique of Piezometer Survey

A piezometric survey was undertaken in the regolith material on the hillslopes of Callow Bank from September 1984 to September 1985. The survey was implemented in order to assess the seasonal changes in pore water pressure values within the regolith mantle, and to establish whether pore water values were reaching critical levels for initiating shallow planar translational failures. Changes in the piezometric levels within the regolith mantle were correlated with respect to rainfall, stream discharge, regolith characteristics and hillslope morphology and geology.

Six slope profiles were selected for the piezometric survey, these included a profile through the main Callow Bank multiple retrogressive landslip (Profile 1, Fig. 3.3), profiles which included slope sections that had undergone failure (Profiles 3, 4 and 6, Figs. 3.9, 3.10 and 3.12), and profiles which appeared to be relatively stable and had not experienced shallow failure (Profiles 2 and 5, Figs. 3.8 and 3.11). The positions of the six piezometer profiles within the Callow Bank study area are shown in Fig. 3.2 (see back pocket).

A standpipe piezometer system was used; consisting of a standpipe tube (i.d. 19mm) with a 30cm Casagrande porous plastic piezometer tip at its lower end, installed down a borehole. Ground water entered

the tube through the porous tip and the water pressure corresponded

to the height of the water column above the piezometer tip. The

water surface was detected using a dip meter probe which was lowered

on a calibrated cable inside the standpipe and emitted an audio

signal on contact with water.

3.4.6 Borehole Installation

Boreholes were drilled to a depth within the regolith mantle in order

to locate the piezometer tip at the weathered/unweathered bedrock

interface. The boundary between bedrock and regolith may be placed

at a depth where fine material forms 25% of the total. Since the

flatter fragments in the upper horizon are found to be orientated

parallel to the slope of the ground surface, the depth at which this

orientation begins or the depth at which the orientation of fragments

as determined by rock structure first becomes disturbed by outcrop

curvature may be taken as the datum (Young, 1963). In some places

this transition area consisted of many large weathered sandstone

blocks. These blocks were broken in the borehole using a Mackintosh

Probe before using a Minuteman drill. Boreholes of 7.6cm in diameter

were drilled using a portable rotary Minuteman drilling rig. The

Minuteman drill is mounted on wheels, and therefore provided the most

appropriate drilling device for drilling boreholes on steep

hillslopes. The lighter Lite-Flite hollow stem augers were used

instead of the heavier standard construction augers.

Slurry was cleared from the bottom of the borehole using a hand auger

designed for use in stony soils before the Casagrande piezometer tip

was installed. Coarse, clean filter sand was then poured into the

borehole around the total length of the piezometer tip. The sand

filter was then tamped down to provide a firm base before sealing the sand filter with a bentonite plug. The borehole was then backfilled with the material drilled out of the borehole and tamped down at the surface. An end cap was placed over the top of the standpipe to prevent blockages occurring (Hanna, 1985).

Piezometers were installed at intervals downslope wherever a suitable platform could be found to locate and stabilise the base plate for the drilling rig. The position of each piezometer within the six hillslope profiles are shown in Profiles 1-6 (Figs. 3.3, 3.8, 3.9, 3.10, 3.11 and 3.12). The hillslope profiles were surveyed using a pantometer (Pitty, 1968). A computer program (PLOTGRAF) was used to convert the data of each profile into a profile graph of slope angle against measured length. Piezometer readings were taken twice a week from September 1984 to September 1985.

3.4.7 Measurement of Rainfall

Two natural-siphon autographic rain guages were installed. This type of instrument provided a continuous graphical record of rainfall against time, based on the movements of a float in a collecting chamber. Its capacity is unlimited since the chamber automatically empties itself when full. The mean reading of the two recorders was used to compile the rainfall data.

3.4.8 Measurement of stream Discharge

Six V-notch weirs (V2-V7), built to the specification of BS3680: Part 4A, Thin Plate Weirs, were installed to measure stream discharge, the position of each weir is shown in Fig. 3.2. Triangular, or V-notch,

weirs permit the accurate measurement of much lower discharges than do horizontal crested weirs. The discharge of this type of weir increases more rapidly with the head than in the case of a horizontal weir.

The basic discharge through a V-notch weir is given by equations (King, 1954):

$$Q = C.\tan\frac{\theta}{2}H^{5/2}$$

$$C = C.\tan\frac{\theta}{2}$$

$$Q = C.H^{5/2}$$

$$Q = 0.15\,H^{2.48}$$

where:

Q = Discharge in litres per second

C = The coefficient of discharge (Lenz, 1943)

H = Head of water over notch in cm

Discharge was also estimated for a dam situated in Dale Bottom at position V1 in Fig. 3.2. The dam took the form of a rectangular weir, therefore an equation for a rectangular horizontal crested weir was used to calculate discharge (King, 1954):

$$Q = C.L.H^3/2$$

where:

Q = Discharge in cubic metres per second

C = Coefficient of discharge (3.19) (Kindsvater & Carter, 1959)

L = Length of horizontal crest

H = Head of water above the crest

3.4.9 Regolith Material Classification

The British Classification for Engineering Purposes (BSCS) as described in the Code of Practice for Site Investigations (BS5930:1981) was used to classify regolith materials on the hillslopes of Callow Bank. The basis of this method of classification was originally put forward by the Engineering Group of the Geological Society and is described in the Quarterly Journal of Engineering Geology, 5,(4), (1972). The BSCS is recommended primarily for soils to be used as construction materials. Any soil can be placed in one of a number of soil groups on the basis of the grading of the constituent particles, and the plasticity of that fraction of the material passing a 425µm B.S. sieve. The soil groups were divided into sub-groups on the basis of laboratory tests. The classification is carried out on material nominally finer than 60mm (i.e. passing the 63mm B.S. test sieve complying with the requirements of BS410); coarser material, consisting of boulders and cobbles, is picked out and its proportion of the whole is estimated and recorded as cobbles (60mm to 200mm) or boulders (over 200mm). The grading and plasticity characteristics are divided into a number of clearly defined ranges, each of which may be referred to by a description name and letter symbol. This method of classification along with the descriptive names and letter symbol is outlined in Table 3.1.

The Liquid Limit (LL) was determined using a Cone Penetrometer (BS1377:1975) and the Plastic Limit (PL) was also determined using the procedure as set out in BS1377:1975. The Plasticity Index (PI) was calculated from the equation PI = LL-PL. Samples of 1kg were taken from a depth of 1m for classification using an Eijkelkamp auger

Table 3.1 British soil classification for engineering purposes
(from BS5930)

Soil groups (see note 1)			Subgroups and laboratory identification				
GRAVEL and SAND may be qualified Sandy GRAVEL and Gravelly SAND, etc. where appropriate (See 41.3.2.2)			Group symbol (see notes 2 & 3)	Subgroup symbol (see note 2)	Fines (% less than 0.06 mm)	Liquid limit %	Name
COARSE SOILS less than 35 % of the material is finer than 0.06 mm	GRAVELS More than 50 % of coarse material is of gravel size (coarser than 2 mm)	Slightly silty or clayey GRAVEL	G — GW / GP	GW / GPu GPg	0 to 5		Well graded GRAVEL / Poorly graded/Uniform/Gap graded GRAVEL
		Silty GRAVEL / Clayey GRAVEL	G F — G-M / G-C	GWM GPM / GWC GPC	5 to 15		Well graded/Poorly graded silty GRAVEL / Well graded/Poorly graded clayey GRAVEL
		Very silty GRAVEL / Very clayey GRAVEL	GF — GM / GC	GML, etc / GCL GCI GCH GCV GCE	15 to 35		Very silty GRAVEL, subdivide as for GC / Very clayey GRAVEL (clay of low, intermediate, high, very high, extremely high plasticity)
	SANDS More than 50 % of coarse material is of sand size (finer than 2 mm)	Slightly silty or clayey SAND	S — SW / SP	SW / SPu SPg	0 to 5		Well graded SAND / Poorly graded/Uniform/Gap graded SAND
		Silty SAND / Clayey SAND	S-F — S-M / S-C	SWM SPM / SWC SPC	5 to 15		Well graded/Poorly graded silty SAND / Well graded/Poorly graded clayey SAND
		Very silty SAND / Very clayey SAND	SF — SM / SC	SML, etc / SCL SCI SCH SCV SCE	15 to 35		Very silty SAND, subdivided as for SC / Very clayey SAND (clay of low, intermediate, high, very high, extremely high plasticity)
FINE SOILS more than 35 % of the material is finer than 0.06 mm	SILTS and CLAYS 35 % to 100 % fines	Gravelly or sandy SILTS and CLAYS 35 % to 65 % fines — Gravelly SILT / Gravelly CLAY (see note 4)	FG — MG / CG	MLG, etc / CLG CIG CHG CVG CEG		< 35 / 35 to 50 / 50 to 70 / 70 to 90 / > 90	Gravelly SILT; subdivide as for CG / Gravelly CLAY of low plasticity / of intermediate plasticity / of high plasticity / of very high plasticity / of extremely high plasticity
		Sandy SILT (see note 4) / Sandy CLAY	FS — MS / CS	MLS, etc / CLS, etc			Sandy SILT; subdivide as for CG / Sandy CLAY; subdivide as for CG
		SILT (M-SOIL) / CLAY (see notes 5 & 6)	F — M / C	ML, etc / CL CI CH CV CE		< 35 / 35 to 50 / 50 to 70 / 70 to 90 / > 90	SILT, subdivide as for C / CLAY of low plasticity / of intermediate plasticity / of high plasticity / of very high plasticity / of extremely high plasticity
ORGANIC SOILS	Descriptive letter 'O' suffixed to any group or sub-group symbol.			Organic matter suspected to be a significant constituent. Example MHO: Organic SILT of high plasticity.			
PEAT	Pt Peat soils consist, predominantly of plant remains which may be fibrous or amorphous.						

NOTE 1. The name of the soil group should always be given when describing soils, supplemented, if required, by the group symbol, although for some additional applications (e.g. longitudinal sections) it may be convenient to use the group symbol alone.

NOTE 2. The group symbol or sub-group symbol should be placed in brackets if laboratory methods have not been used for identification, e.g. (GC).

NOTE 3. The designation FINE SOIL or FINES, F, may be used in place of SILT, M, or CLAY, C, when it is not possible or not required to distinguish between them.

NOTE 4. GRAVELLY if more than 50 % of coarse material is of gravel size. SANDY if more than 50 % of coarse material is of sand size.

NOTE 5. SILT (M-SOIL), M, is material plotting below the A-line, and has a restricted plastic range in relation to its liquid limit, and relatively low cohesion. Fine soils of this type include clean silt-sized materials and rock flour, micaceous and diatomaceous soils, pumice, and volcanic soils, and soils containing halloysite. The alternative term 'M-soil' avoids confusion with materials of predominantly silt size, which form only a part of the group.

Organic soils also usually plot below the A-line on the plasticity chart, when they are designated ORGANIC SILT, MO.

NOTE 6. CLAY, C, is material plotting above the A-line, and is fully plastic in relation to its liquid limit.

designed for sampling stony soils. A sample was taken at 1m at each piezometer site when the period of piezometric survey had been completed. The position of each piezometer site on each hillslope profile is shown in Figs. 3.3, 3.8, 3.9, 3.10, 3.11 and 3.12.

3.4.10 Shear strength of Regolith Materials

A number of studies have taken regolith samples for shear testing using direct shear test apparatus to yield angles of internal shearing resistance (∅'), and these were employed in Infinite Stability Analyses (Skempton & DeLory, 1957). These analyses initially assumed regolith saturation, with the water table at the surface and drainage along flow lines parallel to the surface. Under these conditions the stability model predicts threshold angle (β_l) from:

$$\tan \beta_l = \left[\frac{\gamma_s - m.\gamma_w}{\gamma_s} \right] \tan \phi' \approx \tfrac{1}{2} \tan \phi'$$

where: β_l = Threshold angle of stability

γ_s = Saturated unit weight of soil (kN/m^3)

γ_w = Unit weight of water (kN/m^3)

∅' = Angle of internal shearing resistance

m = Unity, the relative height of water table above the shear plane

The results of such stability analyses suggest that mechanical properties of the regolith may partially explain threshold angles. A number of studies have been undertaken to show the relationship between the angle of shearing resistance (∅') and material sorting (Holtz, 1960; Vucetic, 1958; Kawakami & Abe, 1970). Vucetic (1958)

tested for changes in the shear strength of clayey schist with upper limits on individual fragments at 30, 15, 8 and 4mm. The first three mixtures all approximated to the same value of the angle of shearing resistance ($\emptyset' = 39^{\circ}$) and then the value of $\emptyset'$ suddenly fell to 25° in the case of the 4mm sample. He concluded that the decrease in shear strength with decreasing rock fragment size was discontinuous rather than gradual. Holtz (1960), similarly tested mixtures of gravel and soil and found no change in $\emptyset'$ at first and then a sudden drop and then no further change when decreasing the fraction of gravel in the mixture. With sandy gravel mixtures, the discontinuity occurred at about 20% gravel, and with clayey gravel, at about 35% gravel in the mixture.

Carson & Petley (1970) conducted shear tests on regolith material overlying Shale Grit on Derbyshire hillslopes. They determined peak shear strength, residual shear strength and the maximum stable slope angles for two characteristic straight hillslope inclinations of 21° and 26.5°. The results of their tests are shown in Table 3.2.

Table 3.2 The peak shear strength, residual shear strength and the maximum stable slope angles of regolith on Shale Grit bedrock for two characteristic straight hillslope inclinations of 21° and 26.5° (from Carson & Petley, (1970)).

Slope inclination (β)	Peak shear strength ($\emptyset'$)	Residual shear strength ($\emptyset'r$)	Maximum stable slope angle (when: c'=0 and m=1) (β_l)	
			Peak stress	Residual stress
21°	43°	41.5°	24.8°	23.5°
26.5°	45.9°	37.5°	27.3°	20.9°

Carson & Petley (1970) used conventional direct shear apparatus to test regolith samples of 6 x 6cm and 2cm thick. They acknowledged that this type of apparatus was suitable for material consisting of particles smaller than 2mm only. They also acknowledged that it was impossible to extract samples for laboratory direct shear testing which could be described as undisturbed. Both these points can be regarded as serious criticisms of any attempt by Carson & Petley (1970) to relate shear strength properties measured in laboratory shear tests to phenomena which occur in the field. Two questions of sample representativeness must be considered; firstly as to whether the samples extracted truly represented the material controlling the stability of the slope mantle. This is a problem since the regolith character varies with depth through the weathering profile, with a marked increase in the coarse fraction towards bedrock. Secondly, a problem remains as to the extent to which the tested sample represents the material in the weathering profile. It has been shown (Chandler, 1973) that for non-cohesive sediments laboratory direct shear box tests may give unrepresentative results. When coarse material greater than a critical size (i.e. greater than approx. 8.3% of the shear box length) is included in the sample, because excessive stresses tend to develop where the coarse particles intersect the failure plane. In the absence of infinitely variable shear box dimensions, the necessary exclusion of large particles artificially improves sediment sorting, which may result in underestimation of field strength parameters. It is normal practice in soil mechanics laboratory testing to minimise the sample variability by controlling water content, and particle size, by eliminating organic matter, and often by removing structural discontinuities in the reconstitution of samples. This can still result in widely variable values for even simple classification and index tests (Sherwood, 1970; Sherwood &

Ryley, 1970). Small sample size and the accepted practice of screening variability from samples for laboratory tests more usually results in residual variance and quite acceptable 'average' values. Clearly there is a requirement for a practical alternative shear box design which can be used to test soils containing large fragments in the field. This would overcome some of the problems of disturbance and sample representativeness discussed above.

3.4.11 Shear Tests

The suitability of standard engineering tests and testing equipment for the measurement of soil strength parameters as part of geomorphological research has received little critical evaluation. The accepted use of the Terzaghi-Coulomb criterion of failure (i.e. in terms of the principle of effective stress; see e.g. Bishop & Skinner, 1977) as a means of estimating the two shear strength parameters of a soil, the cohesion (C') and the angle of shearing resistance (∅'), which are almost independent of the test procedure, requires the measurement of normal stress, shear stress and pore water pressure at failure. This precludes the use of vane and penetrometer tests which may be used to determine in situ undrained shear strength but not values of C' and ∅' and the normal stress (σn) can be estimated. Standard laboratory methods of determining shear strength parameters under strictly controlled conditions include direct shear, ring shear and triaxial compression tests which, for civil engineering purposes, were designed to test small samples of relatively homogenous undisturbed or remoulded soil materials. In standard engineering practice pedological soil materials and organic material are excluded from testing because of the effects of structural discontinuities and compositional variation

on shear strength (Skempton & Hutchinson, 1969). Pedological samples containing particles larger than a specified size cannot be tested due to scale effects, or the large particles are removed before testing.

Large scale shear box tests have been designed to test large samples in the field under natural or anticipated design stress conditions in order to overcome the difficulties mentioned (Bishop, 1948; Akroyd, 1957). These in situ tests involve direct shearing along a predetermined shearing plane, although soil or rock deformation properties are derived from plate loading or bearing tests. The preparation and testing of large scale specimens in a field direct shear apparatus are generally very expensive in labour, equipment and time (James, 1969; Franklin et al., 1974). For these reasons a minimum of tests on carefully selected specimens are conducted in order to obtain optimum shear strength and behavioural information. Chandler et al. (1981) list the necessary requirements of a shear strength test for geomorphological purposes as follows:

(1) Sampling the structural and compositional inhomogeneities of shallow pedological soils (1-2m deep residual soils or colluvial mantles) in a statistically significant manner (i.e. sufficient tests should be conducted to determine the variability or range of shear strength response).

(2) Using a specimen large enough to include the roots, organic matter, structures and large particle characteristics of superficial deposits.

(3) Simulating the low _in situ_ geostatic stresses, of the order of $0-20$ kN/m^2, typical of shallow regolith.

(4) Testing soils on steep hillslopes at approximately the same angle and depth as a natural failure zone might occur.

Important considerations in the design of field equipment for in situ testing include portability to remote sites, and a rugged yet simple construction in order to minimise operating costs while optimising the number of tests as noted under (1) above. A review of earlier large scale field shear test aparatus has been described by Chandler _et al._ (1981). They concluded that a practical alternative shear box design is required for sampling soil variability, incorporating undisturbed macroscopic soil structures, simulating in situ geostatic pressures depths and inclinations, and being of inexpensive, simple, robust and portable construction for difficult testing conditions. Chandler _et al._ (1981) suggested a guide for a practical alternative design, was provided by the experimental studies of Endo & Tsuruta, 1969; O'Loughlin, 1974 and O'Loughlin & Pearce, 1976, who employed a winch and simple direct shear box to conduct field tests of the effects of tree roots on soil strength. Chandler _et al._ (1981) designed an Open-sided Field Direct Shear Box based on their design specifications. The shear box has two vertical side shearing planes in addition to the usual basal shearing surface. The design allows rapid and easy preparation of undisturbed samples incorporating lateral as well as vertical roots, large stones and other pedological structures that would not be adequately included in any standard laboratory or conventional shear box test. Field probasal shearing areas should necessarily resemble the same proportion in a natural landslide, where the area of side shearing is relatively minor. The

dimensions (15cm x 30cm) were chosen to ensure adequate sampling representation of heterogeneous soil, provided sufficient tests are conducted, but at the same time the dimensions were limited by practical considerations of portability and partly in order to simplify calculations in data analysis. Normal loadings were applied directly to the top of the soil specimen by a set of weights; in the case of tests conducted by O'Loughlin & Pearce (1976) these were in the order of 1.5 to 8.0 kN/m^2. Shear forces were applied by an anchored winch and cables and were measured through a calibrated proving ring and dial guage. The apparatus is detailed schematically in Fig. 3.13.
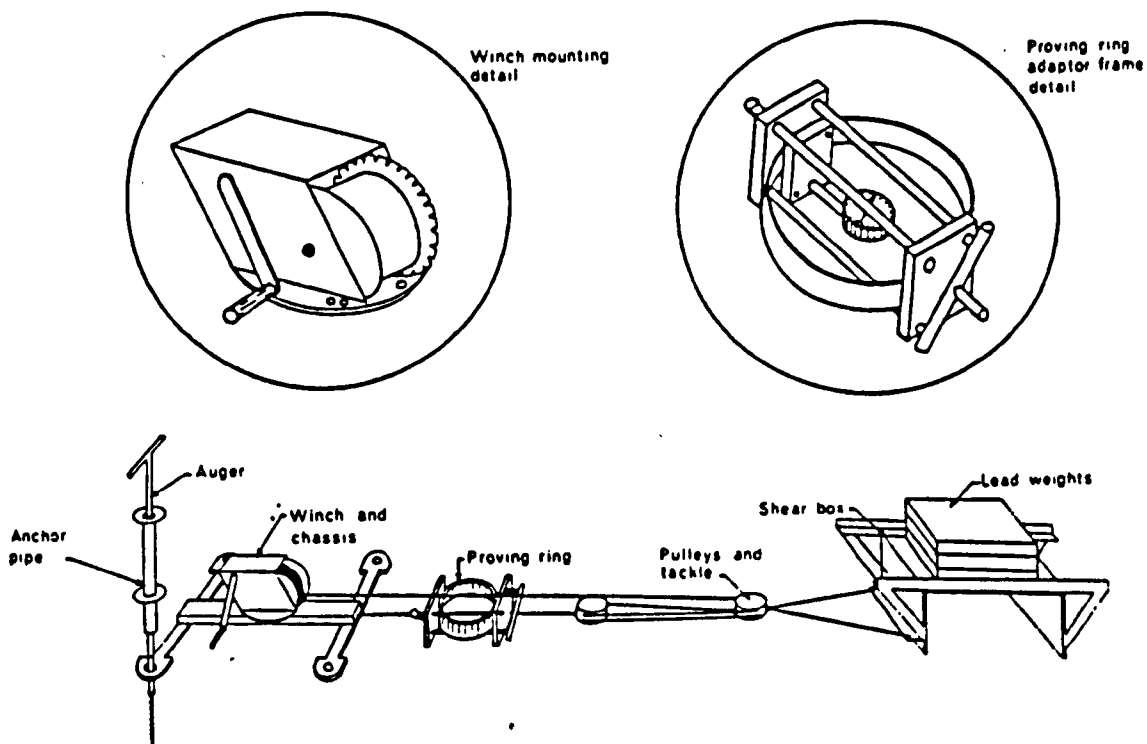
Fig 3.13 Schematic layout of components of the field shear testing apparatus, showing details of the winch mounting and proving ring adaptor frame (NOT TO SCALE), (From Chandler et. al. 1981).

Chandler et al. (1981) gave some details of the engineering specifications of the shear box in the BGRG Technical Bulletin No. 27, however, these were considered to be unsatisfactory, and new detailed engineering drawings of the Open-sided Direct Shear Box were drawn.

3.4.12 Shear Test Procedure

1. Sample Preparation:

Fig. 3.2 shows the location of the shear box tests adjacent to slope profile 3 (Fig. 3.9). A shallow planar translational slide had taken place within the middle slope section of slope profile 3 (Fig. 3.9). The slide is shown in section in Fig. 3.14, the maximum piezometric surface is also shown.
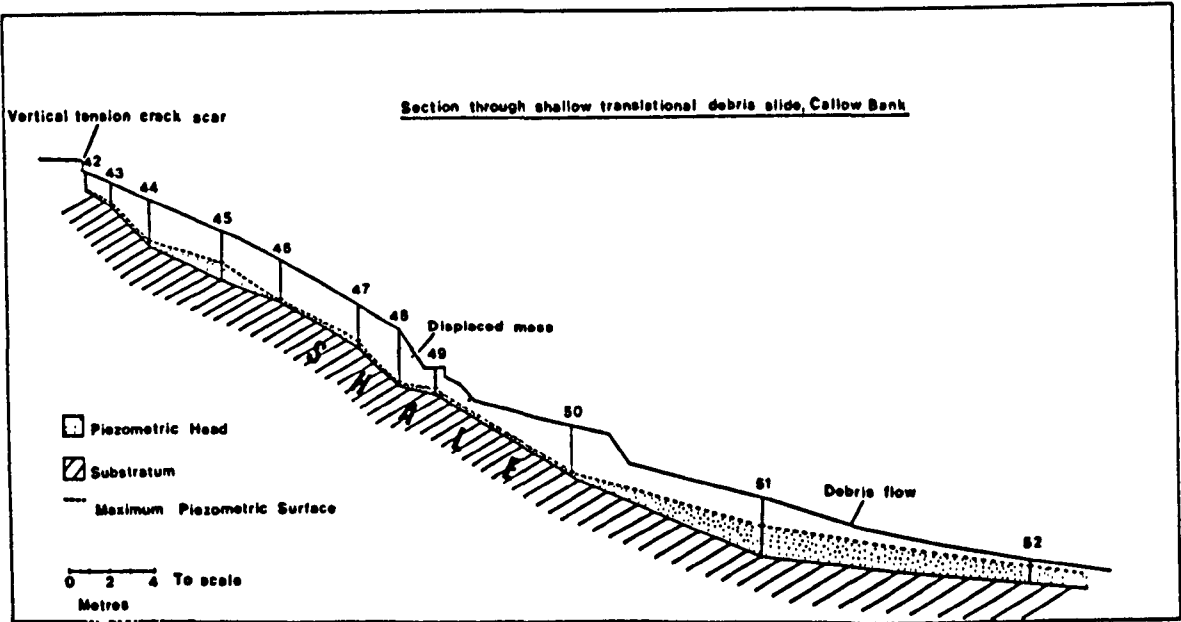
Fig. 3.14 Section through shallow translational debris slide, Callow Bank.

Three sample locations were chosen for shear box testing, by dividing
the total slope profile from the slope crest to the slope base into
three equal sections, upper slope section, middle slope section and
lower slope section. These locations accounted for the main
morphological changes in the slope profile and corresponding regolith
composition changes. There was no evidence for recent shallow
landsliding along this profile. Open-sided Direct Shear Box tests
were conducted on lower $(\beta = 16^\circ)$, middle $(\beta = 24^\circ)$ and upper
$(\beta = 33^\circ)$ sections of this slope profile. Table 3.9 shows the
particle size composition for regolith samples taken at a depth of
0.75m from these three sections. Representative soil profiles of
these three sections are shown in Tables A4, 5 and 6 in the Appendix.

Table 3.9 The particle size composition for regolith samples taken
at a depth of 0.75m from the three slope sections

Slope Profile Section	Gravel >2.00mm	Sand 2.00-0.06mm	Silt 0.06-0.002mm	Clay <0.002mm	Liquid Limit	Plastic Limit	Plasticity Index	BSCS
Lower slope section		24	23	53	30	21	9	FS-CLS
Middle slope section	30	28	24	18	23	17	6	GF-GML
Upper slope section	50	35	6	9	33	24	9	G-F GPC

Five parallel trenches approximately 0.31-0.33m wide were dug along the fall line of the slope for each section. The final inclination of the trench floor (β) determined the inclination of the shear box in the test. The front portion of the trench floor was then dug about 0.15m deeper from a point 0.5m in front of the back wall, keeping the new floor parallel with the former, this created an inclined step. The top of the step being 0.75m below the ground surface. This depth of shear box testing was chosen, according to the depth of tension cracks above a small translational debris slide adjacent to the shear strength test sites, the tension cracks were 0.7-1.0m deep. A niche was then excavated at the back of the step, again to a depth of about 0.15m; this produced an isolated block (0.3x0.3x0.15m). The shear box was carefully placed over the pre-cut block making sure there was no contact between the lower edges of the end plates and the trench floor. The winch was positioned 2.5m downslope from the sample trench and was aligned with the centre line of the trench to preclude torsional components of side friction or shear force. Following the loading of the specimen and the linking of cables to the box, the shear displacement measuring datum pin and rule were set in place. Specific site and test conditions were recorded on a proforma data sheet. The shear force, which was applied in the downslope direction was increased in approximately 11.4 N increments at 30 second intervals after the start of each test until failure occurred. Failure of the specimen was evident from a falling or constancy of the dial guage readings when these were accompanied by large strain readings. In general it was necessary to make more than one test per site; a minimum of three tests is theoretically sufficient to define a straight line Coulomb relation, but according to Chandler <u>et al.</u> (1981), and O'Loughlin (1974) at least 15 tests should be conducted at one site in order to offset the

scatter of data points produced by natural soil variability. The time spent preparing and setting up the tests is minimised if one trench is used for 3 tests. Following completion of the first test, a new level was dug back up the hillside in line with the original trench. Another sample block was prepared as before at the same depth. Fifteen shear tests were conducted under different conditions of loading for each section of slope. With the particular gauge used each load increment was indicated by 10 divisions on the dial (11.4N) this was recorded along with the corresponding reading of shear displacement from the datum pin on the metal rule (see Fig. 3.13)

2. Calculation of Shear and Normal Stress

The raw data from the field tests were modified to an assimilable form for plotting shear strength (S) against normal stress (σ'n) in accordance with the Terzaghi Coulomb failure criterion.

(i) Shear Stress

Shear stress values were derived from the force applied by the winch (Sa); as measured by the proving ring dial guage, and from a component of downslope shear force (Sg) contributed by the gravitational body force of the loaded box and sample block. Values of (Sa), in dial guage divisions, were converted directly to newtons (N) from the manufacturers calibration chart. Overall shear stress was determined from the sum of the two shear force components divided by the area of the shearing surface which was taken to be $0.18m^2$ (i.e. the sum of the base and two sides). Values of shear stress (S) were calculated using the expression:

$$s = \frac{sa + sg}{2A} = \frac{sa + (w + \gamma v)\sin\beta}{2A}$$

$$= \frac{sa}{2A} + \frac{1}{2}\left(\frac{w}{A} + \gamma d\right)\sin\beta$$

where:

w = Load of box and weights (kN)

γ = Soil unit weight (kN/m^3)

V = Volume of soil sample (m^3)

A = Basal shearing area (0.09m^2)

d = Sample thickness (0.15m)

β = Sample inclination (degrees)

Shear stresses at failure were designated Sf for peak strength and Sr for residual strength.

(ii) Normal Stress

In order to simulate soil stresses approximately equivalent to those present at the depth of testing before the trench was excavated a range of applied loads was chosen so that there was little actual difference in surcharge between pre-excavation and test conditions. The shallow depth of testing and relatively short time which elapsed between excavation and replacement of the soil surcharge with weights precluded the development of any significant stress-release phenomena, such as fissuring or base heave. The procedure also eliminated the need for a lengthy consolidation stage in the test.

The combined magnitudes of the normal forces, divided by the total area on which they act, is the best approximation to a relatively

simple single expression for total normal stress:

$$\sigma n = \frac{Pz + 2Py}{2A} = \frac{Pz}{2A} + \frac{Py}{A} = \frac{1}{2}\sigma z + \frac{1}{2}\sigma y$$

where:

Pz = Vertical normal load

Py = Horizontal geostatic normal forces

A = Basal shearing area $(0.09m^2)$

σz = Stresses acting on the basal shear plane

σy = Stresses acting on the side shear planes

$$\sigma n = \frac{1}{2}\left(\frac{W}{A} + \gamma d\right)\cos\beta + \frac{1}{4}K\left(\gamma\left(d + H\right) + \frac{W}{A}\cos\beta\right)$$

where:

W = Load of box and weights (kN)

A = Basal shearing area $(0.09m^2)$

γ = Soil unit weight (kN/m^3)

d = Sample thickness (0.15m)

β = Sample inclination (degrees)

H = Depth normal to top of sample

K = A coefficient of lateral to vertical effective stresses

(iii)   Calculation of lateral coefficient (K)

K is a coefficient used to express lateral to vertical effective stresses; K is related to the stress history of the soil (Lambe & Whitman, 1969). An effective state of overconsolidation results as high pore water tensions become dissipated towards an assumed maximum neutral stress. The ratio of effective stresses in respective dry and wet conditions can yield a value of overconsolidation ratio (OCR), for which values of K can be determined corresponding to a specified PI for the soil.

The overconsolidation ratio (OCR) was calculated from the formula:

$$OCR = \frac{p'c}{p'o} = \frac{p'd}{p'w}$$

where:

P'C = Former maximum effective overburden stress

P'O = Present in situ effective overburden stress

P'd = State of effective stress in dry conditions

P'w = State of effective stress in wet conditions

Example for the calculation of K:

b = Maximum bulk unit weight of soil (18.0 kN/m^3)

Us = Pore water tension (dry soil Us: -40 kN/m^2, wet soil Us = 0)

w = Moisture content (32%)

z = Depth of regolith (1m)

PI = 13

Wet Soil	Dry Soil
γb = 18.0 kN/m^2	γb = $\frac{18.0}{1.32}$ = 13.6 kN/m^2
Pw = 18.0 kN/m^2	Pd = 13.6 kN/m^2
P'w = Pw - Us	P'd = Pd - Us
= 18.0 kN/m^2	= 53.6 kN/m^2

Hence from the charts at PI = 13%, K = 0.7

The charts showing the relationships between PI, OCR and K have been published: (Brooker & Ireland, 1965; Lambe & Whitman, 1969).

(iv) Pore Water Tension (Us)

As the soil becomes drier, the larger capillaries no longer contain water, and the matric potential decreases (pore water tension becomes more negative) because only smaller capillaries are water filled. The slope of the suction moisture curve for each soil depends on the pore size distribution for the soil. Five tensiometers were installed in each of the three slope sections in order to measure soil water matric potentials. The tensiometers were hand built according to the design provided by Burt (1978a). The tensiometer tips were installed at a depth of 80cm. The pressure measurement device used was a mercury manometer made from glass rather than the less accurate plastic tubing manometer used by Burt (1978a). The tensiometers were removed before December in order to prevent them being damaged by frost. Tensiometers can be used to read both positive and negative soil water potentials. Fig. 3.15 shows the mean pore water tension recorded over three months in 1984 for each section of slope, where T1 relates to the upper slope section, T2 the middle slope section and T3 the lower slope section. Fig. 3.15 shows that the middle and lower slope sections attained positive pore water tensions whereas pore water tensions in the upper slope section remained negative during the three month monitoring period. In general one should test soils at or near their 'worst conditions' for landsliding; namely as close to full saturation as possible.

A pore water tension of 0 was used to represent wet soils, and work undertaken by Black et al. (1958) and Burt (1978b) has shown that negative pore water tensions of -40 kN/m^2 can be attained by similar soil in dry conditions, those were used in the calculation of the lateral coefficient K.
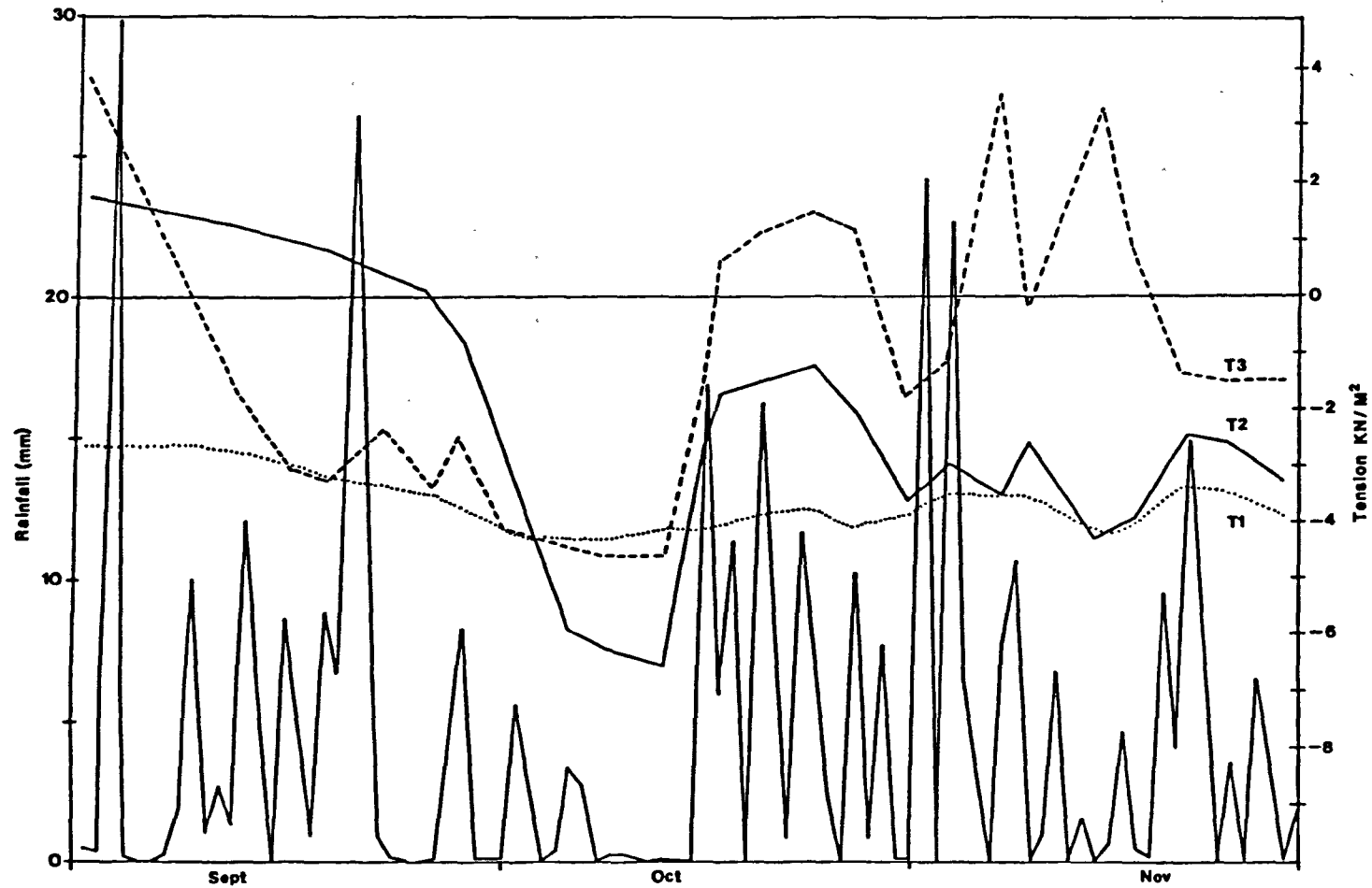
Fig. 3.15 Mean pore water tension (kN/m^2) recorded over three months in 1984, for each section of slope. (T1 = Upper slope section, T2 = Middle slope section, T3 = Lower slope section).

Unit Weight of soil (γ)

The Unit Weight of soil was determined using the sand replacement method (large pouring cyclinder suitable for fine, medium and coarse grained soils) as set out in BS1377. The soil unit weight was determined in situ within the trench for soil samples situated immediately adjacent to the block of soil subsequently prepared for each shear box test. A sample of soil was collected for each bulk density test for laboratory determination of moisture content this information was used to calculate the dry unit weight of soil (Tables A7, A8, A9 (See Appendix)

3.5 RESULTS

3.5.1 Results of the Slope Profile Survey

The division of profiles into best segment and element units showed that both best segments and elements were very restricted. In the case of best elements this was caused by the irregularity of successive measured length slope angles so that the best elements had 25% or less variation of curvature and seldom reached more than 3 or 4 measured lengths. The occurrence of groups of 2 to 3 measured lengths forming segment units covered over 90% of all profiles. For elements the percentage was slightly lower. Such short segments and elements were considered to be of very limited significance in terms of selecting characteristic straight slope angles.

The use of the small measured Pantometer length of 1.5m tended to overemphasise micro relief features. Therefore, no definite straight slope segments in the profiles were found using the system of best

unit analysis (Young, 1972). Thus, the technique did not provide an effective method for identifying characteristic straight slope segment angles.

Fig. 3.16 shows the population sample slope angle frequency histogram for measured slope angles collected in the Callow Bank study area. Significant peaks in the angle frequency distribution occur at 5°, 10°, 15°, 20° and 24°. The asterisks mark the positions of the trimodal distribution of straight slopes (20°, 26° and 33°) identified by Carson & Petley (1970) in their slope analysis of the Southern Pennines of Derbyshire.
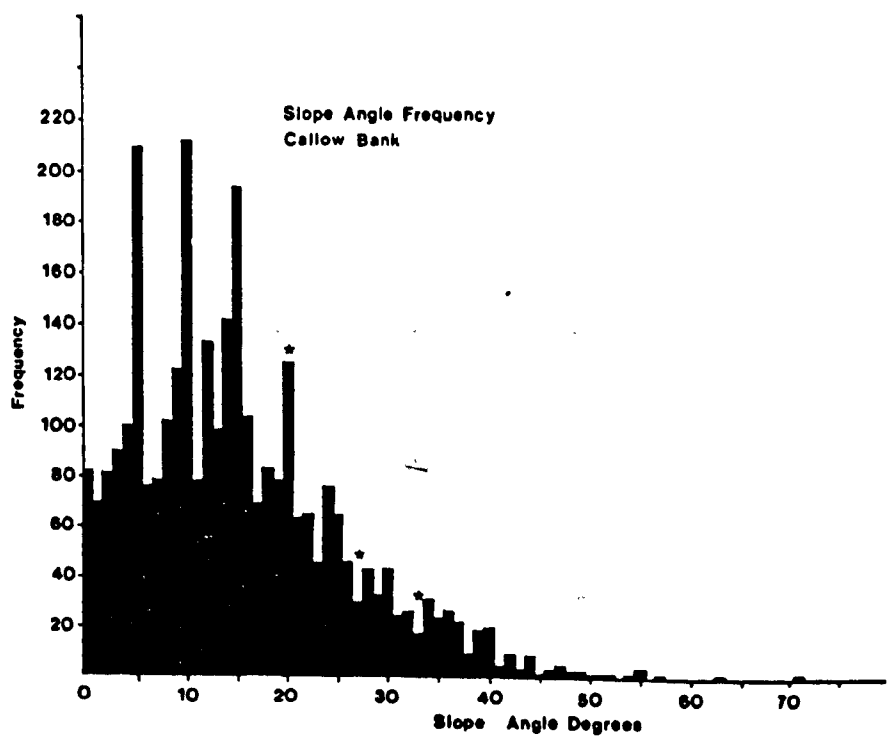
Fig. 3.16 The population sample slope angle frequency histogram for measured slope angles collected in the Callow Bank study area

Fig. 3.17 shows the frequency distribution of the angles of straight slope segments in relation to calculated threshold values for regoliths of sandy soil, taluvium and scree, located on the south Pennine hillslopes of Derbyshire (after Carson, 1969).
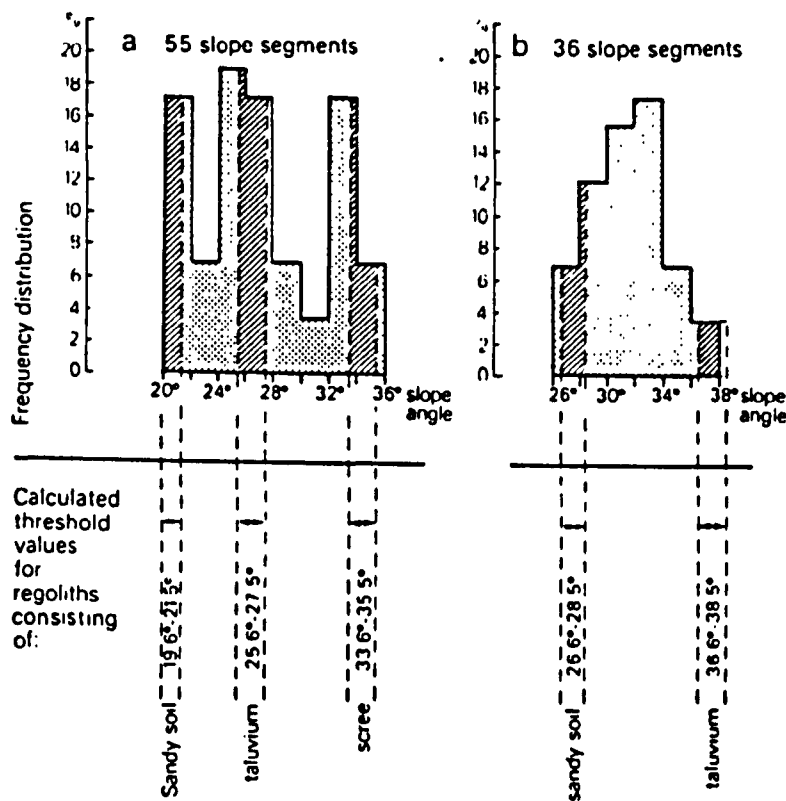
Fig. 3.17 The frequency of the angles of straight slope segments in relation to calculated threshold values in the Pennines and Exmoor (after Carson, 1969).

(a) An example of parallel slope retreat: the modes correspond with the calculated threshold values;

(b) An example of slope flattening: the mode lies between the calculated threshold values.

Although a direct comparison of the frequency of straight slope segments (Carson, 1969) with the slope frequency distribution of Callow Bank may be misleading there does seem to be a definite correspondance in peaks at 20° which is the threshold angle for sandy soil regoliths (19.6°-21.5°). Small peaks in the slope frequency histogram at Callow Bank do occur at 24°-25° and 34° which may be associated with the calculated threshold values of taluvium (25.6°-27.5°) and scree (33.6°-35.5°). Table 3.3 shows the frequency distribution of 23,040 slope angles that were used in the compilation of the regional landslide matrix. The slope angles were calculated using the slope indicator chart of Thrower & Cooke (1968). These slope measurements are very different in kind and scale from those obtained from pantometer measurements. Definite peaks in the frequency distribution occur at 21° 48' and 26° 34' which again correspond closely with the threshold values for regoliths consisting of sandy soil and taluvium. It is interesting to note that a peak in the frequency distribution occurs at 17° 45' which is similar to the predicted mean limiting angle for similar head materials tested in South Wales (β_i = 17.0°-17.2°), (Rouse & Farhan, 1976). Rouse & Farhan (1976) found that this correlated with the confidence interval of the slopes with identified shallow planar failure, 17.4°-18.6°) (95% confidence).

Although Young (1961) defined modal peaks in slope angle histograms as characteristic angles, the statistical significance of such modes has received little attention (Speight, 1971). Slope angle histograms tend to be multi-modal even for sets of angle measured over equal distances within a single profile (Pitty, 1969), and a large proportion of total measured slopes fail to lie in a modal class (Statham, 1975), the significance of modal values is therefore

Table 3.3 Frequency distribution of 23,040 slope angles that were used in the compilation of the regional landslide matrix.

Slope Angle %	Slope Angle (degrees)	Frequency	Slope Angle %	Slope Angle (degrees)	Frequency	Slope Angle %	Slope Angle (degrees)	Frequency
0		447	20	11° 19'	1793	40 *	21° 48'	1172
1		245	21		3	41		1
2		342	22		7	43		5
3		478	23		11	45		50
4	2° 18'	1017	24		9	48		1
5		952	25	14° 02'	1716	50 *	26° 34'	690
6	3° 26'	1265	26		7	51		1
7		32	27		4	54		1
8	4° 34'	2772	28		2	55		11
9		13	29		1	57		1
10	5° 43'	2186	30	16° 42'	972	58		1
11		13	31		20	60 *	30° 58'	206
12		22	32	17° 45'	943	63		3
13	7° 25'	1985	33		4	65		4
14		7	34		5	70		38
15	8° 32'	1140	35		18	72		2
16	9° 05'	1235	36		1	75		126
17		21	37		2	80		15
18		10	38		164	90		16
19		141	39		2	95+		511

debatable. Anderson et al. (1980) discussed problems of relating the predication of a stability analysis to a modal slope angle. An initial problem is the definition of the distribution of slope angles and identification of threshold values. Anderson et al. (1980) contended that the Infinite Slope Model must on occasions result in fortuitous agreement with the observed modal slope angles, because of the simplistic nature of the models specification. Straight slope segments vary systematically in steepness with spatial location in the drainage basin (Carter & Chorley, 1961; Arnett, 1971; Summerfield, 1976). The recognition of the relationship between threshold angles and characteristic straight slope angles for sandstone and granite areas (Carson & Petley, 1970; Carson, 1971) appears to have been somewhat fortuitous inasmuch two discrete semi-frictional threshold angles were identified, as demonstrated to correspond with modal groupings of actual straight slope angles. Studies at Callow Bank have shown that the 'frictional' properties of the regolith may vary appreciably (and not always discontinuously) according to local conditions of parent material, degree of weathering and state of packing and together with the differences in pore pressure conditions, may produce a broad continuum in the threshold angles of an area. This brings into serious question the measuring of a typical slope angle in relation to a specific type of failure or soil material.

3.5.2 Particle size and Index Tests

The results of the regolith classification for each piezometer site are shown in Table 3.4. Each piezometer profile was divided into three equal slope sections as previously described. The upper section (U) corresponded to the slope crest and upper convexity of
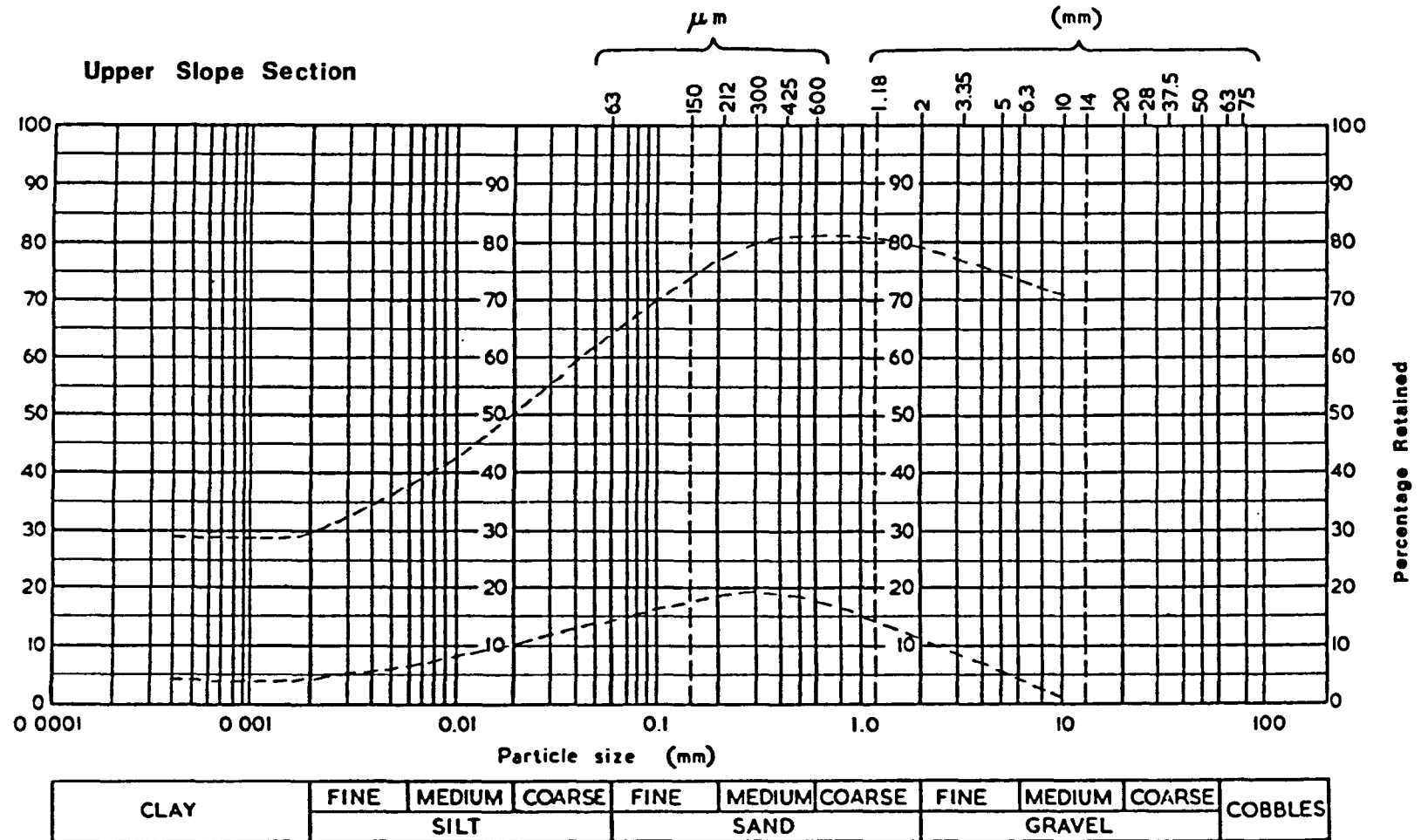
Fig. 3.18   Particle size envelope showing the maximum
           and minimum percentage retained for each
           particle size fraction for all soil samples
           analysed on upper slope sections.
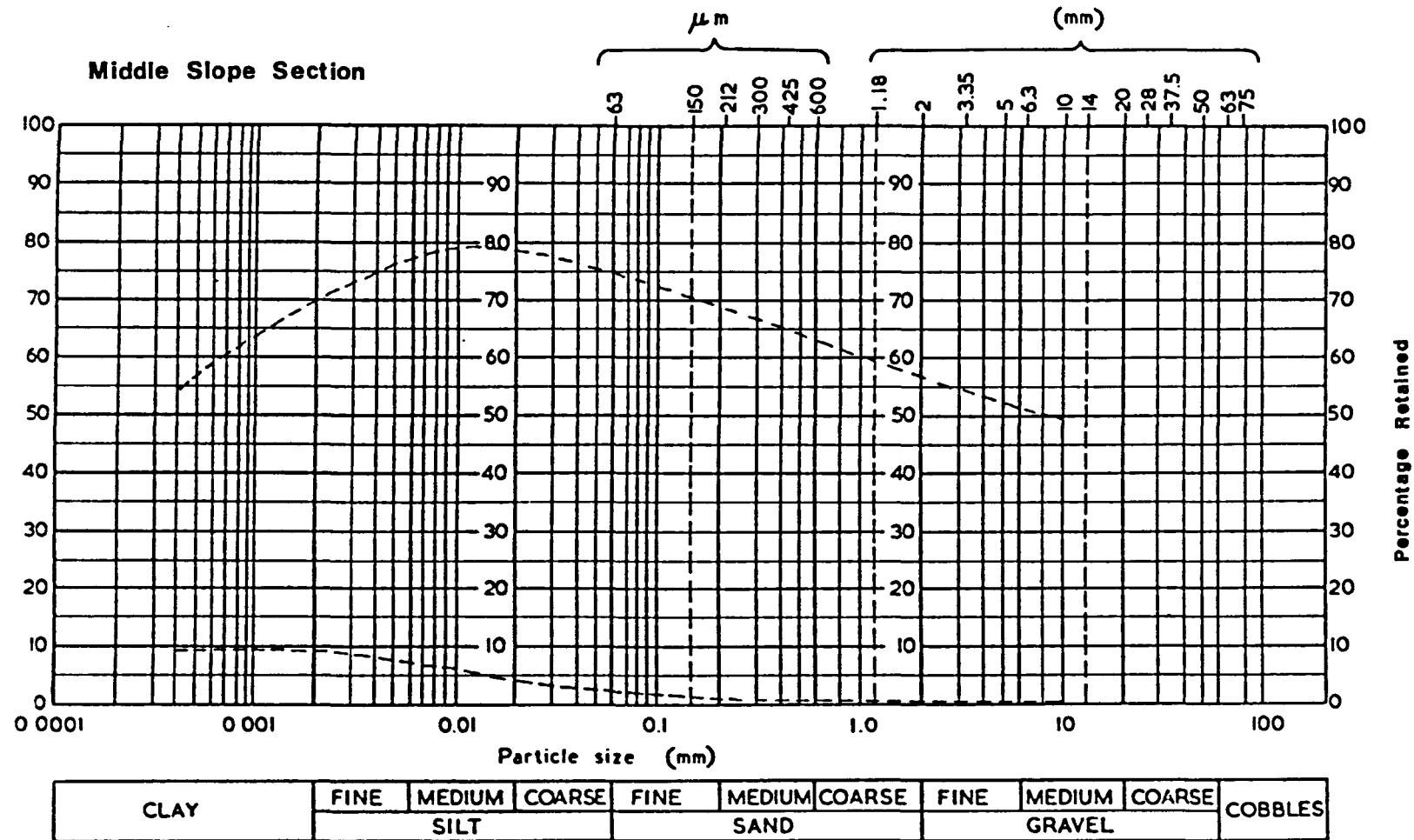
Fig. 3.19 Particle size envelope showing the maximum
and minimum percentage retained for each
particle size fraction for all soil samples
analysed on middle slope sections.
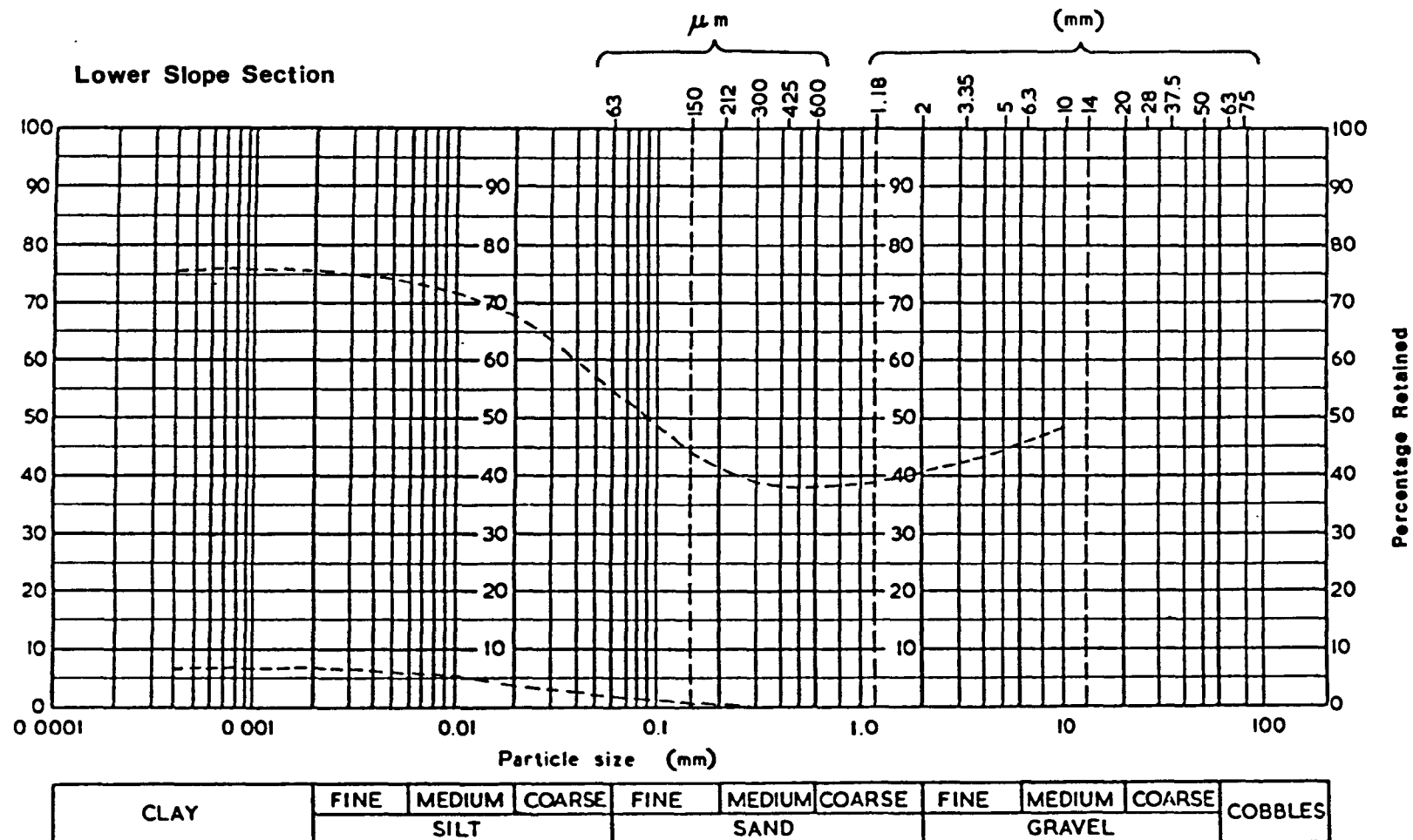
Fig. 3.20 Particle size envelope showing the maximum
and minimum percentage retained for each
particle size fraction for all soil samples
analysed on lower slope sections.

Table 3.4 The results of the Soil classification for each piezometer site.

Slope Section	Piez. No.	Gravel (%) >2.0mm	Sand (%) 2.0-0.06mm	Silt (%) 0.06-0.002mm	Clay (%) <0.002mm	Liquid (%) Limit	Plastic (%) Limit	Plasticity Index	Soil Class (BSCS)	
u	1	42	27	17	14	29	17	12	GF	GCL
u	2	3	59	23	15	27	10	13	FG	CLS
u	3	4	51	25	20	23	12	11	FG	CLS
u	4	48	38	6	8	29	21	8	G-F	GPC
u	5	64	18	9	9	36	22	14	G-F	GPC
u	6	72	19	4	5	31	22	9	G-F	GPC
m	7	6	25	46	23	23	11	12	FS	CLS
m	8	3	23	46	28	19	8	11	FS	CLS
m	9	-	2	59	39	26	19	7	F	CL
m	10	11	14	46	29	23	17	6	FS	MLS
m	11	11	13	46	30	22	17	5	FS	MLS
m	12	2	10	67	21	22	18	4	FS	MLS
m	13	-	22	53	25	30	23	7	FS	CLS
m	14	-	27	60	13	27	21	6	FS	MLS
L	15	-	37	43	20	25	20	7	FG	MLS
L	16	-	24	23	53	30	21	9	FS	CLS
L	17	-	19	34	47	32	23	9	FS	CLS
L	18	-	18	41	41	32	23	9	FS	CLS
L	19	-	24	37	39	32	24	8	FS	MLS
L	20	-	-	25	75	38	23	15	F	CI
L	21	1	1	25	73	36	23	13	F	CL
L	22	11	8	27	54	33	22	11	FS	CLS
u	23	7	64	18	11	27	17	10	SF	SCL
u	24	6	76	11	7	18	9	9	SF	SCL
u	25	4	71	15	10	18	7	11	SF	SCL
u	26	-	43	28	29	22	10	12	FG	CLS
u	27	-	39	33	28	21	12	9	FG	CLS
u	28	-	56	15	29	23	15	8	FG	CLS
m	29	-	50	21	29	35	26	9	FG	CLS
m	30	-	50	23	27	35	25	10	FG	MLS
m	31	-	48	26	26	29	23	6	F	ML
m	32	-	1	63	36	25	20	5	FS	MLS
L	33	2	10	67	21	27	21	6	F	ML
L	34	-	2	64	34	26	20	6	F	ML
L	35	1	3	39	57	27	20	7	F	CL
L	36	48	38	6	8	29	21	8	GF	GCL
u	37	7	57	17	19	23	17	6	FG	MLS
u	38	6	77	6	11	22	17	5	SF	SML
u	39	8	51	30	11	28	21	7	FG	CLS
u	40	8	49	33	10	37	28	9	FG	CLS
u	41	11	53	32	4	24	12	12	FG	CLS
u	42	7	64	19	10	29	23	6	SF	SML
m	43	-	60	22	18	23	17	6	FG	MLS
m	44	-	64	18	18	22	17	5	FG	MLS
m	45	-	53	26	21	25	20	5	FG	MLS
m	46	-	66	15	19	26	20	6	SF	SML

Table 3.4 (continued)

Slope Section	Piez. No.	Gravel (%) >2.0mm	Sand (%) 2.0-0.06mm	Silt (%) 0.06-0.002mm	Clay (%) <0.002mm	Liquid (%) Limit	Plastic (%) Limit	Plasticity Index	Soil Class (BSCS)	
m	47	-	-	79	21	26	20	6	F	ML
m	48	-	30	52	18	25	20	5	FS	MLS
m	49	-	25	61	14	26	20	6	FS	MLS
m	50	3	8	50	39	25	18	7	FS	CLS
m	51	-	43	43	14	25	20	5	FG	MLS
m	52	15	16	40	29	27	20	7	FS	CLS
m	53	20	40	25	15	30	23	7	FG	CLS
m	54	8	47	26	19	22	18	4	FG	MLS
L	55	40	25	19	16	33	20	13	GF	GCL
L	56	53	31	8	8	29	22	7	GF	GCL
L	57	52	33	5	10	31	24	7	G-F	GPM
u	58	-	62	22	16	23	17	6	FG	CLS
u	59	42	27	17	14	29	17	12	GF	GCL
u	60	-	64	21	15	22	17	5	FG	CLS
u	61	-	76	11	13	26	20	6	SF	SML
u	62	20	39	25	16	22	17	5	FS	MLS
m	63	4	38	29	29	23	17	6	FS	MLS
m	64	-	3	66	31	26	19	7	F	CL
m	65	5	26	32	37	37	27	10	FS	MIS
m	66	7	23	30	40	36	23	13	FS	CIS
m	67	4	28	24	44	37	24	13	FS	CIS
m	68	8	32	46	14	30	21	9	FS	CLS
m	69	50	35	6	9	33	24	9	G-F	GPC
L	70	12	3	22	63	29	22	7	FS	CLS
L	71	8	4	47	41	25	20	5	FS	MLS
L	72	-	84	10	6	27	19	8	FS	SCL
u	73	30	28	24	18	23	17	6	GF	GNL
m	74	3	34	45	18	29	23	6	FS	MLS
m	75	-	2	73	25	25	18	7	F	CL
L	76	1	1	26	72	29	21	8	F	CL
L	77	8	3	27	62	38	31	7	F	CI
L	78	4	3	24	69	35	26	9	F	CI
u	79	-	74	20	6	29	23	6	SF	SML
u	80	-	65	27	8	30	24	6	SF	SML
u	81	50	35	6	9	33	24	9	G-F	GPC
u	82	-	64	15	21	27	18	9	GF	GCL
u	83	-	54	25	21	27	19	8	FG	CLS
u	84	-	46	32	22	27	20	7	FG	CLS
u	85	64	18	9	9	36	22	14	GF	GCI
m	86	-	43	36	21	27	20	7	FG	CLS
m	87	29	10	31	30	29	23	6	FG	MLG
m	88	11	8	27	54	30	23	7	FS	CLS
L	89	3	2	25	70	36	23	13	F	CI
L	90	-	-	38	62	34	24	10	F	CL
L	91	10	4	69	17	22	17	5	FS	MLS
L	92	5	5	19	71	32	23	9	FS	CLS

the profile, the middle section (M) corresponded to the straight slope section and the upper part of the lower concave slope and the lower section (L) corresponded to the lower concavity and basal slope of the profile. The letter symbols (u, M, L) in the first column of Table 3.4 indicate the slope section from which the sample was taken.

Table 3.5 shows the mean particle size of soil samples taken from piezometer sites on each slope section. Fine gravel and coarse sand were the dominant components of the upper slope sections and correspond to a clayey-sand (BSCS BS:5930). The regolith in the middle slope sections showed a high proportion of fine sand and silt, they corresponded to a sandy-clay (BSCS BS:5930). Fine silt and clay were the dominant constituents of the regolith situated on the lower slope sections and also corresponded to a sandy-clay.

Table 3.5 Mean particle size of soil samples taken from piezometer sites on each slope section

Slope Section	Gravel >2.00mm	Sand 2.00-0.06mm	Silt 0.06-0.002mm	Clay <0.002mm	Liquid Limit	Plastic Limit	Plasticity Index	BSCS
Upper slopes	16.2	51.1	19.2	14.1	26	18	8	SF SCL
Middle slopes	5.6	29.9	41.4	25.4	27	20	7	FS CLS
Lower slopes	10.4	15.3	31	43.5	31	22	9	FS CLS

The particle size envelopes for the regolith mantle for upper, middle and lower slope sections are shown in Figs. 3.18, 3.19 and 3.20 respectively. The envelopes show the maximum and minimum percentage retained for each particle size fraction for all samples analysed in each slope section. The particle size envelopes illustrate the wide range of particle size within the soils sampled from each slope section indicating that the deposits are poorly sorted. However, the

envelopes do show that there is a distinct downwards fining of grain size. These grain size differences partly reflect bedrock control where the upper slope sections are located on the massive coarse-grained beds of Rivelin Grit whereas the middle and lower slope sections are situated on shales and mudstones. A feature of the weathering and breakdown of shales and mudstones was their disintegration to produce silty clays (Grice, 1969). The differences are also a response to cyclic solifluction and slope wash events removing fines from up-slope locations.

Liquid limits were low, ranging from 18% to 38% for all slope sections. The range of liquid limits for upper slope sections (18%-36%) was slightly greater than the ranges for middle (19%-35%) and lower slope sections (25%-38%). These values indicate that only 18% to 38% of water by weight of sediment is necessary to initiate downslope flowage. The mean liquid limits for each section are shown in Table 3.5. The plastic limits were also low ranging from 10% to 31%, with mean figures of 18%, 20% and 22% for the upper, middle and lower sections respectively. The plasticity index ranged from 4%-15%. The mean plasticity index figures shown in Table 3.5 reflect the small percentage of clay in the sediments. When the liquid limit and plasticity index were plotted on the Casagrande Plasticity Chart they tended to cluster on the A-line boundary between clays of low to medium plasticity and silts of low to medium compressibility (Casagrande, 1949).

3.5.3 Discharge Results

The general model considered appropriate for water flow on the slopes of the Callow Bank catchment is a modification of the 'dynamic

watershed concept' (Tennessee Valley Authority, 1965). Water moves vertically and laterally in the soil mass under unsaturated conditions. The lateral component of flow may be increased by a drop in vertical hydraulic conductivity. This may occur at the regolith/bedrock interface or at some boundary within the soil (illuvial horizon, or iron pan). Where the water table is sufficiently high it may intersect the soil surface and a saturated zone forms which is fed by interflow and rising ground water as return flow. Such a saturated zone may develop where a perched water table becomes established particularly at locations where shale strata outcrops on the hillslope. Saturated flow conditions must exist at the base of the slope for discharge from the slope to occur. This saturated zone is supplied by unsaturated flow from upslope. Instantaneous discharge from the profile is directly related to the hydraulic head in the saturated zone, which in turn is a function of the upslope extent of saturated conditions. Assuming that saturated permeability of the soil is constant upslope, the extent of the saturated zone is dependent only upon unsaturated supply rate. When supply exceeds lateral permeability the saturated zone grows upslope and discharge from the slope base increases (Weyman, 1970).

Figs. 3.21 to 3.27 show the stream discharge plotted for weirs located in the Callow Bank catchment. The positions of the weirs are shown in Fig. 3.2. Figs. 3.21 to 3.27 show discharge (l/s or cumecs) indicated by the broken line plotted against rainfall (shaded bars) for the period September 1984 to September 1985. The hydrographs should only be taken as a very rough indication of stream discharge characteristics in the Callow basin. Inaccuracies must inevitably occur partly because of the crude weir construction used and partly because of the intermittant nature of weir readings. Weir readings
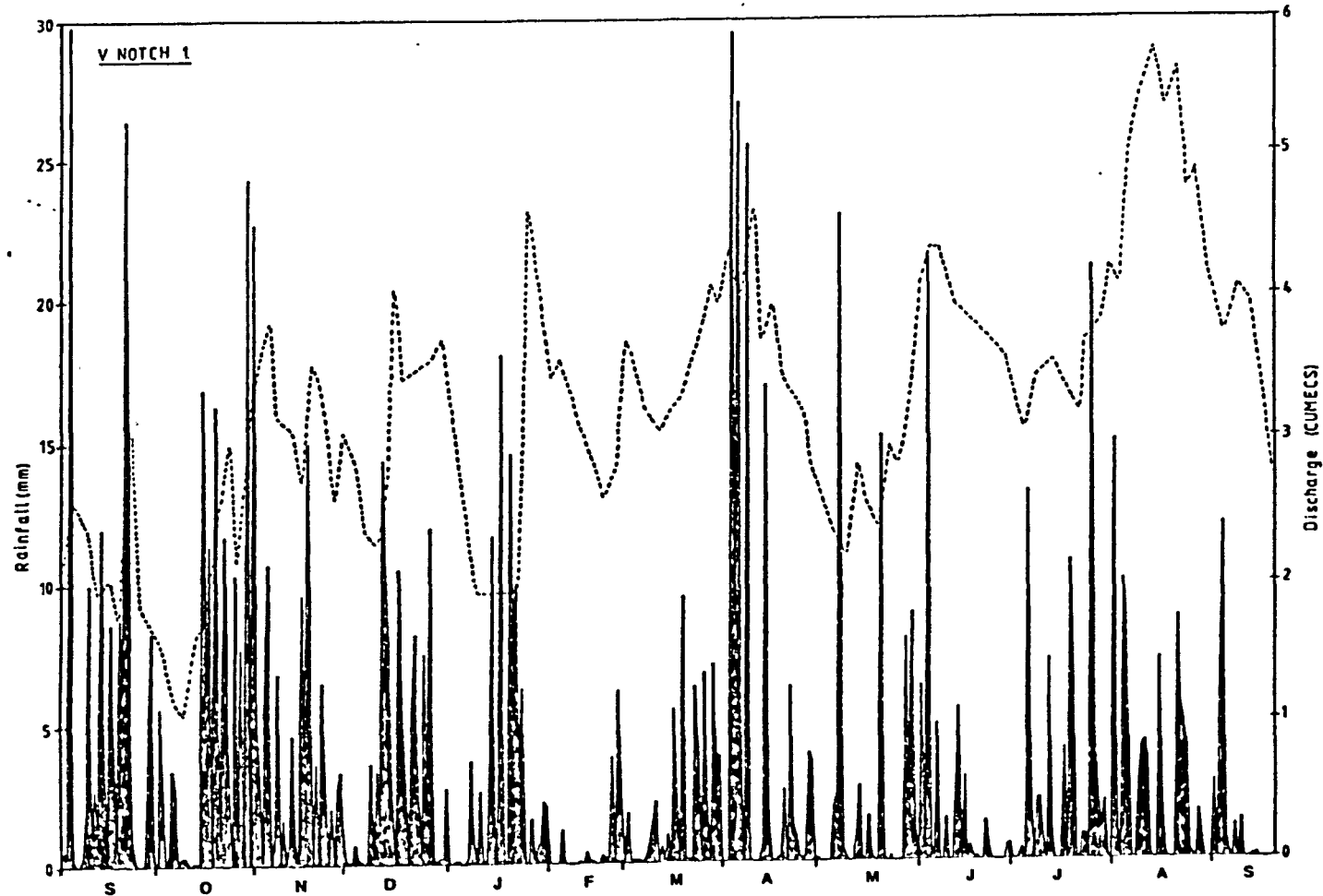
Fig. 3.21 Stream discharge in cumecs for V.Notch weir 1
indicated by the broken line plotted against rainfall (shaded bars)
for the period September 1984 to September 1985.
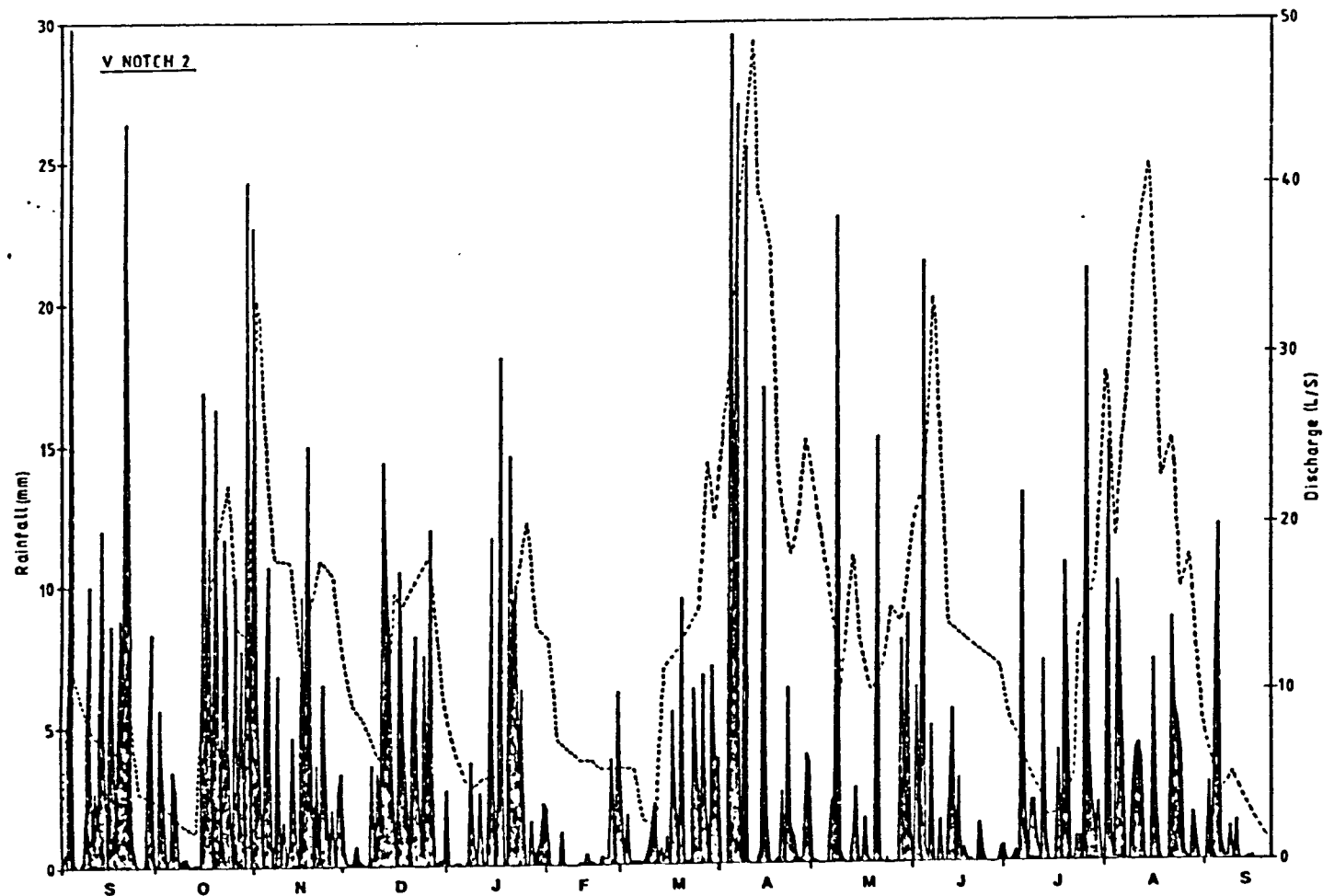
Fig. 3.22 Stream discharge in litres per second for V.Notch weir 2 indicated by the broken line plotted against rainfall (shaded bars) for the period September 1984 to September 1985.
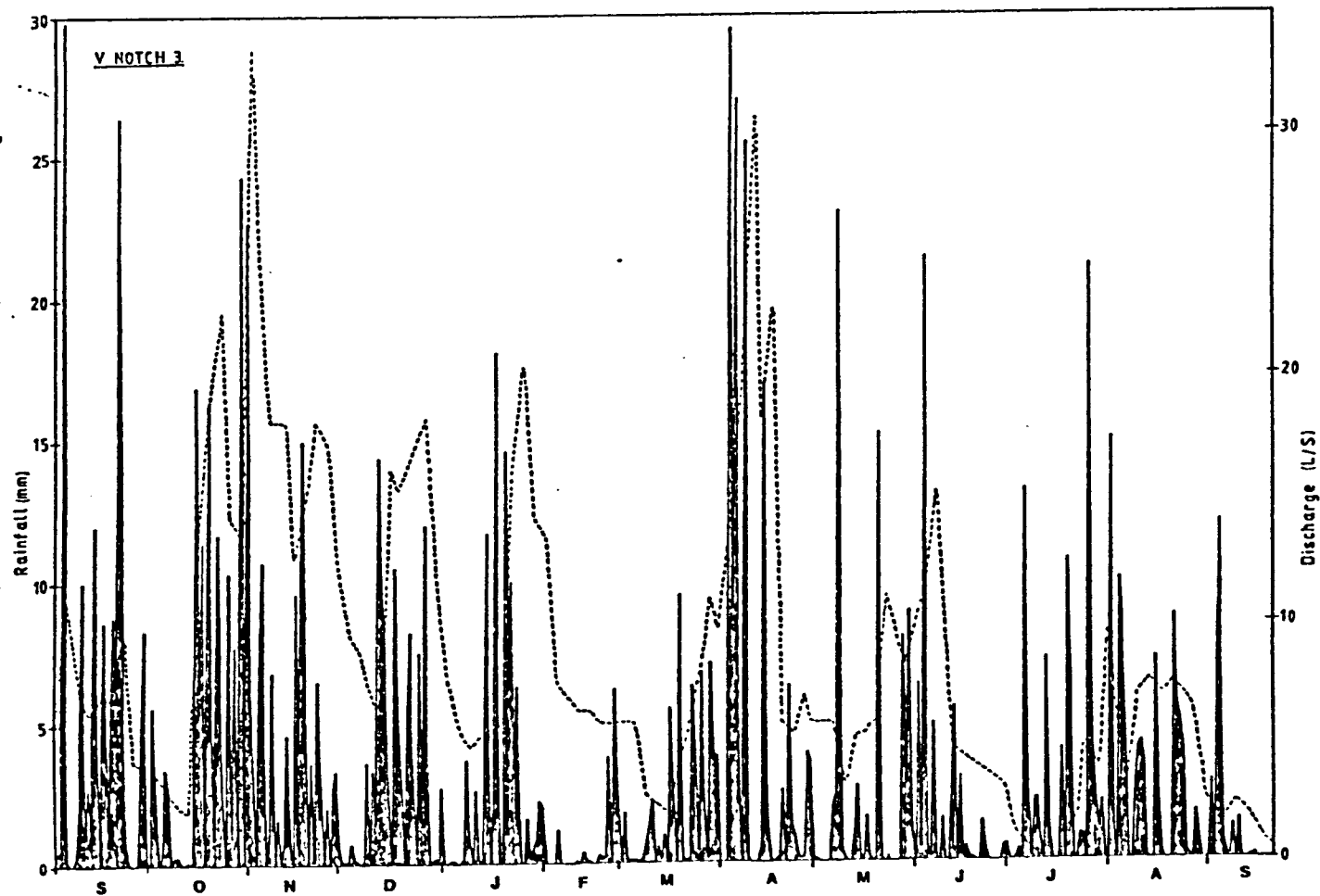
Fig. 3.23 Stream discharge in litres per second for V.Notch weir 3 indicated by the broken line plotted against rainfall (shaded bars) for the period September 1984 to September 1985.
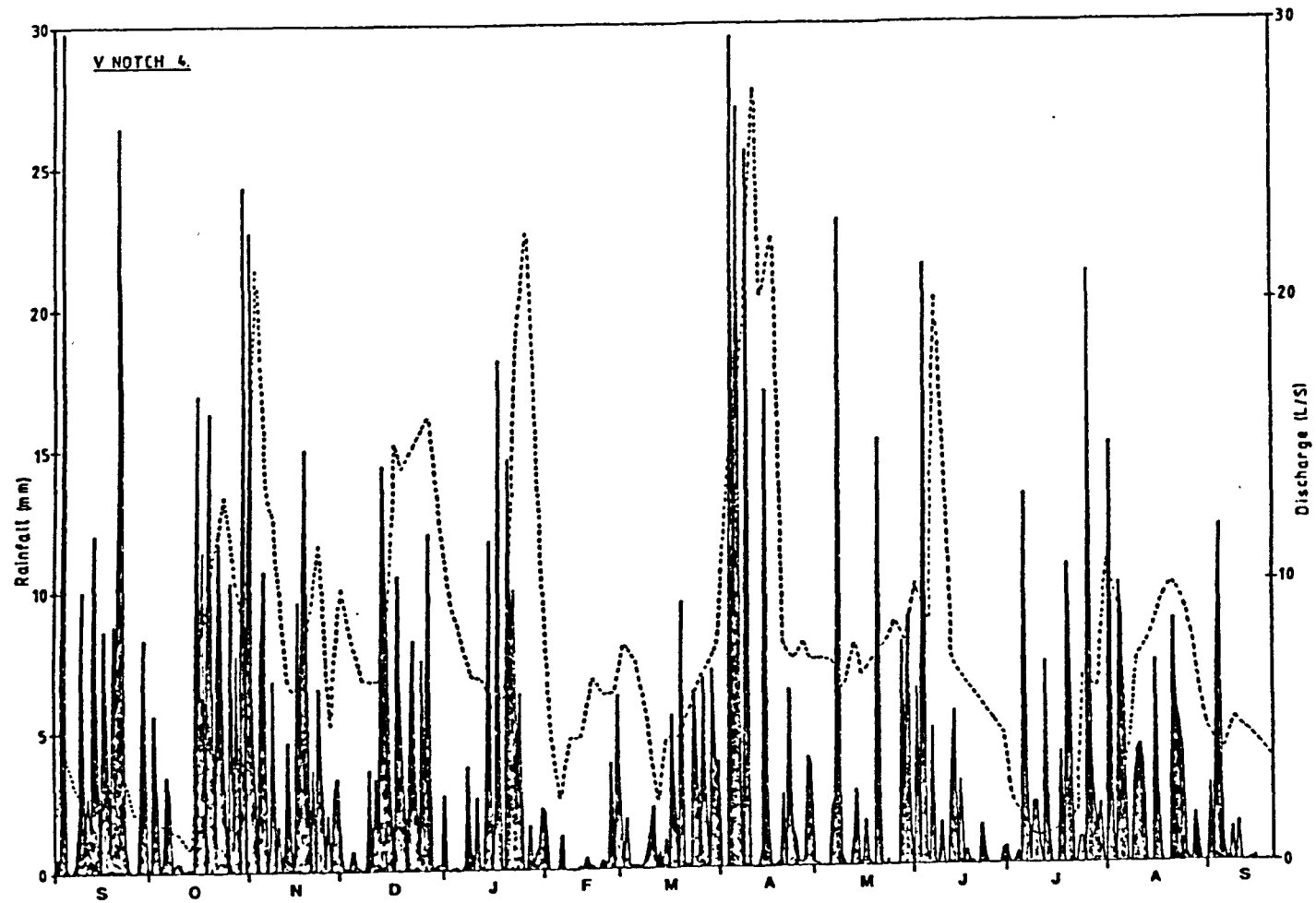
Fig. 3.24 Stream discharge in litres per second for V.Notch weir 4 indicated by the broken line plotted against rainfall (shaded bars) for the period September 1984 to September 1985.
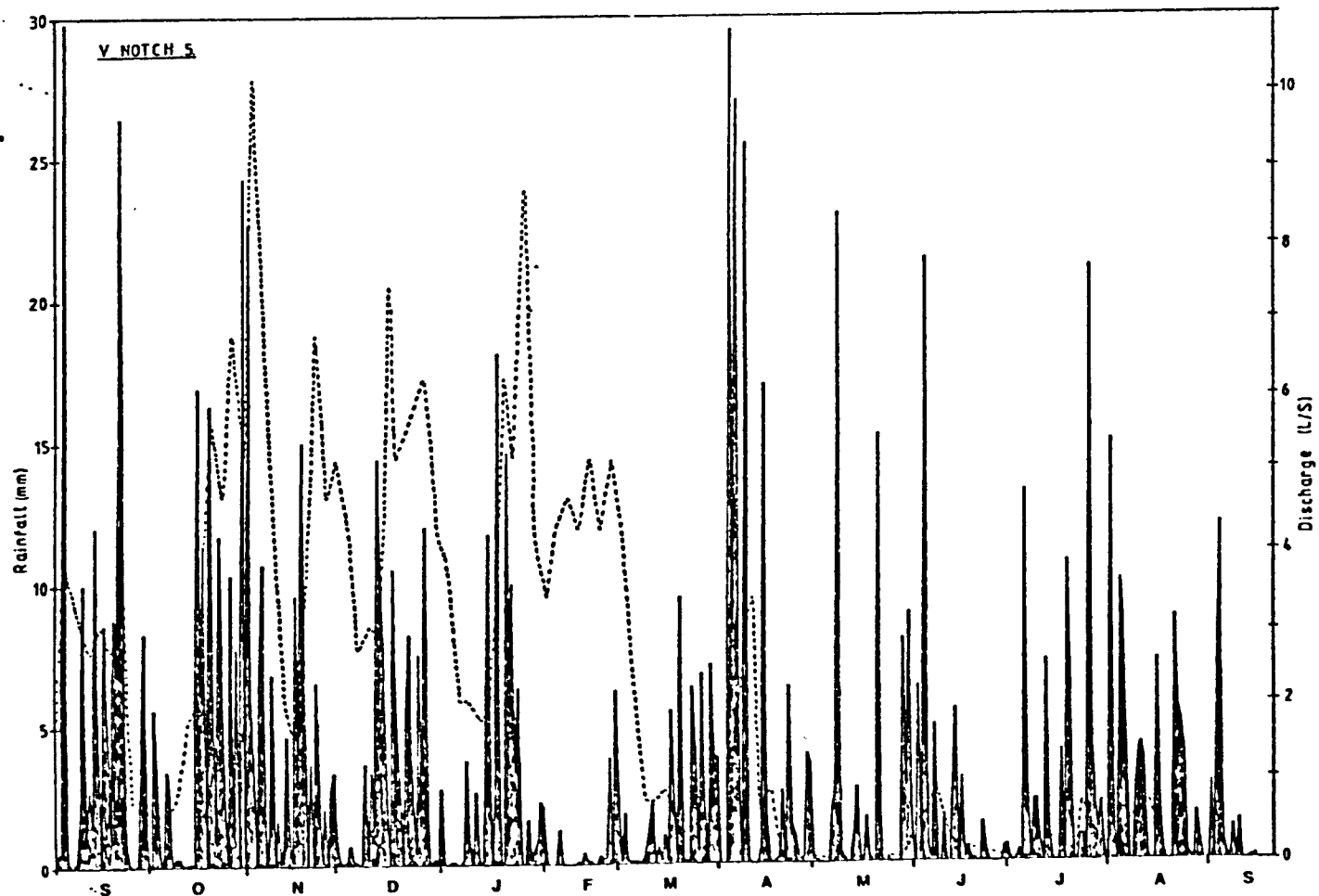
Fig. 3.25 Stream discharge in litres per second for V.Notch weir 5 indicated by the broken line plotted against rainfall (shaded bars) for the period September 1984 to September 1985.
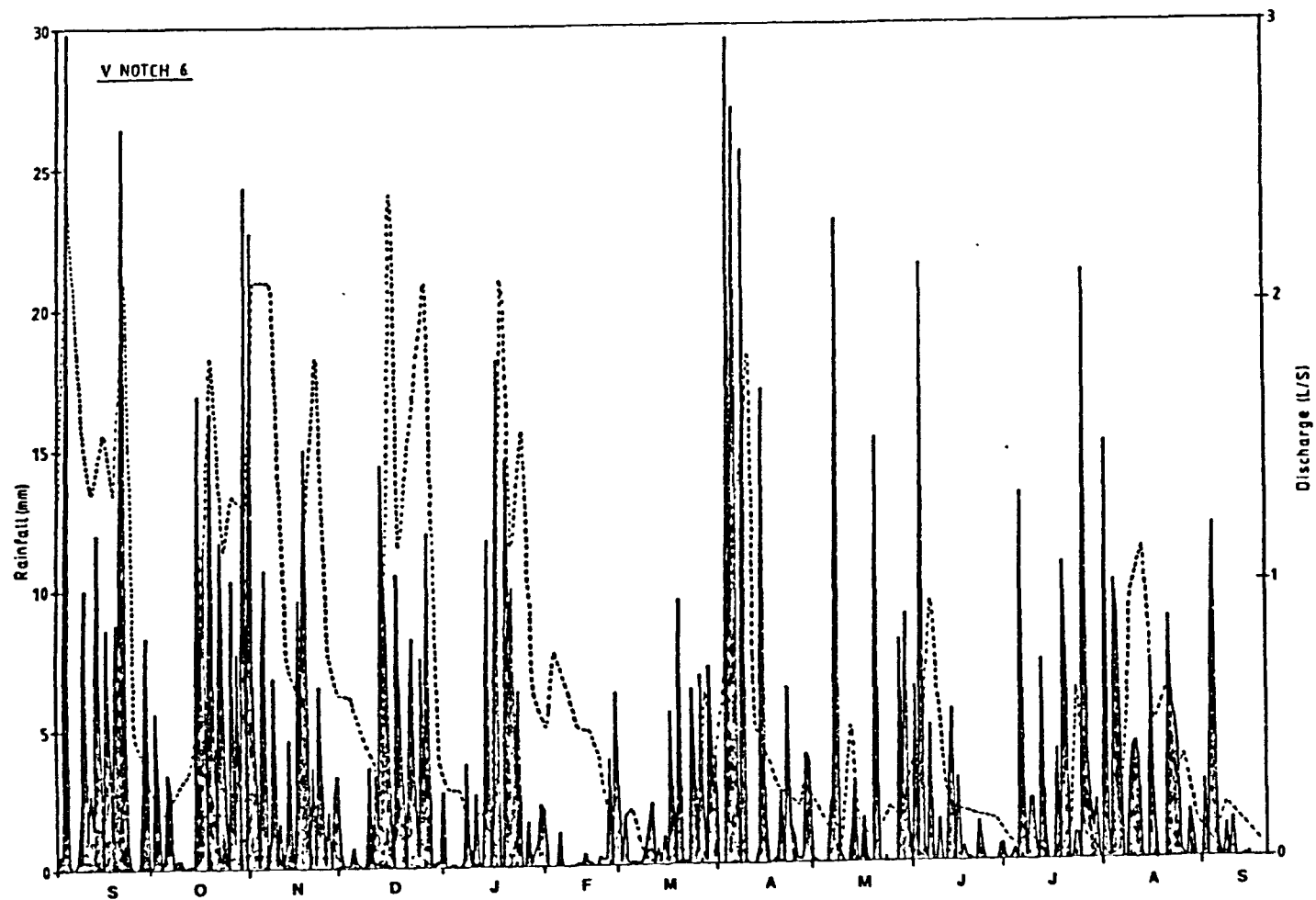
Fig. 3.26 Stream discharge in litres per second for V.Notch weir 6
indicated by the broken line plotted against rainfall (shaded bars)
for the period September 1984 to September 1985.
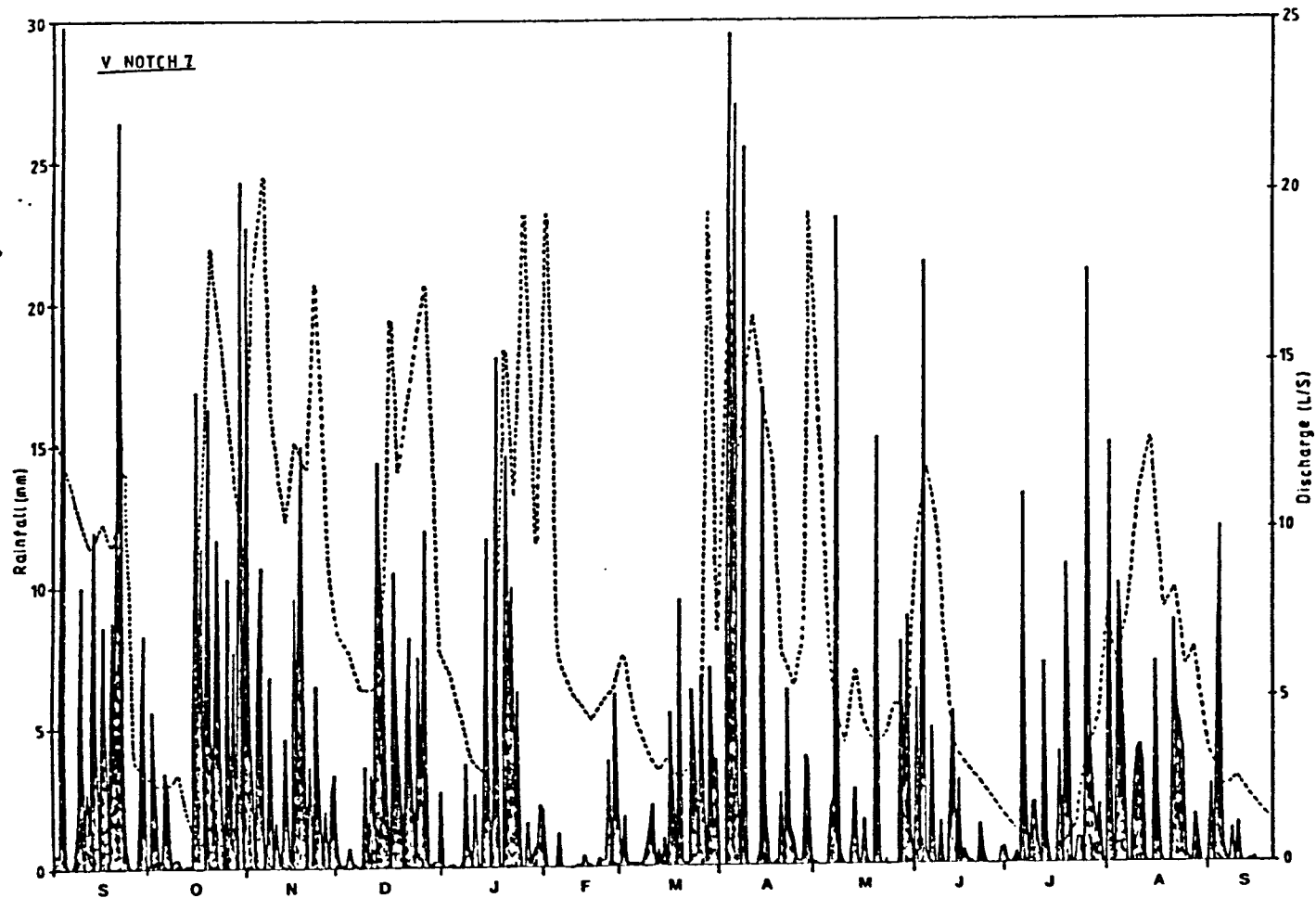
Fig. 3.27 Stream discharge in litres per second for V.Notch weir 7
indicated by the broken line plotted against rainfall (shaded bars)
for the period September 1984 to September 1985.

were taken on only two days each week, therefore, rapid fluctuations in discharge which occurred between recording days may not be accurately represented. However, despite these problems the hydrographs show a general similarity in their characteristics and therefore demonstrate a general unity in discharge patterns for the basin as a whole.

The hydrograph in Fig. 3.21 represents the main weir outflow from the whole basin. The hydrograph shows a close correspondence between rainfall and discharge until June 1985, then the time lag between rainfall peak and discharge peak becomes more prolonged. This extension in time lag between the rainfall peak and discharge peak during the summer months of 1985 may be due to the longer time lag involved in producing saturated throughflow conditions in those areas in which moisture conditions are maintained at or near saturation between storms in the winter months. A major part of the early storm discharge and hydrograph peak appears to be generated as surface flow on areas of top soil saturation particularly stagnogley soils and on unsaturated areas of low infiltration capacity. Large areas are maintained at or close to saturation throughout the winter due to the low sub-surface flow rates. The saturated contributing areas expand and contract dynamically during and between storm rainfalls in a manner that reflects the complexities of soil and topography. Piezometers situated in depressions and small hollows often gave positive pore water pressures throughout the year indicating that these areas maintained saturated conditions.

Weir 2 was situated 90m upstream from weir 1. The discharge response to storm rainfall was more accentuated than compared to the situation in weir 1. The pattern of discharge peaks and troughs in Figs. 3.21

and 3.22 are very similar showing a rapid rise in discharge after rainfall followed by a sharp decrease. Most of the piezometers situated on straight slopes showed that such slopes conducted water by throughflow rapidly thereby causing a rapid discharge response in the main stream channel. None of the piezometers situated on straight or convex slopes at Callow Bank indicated the attainment of saturated conditions. Differences in slope morphology therefore exert a major control in the hydrology of storm response.

V.notch weir 6 was located in the headwater area of the Callow catchment. The hydrograph illustrates the ephemeral nature of this channel situated in the headwater area (Fig. 3.26). The stream conducts water during the winter months then dries up during the summer months. The discharge of this stream is dependant upon small flush areas in hollows and springs which flow during the winter months only. These small flush sites and seeps not necessarily connected directly with the stream appear to be saturated throughout the winter, as a result of both convergent flow and more impermeable soil conditions. Studies by Kirkby et al., 1976, have shown the importance of such flush lines in contributing to the storm hydrograph. Areas of saturation which extend from the head of the channel into flush lines connect areas of low uniform slope along the channel sides that remain saturated throughout the winter.

Weir 5 was situated in a small stream draining a marshy area in a large seepage hollow. The stream discharge was dependant upon saturated conditions being maintained in the seepage hollow. During periods of heavy rainfall during the winter months the saturated area increased, extending the total drainage net leading to peak discharges occurring 2 to 3 days after each rainfall event

(Fig. 3.25). The stream discharge after March 1985 was disrupted by the effects of cattle trampling the banks of the stream channel around the weir; thereby reducing channel flow and affecting subsequent dicharge readings.

The positions of weirs 3 and 4 are close together explaining the similarity of hydrographs (Figs. 3.23 and 3.24). Weir 3 was located downstream from the confluence of a small stream the discharge was therefore slightly higher for the first 9 months, than the discharge at weir 4 situated slightly upstream of the stream confluence. The discharge for weirs 3 and 4 was very similar for the months of June - September 1985 indicating that the contribution of the small stream joining the main channel between weirs was negligible during this period. The hydrograph for weir 7 shows longer lag times between rainfall peaks and discharge peaks compared to the other hydrographs (Fig. 3.27). The lag time delay became longer during the summer months of 1985, this may be explained by the reduction in the extent of saturated areas. Seepage hollows on the western slopes of Overstones catchment and small seepage channels draining the toe area of Callow Bank slide took a longer time to reach a point of threshold saturation in order to permit throughflow, or surface flow thereby delaying response time from such areas.

The rapid response of stream discharge to rainfall in all hydrographs in the winter months appears to be a direct confirmation of the existence of Hortonian overland flow. However, a number of studies including those by Dunne & Black, 1970a, b, have shown that overland flow is rare or non-existant and that which does occur reaches streams too late to make a significant contribution to the measured channel storm hydrograph.

It is now recognised that initial hydrograph responses to storm rainfall are derived from rain falling directly into the channel and from the saturated contributing area immediately adjacent to the stream and seepage hollows further upslope. Summer storms may initially produce Hortonian overland flow from spurs because the hydraulic conductivity of the soils is low and infiltration is at first negligible; only after some hours will soils 'wet up' and infiltration occur at a rate permitted by soil saturated hydraulic conductivity. A number of studies have shown that throughflow is found to be the only process of water transmission effectively contributing to stream flow (Whipkey, 1965a,b; Kirkby & Chorley, 1967; Hewlett & Hibbert, 1965; Beven, 1978; Dunne & Black, 1970b; Anderson & Burt, 1977, 1978a, b, 1979, 1982). The 'quick response' of stream discharge to rainfall is a result of rapid increases in throughflow output as saturated conditions extend upslope. The 'delayed response' of stream discharge and subsequent base flow are both produced by stages in the slow unsaturated drainage of the whole slope, a process which is sufficient to maintain stream flow throughout the year. Overland flow does not contribute to 'quick response' in the stream hydrographs, probably as a resullt of high 'A-horizon' permeability (see Soil Profiles A4, A5 and A6 in the Appendix) and low rainfall intensities. Ground water flow does not appear to contribute to 'delayed flow', although temporary ground water storage must supplement unsaturated throughflow during the year. Beven (1977a, b) showed that convergent slopes and in particular, convergent slopes concave in section deliver the highest peak rates of sub-surface flow and are most likely to generate saturated conditions and return flow at the soil surface. In such areas Beven demonstrated that peak sub-surface flow rates could occur within minutes of the end of the rainfall. The piezometer survey

showed that the areas in which moisture conditions are maintained at or near saturation between storms in winter are found in small convergent hollow areas often associated with intermittent springs and seepage areas associated with underlying shale strata. These areas tend to maintain saturated conditions and facilitate the collection and rapid transmission of surface water to the basin outflow after heavy rainfall.

3.5.4 Piezometer survey

Fluctuations in the level of the water table (i.e. phreatic surface) or the creation of temporary perched water systems, will markedly affect the factor of safety of a hillslope. The association in time between shallow slope failures and periods of heavy rainfall is a widely experienced phenomenon. Even though an actual first time failure may not be associated with heavy rainfall the initiation or possible acceleration of movement of slope material measured by extensometer or inclinometer instrumentation, may be expected, Harper (1975). Slope stability analyses carried out in terms of effective stress require an understanding of the distribution of pore water pressure in the slope. This understanding must be based on the knowledge of the ground water flow system, which is in turn dependant on geological and topographical factors and local changes in hydraulic conductivity.

Slope profiles 1 to 6 (Figs. 3.3, 3.8, 3.9, 3.10, 3.11, 3.12) show the position of each piezometer (numbered square) in relation to the morphology of the hillslope profile. The profiles show in graphical form the maximum and minimum piezometric levels recorded for each piezometer between September 1984 and September 1985. The maximum

Table for Fig.3.3

Section	Piezometer Number	Piezometer Tip Depth (z) (cm)	Min P.L. Below Ground Surface (cm) (Min P.L.)	Max Piez Head (h) (cm) (Max hp)	Max P.L. Below Ground Surface (cm) (Max P.L.)	Min Piez Head (h) (cm) (Min hp)	Mean P.L. Below Ground Surface (cm) (Mean P.L.)	Mean Piez Head (cm) (Mean hp)	Max Pore Pressure (ru) (γw.h/γ.z)	Max Pore Pressure (u) K Pa (γw.h)	Soil Engng. Class BSCS:BS5930 (See Table3.1)
u	1	256	4/11/84 58	198	1/9/84 207	49	145.3	110.7	19.42	0.45	GF GCL
u	2	156	+8	164	29/9/85 21	135	8	156	16.09	0.62	FG CLS
u	3	188	10/11/84 92	96	29/9/85 127	61	120.2	73.8	9.42	0.30	FG CLS
u	4	194	10/11/84 91	103	6/6/85 120	74	108.3	85.7	10.10	0.31	G-F GPC
u	5	167	4/11/84 41	126	13/9/85 77	90	60.5	106.5	12.36	0.44	G-F GPC
u	6	197	30/12/84 16	181	1/9/84 34	163	24.0	173.0	17.76	0.54	G-F GPC
m	7	226	23/9/84 59	167	77	149	69.5	156.5	16.38	0.43	FS CLS
m	8	169	3	166	21	148	13.6	155.4	16.28	0.57	FS CLS
m	9	191	14/4/84 72	119	1/9/84 124	67	91.0	100.0	11.67	0.36	F CL
m	10	188	4/11/84 +2	190	13/9/85 117	71	86	102.0	18.64	0.59	FS MLS
m	11	250	23/9/84 89	161	1/9/84 122	128	109.5	140.5	15.79	0.38	FS MLS
m	12	246	76	170	96	150	157.8	88.2	16.68	0.40	FS MLS
m	13	457	8/11/84 111	346	1/9/84 194	263	163.6	293.4	33.94	0.44	FS CLS
m	14	435	29/9/85 187	248	29/9/85 303	132	245.6	189.4	24.33	0.33	FS MLS
L	15	357	4/11/84 200	157	357	0	340.1	16.9	15.40	0.25	FG MLS
L	16	189	182	7	189	0	187	2	0.69	0.02	FS CLS
L	17	154	153	1	154	0	154	0	0.1	0.004	FS CLS
L	18	458	4/11/84 161	297	10/3/85 369	89	284.5	173.5	29.13	0.38	FS CLS
L	19	101	+9	110	2	98	+6.2	107.2	10.79	0.64	F CI
L	20	134	41	93	29/9/85 108	26	70.6	63.4	9.12	0.41	F CL
L	21	435	25/11/84 182	253	246	189	215.9	219.1	24.82	0.34	F CL
L	22	152	14/4/85 13	139	10/7/85 69	83	38.5	113.5	13.63	0.54	FS CLS

Fig. 3.3

Table for Fig.3.8

Section	Piezometer Number	Piezometer Tip Depth (z) (cm)	Min P.L. Below Ground Surface (cm) (Min P.L.)	Max Piez Head (h) (cm) (Max hp)	Max P.L. Below Ground Surface (cm) (Max P.L.)	Min Piez Head (h) (cm) (Min hp)	Mean P.L. Below Ground Surface (cm) (Mean P.L.)	Mean Piez Head (cm) (Mean hp)	Max Pore Pressure (ru) (γw.h/γ.z)	Max Pore Pressure (u) K Pa (γw.h)	Soil Engng. Class BSCS:BS5930 (See Table3.1)
u	23	128	96	32	128	0	126.8	1.2	0.15	3.14	SF SCL
u	24	326	313	13	326	0	323.7	2.3	0.02	1.28	SF SCL
u	25	226	222	4	226	0	225.7	0.3	0.01	0.39	SF SCL
u	26	88	88	0	88	0	88	0	0	0	FG CLS
u	27	129	126	3	129	0	128.8	0.2	0.29	0.01	FG CLS
u	28	164	132	32	164	0	163.4	0.6	3.14	0.11	FG CLS
m	29	182	182	0	182	0	182	0	0	0	FG CLS
m	30	259	4/11/84 229	30	259	0	231.5	7.5	2.94	0.07	FG CLS
m	31	346	10/11/84 316	30	346	0	328.5	7.5	2.94	0.05	FG MLS
m	32	263	16/4/85 170	93	263	0	229.1	33.9	9.12	0.21	F ML
L	33	163	9/4/84 86	77	163	0	143.5	19.5	7.55	0.28	FS MLS
L	34	163	4/11/84 48	115	27/1/85 145	18	90.0	73.0	11.28	0.41	F ML
L	35	182	4/11/84 94	88	182	0	163.6	18.4	8.63	0.28	F CL
L	36	169	10/11/84 12	157	3/1/85 140	17	100.7	68.3	15.40	0.54	GF GCL

PROFILE 2
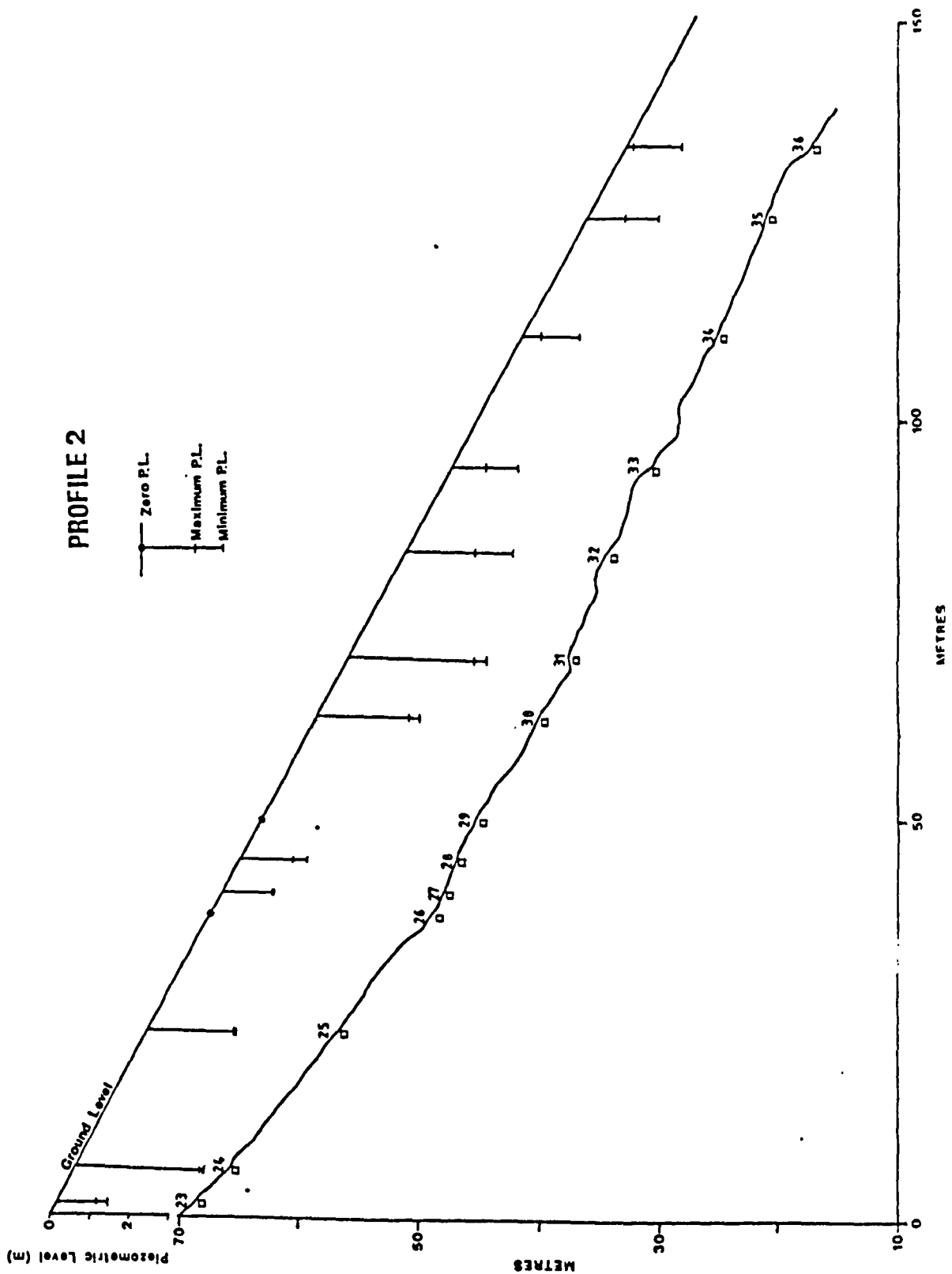
Fig. 3.8

Table for Fig.3.9

Section	Piezometer Number	Piezometer Tip Depth (z) (cm)	Min P.L. Below Ground Surface (cm) (Min P.L.) date	Min P.L. value	Max Piez Head (h) (cm) (Max hp)	Max P.L. Below Ground Surface (cm) (Max P.L.) date	Max P.L. value	Min Piez Head (h) (cm) (Min hp)	Mean P.L. Below Ground Surface (cm) (Mean P.L.)	Mean Piez Head (cm) (Mean hp)	Max Pore Pressure (ru) ($\gamma w.h/\gamma.z$)	Max Pore Pressure (u) K Pa ($\gamma w.h$)	Soil Engng. Class BSCS:BS5930 (See Table3.1)
u	37	88		88	0		88	0	0.	0	0	0	FG MLS
u	38	297		258	39		297	0	287.3	9.7	3.83	0.08	SF SML
u	39	123		111	12		123	0	121.5	1.5	1.18	0.06	FG CLS
u	40	133		118	15		133	0	132.0	1.0	1.47	0.07	FG CLS
u	41	136		130	6		136	0	135.2	0.8	0.59	0.03	FG CLS
u	42	81		81	0		81	0	81	0	0	0	SF SML
m	43	111	31/1/85	92	19		111	0	109.3	1.7	1.86	0.10	FG MLS
m	44	269	14/4/85	205	64		269	0	242.2	26.8	6.28	0.14	FG MLS
m	45	229	25/8/85	152	77		229	0	196.3	32.7	7.55	0.20	FG MLS
m	46	210	9/4/85	184	26		210	0	207.8	2.2	2.55	0.07	SF SML
m	47	205	29/11/84	178	27		205	0	204.1	1.9	2.65	0.08	F ML
m	48	262		256	6		262	0	261.3	1.7	0.59	0.01	FS MLS
m	49	127		99	28		127	0	123.1	3.9	2.75	0.13	FS MLS
m	50	240		234	6		240	0	239.2	0.8	0.59	0.01	FS CLS
m	51	285		127	158		285	0	215.4	69.6	15.50	0.32	FG MLS
m	52	115	14/4/85	38	77		93	22	68.2	46.8	7.55	0.39	FS CLS
m	53	433	14/4/85	303	130	14/10/84	415	18	352.8	80.2	12.75	0.18	FG CLS
m	54	195	10/11/84	89	106		195	0	146.8	48.2	10.40	0.32	FG MLS
L	55	222	9/6/85	191	31		222	0	205.5	16.5	3.04	0.08	GF GCL
L	56	223	8/11/84	91	132		197	26	141.2	81.8	12.95	0.35	GF GCL
L	57	243	6/12/84	17	226		54	189	35.1	207.9	22.17	0.54	G-F GPM

PROFILE 3

Zero P.L.
Maximum P.L.
Minimum P.L.

Ground Level

METRES

Piezometric Level (m)

METRES

Fig. 3.9

Table for Fig. 3.10

Section	Piezometer Number	Piezometer Tip Depth (z) (cm)	Min P.L. Below Ground Surface (cm) (Min P.L.)	Max Piez Head (h) (cm) (Max hp)	Max P.L. Below Ground Surface (cm) (Max P.L.)	Min Piez Head (h) (cm) (Min hp)	Mean P.L. Below Ground Surface (cm) (Mean P.L.)	Mean Piez Head (cm) (Mean hp)	Max Pore Pressure (ru) ($\gamma_w.h/\gamma.z$)	Max Pore Pressure (u) K Pa ($\gamma_w.h$)	Soil Engng. Class BSCS:BS5930 (See Table3.1)
u	58	170	. 77	93	159	11	101.6	68.4	9.12	0.32	FG CLS
u	59	144	27	117	100	44	50.6	93.4	11.48	0.48	GF GCL
u	60	145	9/6/85 49	96	30/7/85 132	13	80.5	64.5	9.42	0.39	FG CLS
u	61	267	14/4/85 129	138	1/9/84 165	102	142.9	124.1	13.54	0.30	SF SML
u	62	176	14/4/85 13	163	30/7/85 138	38	55.4	120.6	15.99	0.54	FS MLS
■	63	109	25/10/84 +4	113	107	2	29.4	79.6	11.09	0.61	F CL
■	64	248	50	198	201	47	108.3	139.7	19.42	0.47	FS MIS
■	65	110	3/2/85 +1	111	30/7/85 92	18	32.3	77.7	10.89	0.59	FS CIS
■	66	114	25/10/84 17	97	114	0	89.3	24.7	9.52	0.50	FS CIS
■	67	103	10/10/84 97	6	103	0	101.5	1.5	0.59	0.03	FS CLS
■	68	143	43	100	96	47	66.6	76.4	9.81	0.41	G-F CPL
■	69	111	58	53	92	19	76.1	34.9	5.20	0.28	FS CLS
L	70	274	196	78	247	27	220.2	53.8	7.65	0.17	FS MLS
L	71	213	54	159	115	98	77.3	135.7	15.60	0.44	FS SCL
L	72	356	30/12/84 71	285	96	260	85.0	271.0	27.96	0.47	

PROFILE 4

Maximum P.L.
Minimum P.L.

Piezometric Level (m)

Ground Level

METRES

METRES

Fig. 3.10

Table for Fig.3.11

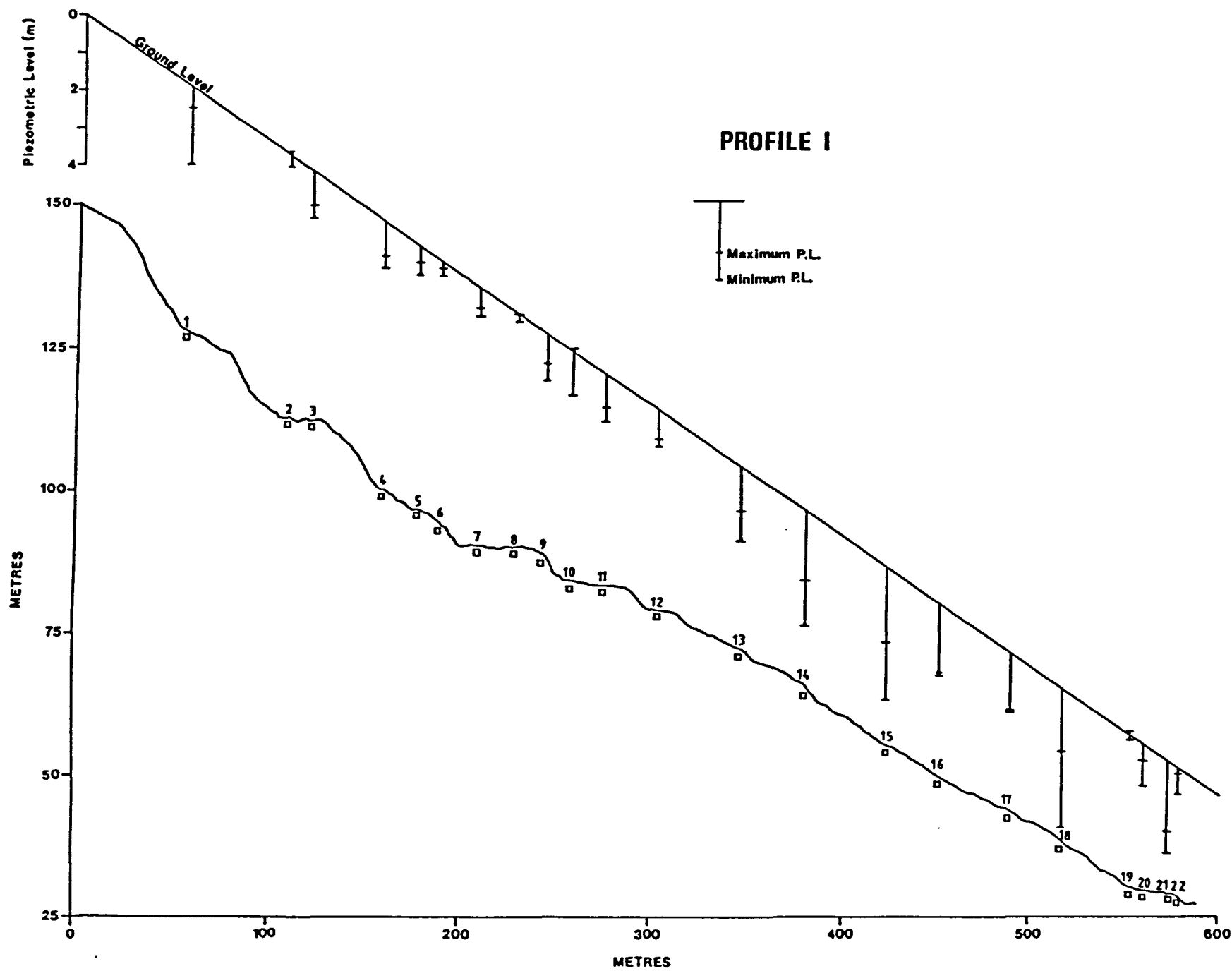| Section	Piezometer Number	Piezometer Tip Depth (z) (cm)	Min P.L. Below Ground Surface (cm) (Min P.L.)		Max Piez Head (h) (cm) (Max hp)	Max P.L. Below Ground Surface (cm) (Max P.L.)		Min Piez Head (h) (cm) (Min hp)	Mean P.L. Below Ground Surface (cm) (Mean P.L.)	Mean Piez Head (cm) (Mean hp)	Max Pore Pressure (ru) ($\gamma w.h/\gamma.z$)	Max Pore Pressure (u) K Pa ($\gamma w.h$)	Soil Engng. Class BSCS:BS5930 (See Table3.1)
u	73	278	23/9/84	81	197		122	156	174.1	103.9	19.33	0.41	GF GML
m	74	248	27/1/85	104	144		218	30	66.5	181.5	14.13	0.34	FS MLS
m	75	248	25/8/85	78	170	14/10/84 156	92		129.1	118.9	16.68	0.40	F CL
L	76	321	12/6/85	216	105	1/9/85 288	33		68.0	253	10.30	0.19	F CL
L	77	264		227	37	1/9/84 264	0		9.0	255	3.63	0.08	F CI
L	78	143	27/1/85	113	30	1/9/84 143	0		1.8	141.2	2.94	0.12	F CI

PROFILE 5
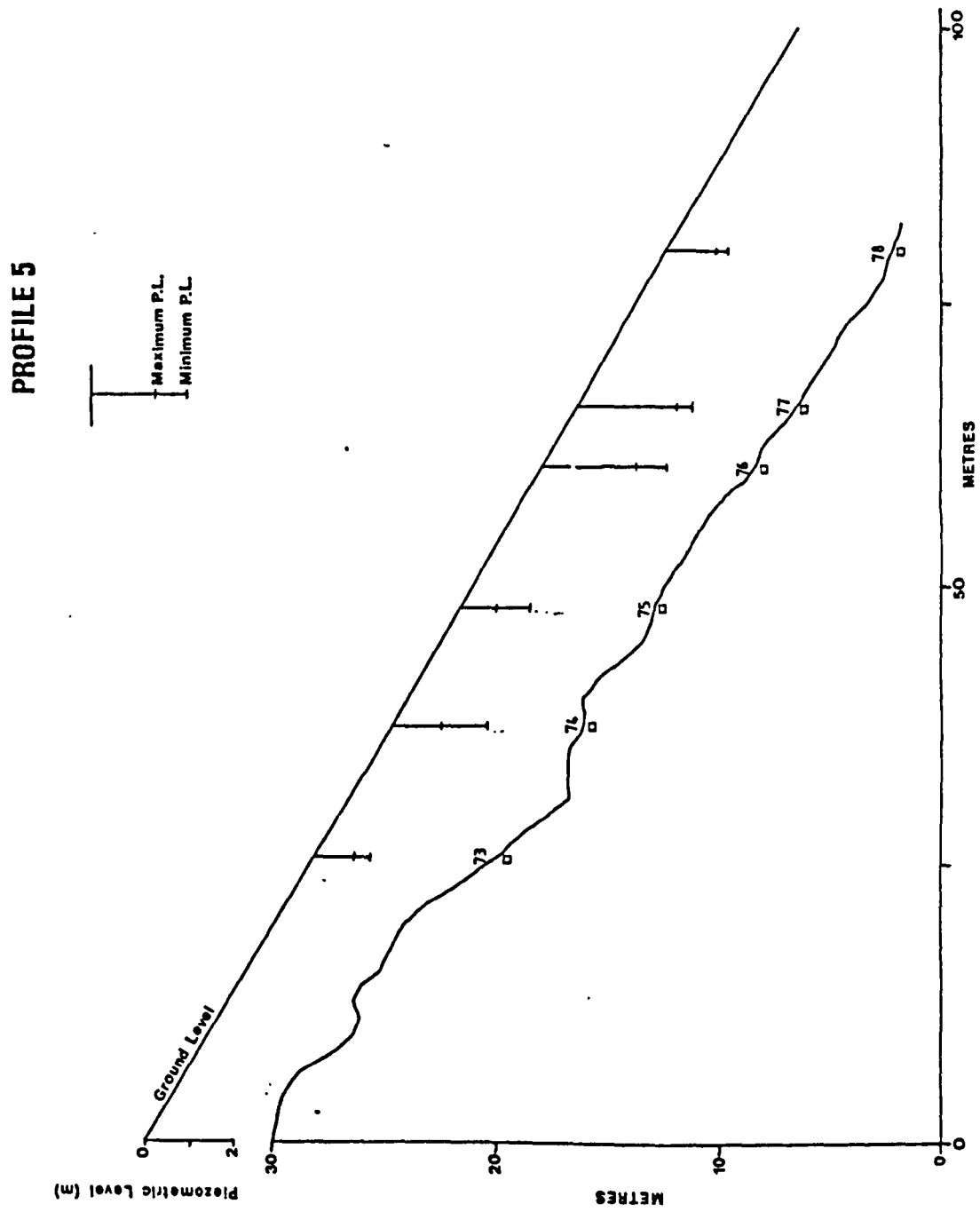
Fig. 3.11

Table for Fig.3.12

Section	Piezometer Number	Piezometer Tip Depth (z) (cm)	Min P.L. Below Ground Surface (cm) (Min P.L.)	Max Piez Head (h) (cm) (Max hp)	Max P.L. Below Ground Surface (cm) (Max P.L.)	Min Piez Head (h) (cm) (Min hp)	Mean P.L. Below Ground Surface (cm) (Mean P.L.)	Mean Piez Head (cm) (Mean hp)	Max Pore Pressure (ru) ($\gamma w.h/\gamma.z$)	Max Pore Pressure (u) K Pa ($\gamma w.h$)	Soil Engng. Class BSCS:BS5930 (See Table3.1)
u	79	185	14/4/85 104	81	20/7/85 131	54	117.6	67.4	7.95	0.26	SF SML
u	80	90	25/10/84 50	40	1/9/84 85	5	69.4	20.6	3.92	0.26	SF SML
u	81	275	14/4/85 168	107	1/9/84 269	6	29.3	60.7	10.50	0.23	G-F GPL
u	82	156	61	95	1/9/84 100	56	77.7	78.3	9.32	0.36	GF GCL
u	83	181	103	78	10/3/85 159	22	128.1	52.9	7.65	0.25	FG CLS
u	84	270	29/8/85 160	110	1/9/84 215	55	186.2	83.8	10.79	0.24	FG CLS
u	85	452	9/4/85 342	110	1/9/84 442	10	373.8	78.2	10.79	0.14	GF GCI
m	86	146	25/8/85 61	85	1/9/84 109	37	78.9	67.1	8.34	0.34	FG CLS
m	87	198	14/4/85 61	137	17/10/84 137	61	90.8	107.2	13.44	0.41	FG MLG
m	88	185	25/8/85 100	85	21/1/85 144	41	122.3	62.7	8.34	0.27	FG CLS
L	89	196	2/12/85 101	95	1/9/84 147	49	117.3	78.7	9.32	0.28	F CI
L	90	290	17/10/84 122	122	168	76	193.5	96.5	11.97	0.25	F CL
L	91	278	181	97	224	54	206.2	71.8	9.52	0.20	FS MLS
L	92	186	115	71	186	0	146.5	39.5	6.97	0.22	FS CLS

PROFILE 6

Maximum P.L.
Minimum P.L.

Ground Level

Piezometric Level (m)

METRES

METRES
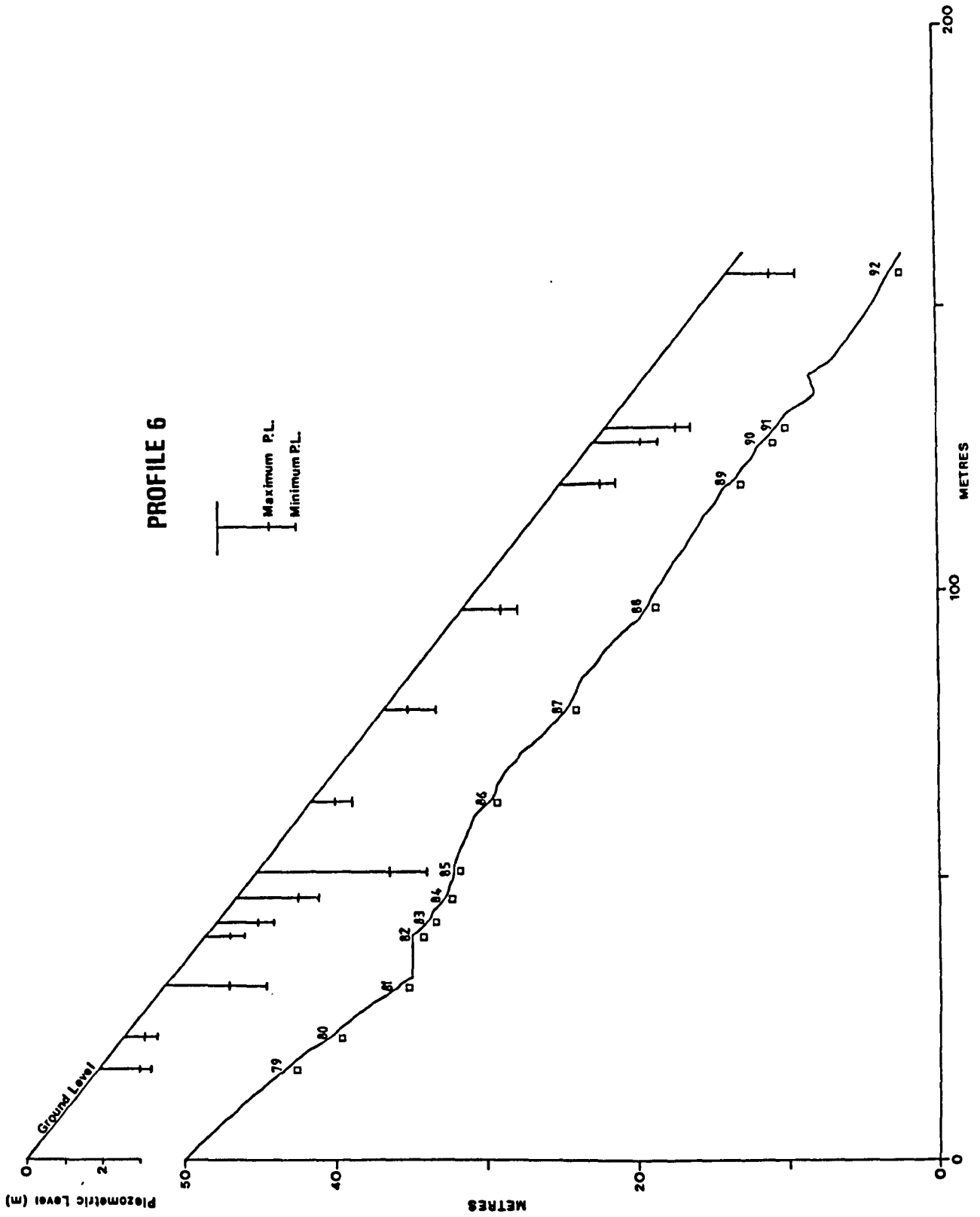
Fig. 3.12

and minimum piezometric levels have been drawn extending vertically from a straight line representing the ground surface rather than the slope profile surface in order to facilitate comparison between piezometric levels. The information in Tables 3.6 to 3.11 correspond to each slope profile, they provide information for each individual piezometer. Dates for the maximum and minimum piezometric levels are also given in the tables. The maximum pore water pressure has been expressed as the ratio ru, where, ru = $u/\gamma z$ = $\gamma w.h/\gamma z$, and as u, where u = $\gamma w.h$. The mean soil unit weight was calculated from the 48 bulk density tests conducted for Field Direct Shear Box testing, (γ = 16.74 kN/m^3). Where seepage is not uniform, and directed out of the slope, it is convenient to use the ratio ru, between pore pressure and the weight of a vertical column of soil. The table also includes the soil engineering classification for each piezometric site, the symbols indicating soil groups correspond to those in Table 3.1.

Profiles 1 to 6 (Figs. 3.3, 3.8, 3.9, 3.10, 3.11, 3.12) show that the piezometric surface on the hillslope is a very complex one. Many hydrological studies have emphasised the role of the dynamic contributing area in controlling saturated surface flow and final discharge (Dunne & Black, 1970a; Kirkby, et al., 1976) and have revealed the significance of small scale local variation in surface saturation (Beven & Kirkby, 1979) and soil moisture tension (Weyman, 1973, 1974; Anderson & Burt, 1978a). These local variations in soil moisture content and slope drainage are controlled by hillslope morphology, soil depth and soil permeability. The piezometric surface is therefore dependant upon a number of factors including rainfall, evapotranspiration, infiltration capacity and ground water or aquifer relationships. The rate of infiltration itself depends on several

parameters and variables, the most important of which are antecedent soil moisture levels particularly in unsaturated areas and the intensity and quantity of surface vegetation (Arnett, 1974, 1976). The field investigation programme was not designed to monitor all the variables known to affect the piezometric surface, therefore, interpretation of results can only be regarded as a precursor to more detailed analyses. Profiles 1 to 6 show that the highest piezometric heads appear to be associated with topographic benches and hollows on the hillslope particularly in the middle and lower sections of the slope. Some of these benches were related to bedrock control, for instance where thin shale bands within the Middle Grit Series outcrop. These sites also tended to be associated with locally high water tables caused by seepage water being maintained on the impermeable shale band (e.g. piezometers 1, 2, 59, 62, 86, 87, 88). Regolith situated on the plateaus created by rotation of blocks in the Callow Bank slide (profile 1) show high piezometric surfaces indicating the development of a perched ground water table system. Piezometers 2 and 8 show that positive piezometric levels were attained in two of these perched water tables. It is difficult to recognise any trend in the pattern of piezometric levels within the regolith along the hillslope profile other than the effect of major topographical controls which are largely a reflection of underlying bedrock geology or mass movement processes. Table 3.6 shows the mean maximum pore water pressures represented by ru and u for upper, middle and lower slope sections. The mean pore water pressure in the upper slope regolith is less than that for both middle and lower sections. Although, one might have expected a higher mean pore-water pressure for basal slope areas this is shown not to be the case on the hillslope profiles studied and the mean pore pressures for regolith in lower slope sections is only slightly greater than that

for mid-slope regolith.

Table 3.6 The mean maximum pore water pressures represented by

(ru) and (u) for upper, middle and lower slope sections

Slope section	Mean maximum pore water pressures (ru) ($Yw.h/ Y.z$)	Mean maximum pore water pressures (kpa) ($Yw.h$)
Upper slopes	0.24	7.75
Middle slopes	0.29	10.19
Lower slopes	0.30	11.62

Seepage hollows, saturated depressions and other areas where perched water table conditions exist could easily be recognised by characteristic vegetation species particularly sphagnum and Juncus. Studies by Rutter, 1955; Bannister, 1964a, 1964b, 1964c; Jones, 1971; Jones & Etherington 1970, have shown convincing regression relationships between percentage of total biomass occupied by individual wet-heath species and water table depth. Gurnell, 1978, 1981, suggested that the composition of vegetation provided a useful indication of surface drainage conditions on a hillslope. Gurnell showed that pore water pressure correlated more closely with properties of the local vegetation canopy than with variations in slope topography as encountered by other workers (e.g. Anderson & Burt, 1978a; Weyman, 1973, 1974). Gurnell demonstrated by using measurements of hydraulic conductivity that larger scale topographic controls on pressure head were confused by local changes in permeability, and that vegetation patterns correlated more closely

with the changes in permeability.

Fig.3.28shows the monthly rainfall at Callow Bank for three years, (1983-1985). Monthly rainfall during January, February and march 1985 was much lower than the previous two years. Rainfall in January and February 1984 was much greater than in 1985 and since monthly rainfall throughout the months September to December 1983 remained high, piezometric levels would have been considerably higher during the winter months in 1984.

Figs. 3.29 to 3.36 show the relationship between rainfall (mm) and piezometric head (cm) for eight selected piezometers from September 1984 to September 1985. Each figure consists of 2 parts, a and b, corresponding to two six monthly periods, this was done in order to show the piezometer fluctuations in relation to individual rainfall events more clearly. The piezometric profiles have been plotted on separate graphs because of the considerable difference in piezometric head on the right axis.

Figs. 3.29 to 3.36 show a clear correlation between fluctuations in piezometric levels and the rainfall histogram. Headworth (1972) suggested that 'the time-lag between the occurrence of rain and the rise in ground water level is both measurable and predictable' and 'the amount of rise in ground water level is proportional to the amount of rainfall'. In each case the piezometric surface both rises and falls rapidly with each rainfall event. For purposes of describing the process of ground water pressure rise due to increased rainfall the problem may be conveniently sub-divided into prediction of the magnitude of pressure rise and measurement of the time-lag between rainfall and the consequent ground water pressure rise. The
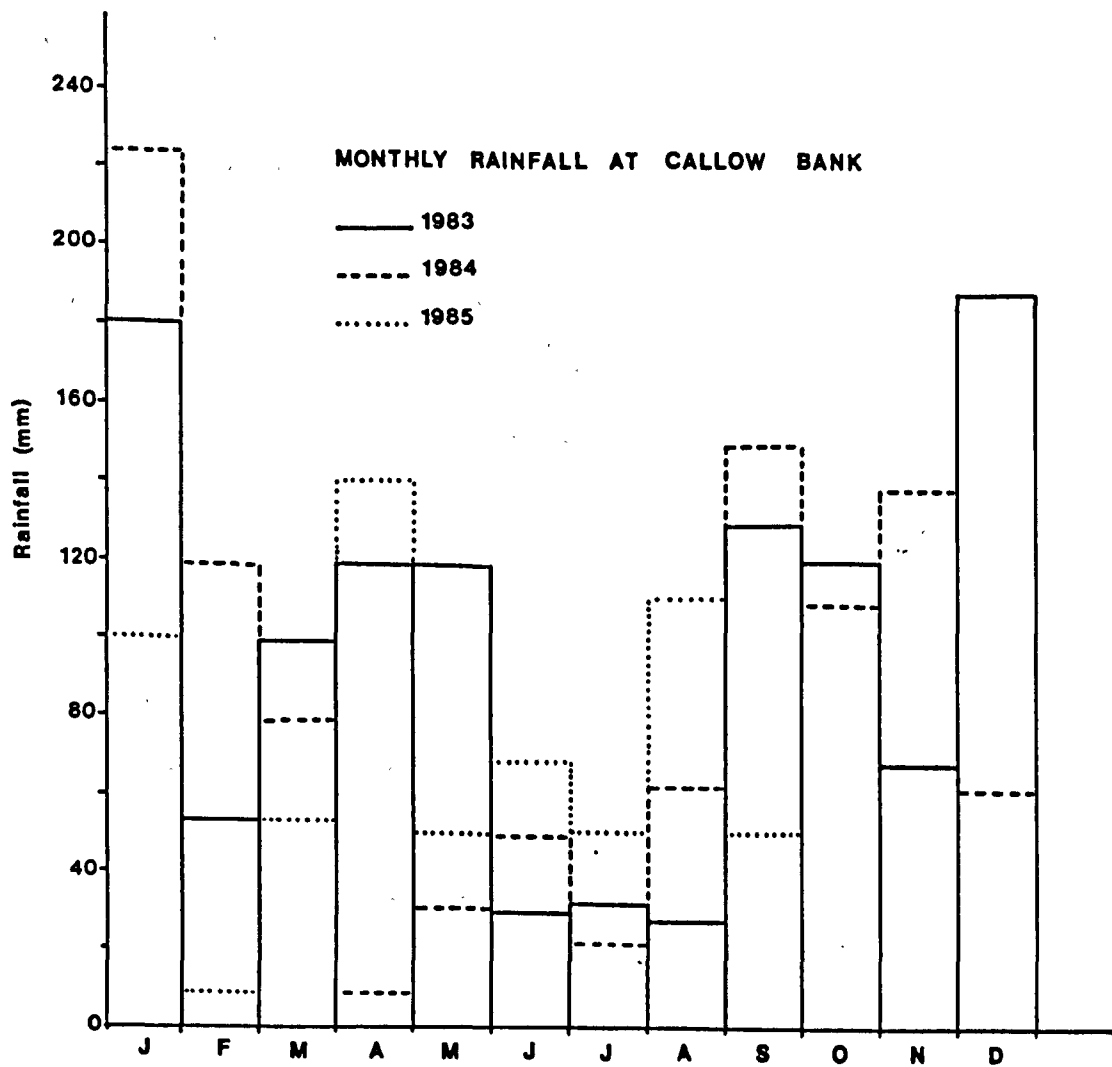
Fig. 3.28 Monthly rainfall (mm) at Callow Bank
from January 1983 to September 1985.

overall pattern of pore water pressure response interval appears to be very short, however, there are slight differences between the selected piezometric profiles. The pore water response interval is dependant upon several factors, such as the depth of the regolith, depth to water table, vegetation type and growth, slope morphology and hydraulic conductivity which is in turn dependant on the nature of the regolith profile and corresponding particle size variations.

The piezometric profile in piezometer 1 (Fig. 3.29) shows that the highest piezometric level (4.11.84) and most prominent fluctuations occurred during the first 6 months, smaller and less fluctuating piezometric levels were recorded for the second 6 months. Maximum piezometric levels in piezometer 1 were attained when winter rainfall was high and evapo-transpiration was low. The response time between the rainfall event and peak piezometric levels varied from 2 to 4 days. Piezometer 1 was located at the head of the Callow basin at the foot of the slip scar of Callow Bank landslide. Seepage springs initiating from beneath the Rivelin Grit maintained relatively high piezometric surface within the regolith throughout the year. The regolith at 1m consisted of clayey gravel derived from shale lower down in the profile. This impermeable shale horizon would have helped to maintain saturated conditions in the regolith.

Piezometer 10 (Fig. 3.30) also showed marked piezometric head fluctuations with rainfall events in the first 6 months, but these fluctuations became less marked in the second 6 months. Dense bracken situated on this slope during summer months increased rainfall interception and soil moisture became rapidly depleted in the sandy silt soil by transpiration and litter evaporation. Studies by Lockwood & Venkatasawmy (1975) estimated a 70% decrease in soil

Fig. 3.29(a)   Correlation between rainfall and piezometric head.

Fig. 3.29(b)   Correlation between rainfall and piezometric head.

Fig. 3.30(a)   Correlation between rainfall and piezometric head.

Fig. 3.30(b)   Correlation between rainfall and piezometric head.

moisture to a depth of 1m during bracken growth in summer. The increase evapotranspiration meant that rainwater was used to recharge the soil moisture; this fact combined with the relatively shallow depth of the regolith minimised the effects of rainfall on the piezometric surface during the summer months.

Piezeometer 14 (Fig. 3.31) was located at a depth of 4.35m in the debris flow material of the Callow Bank slide. The piezometer continued to show marked piezometric fluctuations with rainfall throughout the year. This was probably because of its location near to seepage water issuing from beneath the lowest rotated unit of the Callow Bank slide. The regolith was classified as a well drained sandy silt, this factor coupled with deeper regolith and the presence of short pasture grasses rather than bracken led to a rapid response in piezometric levels with rainfall.

Piezometer 18 (Fig. 3.32) was located in sandy clay at the toe of the Callow Bank slide. The piezometric surface did not fluctuate to the same extent as other piezometric profiles; the peaks were more subdued when compared with the other profiles and the peak of the piezometric level after rainfall took slightly longer in the sandy clay material (approximately 4-5 days). There was a dramatic drop in the piezometric level following the relatively dry February and March and levels did not appear to recover during rainstorm events in the following six months. This may be the result of the cessation of seepage water draining towards the toe area of the landslide after February.

Piezometer 44 (Fig. 3.33) showed a rapid response (48 hours) to rainfall events, however, the maximum piezometric head was still very
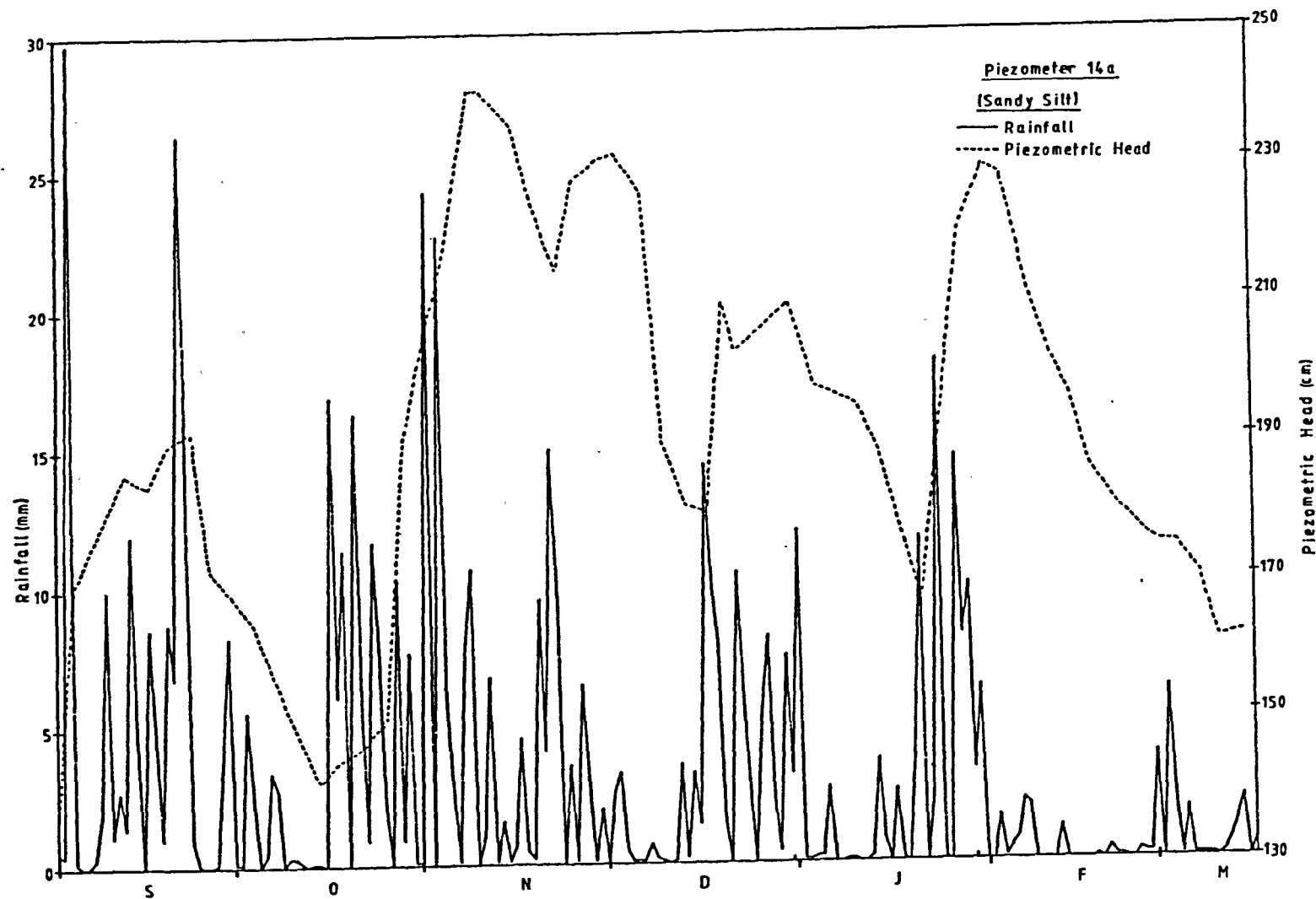
Fig. 3.31(a)   Correlation between rainfall and piezometric head.
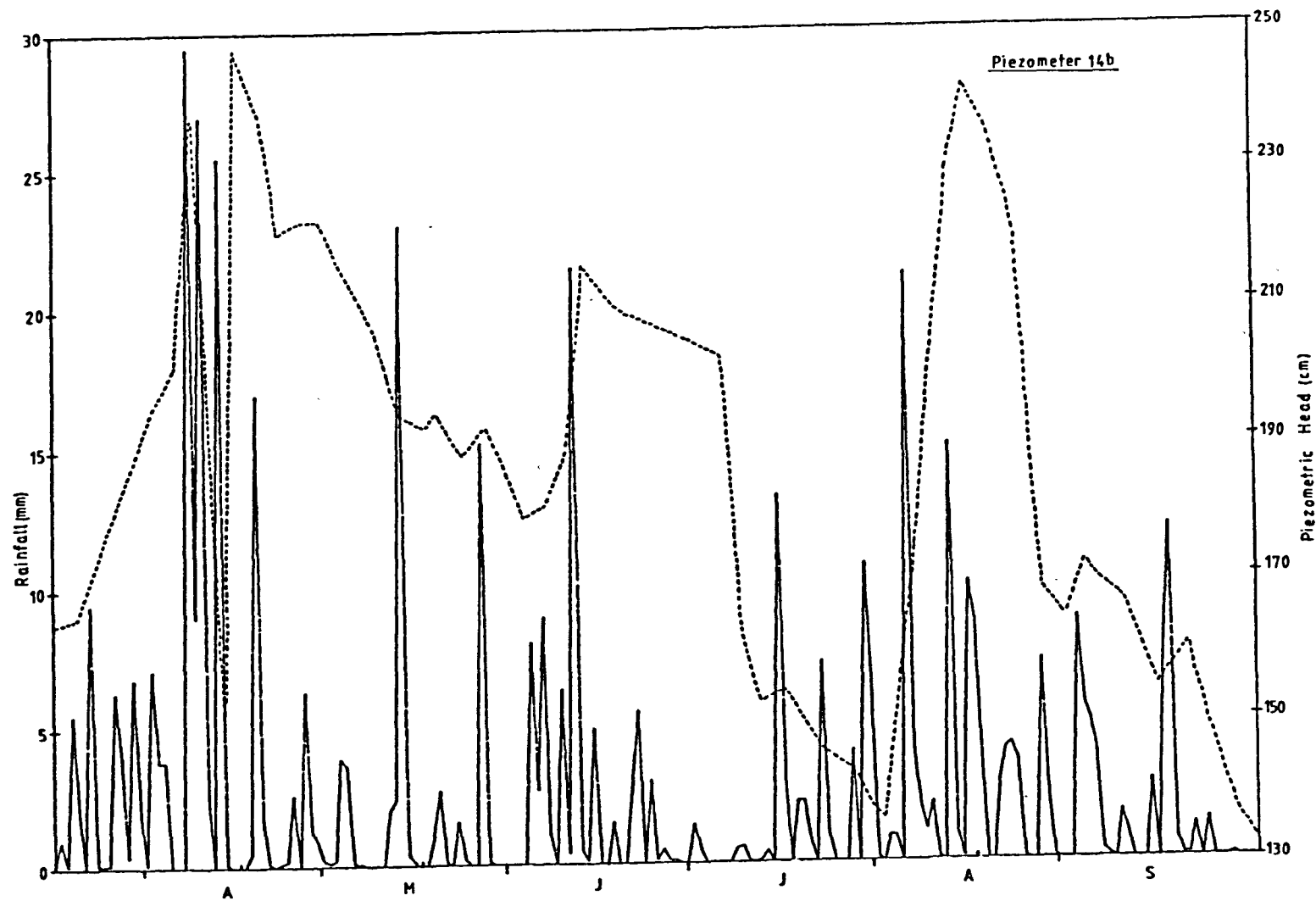
Fig. 3.31(b)   Correlation between rainfall and piezometric head.
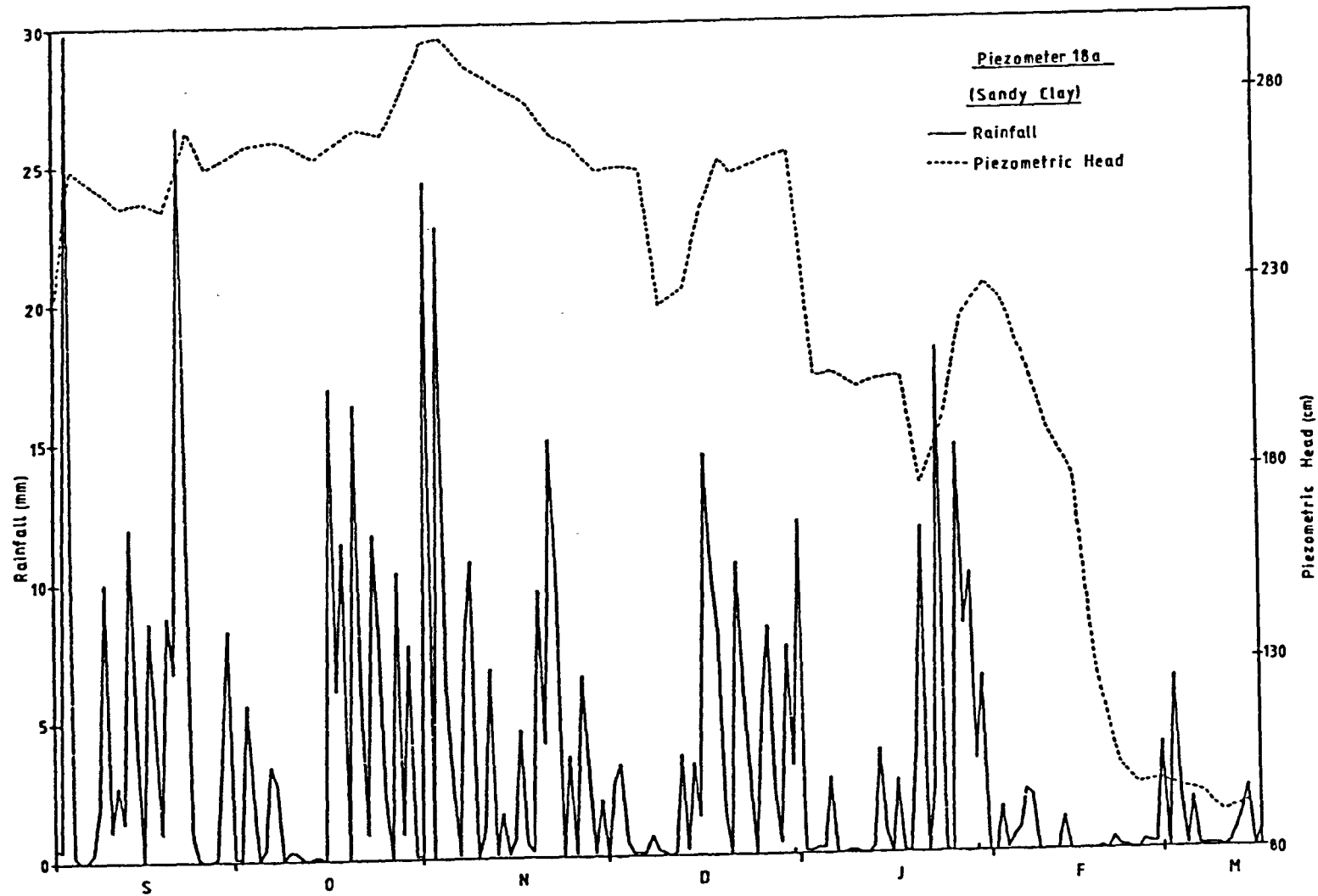
Fig. 3.32(a)   Correlation between rainfall and piezometric head.
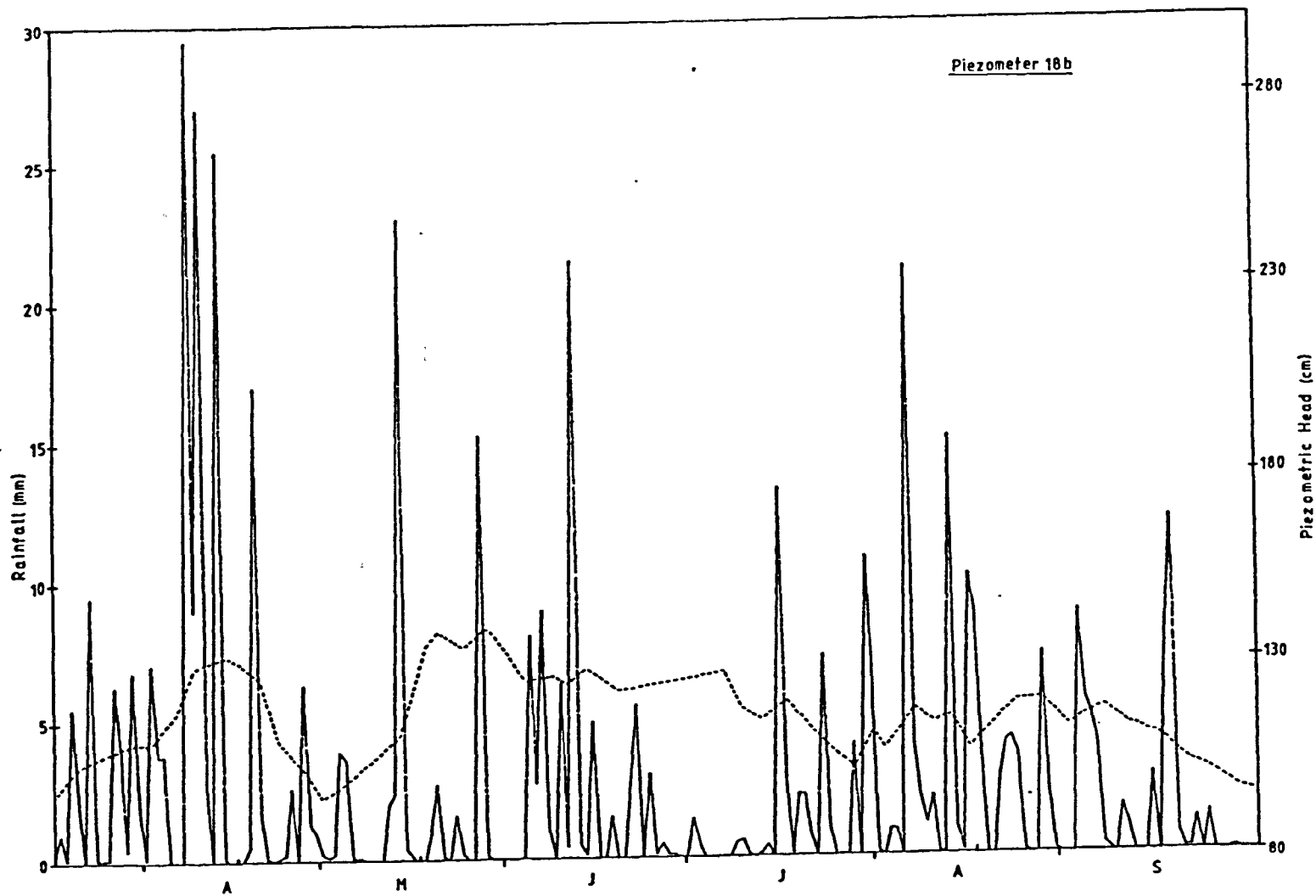
Fig. 3.32(b) Correlation between rainfall and piezometric head.
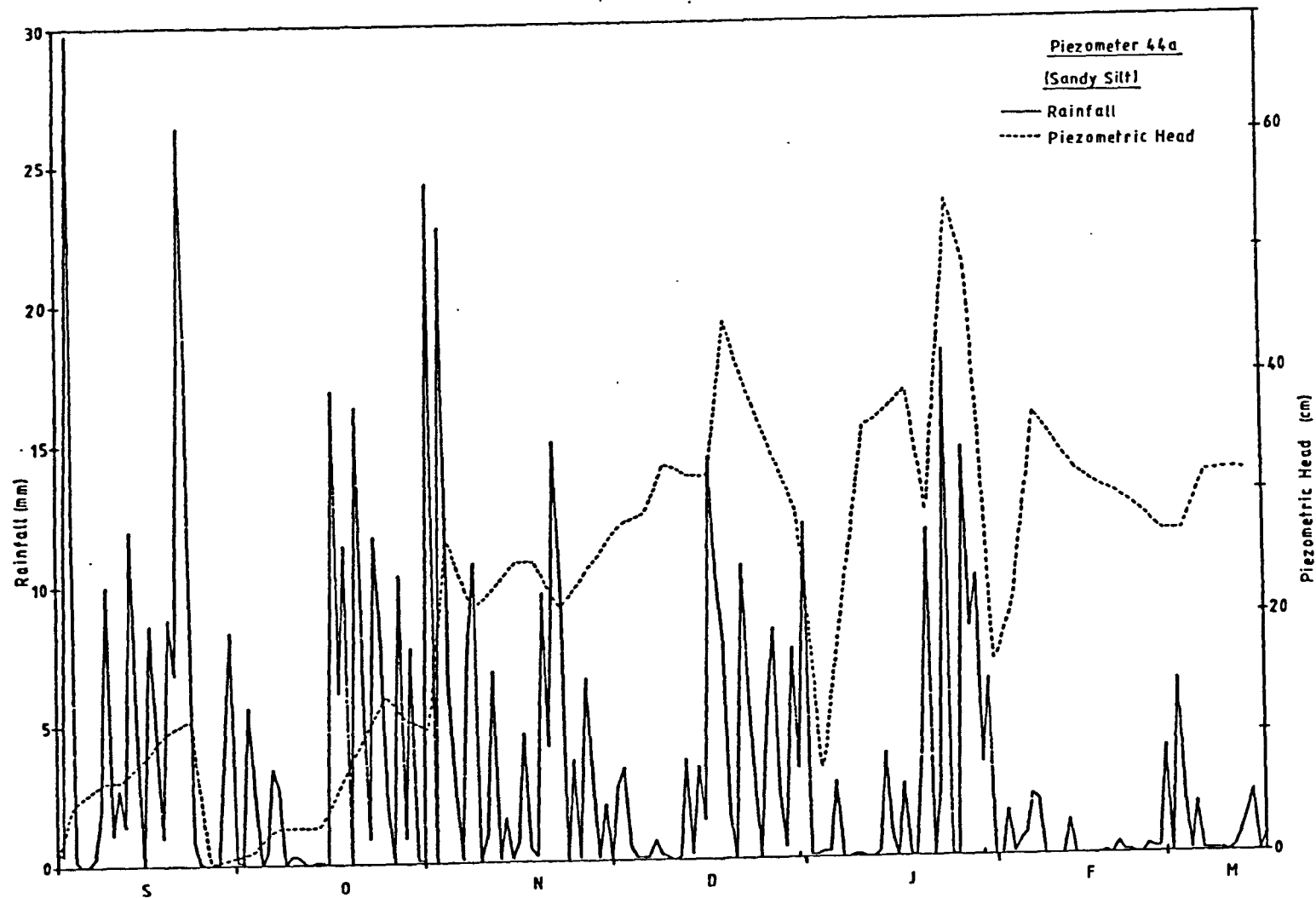
Fig. 3.33(a)   Correlation between rainfall and piezometric head.
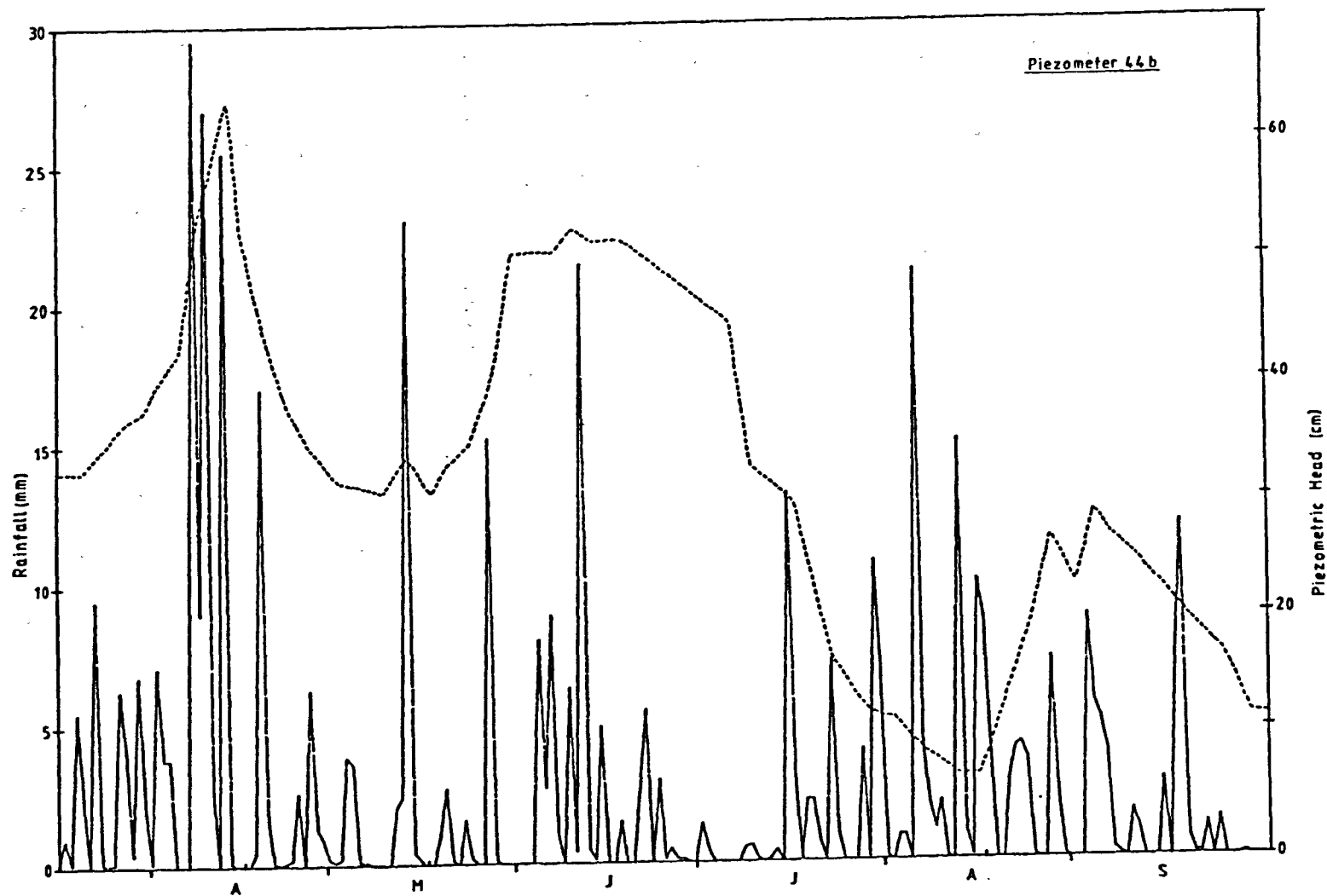
Fig. 3.33(b)   Correlation between rainfall and piezometric head.

small. This piezometer was located just below the backscar of a shallow translational debris slide, the continuous response of the piezometer throughout the second six months was an indication that the bedrock/regolith interface remained reasonably saturated throughout the year.

Piezometer 76 (Fig. 3.34) was located in a basal slope depression in clay regolith. The piezometer continues to respond to rainfall throughout the year indicating that the lower sediments in the hollow remained saturated throughout the year. The piezometric levels increased fairly rapidly with each rainfall event but dropped more gradually than piezometric levels in clayey sands and sandy silt regoliths.

Piezometric levels in piezometer 79 (Fig. 3.35) remained low throughout the year, one might have expected a more marked response to rainfall events in the silty sand regolith, but perhaps the steepness of the slope meant that rapid throughflow prevented the attainment of high piezometric levels.

Piezometer 81 (Fig. 3.36) was located below the shale backscar of a small rotational slide and above a minor road. Springs emerging from the back scar despite attempts to drain them beneath the minor road have maintained piezometric levels throughout the year (mean P.L. 61cm). The piezometric levels increased rapidly with rainfall then tapered-off more gently, this indicated that the drainage in the slip area continued to be a problem despite attempts to drain away seepage water. Slippage continues to occur on the downslope side of the road and it has become necessary to patch up the road each year at this site.
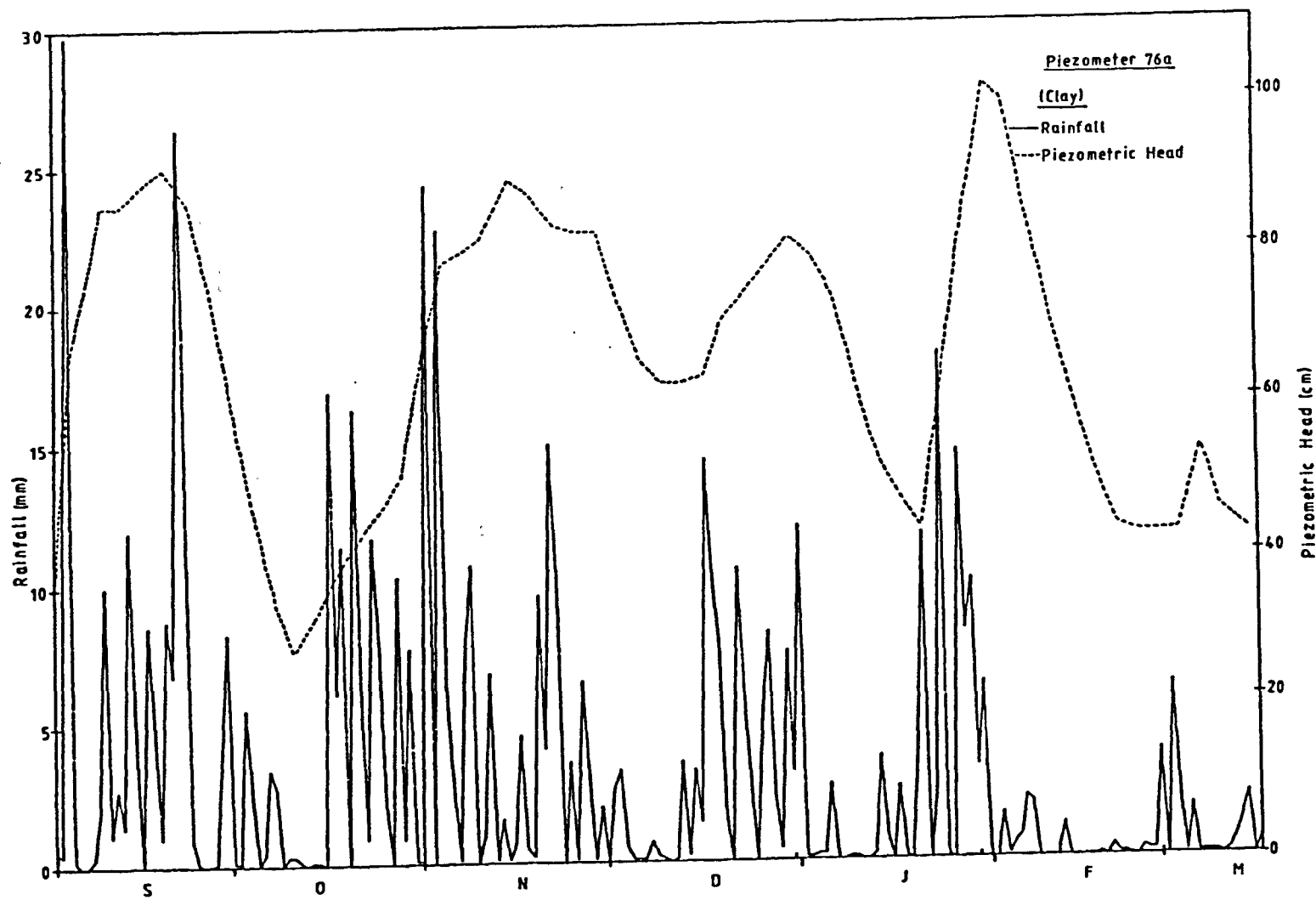
Fig. 3.34 (a)   Correlation between rainfall and piezometric head.
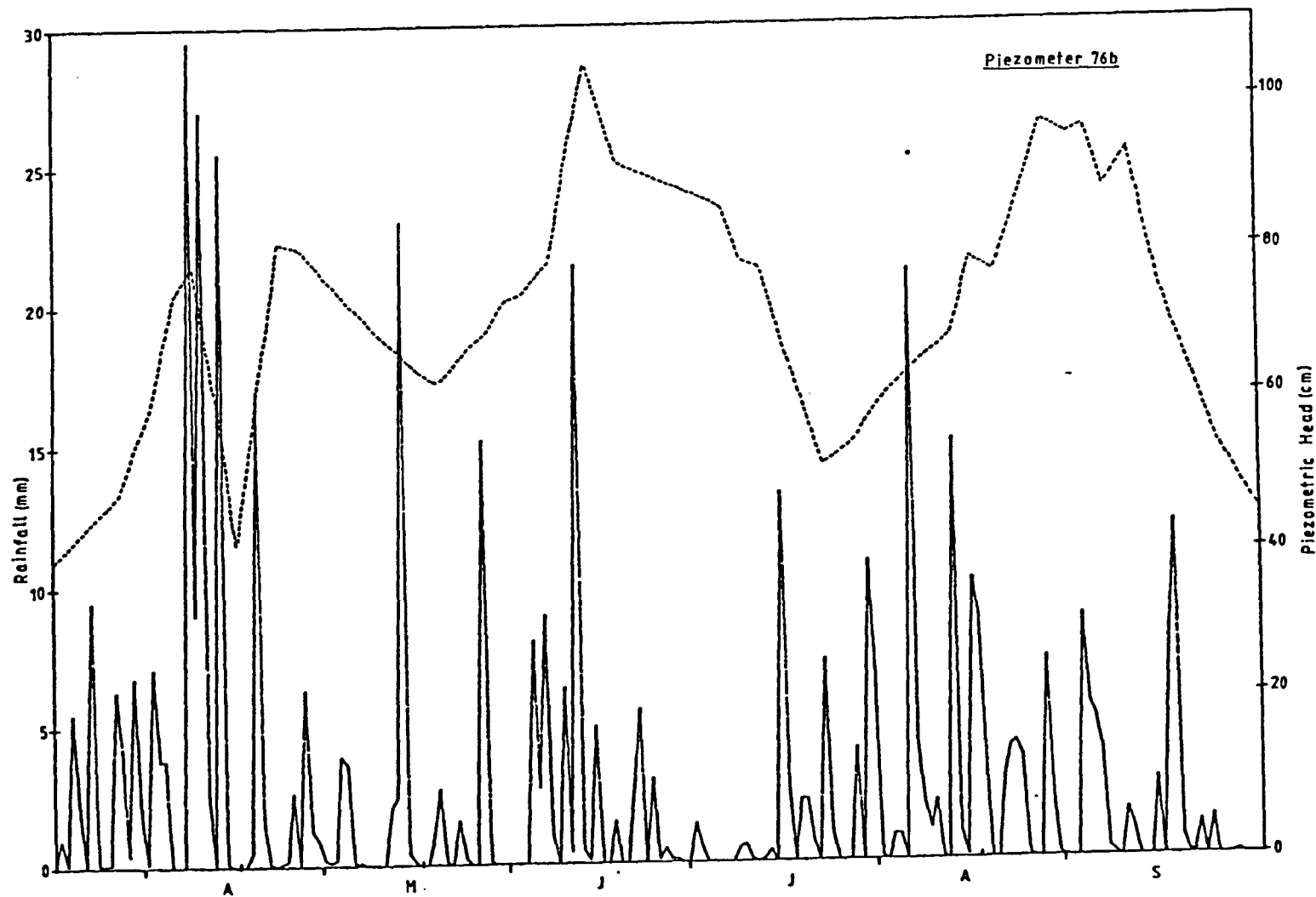
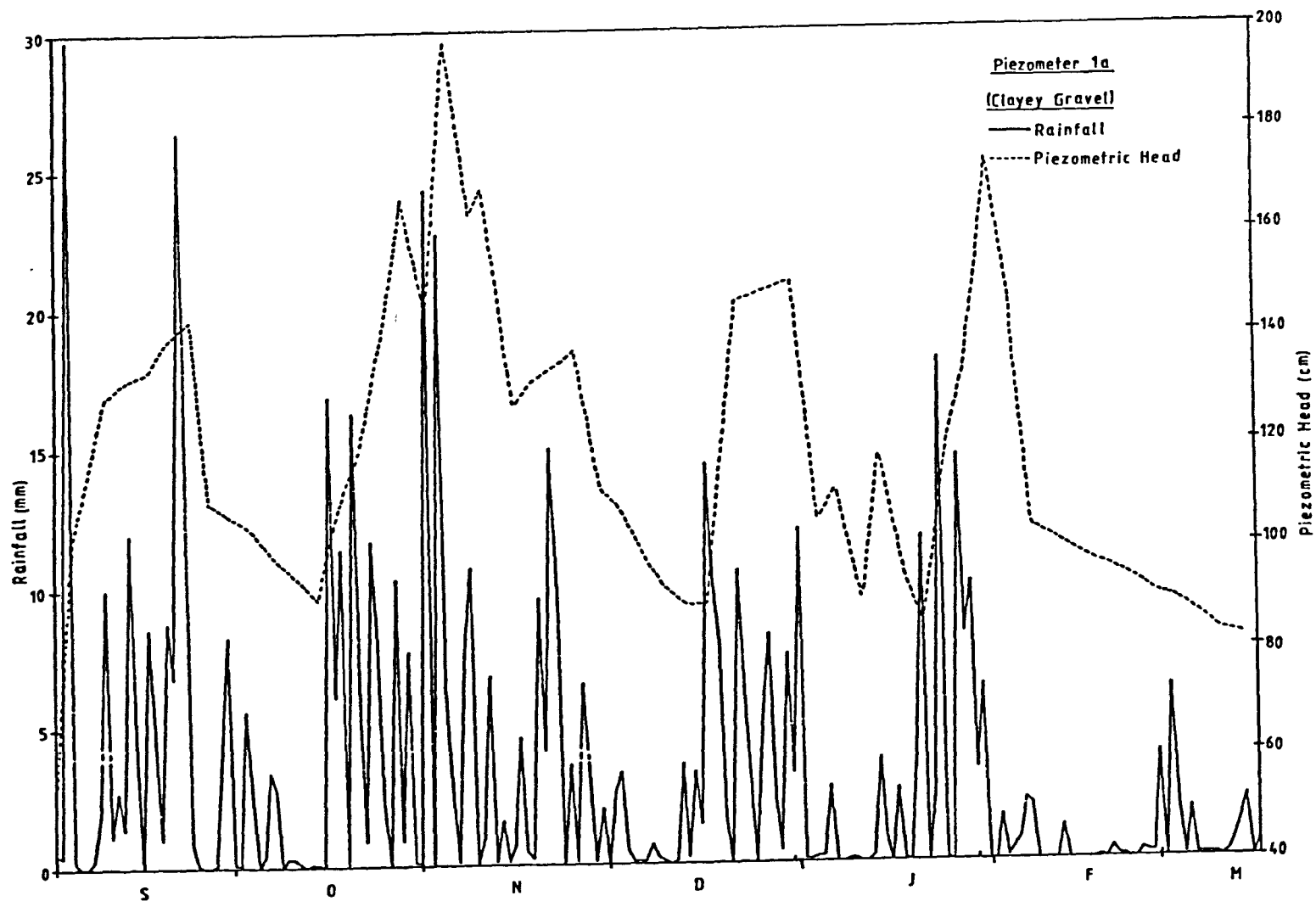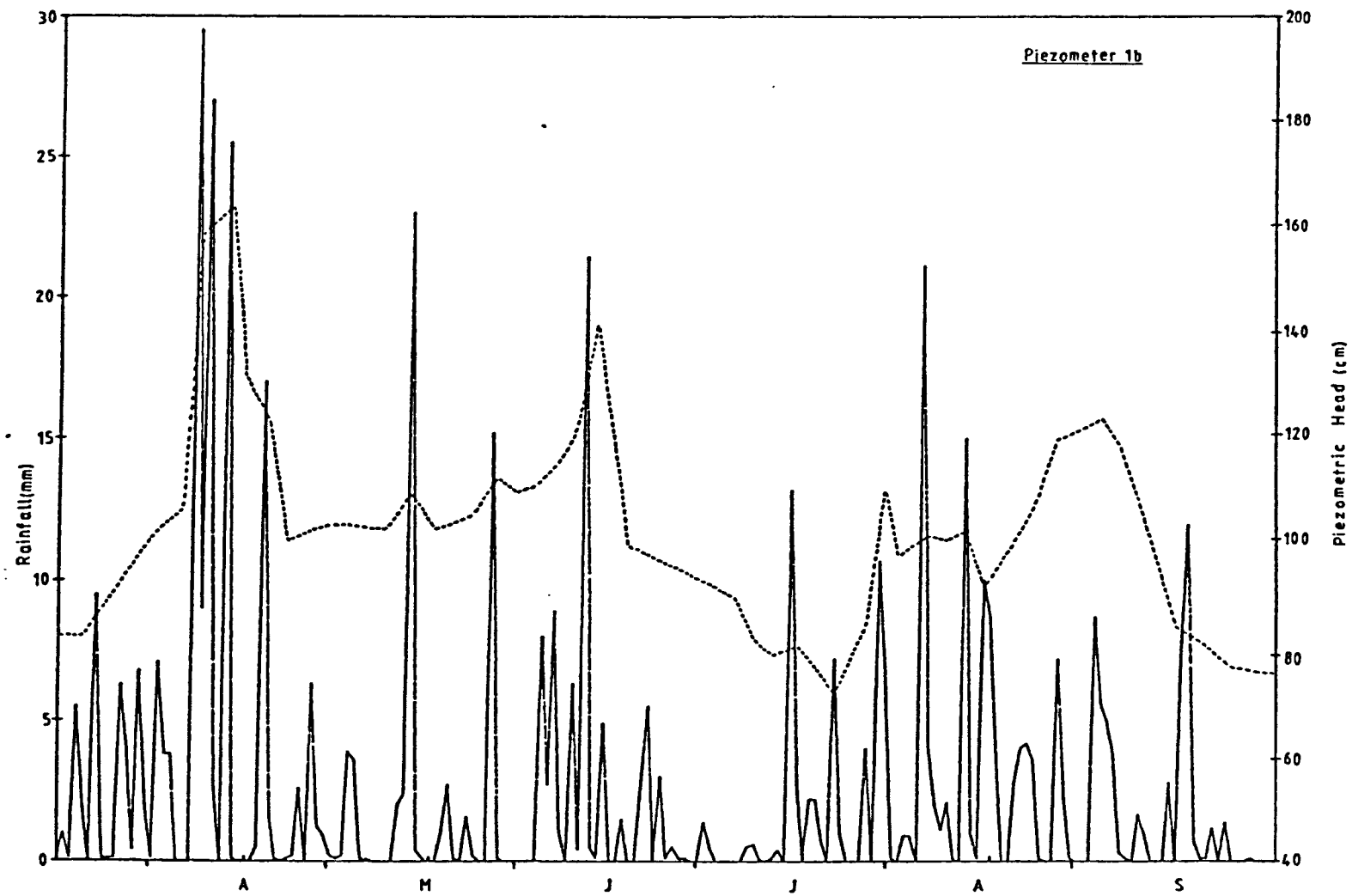Fig. 3.34(b)   Correlation between rainfall and piezometric head.
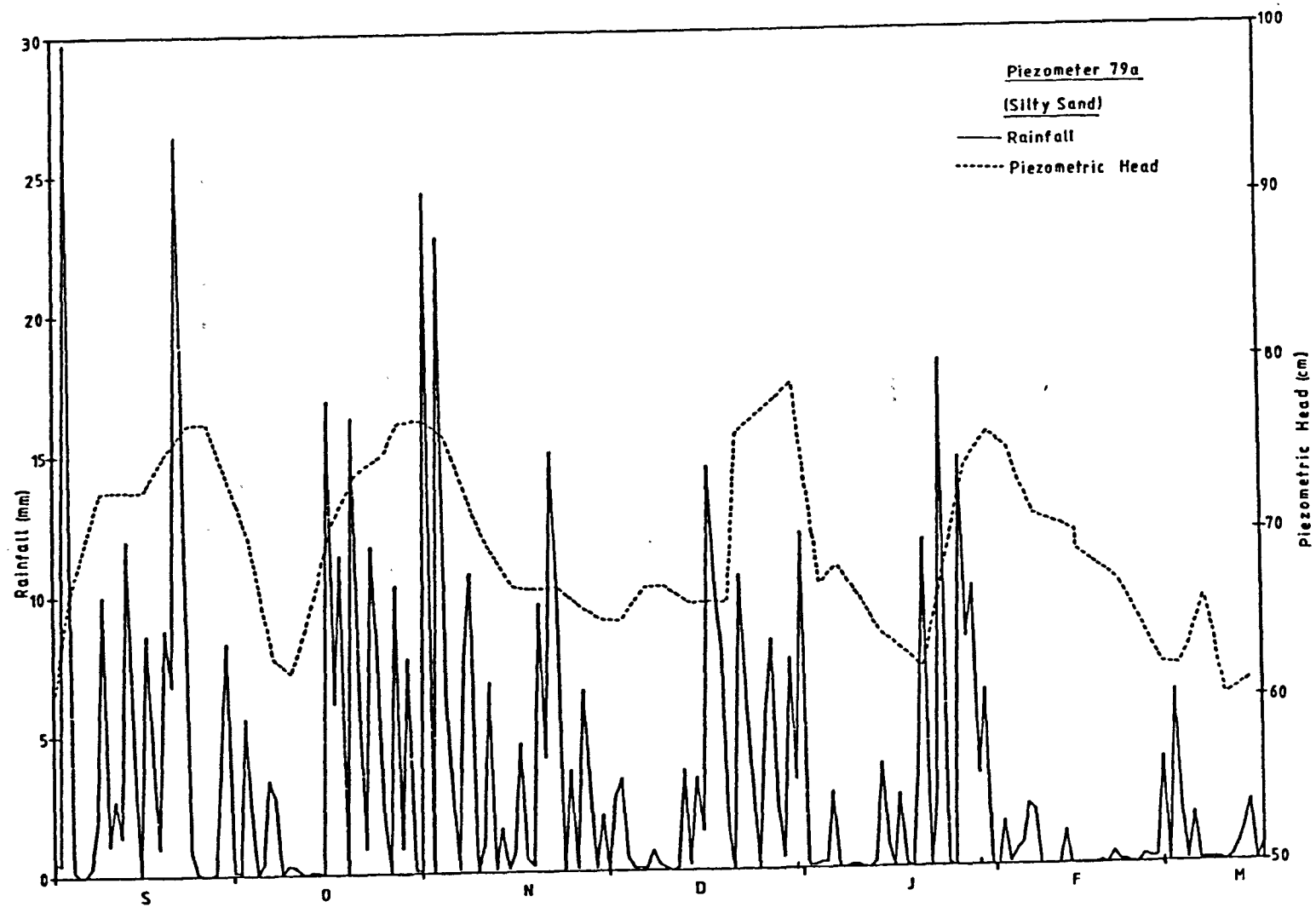
Fig. 3.35(a) Correlation between rainfall and piezometric head.
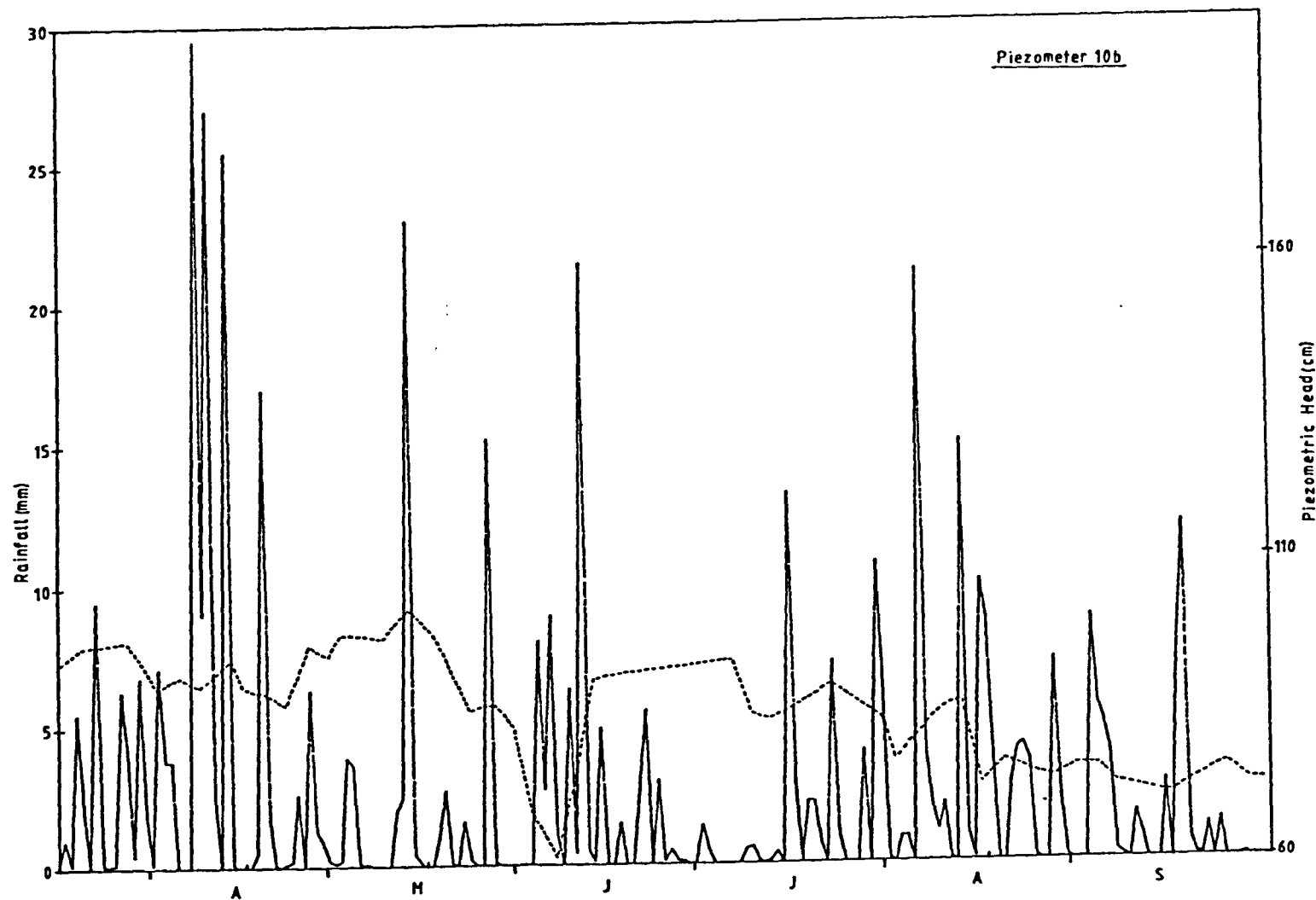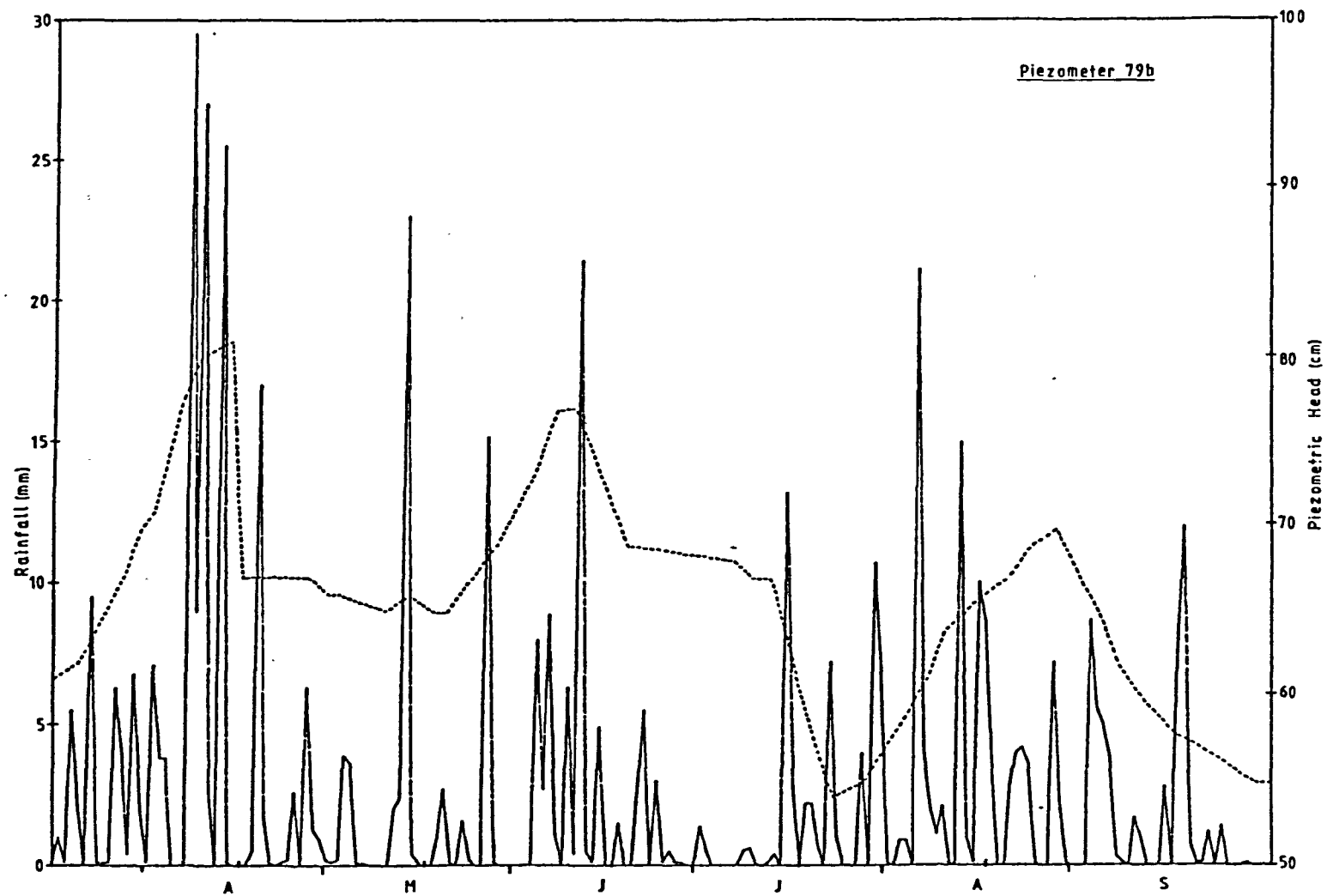
Fig. 3.35(b)   Correlation between rainfall and piezometric head.
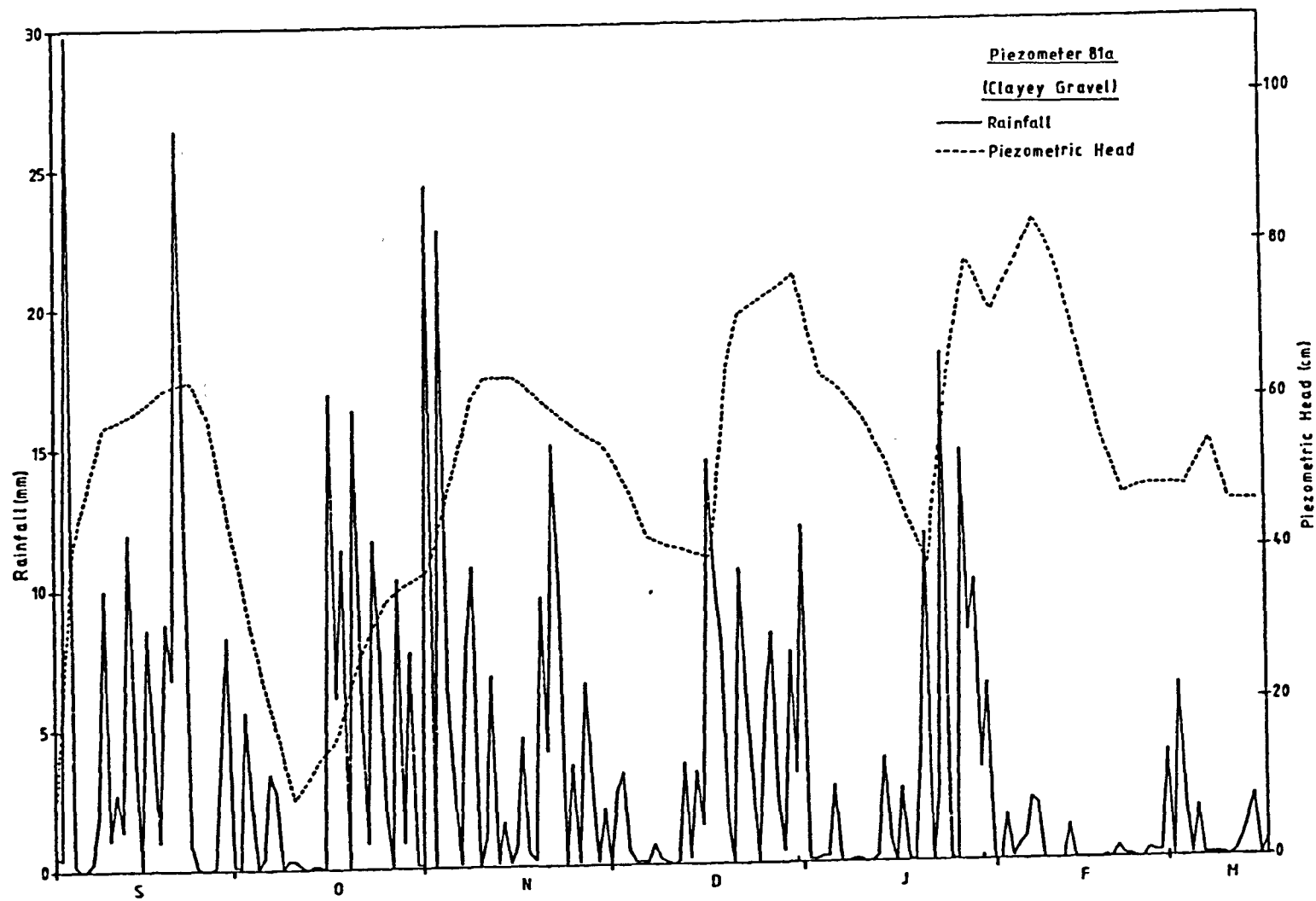
Fig. 3.36(a)   Correlation between rainfall and piezometric head.

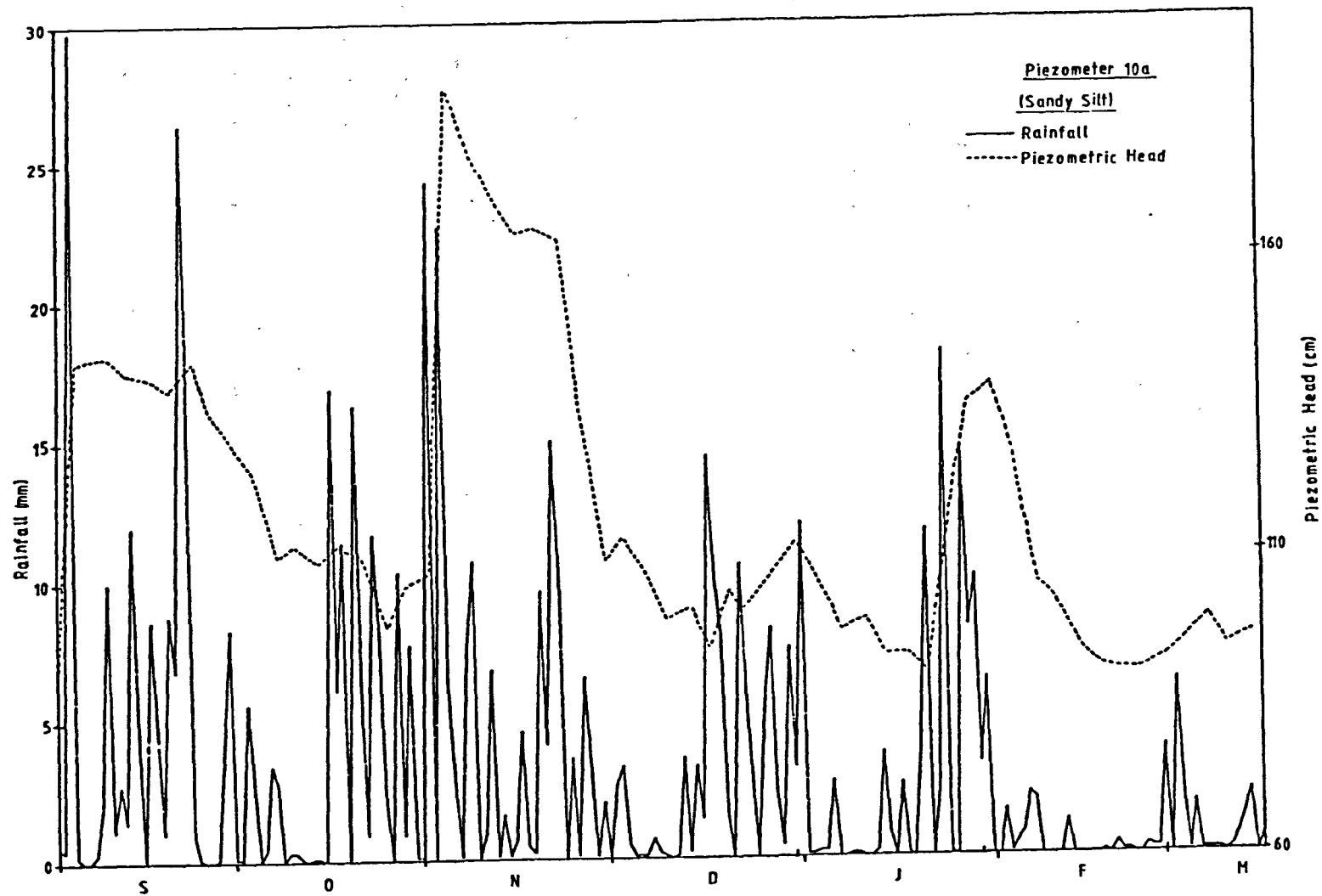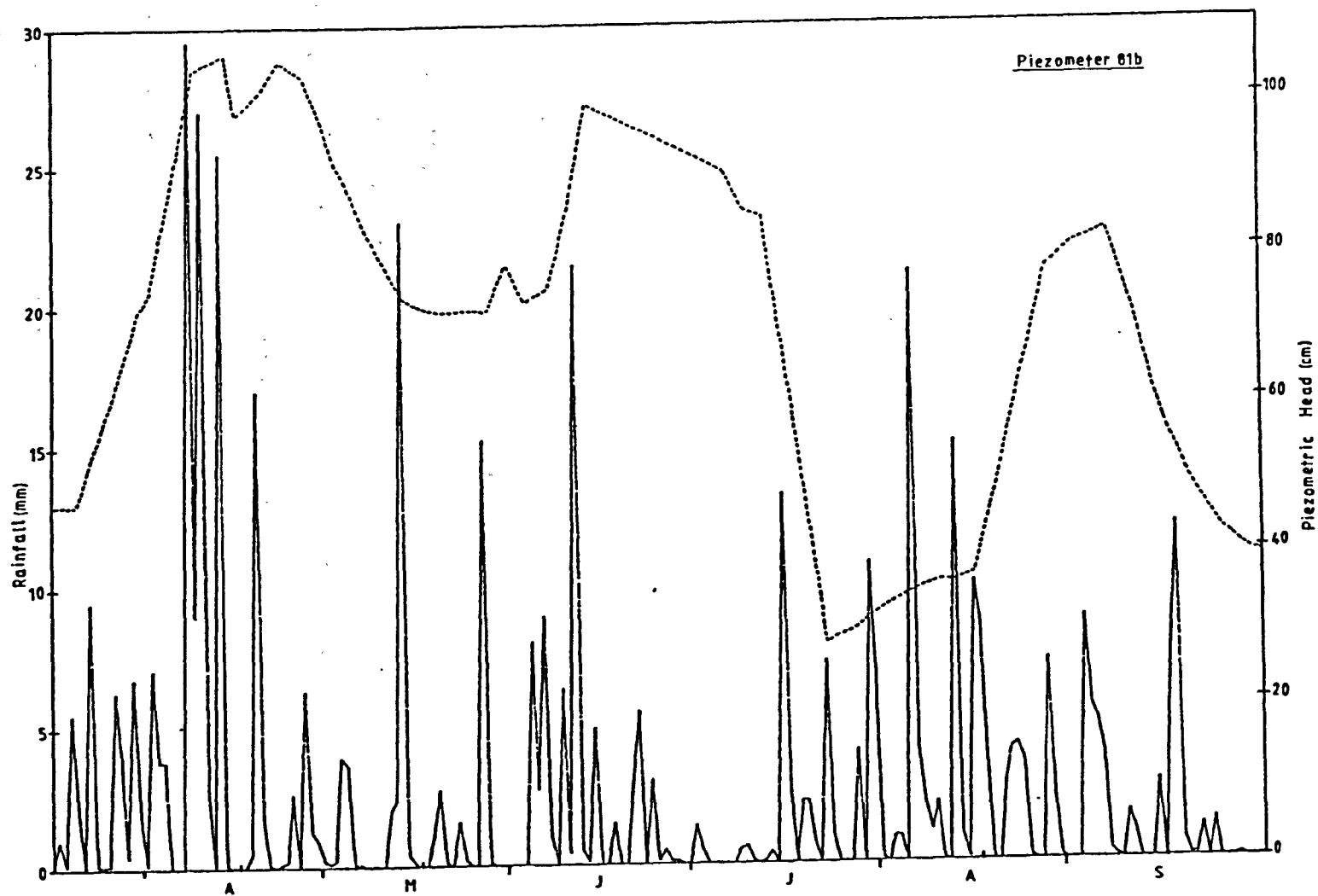Fig. 3.36(b)   Correlation between rainfall and piezometric head.

Table 3.7   The mean pore water pressure represented by (ru) for different

soil groups

Soil Name	Group	Symbol	Mean ru	Soil Groups	Mean ru for Soil Group
Silty gravel	G-F	GM	0.54	Clayey Gravels:	
Clayey gravel	G-F	GC	0.36	More than 50% of the	0.37
Very silty gravel	GF	GM	0.41	coarse material is of	
Very clayey gravel	GF	GC	0.34	gravel size (coarser than 2mm)	
Very silty sand	SF	SM	0.16	Sands: more than 50% of the coarse material is	
Very clayey sand	SF	SC	0.06	of sand size (finer than 2mm)	0.13
Sandy silt	FG	MG	0.20	Sandy silts and clays:	
Sandy clay	FG	CG	0.19	(35% to 65% fines)	0.19
Very sandy silt	FS	MS	0.40		
Very sandy clay	FS	CS	0.30	Silt and clays	
Silt	F	M	0.23	65% to 100% fines	0.32
Clay	F	C	0.29		

Table 3.7 shows the mean pore water pressure represented by (ru) for different soil groups. The highest mean pore water pressures (0.37) was attained in regolith consisting predominantly of clayey gravels. These gravels tended to be associated with shale strata at a shallow depth, thereby creating impermeable conditions and the development of perched water tables. Clay regoliths derived from the in situ weathering and breakdown of shales and mudstone gave the second highest mean pore water pressure (0.32). The clay regolith profiles conformed to that of a stagnogley soil indicating seasonal waterlogging. Free draining sandy regoliths usually associated with the Rivelin Grit on steeper upper slope sections gave the lowest mean pore water pressure (0.13) as might be expected.

3.5.5 Results of the shear strength Tests

The maximum shear stress at incipient failure and the confining stress created by the weight of the applied load, the shear box and the soil block on the failure plane, were obtained from each test and were plotted in order to obtain a Mohr failure envelope. The considerable variability of data points as measured in field tests reflect the expected non-homogeneous pedological and biological conditions prevailing in the regolith soils. Because of the ability of the Open-Sided Shear Box to incorporate those components of the soil which contribute most substantially to variations in the shear strength of shallow soils (i.e. roots, fissures, spatial variations of particle size) a wider more representative range of results may be obtained. Forty five successful tests were completed, fifteen for each slope section. The results of the fifteen successful field shear box tests conduction for each slope section are shown in Table 3.8. The Coulomb failure envelopes were estimated by fitting the least squares regression line to the plots of maximum shear stress (sf) against effective normal stress ($\sigma'n$) (see Fig. 3.37). Peak shear strengths, not residuals, were plotted because they more closely match 'first-time' failure strength of landslides (Skempton, 1970). The soil strength parameters, cohesion (c') and the internal friction angle ($\emptyset'$) were estimated from the envelope-ordinate intercept and the envelope slope respectively (Lambe & Whitman, 1969). Estimates of the angle of internal friction $\emptyset'$ and c' are shown at the foot of Table 3.8. Details of the testing and analysis techniques are presented in O'Loughlin, 1974, and Chandler et al., 1981. In order to use the data analytically, however, comparison should be made with laboratory and other results to confirm acceptable absolute values of the field strength parameters. Direct comparison of laboratory and
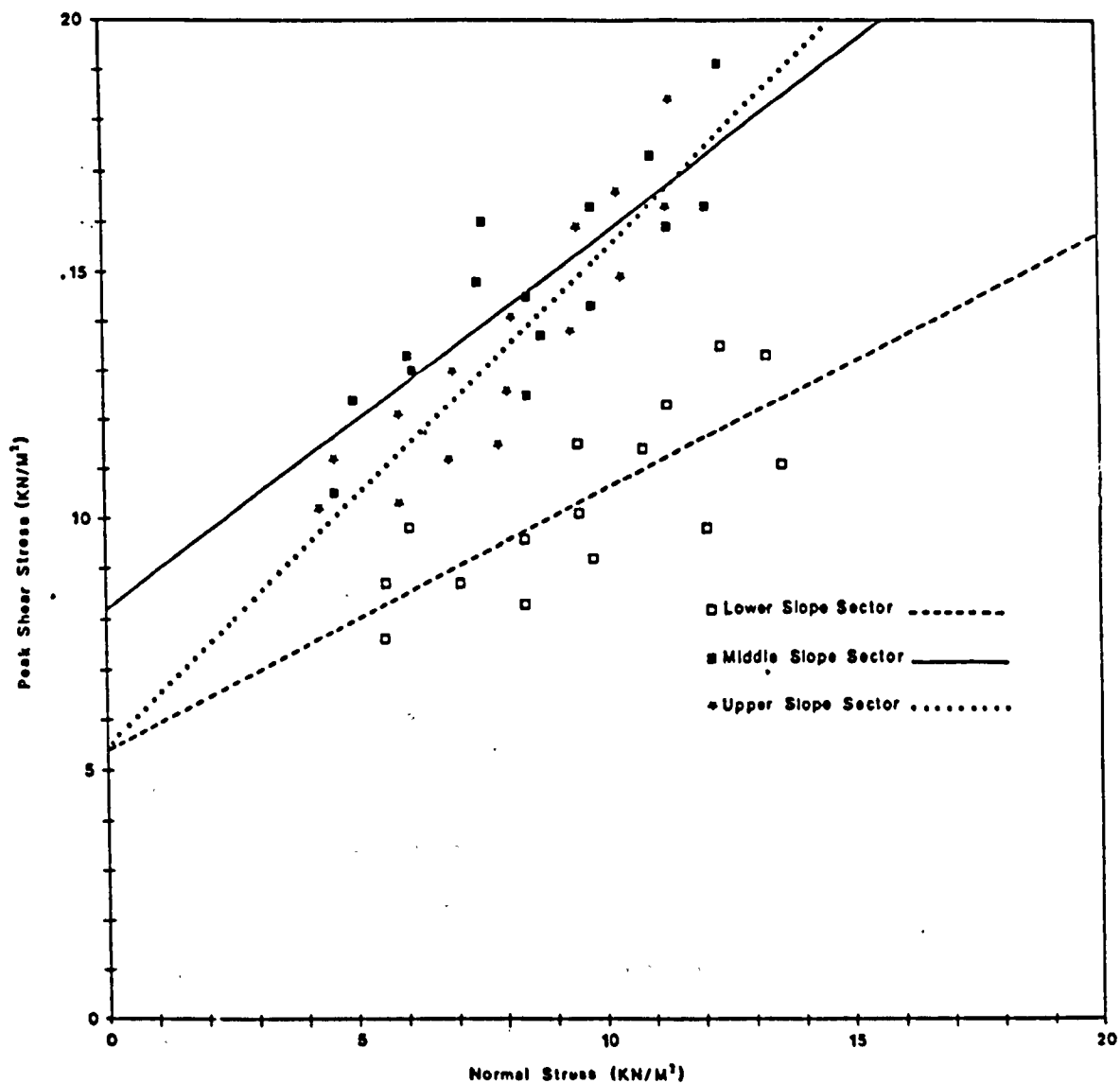
Fig. 3.37 Distribution of 45 successful shear box tests obtained by plotting peak shear stress (sf) against normal stress ($\sigma'n$). The Coulomb failure envelopes shown were estimated by fitting the least squares regression line to the plots for the shear test results of each slope section. The soil strength parameters, effective cohesion (c') and the internal friction angle ($\emptyset'$) were estimated from the envelope-ordinate intercept and the envelope gradient respectively.

field results should be made with reservation due to the influence of measured strength, of differences in drainage conditions, sample size and testing rate, and the degree of sample disturbance (Skempton & Hutchinson, 1969). As a generalisation it is to be expected that tests over a large range of σ'n would give a curved empirical failure envelope. By simplifying the curve into a sequence of straight line segments, each conforming to a Coulomb-failure criterion for limited specified ranges of σ'n it can be envisaged that tests under lower stresses could exhibit lower c' and higher $\emptyset$' than those at higher stresses.

The values of $\emptyset$' are obviously related to the particle sorting; regolith samples consisting of high proportions of gravel and sand gave higher values of $\emptyset$' (see Table 3.8). Regolith samples collected from the upper and middle sections of the slope contained significant proportions of gravel and sand whereas the regolith samples collected from the lower slope contained significant proportions of clay and silt (see Table 3.9). The results of ($\emptyset$') obtained appear to correspond reasonably well with those for similar regolith materials sampled from Derbyshire hillslopes by Carson & Kirkby, 1972; Carson, 1975, and Carson & Petley, 1970.

Table 3.9 The particle size composition for regolith samples taken at a depth of 0.75m from the three slope sections.

Slope Profile Section	Gravel >2.00mm	Sand 2.00-0.06mm	Silt 0.06-0.002mm	Clay <0.002mm	Liquid Limit	Plastic Limit	Plasticity Index	BSCS
Lower slope section		24	23	53	30	21	9	FS-CLS
Middle slope section	30	28	24	18	23	17	6	GF-GML
Upper slope section	50	35	6	9	33	24	9	G-F GPC

Table 3.8   Normal and Peak Shear Stresses at failure for Field
Direct Shear tests for the three slope sections, Callow Bank.

Test Number	Lower Slope Section		Middle Slope Section		Upper Slope Section	
	Peak Shear stress at failure (kN/m²)	Normal stress at failure (kN/m²)	Peak Shear stress at failure (kN/m²)	Normal stress at failure (kN/m²)	Peak Shear stress at failure (kN/m²)	Normal stress at failure (kN/m²)
1	5.6	7.6	4.6	10.5	4.3	10.2
2	5.6	8.7	5.0	12.4	4.6	11.2
3	6.1	9.8	6.1	13.3	5.9	10.3
4	7.1	8.7	6.2	13.0	5.9	12.1
5	8.4	8.3	7.5	14.0	6.9	11.2
6	8.4	9.6	7.6	16.0	7.0	13.0
7	9.5	10.1	8.5	12.5	7.9	11.5
8	9.5	11.5	8.5	14.5	8.1	12.6
9	9.8	9.2	8.8	13.7	8.2	14.1
10	10.8	11.4	9.8	14.3	9.4	13.8
11	11.3	12.3	9.8	16.3	9.5	15.9
12	12.1	9.8	11.0	17.3	10.3	16.6
13	12.4	13.5	11.3	15.9	10.4	14.9
14	13.3	13.3	12.1	16.3	11.3	16.3
15	13.6	11.1	12.4	19.1	11.4	18.4

$\beta = 16°$ $\beta = 24°$ $\beta = 33°$

$C' = 5.4$ kN/m² $C' = 7.8$ kN/m² $C' = 5.5$ kN/m²

$\phi' = 27.3°$ $\phi' = 38.4°$ $\phi' = 45°$

The variation in the effective cohesion (c') appears to be associated with vegetation changes causing corresponding changes in the mechanical reinforcement of soil by roots. The effective cohesion (c') was higher for the middle slope section where bracken (Pteridiun aquilinum) was dominant. The bracken roots extended to depths within the regolith mantle over 1m. Bracken was absent on the lower and upper slope profile sections, grasses (Nardus stricta, Agrostis spp, Festuca spp) were the dominant plant species of these sections. A model of the cohesive strength imparted by roots to soil, based on the engineering theory of reinforced earth, has been presented by Waldron (1977). It appears that the shear strength tests provided a practical way of measuring the contribution of root systems of different vegetation cover to soil cohesive strength.

3.6 STABILITY ANALYSIS

3.6.1 Calculation of the threshold slope angle:

The threshold slope angles were determined for each of the three slope sections using the stability model expressed by:

$$\beta_l = \text{arc tan} \left[\left(1 - \frac{\gamma_s - m.\gamma_w}{\gamma_s} \right) \tan \phi' \right] \qquad (1)$$

where: β_l = Limiting angle of valley side slope i.e. minimum slope on which movement can occur (degrees):

γw = unit weight of water (kN/m3)

γs = saturated unit weight of soil (kN/m^3)

$\emptyset'$ = angle of shearing resistance

m = position of the phreatic surface with respect to ground level

(i.e. m = 1 when the phreatic surface and ground level coincide)

Assuming regolith saturation (m = 1) and drainage along flow lines parallel to the ground surface, the stability model predicted threshold slope angles of 13.4°, 19.2° and 24.1° for the lower, middle and upper slope sections respectively (see Table 3.10).

Table 3.10   Parameters used to calculate the predicted threshold slope angle (β_l) for each slope section

Slope Section	Slope inclination β	Unit weight of water γw kN/m2	Saturated unit weight of soil γs kN/m2	Angle of shearing Resistance $\emptyset'$°	Limiting angle β_l°
Lower slope	16	9.81	18.2	27.3	13.4
Middle slope	24	9.81	17.5	38.4	19.2
Upper slope	33	9.81	17.7	45	24.1

The landslides affecting the regolith mantle tend to be long in relation to their width and are uniformly shallow with planar surfaces of failure.   A conventional 'Infinite Slope' method of stability analysis therefore seemed an appropriate model to use (e.g. Skempton & Weeks, 1976).

For limiting equilibrium of a soil sheet lying on an inclined surface the shear stress (τ) on the plane is given by:

$$\tau = \gamma z \sin \beta \cos \beta$$

and it should become equal to the shear strength:

$$s = c' + (\gamma z \cos^2 \beta - u) \tan \phi' \qquad (2)$$

If the piezometric height is h then:

$$u = \gamma w h \qquad (3)$$

In general the available shear resistance may be equal to or exceed the shear stress. In the latter case the slope can be said to have a factor of safety (F), defined by the ratio $F = s/\tau$. Thus:

$$F = \frac{\dfrac{c'}{\gamma z} \left(\cos^2 \beta - \dfrac{\gamma_w h}{\gamma z} \right) \tan \phi'}{\sin \beta \; \cos \beta} \qquad (4)$$

where the forces promoting stability are exactly equal to the forces promoting instability $F = 1$; where $F < 1$ is in a condition for failure; where $F > 1$ the slope is likely to be stable. Solutions of equation 4 for each slope section are given in Table 3.11.

Table 3.11   Slope stability analysis: parameters determined shown in column 1, include the factor of safety (F) for each slope section

Parameter	Lower slope section	Middle slope section	Upper slope section
c'	5.4 kN/m^2	7.8 kN/m^2	5.5 kN/m^2
γ	17.97 kN/m^2	15.88 kN/m^2	16.36 kN/m^2
z	1.51m	1.75m	1.58m
β	16°	24°	33°
γw	9.81 kN/m^2	9.81 kN/m^2	9.81 kN/m^2
h	0.91m	0.41m	0.13m
ϕ'	27.3°	38.4°	45°
u	8.93 kPa	4.02 kPa	1.28 kPa
(F=1) h	2.20m	2.04m	1.21m
ru	0.33	0.14	0.05
(F=1) ru	0.80	0.72	0.46
(h=z) ru	0.54	0.62	0.60
F	1.91	2.23	1.89

The angle of friction with respect to effective stresses (∅') and effective cohesion (c') were obtained from the failure envelope fitted by linear regression (see Fig. 3.37). The unit weight of soil (γ) was calculated from the mean unit weight of 15 soil samples taken for each shear box test on each slope section (see Table 3.11). The unit weight of water (γw) was taken as 9.81 kN/m^2. The depth of the regolith mantle (z) was measured in the field, details of the soil profiles are given in Figs. A4, A5 & A6. The angle of slope inclination (β) for each slope section was measured using a pantometer. The piezometric height (h) in metres, was calculated from the mean ratio of the mean maximum piezometric height/mean regolith depth recorded over the field study period (September 1984 to September 1985) for sequences of piezometers situated in each slope section adjacent to the shear box testing sites.

All three slope sections are remarkably stable using the stability model expressed by equation (4) above, under the present maximum pore water pressures recorded during field investigations. Using equation (4) above it is possible to calculate the critical piezometric height for instability to occur i.e. when F = 1:

$$F = \frac{\dfrac{c'}{\gamma z} + \left(\cos^2 \beta - \dfrac{\gamma w h}{\gamma z}\right) \tan \phi'}{\sin \beta \cos \beta}$$

$$F \sin \beta \cos \beta = \frac{c}{\gamma z} + \left(\cos^2 \beta - \frac{\gamma w h}{\gamma z}\right) \tan \phi'$$

$$\frac{F \sin \beta \cos \beta - \dfrac{c'}{\gamma z}}{\tan \phi'} = \cos^2 \beta - \frac{\gamma wh}{\gamma z}$$

$$\frac{\gamma wh}{\gamma z} = \cos^2 \beta - \frac{F \sin \beta \cos \beta - \dfrac{c'}{\gamma z}}{\tan \phi'}$$

$$h = \frac{\gamma z}{\gamma w} \left(\cos^2 \beta - \frac{F \sin \beta \cos \beta - \dfrac{c'}{\gamma z}}{\tan \phi'} \right) \qquad (5)$$

The piezometric height necessary for failure (i.e. when F = 1) to occur is shown in Table 3.11, this equates to piezometric surfaces of 0.69cm and 0.29cm above the ground surface for the lower and middle slope sections respectively and a piezometric level of 0.37cm below the ground surface in the upper slope section.

Under most conditions the free soil water level cannot rise above the soil surface and the pore water pressure (u) is given by:

$$u = \gamma wh \qquad (6)$$

where h is the piezometric head measured from a piezometer and γw is the unit weight of water. Where seepage is not uniform, and directed out of the slope, it is convenient to use the ratio ru between pore water pressure and the weight of a vertical column of soil to express pore pressure:

$$ru = u/\gamma z = wh/\gamma z \qquad (7)$$

For failure to occur (i.e. when F = 1) the pore pressure ratio (ru) would need to be 0.80, 0.72 and 0.46 for the lower, middle and upper slope sections analysed. This requires that for the slices analysed the mean maximum piezometric height recorded during the field investigation would have to rise by 1.29m, 1.90m and 1.08m for the lower, middle and upper slope sections to fail respectively.

The values of ru when F = 1 are unusually high for the lower and middle slope sections. For the case where hydrostatic pressures exist at the failure plane when the piezometric height (h) equals the depth of soil (z), values of (ru) for the lower and middle slope sections are 0.54 and 0.62 respectively. For conditions when the soil is 'saturated' and rainfall intensities are low enough to permit the soil to drain at a rate close to that of the infiltration rate the values of (ru) when h = z would be the levels of pore water pressure most likely to develop in order for failure to occur on the regolith mantles of the three slope sections.

Solutions to the stability equation (4) are given in Figs. 3.38 to 3.43. They illustrate how the factor of safety against shallow planar landsliding changes as one parameter only varies. The parameter values are shown in Table 3.11. Piezometric heights (h) of 2.04m and 1.21m were used (i.e. values of h when F = 1) in the infinite slope analysis of the middle and upper slope profile sections respectively. The graphs have been constructed to show how the factor of safety (F) varies with changes in the value of the parameters for the upper and middle slope profile sections represented by lines (u) and (m) respectively (see Table 3.12 and Figs. 3.38 to 3.43.

Fig. 3.42. Graph to show how the factor of
safety against shallow planar landsliding
changes as parameter angle of internal
friction ($\emptyset'$) varies in Infinite slope
analysis for the middle and upper slope
profile sections.

Fig. 3.43. Graph to show how the factor of
safety against shallow planar landsliding
changes as parameter soil unit weight (γ)
varies in Infinite slope analysis for the
middle and upper slope profile sections.

Fig. 3.42 and Fig. 3.43
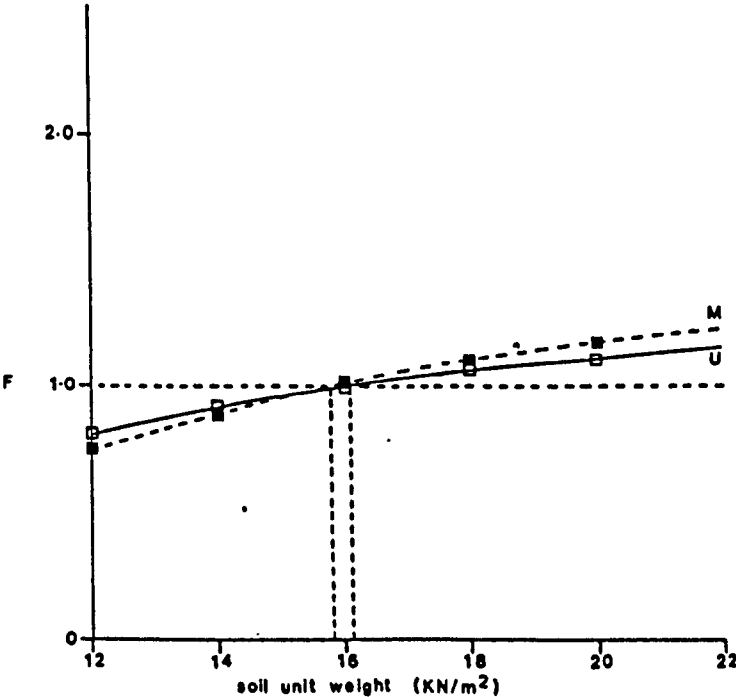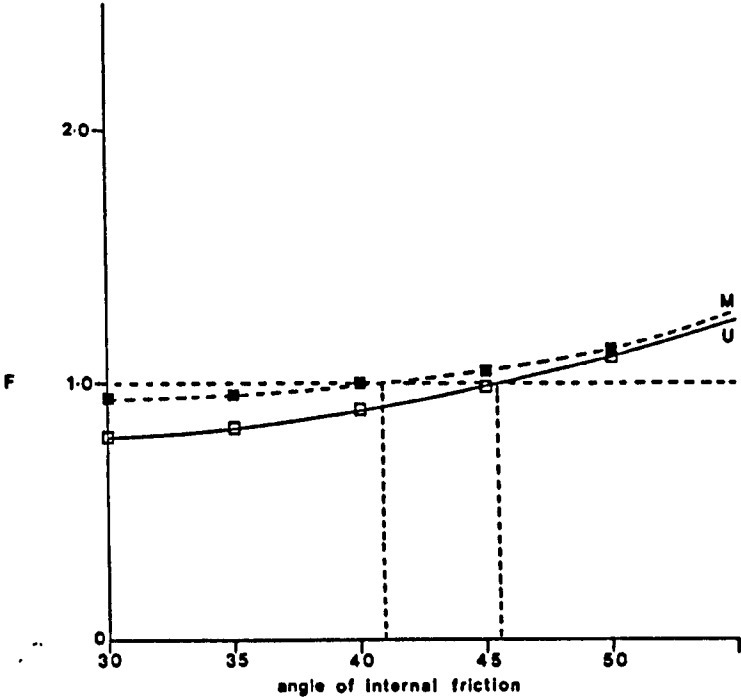
Fig. 3.40. Graph to show how the factor
of safety against shallow planar landsliding
changes as parameter cohesion (C') varies
in Infinite slope analysis for the middle
and upper slope profile sections.

Fig. 3.41. Graph to show how the factor
of safety against shallow planar landsliding
changes as parameter soil depth (z) varies
in Infinite slope analysis for the middle
and upper slope profile sections.

Fig. 3.40 and Fig. 3.41
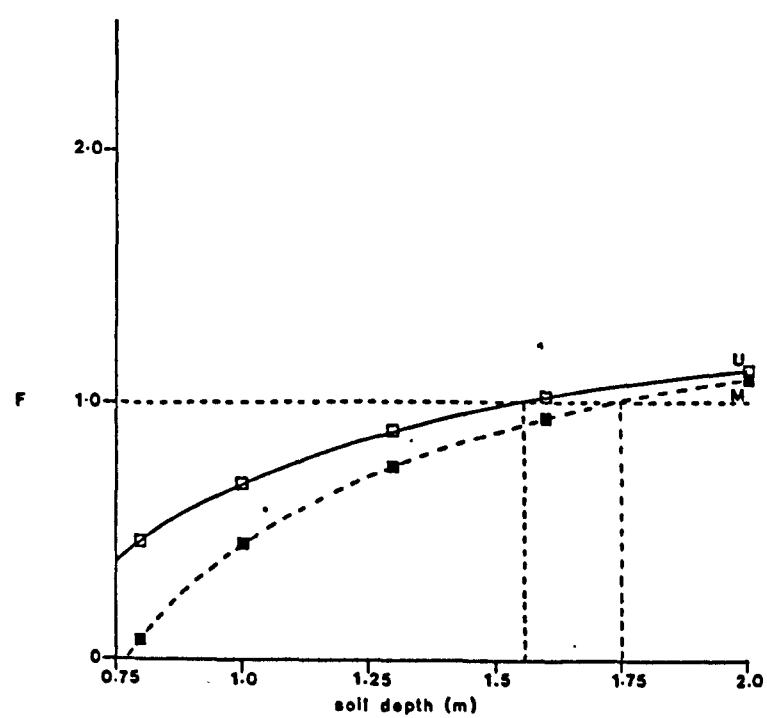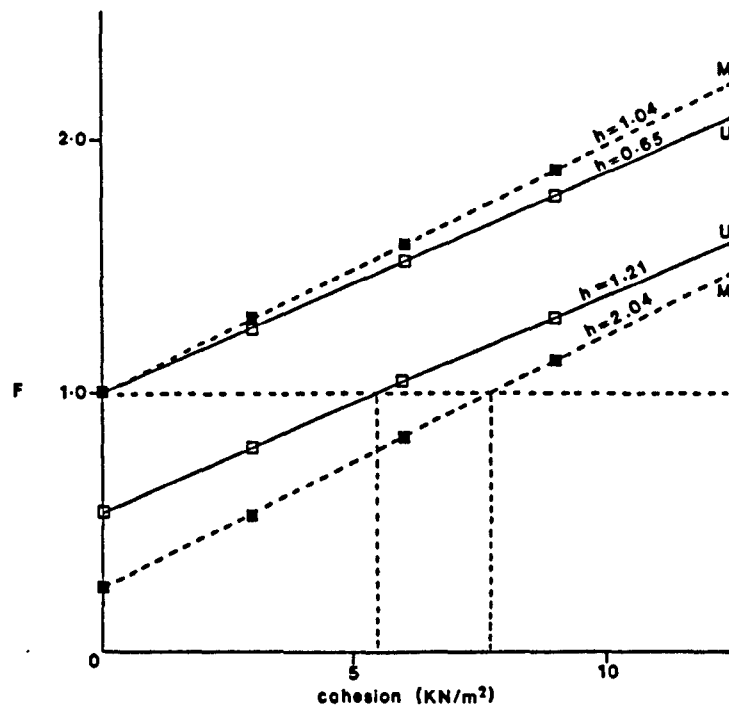
Fig. 3.38. Graph to show how the factor
of safety against shallow planar landsliding
changes as parameter piezometric height (h)
varies. Piezometric heights (h) of 2.04m
and 1.21m were used (i.e. values of h when
F = 1) in the Infinite slope analysis of
the middle and upper slope profile sections
respectively.

Fig. 3.39. Graph to show how the factor of
safety against shallow planar landsliding
changes as parameter slope inclination (β)
varies in Infinite slope analysis for the
middle and upper slope profile sections.

Fig. 3.38 and Fig. 3.39
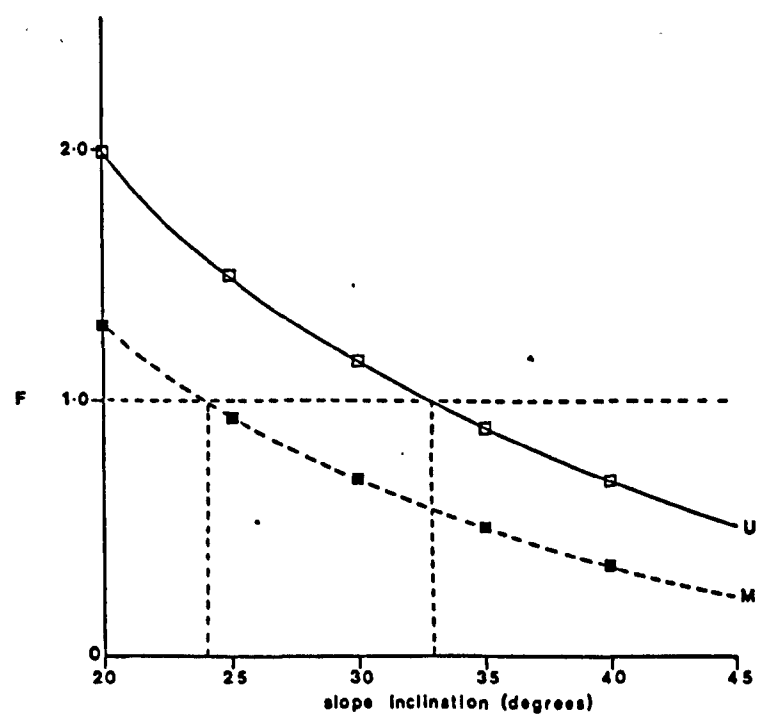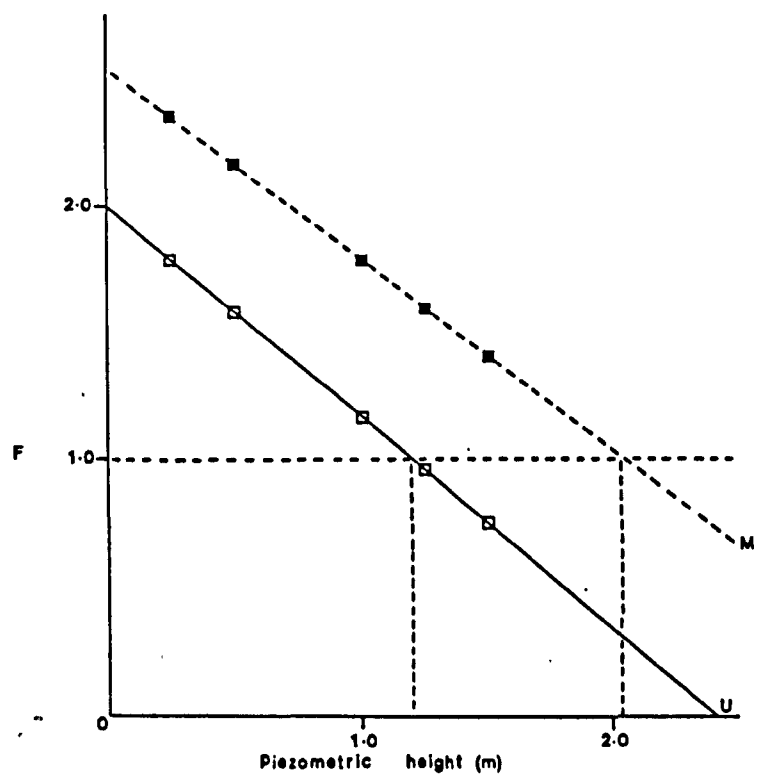
Table 3.12 Variation in the factor of safety against shallow
landsliding, derived from Infinite Slope Analyis, as
one parameter only varies

Slope Section	Parameter value when $F = 1$					
	h(m)	β	$\emptyset'^{O}$	$\gamma(kN/m^3)$	$c'(kN/m^2)$	z(m)
Upper slope section (u)	1.21	33°	45°	16.1	5.5	1.56
Middle slope section (m)	2.04	24°	39°	15.7	7.6	1.75

Figs. 3.38 to 3.43 show that the value of F is very sensitive to
changes in the value of effective cohesion (c') and piezometric
height (h), moderately sensitive to changes in the values of regolith
depth (z) and the angle of slope inclination (β) and rather
insensitive to changes in the values of the angle of friction with
respect to effective stresses ($\emptyset'$) and soil unit weight (γ).

Infinite Slope Stability Analysis (Skempton & DeLory, 1957) has been
widely used as a model with which to interpret the observed limiting
or threshold inclination of slope thought to be declining as a result
of landslide processes. Many of the slope stability formulae used by
geomorphologists including Infinite Slope Stability Analysis involve
the concept of a unique value of pore water pressure acting on the
failure plane, at which the shear strength generated within the slope
is overcome by the forces promoting failure. However, the observed
pattern of pore water pressure at Callow Bank suggest that this may
not be a sensible model to use. Piezometric analysis has shown that
the pore water pressures monitored from September 1984 to September
1985 are proportionately less than the pressures required to initiate
movement using the Infinite Slope Stability Model. However, such low
piezometric levels do not explain why shallow translational movements
are still very common on Derbyshire hillslopes. Perhaps the
mechanism for small localised shallow failures involves the
consideration of other variables which have not been incorporated
into the Infinite Slope Stability Model. From piezometric analyses
at Callow Bank, prolonged rainfall lasting several days would be
required to elevate piezometric levels to a level sufficient to cause
failure. The rainfall during the Winter months of 1984 was
considerably less than the two previous years. Clearly a piezometric
analysis over several years would be necessary in order to assess the
maximum pore water pressure likely to occur in the regolith mantle.
Perhaps the rainfall and consequently piezometric levels during the
period September 1984 to September 1985 were abnormally low.

For different reasons, the relationships between pore-water pressure and stability are complex. A number of studies have looked at the relationship between rainfall and slope failure. These studies have shown that shallow failures cannot be fully explained by the effect of the amount of rainwater alone. For example, some shallow failures have been reported to have occurred before saturation of the surface layer, while in contrast, saturated surface soil layers have remained stable or failures have occurred many hours later when the rainfall had stopped (Tanaka, 1963; Okimura, 1983). Some reports have claimed that immediately after such failures a large amount of ground water flowed out from the site where failure took place (Tanaka et al., 1972; Selby, 1976). Studies by Aboshi (1979); Okimura (1983); McGreal & Craig (1982); and Anderson et al., (1980) have shown that shallow translational failures occurred when the intensity of rainfall suddenly increased and that failure tended to occur 2-3 hours after the intensity of the rainfall reached a maximum. Okimura (1983), demonstrated that when the discharge in throughflow exceeded a particular value, piezometric level acceleration increased in proportion to the discharge of ground water, which was found to be directly related to rainfall intensity. Anderson et al. (1980), noted that an embankment failure had taken place after the moment of peak pore pressures; they suggested that this reflected the distribution of saturated conditions over the slope profile, increasing average normal load temporarily. Subsequent saturated soil water drainage towards the slope base increased basal pore pressures at the failure plane and reduced the normal load higher up the slope. Brief periods of intense rainfall generate a subsequent transient pressure rise in the slope material and this brief pressure wave may change a condition of stability in the slope to one of instability.

Studies by a number of workers have shown that many shallow
translational slides have taken place during high intensity summer
rainstorms after prolonged dry periods where soil fissures and
tension cracks have developed (Selby, 1976; Campbell, 1974). Soil
shrinkage upon drying is caused by capillary tension, the extent of
cracking is controlled by the type and proportion of clay minerals
present (Mitchell, 1976). Since the capillary tension can occur both
horizontally and vertically, shrinkage caused by dessication in dry
periods generates the separation of soil structural units, but even
more significantly promotes the formation of vertical tension cracks
normal to the soil surface. Cracks within the slope mantle lower
stability by reducing the length of the surface of failure over which
the shearing resistance is mobilised. If water enters the crack and
is unable to escape it can exert a hydrostatic pressure on the sides
of the crack which contributes to the disturbing forces. When
shrinkage cracks are open to the ground surface the potential
infiltration rate is increased as the tension cracks permit the rapid
transfer of water to sub-surface soil horizons during periods of
rainfall.. Vertical tension cracks of 1m depth and transversely
extending several metres had developed in several areas on the
hillslopes of Callow Bank. Such tension crack systems may be crucial
micro-morphological features facilitating rapid infiltration of
rainwater into the hillslope regolith of Callow Bank. It is highly
probable that the formation of these tension cracks is an important
precursory factor before shallow translational slides can occur.

After heavy and intense rainfall, pore water pressures are higher in
cracks and fissures within the regolith mantle, than the general
water table. This suggests a relationship between slope failure,
high rainfall intensities and locally high pore water pressure with

average ground water levels lagging somewhat behind. The presence of tension cracks and fissures before failure make environmental reconstruction from stability analyses extremely difficult if not impossible, because of the wide range of parameters permitted. If the Infinite Slope Stability Model is applied to slopes where the worst pore pressure conditions are assumed to have been associated with ground water flow parallel to the surface, underprediction of threshold slope angles will occur if in reality the worst pore pressure conditions were associated with a line of zero pore-water pressure converging towards the slope base. Anderson et al., (1980) showed that the Infinite Slope model tends to underpredict the threshold angle of stability, they suggested that this may be due to inadequate representation of pore water conditions when soil water potential lines depart significantly from the normal to the slope surface assumed by the Infinite Slope Model. Therefore, a slope may be modelled either by an Infinite Slope Model with the water-table parallel to the surface, or by a model in which the water-table converges towards the surface at the base of the slope. According to Anderson et al., (1980) the former model may be more applicable under permafrost conditions, or possibly where very strong permeability contrasts within the soil create a perched water-table. The latter condition is more appropriate for contemporary and post-glacial rainfall-induced pore-pressure variation. In order to distinguish the origin of slope form, and the details of the process, additional information from datable material, or soil micro-structural analysis demonstrating prior segregation ice formation is required. In attempts to infer environmental conditions at the time of failure from successfully fitted stability models, the problem remains that the knowledge of relationships between pore-pressure and rainfall variation is limited or non-existant.

Clearly there is a requirement for more detailed field investigation of piezometric levels, rainfall intensity and micro-morphology at Callow Bank. It would have been interesting to monitor in more detail the changes in piezometric level with rainfall intensity within tension cracks for particular rainstorm events. Observations of short term pore-pressure variation using simple Casagrande Standpipe piezometers is not a very accurate method of establishing accurate piezometric levels during high intensity Summer rainstorms because of the delay in response time of such instruments. Anderson et al., (1980) compared an automatic tensiometer monitoring system with a standpipe piezometer system and showed the lagged response of the standpipe piezometer system compared to the tensiometer system, sometimes in the order of several hours which had the effect of dampening pore-water pressure fluctuation. The results implied that a standpipe piezometer system might suggest slope failure at lower pore pressures than those actually experienced. It is possible that the Casagrande porous plastic piezometer tips used at Callow Bank may also have indicated lower piezometric levels than those actually attained in the slope regolith. A sensitive tensiometer system might have provided a more accurate means of measuring rapid pore-water fluctuations during storm events. An integrated monitoring system which incorporated an automatic tensiometer Scani-valve system (Burt, 1978b) combined with an automatic raingauge capable of measuring rainfall intensities accurately over short time periods linked with a horizontal rod extensometer fitted with displacement transducers suitable for measuring tension crack movements each terminating to a central data logger would have provided an ideal instrumentation set-up. However, such an instrumental system is very expensive and the system would have to be purpose built.

Until recently there was no automatic means of directly monitoring water levels in remote standpipes and Casagrande piezometers. All previous methods relied one way or another on sensing water pressure, usually using transducers to translate this pressure into a form suitable for automatic recording. During the last few years a system has been developed which measures depth to water. A small device called a transponder is fixed to the top of the standpipe or piezometer tubing. This emits a sonic pulse which travels down the tube and is reflected by the water surface. The time elapsed between the signal leaving the transponder and the echo from the water surface returning to it is directly proportional to the distance travelled. This time interval is precisely measured with reference to a quartz oscillator. The advantage of this is that sensitivity of 1mm depth is achieved, and the readings are free from time dependant drift. Bands and kinks in the tubing present no difficulty, and readings have been achieved in tubes impassible to a conventional dip meter. Range, however, is limited to 15m. The transponder is connected by an electrical cable to the data logger unit. The logger consists of solid state electronics and contains no moving parts. The basic unit can automatically record readings from up to 50 transponders at intervals selected between 5 minutes to 1 day. The system uses C.M.O.S. microprocessor technology and as each reading takes only a few seconds, the power consumption is very low; the unit can run for months on its internal batteries before needing recharging.

Durham et al. (1986a,b) describe a data logging system that uses pulse-width modulated a.c. signals transmitted from transducers equipped with address recognition circuits. The system was used to monitor a hydrologic network consisting of 30 piezometers, one

tipping-bucket rain gauge and one weir-stage recorder, and provided the control signals for a 24 bottle water sampler. The tipping-bucket rain gauge, weir-stage recorder and the 30 piezometers were read every 10 minutes. The data from each piezometer was retained only when the water level changed by ± 6mm. The system was designed to meet the following requirements:

(a) The ability to monitor a large number of transducers of similar type via a single cable: address transmission and recognition circuitry is included in the logger and at the remote measured points, thereby allowing data transmission from many transducers connected via a single cable to the logger.

(b) Interrogation, processing and recording of data according to a preset but flexible specification, and to activate external devices on command: a low-power micro-computer is dedicated to provide programmable control for the tasks of addressing and interrogating transducers, storing data in solid state memory and transmitting trigger signals to activate external devices.

(c) Elimination of problems associated with transmitting d.c. signals over long distances: pulse-width-modulation circuits are built into each transducer at the point of measurement to allow data to be transmitted as variable pulse-width signals. Data transmitted in this form are insensitive to supply voltage and line resistance, and bypass ground loop problems Durham, (1986a,b). The system has proven to be particularly suited to experimental installations where a large number of similar transducers have been employed, and where it is important to know the precise relative timing of changes in the various transducers.

A micromatic pneumatic piezometer system linked to a central data logger would have provided an alternative low cost technique for measuring rapid pore water pressure fluctuations. A more expensive but very accurate system of pore pressure monitoring would have been the use of a network of vibrating wire piezometers terminating to a central data logger.

Difficulties arise in relating slope failure to rainfall conditions because of the influence of hydraulic conductivities of different sediments. High intensity rainstorms often do not cause slope failure in highly permeable sediments. Thus the intensity of the rainfall and the relative frequency of storm events required to cause failure may depend on the permeability of the superficial sediments concerned. A useful experiment would have been to undertake hydraulic conductivity tests of the regolith in order to accurately determine infiltration rates. An experimental set-up in order to measure throughflow rates at different levels within the regolith profile would also have provided useful information on sub-surface channelling. The Linear Shrinkage Test would have provided important additional information as to the likelihood of tension-crack and fissure formation within the regolith material.

Uncertainties arising from such factors as fissures, tension cracks, variable regolith properties and sub-surface channelling make determination of true pore-water pressure at failure extremely difficult if not impossible. The piezometric observations of ground water conditions at Callow Bank can only be regarded as a crude indication of the widespread pattern of pore pressures within the material at the regolith/bedrock interface. Although, from the data presented here there does seem to be a range of pore-water pressure

values over which mass movement may occur, it is clear that a more

sophisticated and sensitive system for monitoring ground water

fluctuations at specific sites is required, in order to assess more

accurately how changes in pore-water pressure affect stability. The

relationship between the trend of pore-water pressure with rainfall

intensity needs to be monitored carefully particularly the timing and

magnitude of the transient water pressure wave in relation to

specific rainfall intensities. This information in the form of a

mathematical model along with the knowledge of storm return periods

would provide a useful indication to geotechnical engineers as to

when shallow translational failures might occur particularly on

metastable slopes. While variations of the Infinite Slope Stability

Model may provide a useful first approximation to real slope failure

situations, the engineering geomorphologist must not hesitate to

modify these models in order to fit field observations.

Back calculations have shown that a piezometric height below the

slope surface (0.37m beneath the surface) would be required to cause

failure in the Upper Slope Section at Callow Bank. The stability

analysis used in the investigations at Callow Bank may be modified by

assuming a water-table parallel to, but beneath the surface, its

position defined by the parameter (m). If the water-table is partly

below the ground surface, part of the overburden of regolith is

unsaturated so that the normal load is reduced. The equation given

below is a more precise formulation of the stability analysis for a

partially saturated slope:

$$\tan \beta_t = \left[\frac{m \ \Upsilon_s + (1 - m) \ \Upsilon_d - m \ \Upsilon_w}{m \ \Upsilon_s + (1 - m) \ \Upsilon_d} \right] \tan \phi'$$

The Infinite Planar Slide Model may be modified in detail but these modifications should not be restricted to the location of the water-table. For example, although most shallow failures are usually of limited lateral extent, in time successive failures may regrade the full horizontal extent of a straight slope section. Therefore, individual slides are subject to significant lateral pressures which will have the effect of maintaining stability to angles in excess of those predicted by the Infinite Slide Model for given pore water pressure conditions (Chandler, 1972a).

From field investigations at Callow Bank a more sophisticated stability model that can accommodate a non-linear failure surface and variations in pore-water pressure along the failure plane would provide a more accurate analytical model. However, such a model cannot be readily used to determine threshold slope angles in the geomorphological context as suggested by Carson & Petley's analysis (1970). The analytical formulation in models more complex than the Infinite Slope Stability model deal only in terms of force resolution with respect to the failure surface inclination; hence back calculation of the threshold slope angle (β_t) cannot be uniquely achieved.

Threshold slopes have been determined by using the Infinite Slope

Stability Model because of its simplistic nature, since it requires

only the selection of the worst pore-water conditions if effective

cohesion can be assumed to be zero. Such conditions are usually

assumed to have occurred in Britain in the periglacial periods of the

Late Devensian, with the water-table at the surface (m = 1).

Although, a more sophisticated stability model may be analytically

more desirable as indicated above, this would present a major problem

in the selection of shear-plane configuration and depths of the zero

pore pressure line, as well as varying pore-water conditions along

the shear plane. Clearly there is no satisfactory way in which these

variable options can be selected with respect to past climatic

conditions to yield threshold angles.

The formation of complex mathematical models provided by stability

analyses are potentially far more sophisticated than the data

available for their calibration, particularly in relation to the

explanation of long term slope evolution. The ability to select an

appropriate model is severely limited by the absence of detailed

morphological and pore-pressure data, and it is evident that

arbitrary selection of imput parameters to stability models can lead

to fortuitous agreement between model predictions and observed

threshold slopes, and equivalent agreement by various alternative

models. The minor details of lateral pressure, tension cracks, and

water-table gradient exert a particularly significant influence over

threshold angles when the failures are shallow slides in a

superficial regolith material.

3.8 SUMMARY

Landslide Distribution

The Derbyshire case study has shown that separate distributions may be defined for deep-seated and shallow mass movements since each of these respond to different controls. Similarly separate distributions may exist for a given type of landslide according to temporal conditions of soil moisture or ground water levels.

Deep-seated failures tend to occur in intact cohesive materials and involve mobilisation of shear strengths in excess of residual, particularly where massive Millstone Grit overlies weaker shale strata. As shown in the Derbyshire case study, slope height and angle are both important influences, and instability occurs if basal erosion either increases slope height beyond a critical value at a given slope angle, or steepens the slope until the actual height equals the limiting height.

Shallow translational slides generally occur in cohesionless regolith at near residual strengths and are independant of slope height. Slope angle is critical and shallow failure restores stability on oversteepened slopes by lowering the angle to approximately the residual angle of friction in the absence of positive pore-water pressures which result in even lower stable angles.

Landslide causes

It appears from field evidence in the Peak District that the first slip movement that took place for many of the large deep-seated

rotational slides developed from outward bulging and deformation at the foot of the slope. Retrogression then took place either where tensional stresses caused movement outwards and downwards from the original slope or where stream undercutting permitted further slip movement on the slide surface. Failure in the less competent shale strata depended upon the susceptibility of a particular bed to mechanical and chemical breakdown, but was also influenced by the thickness and weight of the load bearing down upon it. The presence of thick permeable sandstone in the upper slope greatly increased the load that had to be supported. It would appear from morphological evidence that the failure path for the most part was in the mudstone or shale strata situated at the base of slopes. This is in the zone of contact between impermeable rocks and where the ground water flow is strongly anisotropic being determined by the dip of the beds In such zones high pore water pressures can be generated with higher pressure gradients within the slopes. Equally important, chemical and mechanical weathering in such zones reduces the rock to very low shear strength levels.

The maintenance of a high water table and a strong pore-water pressure gradient in the hillslope during the Devensian glacial period must have caused a weakening of rock strength, but the most extensive landslides appear to have occurred after the more temperate Boreal climatic regime.

The immediate cause of all landsliding appears in all cases to have been slope failure resulting from a progressive weathering of the rocks at the base of the old hillslope. This can be seen as a natural process of hillslope evolution controlled by local geological conditions.

Time of failure
==================

There is some evidence that environmental changes might also have

been involved in actually triggering slide movements. For example,

climatic change towards increased wetness, could perhaps be invoked

as a trigger mechanism. However, it is evident from studies

undertaken in the Peak District that landsliding has occurred at

times when geomorphological processes were less intensive than they

had been during periods in the Pleistocene. The slopes of the Peak

District experienced, for long periods, climatic regimes similar to

and more severe than those today; the slopes only failed when some of

their constituent strata became progressively weakened to a point of

critical 'threshold' stage. When this point was reached, the slope

failed, regardless of climatic conditions, steepness of slope or any

other factor. The actual site of a landslide is therefore determined

mostly by local conditions, particularly where structure and

lithology favour the concentration of ground water into an area of

steep surface slope. Thus whilst it is probably true that most

landslides in the study region occurred during climatic periods when

the rate of weathering was accelerated, it would be wrong to conclude

that all Pennine landslides took place during these periods. Clearly

more research is needed to investigate dateable deposits above and

below landslide material and also within river terrace gravels and

solifluction deposits associated with the landslide debris, in order

to construct more exactly the date of inception of landslide events

in the Peak District.

Shallow planar translational sliding remains an important process of

slope evolution. Where cohesionless regoliths occur on steep slopes

sliding occurs when weathering has proceeded far enough to reduce

soil strength towards a failure condition and where there is sufficient thickness and water pressure.

The Matrix Assessment Approach

There is an increasing requirement for slope stability information in planning/engineering management decision-making as the demand for roads, structures, recreational facilities etc grows. Large-scale/ extensive civil engineering works, planning and land-management in areas known to have a landslide problem require large area or regional landslide susceptibility threshold evaluation.

The Matrix Assessment Approach provides a useful technique for identifying those geological/geomorphological features and structures indicative of instability. This information is useful for the simultaneous delineation of areas of hillslope instability and areas of potential instability. The user would be able to distinguish unstable areas from adjacent areas of stable ground before engineering works commence.

The Matrix Assessment Approach is a quantitative method for establishing an index of stability-states over large areas. The method allows the relative landslide potential/susceptibility to be evaluated over large areas using a discrete combination of measureable stability factors/parameters and follows a well defined procedure. A map of existing landslides serves as a basic data source for understanding the macro threshold conditions controlling slope stability.

The Matrix Assessment Approach coupled with an on-line interactive graphics facility enables the user to test hypotheses concerning:-

(a)   The essential geological/geomorphological parameters needed to explain slope failures over the region of interest.

(b)   The spatial pattern of slope susceptibility to failure for large areas.

The Derbyshire case study area has also shown that the matrix combinatorial model:-

(i)   Is sensitive to changes in the combination of variables/ parameters used.

(ii)   Is less sensitive to changes in classification.

(iii)   Confirmed that bedrock geology and slope steepness were the most important variables used, but relative relief, slope aspect and soils also appeared to be important susceptibility variables.

The results of the field survey illustrated the potential of MAP for classifying slope stability in the northern and southern sectors of the study region. The technique successfully identified a number of previously unmapped landslide sites.

MAP therefore provides a useful preliminary technique to be introduced during the reconnaisance stage of a proposed engineering project. The resulting landslide susceptibility map should be considered primarily as a guide to slope instability and not an absolute indicator of landslides. The LSI values would assist highway planners and engineers to choose the most appropriate highway route from the feasible routes. A more intensive ground investigation which includes detailed geomorphological, geotechnical and perhaps geophysical investigation could be instigated in those areas along the route where high LSI values are prevalent. In those areas, where the planned highway intersects high LSI values, borehole investigation and field instrumentation could be concentrated. A programme of inclinometer, piezometer and settlement instrumentation could be devised for those areas where a particularly high landslide susceptibility value had been predicted.

At the construction stage more detailed site geotechnical investigations would be required in recognised areas (i.e. those cells containing high LSI values) to determine precise local variation. The basic data collected for the landslide susceptibility assessment could also be used by other specialists to carry out a variety of environmental investigations as part of a single multi-disciplinary and multi-purpose projects, e.g. land-resource evaluation or for planning purposes. The application of MAP in the study area has also provided a useful example of how techniques of automated cartography and numerical analysis can be integrated with geological/geomorphological knowledge not only to provide a better understanding of the landslide susceptibility problem, but also to further the development of interactive display software systems of practical use to researchers, planners and civil engineers.

An interesting exercise given further time would have been to use MAP on one type of landslide rather than for all classes of landslide encountered in the Derbyshire case study. By applying MAP, for each type of landslide identified, it will be possible to establish which variables are more important for each landslide type. Separate landslide suseptibility maps could be created for each identified landslide type in the study region. The spatial distribution of high susceptibility index values for each type of landslide could then be compared and vulnerable areas for specific types of landslide could be identified and delineated. Such an investigation would be very useful in planning the position and type of monitoring instrumentation or the appropriate type of remedial engineering measures necessary to prevent failure occurring in predicted high risk areas.

Callow Bank Case Study

Unlike deep-seated failures, surface failures in the form of shallow rotational slips or translational slides may not have the effect of preventing the exploitation of areas above and below the slope. However, they can cause considerable inconvenience and expense when the necessary repairs have to be made. Deep-seated failures are now routinely analysed and compensated for in new earthworks and remedial measures, and are now relatively rare events. On the other hand, scant regard has been paid to designing against shallow failures, the consequences of which are evident to users of motorways and trunk roads in the British Isles.

Section III of this thesis, which examined the meso/micro stability
threshold conditions, showed that critical geomorphological threshold
states can be identified within the superficial materials on
hillslopes, with respect to shallow planar translational slides in
regolith.

In order to monitor the present dynamics of the threshold state of
shallow planar sliding, a series of geomorphological techniques were
successfully applied. These techniques involved a network of
monitoring instruments which included standpipe piezometers placed in
the hillslope regolith, V.notch weirs, and raingauges along with
standard techniques of slope profile analysis, in situ shear box
testing and laboratory testing of soils.

Slope Analysis

No definite straight slope segments in the slope profiles
investigated at Callow Bank were found using the system of 'best unit
analysis'. This technique, therefore, did not provide an effective
method for identifying characteristic slope segment angles.

Slope angle studies along with particle size analyses at Callow Bank
have shown that the 'frictional' properties of the regolith vary
appreciably according to the local conditions of the parent material,
the degree of weathering, and the state of packing. These regolith
characteristics together with differences in pore water pressure
conditions produce a broad continuum in the threshold slope angles of
an area.

Particle size Analysis

Fine gravel and coarse sand were the dominant constituents of regolith sampled from the upper slope sections and corresponded to a clayey sand. The regolith of the middle slope sections showed a high proportion of fine sand and silt; they corresponded to a sandy clay. Fine silt and clay were the dominant constituents of the regolith studied on the lower slope sections and also corresponded to a sandy clay. The particle size differences partly reflect bedrock control, since the upper slope sections tended to be located on the massive coarse-grained beds of Rivelin Grit and the middle and lower slope sections were situated on shales and mudstone strata.

The range of liquid limits for upper slope sections (18% to 36%) was slightly greater than the ranges for the middle (19% to 35%) and lower slope sections (25% to 38%). The plastic limits were also low, ranging from 10% to 31% with mean figures of 18%, 20% and 22% for the upper, middle and lower slope sections.

Stream Discharge

The stream hydrographs demonstrated the rapid response of stream discharge to rainfall in the winter months. The stream hydrograph responses to rainfall are derived from rain falling directly into the stream channel and from the saturated contributing area immediately adjacent to the stream and seepage hollows further upslope. The piezometer survey showed that the areas in which moisture conditions were maintained at or near saturation between storms in winter are located in small convergent hollow areas often associated with intermittent springs and seepage areas associated with underlying

shale strata. These areas tend to maintain saturated conditions and facilitate the collection and rapid transmission of surface water to the basin outflow after heavy rainfall.

Piezometer Results

The highest mean pore water pressures (ru = 0.37) was recorded in regolith consisting predominantly of clayey gravels. These gravels tended to be associated with shale strata at shallow depth, thereby creating impermeable conditions and the development of perched water tables. Clay regolith derived from the in situ weathering and breakdown of shales and mudstone gave the second highest mean pore water pressure (ru = 0.32). The clay regolith profiles conformed to that of a stagnogley soil indicating seasonal waterlogging. Free draining sandy regoliths usually associated with the Rivelin Grit on steeper upper slope sections gave the lowest mean pore water pressure (ru = 0.13) as might be expected.

Seepage hollows, saturated depressions and other areas where perched water table conditions existed could easily be recognised by characteristic vegetation, particularly Sphagnum and Juncus species. There is a strong correlation between pore water pressures and properties of the local vegetation canopy. Engineers should be aware of particular plant indicator species as a means of locating the presence of perched water tables.

Effective Cohesion

The values of ϕ' are related to the particle sorting; regolith samples consisting of high proportions of gravel and sand gave higher values of ϕ'. Values of ϕ', therefore, tended to be higher for regolith material sampled from the upper and middle slope sections. The variation in the effective cohesion (c') appears to be associated with vegetation changes causing corresponding changes in the mechanical reinforcement of soil by roots. The effective cohesion (c') was higher for the middle slope section where bracken (Pteridium aquilinum) was dominant. The bracken roots and rhizomes mechanically bind or reinforce the soils they are growing in. Even a small increase in cohesion or shear strength will counter the loss of strength of unsaturated soils caused by an increase in pore water pressures resulting from infiltration due to prolonged rainfall or ground water seepage. This increased shear resistance resulted in a significant increase in the factor of safety for the slope against shallow-seated failures. Through the increased use of specially selected varieties of plants e.g. certain grasses and legumes with potential to establish deep-root systems in a wide range of soils, along with the combined use of geotextiles in extremely critical areas, it will be possible for engineers to provide an economical and effective natural means of enhancing the stability of slopes with respect to shallow translational failures.

Infinite Slope Stability Analysis

Using conventional Infinite Slope Stability Analysis (ISSA), it was possible to define the precise 'critical state' of a series of geomorphological parameters (i.e. effective cohesion (c'),

piezometric head (h), depth of regolith (z), angle of internal
friction with respect to effective stresses (Ø'), pore-water pressure
(u) etc) associated with the overall threshold instability state.
The application of ISSA showed that all three slope sections studied
at Callow Bank were stable under the present maximum pore water
pressures recorded during field investigations. The piezometric
height necessary for failure to occur equated to piezometric surfaces
of 0.69 m and 0.29 m above the ground surface for the lower and
middle slope sections and a piezometric level of 0.37 m below the
ground surface in the upper slope section. For failure to occur
(i.e. where F = 1) the pore pressure (ru) would need to be 0.80, 0.72
and 0.46 for the respective lower, middle and upper slope sections
analysed.

From back calculations based on the Infinite Slope Stability Model it
was possible to show how the factor of safety against shallow planar
sliding changed as one geomorphological parameter only varied. The
value of the factor of safety was found to be very sensitive to
changes in the value of effective cohesion and piezometric height,
moderately sensitive to changes in the values of regolith depth and
angle of slope inclination and rather insensitive to changes in the
values of the angle of friction with respect to effective stress and
soil unit weight.

The low piezometric levels do not explain why shallow translational
movements are still very common on Derbyshire hillslopes. This
suggests that the mechanism for small localised shallow failures
involves the consideration of other variables which have not been
incorporated into the Infinite Slope Stability Model. Uncertainties
arising from such factors as fissures, tension cracks, variable

regolith properties and subsurface channelling make determination of true pore water pressures at failure extremely difficult. There would also appear to be some misgivings in the type of instrumentation used at Callow Bank to monitor the relationship between the pore water pressures, rainfall and slope failure at critical points in the slope material. More detailed field investigation of the relationship between piezometric levels, rainfall intensity and micro-morphology at Callow Bank are necessary.

The relationship between pore water pressure and rainfall intensity requires to be accurately monitored, particularly the timing and magnitude of the transient water pressure wave in relation to specific rainfall intensities. This information, in the form of a mathematical model, along with the knowledge of storm return periods would alert geotechnical engineers as to when shallow translational failures might occur particularly on metastable slopes. The recognition of such meso/micro geomorphological thresholds is not only important for geomorphologists concerned with landform evolution, it is also fundamental to successful and safe engineering practices. Investigations carried out at Callow Bank have provided a useful insight into the nature and dynamic behaviour of shallow landsliding in regolith. An awareness of the variables involved in shallow planar translational landsliding along with the knowledge of critical thresholds of certain geomorphological parameters establishes the basic context by which correct engineering decisions can be made.

REFERENCES

Aboshi, H. (1979). Failure of granite slopes in Chugoku District under heavy rain: shearing strength at failure. Natural Disaster Science 1; 77-87.

Ackroyd, T.N.W. (1957). Laboratory testing in soils engineering. Geotechnical Monograph No. 1. Soil Mechanics Ltd., London. 233pp.

Aitkenhead, N. and Chisholm, J.I. (1982). A standard nomenclature for the Dinantian formations of the Peak District of Derbyshire and Staffordshire. Report of the Institute of Geological Science No. 82/8. British Geological Survey, Keyworth, Nottingham.

Alfors, J.T., Burnett, J.L. and Gay, T.E. (1973). Urban geology masterplan for California - the nature, magnitude and costs of geologic hazards in California and recommendations for their mitigation. California Division of Mines and Geology Bulletin; No. 198; 122pp.

Allen, J.R.L. (1960). The Mam Tor sandstones: A 'Turbidite' facies of the Namurian deltas of Derbyshire, England. Journal of Sedimentary Petrology, 30; 193-208.

Anderson, M.G. and Burt, T.P. (1977). Automatic monitoring of soil moisture conditions in a hillslope spur and hollow. Journal of Hydrology, 33; 27-36.

Anderson, M.G. and Burt, T.P. (1978a). The role of topography in controlling throughflow generation. Earth Surface Processes and Landforms, 3; 331-344.

Anderson, M.G. and Burt, T.P. (1978b). Time synchronised stage recorders for the monitoring of incremental discharge inputs in small streams. Journal of Hydrology, 37; 101-109.

Anderson, M.G. and Burt, T.P. (1979). Toward more detailed field monitoring of variable source areas. Water Resource Research, 14; 1123-1131.

Anderson, M.G. and Burt, T.P. (1982). The contribution of throughflow to storm runoff: An evaluation of a chemical mixing model. Earth Surface Processes and Landforms, 7; 565-574.

Anderson, M.G., Richards, K.G. and Kneale, P.E. (1980). The role of stability analysis in the interpretation of the evolution of threshold slopes. Transactions of the Institute of British Geographers, New Series, 5; 100-112.

Anderson, P. and Shimwell, D. (1981). Wild Flowers and Other Plants of the Peak District. Moorland Publishing, Ashbourne, Derbyshire. 192pp.

Anselmo, V. and Gedone, F. (1976). A method for drawing slope maps from aerial photographs. Bulletin of the Society of Geology of Italy, 95; 75-80.

Arnett, R.R. (1971). Slope form and geomorphological process: An Australian example. Institute of British Geographers Special Publication, 3; 81-92.

Arnett, R.R. (1974). Environmental factors affecting the speed and volume of top soil interflow. Institute of British Geographers Special Publication, No. 6; 7-22.

Arnett, R.R. (1976). Some pedological features affecting the permeability of hillside soils in Caydale, Yorkshire. Earth Surface Processes and Landforms, 1; 3-16.

Avery, B.W. (1980). Soil classification for England and Wales (Higher categories). Soil Survey Technical Monograph, No. 14; Soil Survey, Harpenden. 67pp.

Badger, C.W., Cummings, A.D. and Whitmore, R.L. (1956). The disintegration of shale. Journal of the Institute of Fuel, 29; 417-423.

Bailey, R.G. (1971). Landslide Hazards Related to Land Use Planning in Teton National Forest, North West Wyoming. U.S.D.A. Forest Service, Inter-mountain Region, Ogden, Utah. 131pp.

Bannister, P. (1964a). The water relations of certain heath plants with reference to their ecological amplitude. I. Introduction: Germination and establishment. Journal of Ecology, 52; 423-432.

Bannister, P. (1964b). The water relations of certain heath plants with reference to their ecological amplitude. II. Field studies. Journal of Ecology, 52; 481-497.

Bannister, P. (1964c). The water relations of certain heath plants with reference to their ecological amplitude. III. Experimental studies and general conclusions. Journal of Ecology, 52; 499-509.

Barton, N. (1973). Review of a new shear-strength criterion for rock joints. Engineering Geology, 7; 287-332.

Barton, N. (1976). The shear strength of rock and rock joints. International Journal of Rock Mechanics and Mining Science, 13; 255-279.

Barton, N. and Choubey, V. (1977). The shear strength of rock joints in theory and practice. Rock Mechanics, 10; 1-54.

Bazynski, J. (1977). Studies of the landslide areas and slope stability forecast. Bulletin of the

International Association of Engineering Geology, 16; 77-80.

Beven, K.J. (1977a). Hillslope hydrographs by the finite element method. Earth Surface Processes and Landforms, 2; 13-28.

Beven, K.J. (1977b). Experiments with a finite element model of hillslope hydrology: the effect of topography. Proceedings of the 3rd International Hydrology Symposium, Fort Collins, Colorado, 1, 84-102.

Beven, K.J. (1978). The hydrological response of headwater and sideslope areas. Hydrological Science Bulletin 23; 419-437.

Beven, K.J. and Kirkby, M.J. (1979). A simple physically based, variable contributing area model of basin hydrology. Hydrological Science Bulletin, 24; 43-69.

Bishop, A.W. (1948). A large scale shear box for testing sands and gravels. Proceedings of the 2nd International Conference on Soil Mechanics and Foundation Engineering, Rotterdam, 1; 207-211.

Bishop, A.W. and Skinner, A.E. (1977). The influence of high pore water pressure on the strength of cohesionless soils. Philosophical Transactions of the Royal Society, London. Series A, 284; 91-130.

Bjerrum, L. (1967). Progressive failure in slopes of over-consolidated plastic clay and clay shales. Proceedings of the American Society of Civil Engineers 93, No. SM5; 1-49.

Bjerrum, L. and Jørstad, F.A. (1968). Stability of rock slopes in Norway. Norwegian Geotechnical Institute Publication, 79, 1-11.

Black, W.P.M., Croney, D. and Jacobs, J.C. (1958). Field studies of the movement of soil moisture. Road Research Technical Paper, No. 41; HMSO, London; 72pp.

Bolt, B.A., Horn, W.L., Macdonald, G.A. and Scott, R.G. (1975). Geological Hazards. Springer Verlag, Berlin; 328pp.

Brabb, E.E. (1982). Preparation and use of a landslide susceptibility map for a county near San Francisco, California. In: Landslides and Mudflows: Reports of Alma-Ata International Seminar October 1981. UNESCO/UNEP. Centre of International Projects, GKNT, Moscow, p. 407-419.

Brabb, E.E. (1984). Innovative approaches to landslide hazard and risk mapping. Proceedings of the 4th International Symposium on Landslides, Toronto, 1; 307-324.

Brabb, E.E., Pampeyan, E.H. and Bonilla, M.G. (1972).
     Landslide susceptibility in San Mateo County,
     California, U.S. Geological Survey Miscellaneous Field
     Studies Map. No. MF 360., Scale 1:62,500.

Bradley, R. and Hart, C. (1983). Prehistoric settlement in
     the Peak District during the third and second millenia
     BC: a preliminary analysis in the light of recent
     fieldwork. Proceedings of the Prehistorical Society,
     49; 177-193.

Briggs, D.J. and Burek, C. (1985). Quaternary deposits in
     the Peak District. In: Peak District and Northern
     Dukeries, Field Guide, (Ed. Briggs, D.J., Gilbertson,
     D.D. and Jenkinson, R.D.S.). Quaternary Research
     Association, University of Sheffield. p. 15-30.

British Standards Institution (1975). Methods of Testing
     Soils for Civil Engineering Purposes. B.S. 1377.
     British Standards Institution, London, 143pp.

British Standards Institution (1980). Methods of
     Measurement of Liquid Flow in Open Channels, Part 4A.
     Thin Plate Weirs. B.S. 3680. British Standards
     Institution, London, 46pp.

British Standards Institution (1981). Code of Practice for
     Site Investigations. B.S. 5930. British Standards
     Institution, London, 147pp.

Brooker, E.W. and Ireland, H.O. (1965). Earth pressures at
     rest related to stress history. Canadian Geotechnical
     Journal, 2; 1-15.

Brown, C.B. and Sheu, M.S. (1975). Effects of deforestation
     on slopes. Journal of the Geotechnical Engineering
     Division, American Society of Civil Engineers, GT2;
     147-165.

Brückl, E. and Scheidegger, A.E. (1972). The rheology of
     spatially continuous mass creep in rock. Rock
     Mechanics, 4; 237-250.

Brunsden, D. (1974). The degradation of a coastal slope,
     Dorset, England. Institute of British Geographers
     Special Publication, 7; 79-98.

Brunsden, D. (1979). Mass Movements. In: Process in
     Geomorphology. (Ed. Embleton, C. and Thornes, J.).
     Arnold, London, p. 130-186.

Brunsden, D., Doornkamp, J.C., Fookes, P.G., Jones, D.K.C.
     and Kelly, J.H.M. (1975a). Large scale
     geomorphological mapping and highway engineering
     design. Quarterly Journal of Engineering Geology, 8;
     227-253.

Brunsden, D., Doornkamp, J.C., Fookes, P.G., Jones, D.K.C. and Kelly, J.H.M. (1975b). Geomorphological mapping techniques in highway engineering. Journal of the Institute of Highway Engineering, 22; 35-41.

Brunsden, D. and Jones, D.K.C. (1972). The morphology of degraded landslide slopes in South West Dorset. Quarterly Journal of Engineering Geology, 5; 205-222.

Brunsden, D. and Jones, D.K.C. (1976). The evolution of landslide slopes in Dorset. Philosophical Transactions of the Royal Society, London, Series A, 283; 605-631.

Brunsden, D. and Thornes, J.B. (1979). Landscape sensitivity and change. Transactions of the Institute of British Geographers, New series, 4; 463-484.

Burek, C.V. (1977). An unusual occurrence of sands and gravels in Derbyshire. Mercian Geologist, 6; 123-130.

Burt, T.P. (1978a). Three simple and low cost instruments for the measurement of soil moisture properties. Internal Publication Series, Occasional Paper No. 6. Department of Geography, Huddersfield Polytechnic. 24pp.

Burt, T.P. (1978b). An automatic fluid-scanning switch tensiometer system. British Geomorphological Research Group, Technical Bulletin No. 21, Geo Abstracts Ltd., Norwich. 30pp.

Caine, N. (1980). Rainfall intensity-duration control of shallow landslides and debris flows. Geografiska Annaler 62A; 23-27.

Campbell, R.H. (1974). Debris flows originating from soil slips during rainstorms in southern California. Quarterly Journal of Engineering Geology, 7; 339-349.

Campbell, R.H. (1975). Soil slips debris flows and rainstorms in the Santa Monica Mountains and vicinity, southern California. United States Geological Survey Professional Paper 851; 51pp.

Canuti, P., Focardi, P. and Garzonio, C.A. (1985). Correlation between rainfall and landslides. Bulletin of the International Association of Engineering Geology 32; 49-54.

Carney, J.N. (1974). The use of stereoscopic aerial photographs in the detection and study of mass movement phenomena: with particular reference to ancient or small scale occurrences. Institute of Geological Sciences Photogeology Unit Special Publication, British Geological Survey, Keyworth, Nottingham, 15pp.

Carrara, A. and Merenda, L. (1976). Landslide inventory in northern Calabria, Southern Italy. Bulletin of the Geological Society of America, 87; 1153-1162.

Carrara, A., Catalano, E., Sorriso-Valvo, M., Realli, C., Merenda, L. and Rizzo, V. (1977a). Landslide morphology and typology in two landslide zones, Calabria, Italy. Bulletin of the International Association of Engineering Geology, 16; 8-13.

Carrara, A., Pugliese-Carratelli, E. and Merenda, L. (1977b). Computer-based data bank and statistical analysis of slope instability phenomena. Zeitschrift für Geomorphologie, 21; 187-222.

Carrara, A., Catalano, E., Sorriso-Valvo, M., Realli, C. and Ossi, I. (1978). Digital terrain analysis for land evaluation. Geologica Applicata e Idrogeologia, 13; 69-127.

Carson, M.A. (1969). Models of hillslope development under mass failure. Geographical Analysis, 1; 76-100.

Carson, M.A. (1971). Application of the concept of threshold slopes to the Laramie Mountains, Wyoming. Institute of British Geographers Special Publication, 3; 31-48.

Carson, M.A. (1975). Threshold and characteristic angles of straight slopes. In: Mass Wasting (Ed. Yatsu, E., Ward, A.J. and Adams, F.). 4th Guelph Symposium on Geomorphology, Geo Abstracts Ltd., Norwich. p. 19-34.

Carson, M.A. and Kirkby, M.J. (1972). Hillslope Form and Process. Cambridge University Press, Cambridge. 475pp.

Carson, M.A. and Petley, D. (1970). The existence of threshold hillslopes in the denudation of the landscape. Transactions of the Institute of British Geographers, 49; 71-96.

Carter, R.S. and Chorley, R.J. (1961). Early slope development in an expanding stream system. Geological Magazine, 98; 117-130.

Casagrande, A. (1949). Notes on swelling characteristics of clay shales. Harvard Soil Mechanics Series, Harvard University, Cambridge, Massachusetts. 77pp.

Chandler, M.P. and Hutchinson, J.N. (1984). Assessment of relative slide hazard within a large, pre-existing coastal landslide at Ventnor, Isle of Wight. Proceedings of the 4th International Symposium on Landslides, Toronto, 2; 517-522.

Chandler, M.P., Parker, D.C. and Selby, M.J. (1981). An opensided field direct shear box with applications in

geomorphology. Technical Bulletin No. 27, British Geomorphological Research Group, Geo Abstracts Ltd., Norwich. 44pp.

Chandler, R.J. (1970a). The degradation of Lias Clay slopes in an area of the East Midlands. Quarterly Journal of Engineering Geology, 2; 161-181.

Chandler, R.J. (1970b). Solifluction on low angled slopes in Northamptonshire. Quarterly Journal of Engineering Geology, 3; 65-69.

Chandler, R.J. (1970c). A shallow slab slide in the Lias Clay near Uppingham, Rutland. Géotechnique, 20; 253-260.

Chandler, R.J. (1971). Landsliding on the Jurassic escarpment near Rockingham, Northamptonshire. Institute of British Geographers Special Publication 3; 111-128.

Chandler, R.J. (1972a). Lias Clay: weathering processes and their effect on shear strength. Géotechnique, 22; 403-431.

Chandler, R.J. (1972b). Periglacial mudslides in Vest-Spitsbergen and their bearing on the origin of fossil 'Solifluction Shears' in low angle clay slopes. Quarterly Journal of Engineering Geology 5; 223-241.

Chandler, R.J. (1973). The inclination of talus, Arctic talus terraces and other slopes composed of granular materials. Journal of Geology, 81; 1-14.

Chandler, R.J. (1974). Lias Clay: the long term stability of cutting slopes. Géotechnique, 24; 21-38.

Chandler, R.J. (1982). Lias Clay slope sections and their implications for the prediction of limiting or threshold slope angles. Earth Surface Processes and Landforms, 7; 427-438.

Chandler, R.J. and Skempton, A.W. (1974). The design of permanent cutting slopes in stiff, fissured clay. Géotechnique, 24; 457-466.

Chaplow, R. (1983). Engineering geomorphological investigations of a possible landslide, Killiecrankie Pass, Scotland. Quarterly Journal of Engineering Geology, 16; 301-308.

Chappel, B.A. (1974). Deformational response of differently shaped and sized test pieces of shale rock. International Journal of Rock Mechanics and Mining Science, 11; 21-28.

Clark, A.R. and Johnson, D.K. (1975). Geotechnical mapping as an integral part of site investigation, two case

histories. Quarterly Journal of Engineering Geology, 8; 211-224.

Clayden, B. and Hollis, J.M. (1984). Criteria for differentiating soil series. Soil Survey Technical Monograph No. 17, Soil Survey, Harpenden. 132pp.

Collinson, J.D. (1969). The sedimentology of the Grindslow Shales and Kinderscout Grit: a deltaic complex in the Namurian of northern England. Journal of Sedimentary Petrology, 39; 194-221.

Conway, B.W. (1974). The Black Ven landslip, Charmouth, Dorset. An example of the effect of a secondary reservoir of ground water in an unstable area. British Geological Survey, Keyworth, Nottingham. Institute of Geological Sciences. Report No. 74/3, 16pp.

Conway, B.W. (1976). Coastal terrain evaluation and slope stability of the Charmouth/Lyme Regis area of Dorset. Institute of Geological Sciences, Geophysics Division Engineering Geology Unit. Report No. EG 76/10, British Geological Survey, Keyworth, Nottingham. 100pp.

Conway, B.W., Forster, A., Northmore, K.J. and Barclay, W.J. (1980). South Wales coalfield landslip survey. Institute of Geological Science Special Survey Division, Engineering Geology Unit. Report EG 80/4, British Geological Survey, Keyworth, Nottingham. 218pp.

Conway, B.W., Forster, A. and Northmore, K.J. (1983). A study of two landslipped areas in the South Wales Coalfield. Institute of Geological Science Engineering Geology Unit. Report EG 83/6, British Geological Survey, Keyworth, Nottingham. 68pp.

Conway, V.M. (1954). Stratigraphy and pollen analysis of southern Pennine blanket peats. Journal of Ecology, 42; 117-147.

Cooke, R.U. and Doornkamp, J.C. (1974). Geomorphology in Environmental Management. Oxford University Press, Oxford. 413pp.

Cope, F.W. (1949). Woo Dale borehole, near Buxton, Derbyshire. Quarterly Journal of the Geological Society, London, 105; 4.

Cope, F.W. (1973). Woo Dale borehole, near Buxton, Derbyshire. Nature, London (Physical Sciences), 243; 29-30.

Cotecchia, V. (1978). Systematic reconnaissance mapping and registration of slope movements. Bulletin of the

International Association of Engineering Geology, 17; 5-37.

Cratchley, C.R. and Denness, B. (1972). Engineering geology in Urban Planning with an example from the new city of Milton Keynes. Proceedings of the International Geological Congress, 24th Session, Montreal. Section 13; 13-22pp.

Cripps, J.C. and Taylor, R.K. (1981). The engineering properties of mudrocks. Quarterly Journal of Engineering Geology, 14; 325-346.

Crockett, D.H. (1966). A geologic-stability report of the proposed Snake Canyon Alpine Impoundment area, Teton, Bridger and Targhee National Forests. United States Department of Agriculture, Forest Services, Intermountain Region, Ogden, Utah. 9pp.

Crozier, M.J. (1973). Techniques for the morphometric analysis of landslips. Zeitschrift für Geomorphologie, 17; 78-101.

Crozier, M.J. (1982). A technique for predicting the probability of mudflow and rapid landslide occurrence. In: Landslides and Mudflows: Reports of Alma-Ata International Seminar October 1981. UNESCO/UNEP. Centre of International Projects, GKNT, Moscow. p. 420-430.

Crozier, M.J. (1986). Landslides: Causes, Consequences and Environment. Croom Helm, London. 252pp.

Dalrymple, J.B., Blong, R.J. and Conacher, A.J. (1968). A hypothetical nine unit landsurface model. Zeitschrift für Geomorphologie, 12; 60-76.

Daughton, G., Noake, J.S. and Siddle, H.T. (1977). Some hydrogeological aspects of hillsides in South Wales. Proceedings of the Conference on Rock Engineering, University of Newcastle-upon-Tyne. British Geotechnical Society, 1; 423-439.

Dearman, W.R. and Fookes, P.G. (1974). Engineering geological mapping for civil engineering practice in the United Kingdom. Quarterly Journal of Engineering Geology, 7; 223-256.

Deere, D.U. and Patton, F.D. (1967). Effect of pore pressure on the stability of slopes. Proceedings of the American Society of Civil Engineers, 93, No. SM4; 235-248.

DeGraff, J.V. (1977). A procedure for developing an empirical mass failure rule. In: ECOSYM - An ecosystem classification and data storage system for natural resource management. (Ed. Henderson, J.A., Davis, L.S. and Ryberg, E.M.). Department of Forestry and Outdoor Recreation, Utah State University, Logan, Utah. Appendix 33, 49pp.

DeGraff, J.V. (1978). Regional landslide evaluation: two Utah examples. Environmental Geology, 2; 203-214.

DeGraff, J.V. and Romesburg, H.C. (1980). Regional landslide susceptibility assessment for wildland management, a matrix approach. In: Thresholds in Geomorphology. (Ed., Coates, D.R. and Vitek, J.D.). Allen and Unwin, London. p. 401-414.

Denness, B. (1972a). The reservoir principle of mass movement. Institute Geological Sciences Report. No. 72/7, British Geological Survey, Keyworth, Nottingham. 13pp.

Denness, B. (1972b). End of the landslide menace. New Scientist. p. 417.

Dines, H.G., Hollingworth, S.E., Edwards, W., Buchan, S. and Welch, F.B.A. (1940). The mapping of Head deposits. Geological Magazine, 77; 198-226.

Dougherty, M.J. and Barsotti, N.J. (1972). Structural damage and potentially expansive sulphide minerals. Bulletin of the International Association of Engineering Geology, 9; 105-125.

Dunham, K.C. (1973). A recent deep borehole near Eyam, Derbyshire. Nature, 241; 84-85.

Dunne, T. and Black, R.G. (1970a). An experimental investigation of runoff production in permeable soils. Water Resources Research, 6; 478-490.

Dunne, T. and Black, R.G. (1970b). Partial area contributions to storm runoff in a small New England Watershed. Water Resources Research, 6; 1296-1311.

Durham, I.H., O'Loughlin, E.M. and Moore, I.D. (1986a). Electronic acquisition of hydrological data from intensively instrumented hillslopes. Hydrological Processes, 1; 79-87.

Durham, I.H., O'Loughlin, E.M. and Moore, I.D. (1986b). Design and circuitry of a low powered data logger for use with pulse-width modulation transducers. CSIRO Division Water and Land Resources Technical Memorandum, No. 309, 42pp.

Early, K.R. and Skempton, A.W. (1972). Investigations of the landslide at Walton's Wood, Staffordshire. Quarterly Journal of Engineering Geology, 5; 19-41.

Eden, R.A., Stevenson, I.P. and Edwards, W. (1957). Geology of the country around Sheffield. Memoir of the Geological Survey of England and Wales, HMSO, London. 238pp.

Eden, R.A., Orme, G.R., Mitchell, M. and Shirley, J. (1964). A study of part of the margin of the Carboniferous Limestone 'massif' in the Pindale area, Derbyshire. Bulletin of the Geological Survey of Great Britain, No. 21, 73-118.

Edwards, W. (1956). Geology. In: Sheffield and its Region. (Ed., Linton, D.L.). British Association for the Advancement of Science, London. p. 3-23.

Edwards, W. and Trotter, F.M. (1962). The Pennines and Adjacent Areas. British Regional Geology Survey, HMSO, London. 40pp.

Endo, T. and Tsuruta, T. (1969). On the effect of tree roots upon the shearing strength of soil. Annual Report of the Hokkaido Branch, Tokyo Forest Experiment Station, 18; 176-182.

Evans, I.S. (1972). General geomorphometry, derivatives of altitude and descriptive statistics. In: Spatial Analysis in Geomorphology. (Ed. Chorley, R.J.). Methuen, London. p. 17-90.

Evans, I.S. (1978). An integrated system of terrain analysis and slope mapping. Grant DA-ERO-591-73-G0040, Statistical characterisation of altitude matrices by computer, Report 6. Department of Geography, University of Durham. 192pp.

Farhan, Y.I. (1976). A geomorphological engineering approach to terrain classification. Unpublished Ph.D. Thesis, University of Wales, Swansea. 355pp.

Farhan, Y.I. (1978). Terrain classification based on engineering geomorphological parameters: a multivariate approach. Proceedings of the Digital Terrain Models (DTM) Symposium, St. Louis, Missouri. p. 428-464.

Fasiska, E., Wagenblast, N. and Dougherty, M.T. (1974). The oxidation mechanism of sulphide minerals. Bulletin of the Association of Engineering Geologists, 11, p. 75-82.

Flint, R.F. (1971). Glacial and Quarternary Geology. Wiley, New York. 892pp.

Fookes, P.G. and Wilson, D.D. (1966). The geometry of discontinuities and slope failures in Siwalik Clay. Géotechnique, 16; 305-320.

Ford, T.D. (1966). The underground drainage systems of the Castleton area, Derbyshire, and their evolution. Cave Science, 5; 369-396.

Ford, T.D. (1977). Limestones and Caves of the Peak District. Geo Abstracts Ltd., University of East Anglia, Norwich. 469pp.

Ford, T.D. and Burek, C.V. (1977). Anomalous Limestone gorges in Derbyshire. Mercian Geologist, 6; 59-66.

Ford, T.D., Gascoyne, M. and Beck, J.S. (1983). Speleothem dates and Pleistocene chronology. Cave Science, 10; 103-15.

Franklin, J.A. and Chandra, R. (1972). The slake durability test. International Journal of Rock Mechanics and Mining Science, 9; 325-341.

Franks, J.F. and Johnson, R.H. (1964). Pollen analytical dating of a Derbyshire landslip. New Phytologist, 63; 209-216.

Franklin, J., Manailoglou, J. and Sherwood, D. (1974). Field determination of direct shear strength. Proceedings of the 3rd Congress of the International Society for Rock Mechanics, Denver. 2A; 233-240.

Fu, K.S. (1974). Syntactic Methods in Pattern Recognition. Academic Press, New York. 295pp.

Garrels, R.M. and Thompson, M.E. (1960). Oxidation of pyrite by iron sulfate solutions. American Journal of Science, 258a; 57-67.

Geological Society Engineering Group Working Party (1972). The preparation of maps and plans in terms of engineering geology. Quarterly Journal of Engineering Geology, 5; 293-381.

Geological Society of London (1983). Working Party reports on land surface evaluation. Quarterly Journal of Engineering Geology, 15; 1-168.

Germann, P.F. (1986). Rapid drainage response to precipitation. Hydrological Processes, 1; 3-13.

Germann, P. and Beven, K. (1986). A distribution function approach to water flow in soil micropores based on kinematric wave theory. Journal of Hydrology, 83; 173-183.

Gerrard, A.J.W. and Robinson, D.A. (1971). Variability in slope measurements. Transactions of the Institute of British Geographers, 54; 45-54.

Gibson, H. and Wedd, C.B. (1913). The geology of the northern part of the Derbyshire coal field and bordering tracts. Memoirs of the Geological Survey of Great Britain. H.M.S.O., London. 186pp.

Gil, E., Gilot, E.G., Kotarba, A., Starkel, L. and Szczepanek, K. (1974). An early Holocene landslide in the Neski Beskid and its significance for palaeogeographical reconstructions. Studia Geomorphologica Carpatho-Balcanica, Krakow, 8; 69-83.

Godwin, H., Suggate, R. and Willis, E. (1958). Radiocarbon dating of the eustatic rise in ocean level. Nature, 181; 1518-1519.

Goudie, A. (1981). Geomorphological Techniques. Allen & Unwin, London. 395pp.

Gray, D.H. (1970). Effects of forest clear-cutting on the stability of natural slopes. Bulletin of the Association of Engineering Geology, 7; 45-66.

Green, A.H., Le Neve Foster, C. and Dakyns, J.R. (1887). The geology of the Carboniferous Limestone, Yoredale Rocks and Millstone Grit of north Derbyshire. Memoirs of the Geological Survey of England and Wales. HMSO, London. 212pp.

Greensmith, J.T. (1956). Sedimentary structures in the Upper Carboniferous of north and central Derbyshire, England. Journal of Sedimentary Petrology, 26; 345-355.

Greensmith, J.T. (1957). Lithology, with particular reference to cementation of upper Carboniferous sandstones in north Derbyshire, England. Journal of Sedimentary Petrology, 27; 405-416.

Greensmith, J.T. (1960). Upper Carboniferous sedimentation in Derbyshire. Journal of Sedimentary Petrology, 30; 628.

Grice, R.H. (1969). Test procedures for the susceptibility of shale to weathering. Proceedings of the 7th International Conference on Soil Mechanics Foundation Engineering, Mexico City, 3; 884-889.

Gurnell, A.M. (1978). The dynamics of a drainage network. Nordic Hydrology, 9; 293-306.

Gurnell, A.M. (1981). Heathland vegetation, soil moisture and dynamic contributing area. Earth Surface Processes and Landforms, 6; 553-570.

Hanna, T.H. (1985). Field Instrumentation in Geotechnical Engineering. Trans-Technical Publications, Cleveland, Ohio. 843pp.

Hansen, A. (1984). Landslide hazard analysis. In: Slope Instability. (Ed. Brunsden, D. and Prior, D.B.). Wiley, Chichester, p. 523-602.

Harper, T.R. (1975). The transient groundwater pressure response to rainfall and the prediction of rock slope instability. International Journal Rock Mechanics and Mining Science Geomechanics Abstracts, 12; 175-179.

Harrison, D.J. and Adlam, K.A.M. (1984). The limestone and dolomite resources of the Peak District of Derbyshire and Staffordshire. Description of parts of 1:50,000 geological sheets 99, 111, 112 and 125. Mineral Assessment Report, British Geological Survey No. 144. HMSO, London. 45pp.

Hawke-Smith, C. (1981). Landuse, burial practice and territories in the Peak District, Circa 2000-1000 BC. In: Prehistoric Communities in Northern England. (Ed. Barker, G.). Sheffield University Department of Prehistory and Archaeology.

Hawkins, A.B. and Privett, K.D. (1979). Engineering geomorphological mapping as a technique to elucidate areas of superficial structures; with examples from the Bath area of the south Cotswolds. Quarterly Journal of Engineering Geology, 12; 221-233.

Headworth, H.G. (1972). The analysis of natural groundwater level fluctuations in the chalk of Hampshire. Journal of the Institution Sanitary Engineers, 37; 107-124.

Henkel, D.J. (1967). Local geology and the stability of natural slopes. American Society of Civil Engineers Journal of Soil Mechanics and Foundation Engineering Division, 93; 437-446.

Henkel, D.J. and Skempton, A.W. (1954). A landslide at Jackfield, Shropshire, in an over-consolidated clay. Proceedings of the Conference on the Stability of Earth Slopes, Stockholm, 1; 90-101.

Hewlett, J.D. and Hibbert, A.R. (1967). Factors affecting the response of small watersheds to precipitation in humid areas. In: Forest Hydrology. (Ed. Sopper, W.E. and Lull, H.W.). Pergamon, Oxford, p. 275-290.

Hicks, S.P. (1971). Pollen analytical evidence for the effect of prehistoric agriculture on the vegetation of north Derbyshire. New Phytologist, 70; 647-67.

Higginbottom, I.E. and Fookes, P.G. (1971). Engineering aspects of periglacial features in Britain. Quarterly Journal of Engineering Geology, 3; 85-117.

Hill, H.P. (1949). The Ladybower Reservoir. Journal of the Institution of Water Engineers, 3; 414-433.

Hodge, R.A.L. and Freeze, R.A. (1977). Ground water flow systems and slope stability. Canadian Geotechnical Journal, 14; 466-476.

Hoek, E. and Bray, J.W. (1977). Rock Slope Engineering, 2nd Edition, Institute of Mining & Metallurgy, London. 402pp.

Hollingworth, S.E., Taylor, J.H. and Kellaway, G.A. (1944). Large scale superficial structures in the Northampton Ironstone field. Quarterly Journal of the Geological Society, London; 100; 1-44.

Höltz, W.G. (1960). Effect of gravel particles on the friction angle. Proceedings of the American Society of Civil Engineers, Research Conference on Shear Strength of cohesive soils. Boulder, Colorado, 1, 1000-1001.

Hudson, R.G.S. (1943). The Namurian of Alport Dale, Derbyshire. Proceedings of Yorkshire Geological Society, 25; 142-73.

Hudson, R.G.S. and Cotton, G. (1945). The carboniferous rocks of the Edale anticline, Derbyshire. Quarterly Journal of the Geological Society, London, 101; 1-36.

Hutchinson, J.N. (1965). The stability of cliffs composed of soft rocks with particular reference to the coasts of south-east England. Unpublished Ph.D. Thesis, University of Cambridge.

Hutchinson, J.N. (1968a). The free degradation of London Clay cliffs. Proceedings of the Geotechnical Conference on Shear Strength Properties of Natural Soils and Rocks, Norwegian Geotechnical Institute, Oslo, 1; 113-118.

Hutchinson, J.N. (1968b). Surveys of coastal landslides, Kent. Building Research Station, Report EN 35/65. Building Research Establishment, Watford.

Hutchinson, J.N. (1968c). Surveys of coastal landslides, Essex and south Suffolk. Building Research Station, Report EN 35/67. Building Research Establishment, Watford.

Hutchinson, J.N. (1968d). Field meeting on the coastal landslides of Kent. Proceedings of the Geologists' Association, 79; 227-37.

Hutchinson, J.N. (1968e). Mass movement. In: Encyclopaedia of Earth Science. (Ed. Fairbridge, R.W.). Reinhold, New York, p. 688-695.

Hutchinson, J.N. (1969). A reconsideration of the coastal landslides at Folkestone Warren, Kent. Géotechnique, 19; 6-38.

Hutchinson, J.N. (1970). A coastal mudflow on the London Clay cliffs at Beltinge, North Kent. Géotechnique, 20; 412-438.

Hutchinson, J.N. (1971a). The response of London Clay cliffs to differing rates of erosion. Proceedings of a Conference on Natural Slope Stability and Conservation I.R.P.I., Naples, 1, 47-65.

Hutchinson, J.N. (1971b). Field and laboratory studies of a fall in Upper Chalk cliffs at Joss Bay, Isle of Thanet. In: Stress - Strain Behaviour of Soils. (Ed. Parry, R.H.G.). Roscoe Memorial Symposium, Cambridge University, p. 692-706.

Hutchinson, J.N. (1973). The response of London Clay cliffs to differing rates of toe erosion. Geologia applicata Idrogeologia, 8; 221-239.

Hutchinson, J.N. and Brunsden, D. (1974). Mudflows: a review and classification (abstract). Quarterly Journal of Engineering Geology, 7; 328.

Hutchinson, J.N. and Gostelow, T.P. (1976). The development of an abandoned cliff in London Clay at Hadleigh, Essex. Philosophical Transactions of the Royal Society, London, Series A, 283; 557-604.

Ingold, T.S. (1975). The stability of highways in landslipped areas. The Highway Engineer, 12; 14-22.

Ives, J.D. and Bovis, M.J. (1978). Natural hazard maps for landuse planning, San Juan Mountains, Colorado, U.S.A. Arctic and Alpine Research, 10; 185-212.

Jacobi, R.M., Tallis, J.H. and Mellars, P.A. (1976). The southern Pennine Mesolithic and ecological record. Journal of Archaeological Science, 3; 307-320.

Jackson, J.W. (1925). The relation of the Edale Shales to the Carboniferous Limestones in north Derbyshire. Geological Magazine, 62; 267-274.

Jackson, J.W. (1927). The succession below the Kinderscout Grit in north Derbyshire. Journal of the Manchester Geological Association, 1; 15-32.

Jackson, R.J. (1966). Slips in relation to rainfall and soil characteristics. Journal of Hydrology (New Zealand), 5; 45-53.

James, P.M. (1969). In situ shear tests at Muda Dam. Proceedings of the 7th International Conference on Soil

Mechanics and Foundation Engineering, Mexico City, 1, 75-81.

Johnson, R.H. (1957). An examination of the drainage pattern of the eastern part of the Peak District of north Derbyshire. Geographical Studies, 4; 46-55.

Johnson, R.H. (1965). A study of the Charlesworth landslides near Glossop, north Derbyshire. Transactions of the Institute British Geographers, 37; 111-126.

Johnson, R.H. (1967). Some glacial, periglacial and karstic landforms in the Sparrowpit-Dove Holes area of north Derbyshire. East Midland Geographer, 4; 421-426.

Johnson, R.H. (1968). Four temporary exposures of solifluction deposits on Pennine hillslopes in north east Cheshire. Mercian Geologist, 2; 379-387.

Johnson, R.H. (1969a). The glacial geomorphology of the area around Hyde, Cheshire. Proceedings of the Yorkshire Geological Society, 37; 189-230.

Johnson, R.H. (1969b). The Derwent - Wye confluence re-examined. East Midland Geographer, 4; 421-426.

Johnson, R.H. (1980). Hillslope stability and landslide hazard: a case study for Longdendale, north Derbyshire, England. Proceedings of the Geologists' Association, 91; 315-325.

Johnson, R.H. (1981). Four maps for Longdendale: a geomorphological contribution to environmental management in an upland Pennine valley. Manchester Geographer, 2; 6-34.

Johnson, R.H. and Walthall, S. (1979). The Longdendale landslides. Geological Journal, 14; 135-58.

Jones, H.E. (1971). Comparative studies of plant growth and distribution in relation to waterlogging. III. The response of Erica cinerea L. to waterlogging in peat soils of differing iron content. Journal of Ecology, 59; 583-591.

Jones, H.E. and Etherington, J.R. (1970). Comparative studies of plant growth and distribution in relation to waterlogging. I. The Survival of Erica cinerea L. and Erica tetralix L. and its apparent relationship to iron and manganese uptake in waterlogged soils. Journal of Ecology, 58; 487-496.

Jones, O.T. (1942). The structure of the Edale Mam Tor and Castleton area. Geological Magazine, 79; 188-96.

Kawakami, H. and Abe, H. (1970). Shear characteristics of saturated gravelly clays. Transactions of the Japanese Society of Civil Engineers, 2; 295-8.

Kellaway, G.A. and Taylor, J.H. (1968). The influence of landslipping on the development of the City of Bath, England. Proceedings of the 23rd International Geological Congress, Czechoslovakia. Session 12; 65-76.

Kennard, M.F., Knill, J.L. and Vaughan, P.R. (1967). The geotechnical properties and behaviour of Carboniferous shale at Balderhead Dam. Quarterly Journal of Engineering Geology, 1; 3-24.

Kent, P.E. (1966). The structure of the concealed Carboniferous rocks of north-eastern England. Proceedings of the Yorkshire Geological Society, 35; 323-52.

Kesseli, J.E. (1943). Disintegrating soil slips of the coast ranges of Central California. Journal of Geology, 51; 342-352.

Kienholz, H. (1978). Maps of geomorphology and natural hazards of Grindelwald, Switzerland, Scale 1:10,000. Arctic and Alpine Research, 10; 169-184.

Kindswater, C.E. and Carter, R.W. (1959). Discharge characteristics of rectangular thin-plate weirs. Proceedings of the American Society of Civil Engineers, 124; 772-822.

King, H.W. (1954). Handbook of Hydraulics. IV Ed., McGraw-Hill, London, 556pp.

Kirkby, M.J. (1973). Landslides and weathering rates. Geologia Applicata e Idrogeologia, Bari, 8; 171-183.

Kirkby, M.J., Callen, J., Weyman, D.R. and Wood, J. (1976). Measurement and modelling of dynamic contributing areas in very small catchments. Working Paper No. 167, Department of Geography, University of Leeds. 19pp.

Kirkby, M.J. and Chorley, R.J. (1967). Throughflow, overland flow and erosion. Bulletin of the International Association of Scientific Hydrology, 12; 5-21.

Krinitzsky, E.L. and Kolb, C.R. (1969). Geological influences on the stability of clay shale slopes. Proceedings of the 7th Symposium on Engineering Geology and Soils Engineering, Moscow, Idaho. Idaho Department of Highways, Idaho State University; 160-175.

Kyunttsel, V.V., Maksimov, M.M. and Sheko, A.I. (1978). Experience of a regional prediction of some exogenic geologic processes. Proceedings of the 3rd

International Conference of the International
Association of Engineering Geologists. Section 1,
112-228.

Laird, R.T., Perkins, J.B., Bainbridge, D.A., Baker, J.B.,
Boyd, R.T., Huntsman, D., Staub, P.E. and Zucker, H.B.
(1979). Quantitative land-capability analysis. United
States Geological Survey Professional Paper, 945.
115pp.

Lamb, H.H. (1966). The Changing Climate: Selected papers.
Methuen, London. 236pp.

Lambe, T.W. and Whitman, R.V. (1969). Soil Mechanics.
Wiley, New York. 553pp.

Leadbeater, A.D. (1985). A57 Snake Pass, remedial work to
slip near Alport Bridge. In: Failures in Earthworks.
Thomas Telford Ltd., London, p. 29-38.

Leighton, F.B. (1976). Urban Landslides: targets for land-
use planning in California. In: Urban Geomorphology
(Ed. Coates, D.R.). Geological Society of America
Special Paper, 174; 37-60.

Lenz, A.T. (1943). Viscosity and surface tension effects on
V-notch Weir Coefficients. Proceedings of the American
Society Civil Engineers, 69; 759-802.

Linton, D.L. (1951). Midland drainage: some considerations
bearing on its origin. British Association for the
Advancement of Science, London, 7; 449-56.

Linton, D.L. (1956). Geomorphology. In: Sheffield and its
Region. (Ed. Linton, D.L.). British Association for
the Advancement of Science, London, p. 24-43.
Linton, D.L. (1963). Geomorphology of the southern
Pennines. In: Field Studies in the British Isles.
(Ed. Steers, J.). Nelson, London. p. 138-154.

Lockwood, J.G. and Venkatasawmy, K. (1975). Evapotrans-
piration and soil moisture in upland grass catchments
in the eastern Pennines. Journal of Hydrology, 26;
79-94.

Lumb, P. (1966). The variability of natural soils.
Canadian Geotechnical Journal, 3; 74-97.

Lumb, P. (1972). Probabilistic aspects of slope stability.
Proceedings of the 1st International Symposium on
Landslide Control, Japanese Society of Landslides.
Kyoto, Japan. 1; 125-128.

Manley, G. (1959). The late-glacial climate of north-west
England. Liverpool and Manchester Geological Journal,
2; 188-215.

Maroof, S.I. (1976). The structure of the concealed pre-Carboniferous basement of the Derbyshire Dome from gravity data. Proceedings of the Yorkshire Geological Society, 41; 59-69.

Martin, R.P. (1978). The application of some low-cost geomorphological techniques to highway engineering, with special reference to mass movement. Unpublished Ph.D. Thesis University of London. 494pp.

Matula, M. and Nemčok, A. (1965). Verbreitung und Charakter der Rutschungen in Westkarpaten. Proceedings of the 7th Congress CBGA, Sofia, Section 5; 103-110.

McArthur, J.L. (1977). Quaternary erosion in the upper Derwent basis and its bearing on the age of surface features in the southern Pennines. Transactions of the Institute of British Geographers, 2; 490-497.

McArthur, J.L. (1981). Periglacial slope planation in the southern Pennines, England. Biuletyn Peryglacjainy, 28; 85-97.

McGreal, W.S. and Craig, D. (1982). Mass movement activity: an illustration of differing responses to groundwater conditions from two sites in Northern Ireland. Irish Geographer, 10; 28-35.

Mead, W.J. (1936). Engineering geology of dam sites. Transactions of the 2nd International Congress on Large Dams, Washington, D.C., 4; 183-198.

Melton, M.A. (1965). Debris-covered hillslopes of the Southern Arizona Desert, consideration of their stability and sediment contribution. Journal of Geology, 73; 715-729.

Mitchell, J.K. (1976). Fundamentals of Soil Behaviour. Wiley, New York. 522pp.

Mitchell, G.F., Penny, L.F., Shotton, F.W. and West, R.C. (1973). A correlation of Quaternary deposits in the British Isles. Geological Society of London, Special Report No. 4, 99pp.

Moon, B.P. (1984). Refinement of a technique for determining rock mass strength for geomorphological purposes. Earth Surface Processes and Landforms, 9; 189-193.

Morgenstern, N.R. and Eigenbrod, M.D. (1974). Classification of argillaceous soil and rocks. Proceedings of the American Society Civil Engineers, Journal of the Geotechnical Engineering Division, GT10, 100; 1137-56.

Muller, R. (1979). Investigating the age of a Pennine landslip. Mercian Geologist, 7; 211-218.

Nemčok, A., Pašek, J. and Rybář, J. (1972). Classification of landslides and other mass movements. Rock Mechanics, 4; 71-78.

Newman, E.B., Paradis, A.R. and Brabb, E.E. (1978). Feasibility and cost of using a computer to prepare landslide susceptibility maps of the San Francisco Bay region of California. United States Geological Survey Bulletin No. 1443. 27pp.

Nilsen, T.H., Taylor, F.A. and Brabb, E.E. (1976a). Recent landslides in Alameda County, California (1940-71): an estimate of economic losses and correlations with slope, rainfall and ancient landslide deposits. United States Geological Survey Bulletin No. 1398. 21pp.

Nilsen, T.H., Taylor, F.A. and Dean, R.M. (1976b). Natural conditions that control landsliding in the San Francisco Bay region: an analysis based on data from the 1968-69 and 1972-73 rainy seasons. United States Geological Survey Bulletin No. 1424. 35pp.

Nilsen, T.H., Wright, R.H., Vlasic, T.C. and Spangle, W. (1979). Relative slope stability and land-use planning in the San Francisco Bay region, California. United States Geological Survey Professional Paper No. 944. 96pp.

Norman, J.W. (1970). The photogeological detection of unstable ground. Journal of the Institute of Highway Engineers, 17; 19-22.

Norman, J.W., Leibowitz, T.H. and Fookes, P.G. (1975). Factors affecting the detection of slope instability with air photographs in an area near Sevenoaks, Kent. Quarterly Journal of Engineering Geology, 8; 159-176.

Northmore, K.J., Denness, B. and Conway, B.W. (1977). South Essex geological and geotechnical survey. Part 3. Engineering Geology. Institute of Geological Sciences, Report 1406, 100, 3/77. British Geological Survey, Keyworth, Nottingham. 104pp.

Okimura, T. (1983). Rapid mass movement and groundwater level movement. Zeitschrift für Geomorphologie, 46; 35-54.

O'Loughlin, C.L. (1974). The effect of timber removal on the stability of forest soils. Journal of Hydrology, (New Zealand) 13; 121-134.

O'Loughlin, C.L. and Pearce, A.J. (1976). Influence of Cenozoic geology on mass movement and sediment yield response to forest removal, north Westland, New Zealand. Bulletin of the International Association of Engineering Geology, 14; 41-46.

Palmer, J. and Radley, J. (1961). Gritstone tors of the English Pennines. Zeitschrift für Geomorphologie, 5; 37-52.

Parkinson, D. (1947). The Lower Carboniferous of the Castleton district, Derbyshire. Proceedings Yorkshire Geological Society, 27; 99-124.

Parkinson, D. (1957). The Lower Carboniferous reefs of north England. Bulletin of the American Association of Petrology and Geology, 41; 511-37.

Parkinson, D. (1965). Aspects of the Carboniferous stratigraphy of the Castleton-Treak area of north Derbyshire. Mercian Geologist, 1; 161-80.

Pašek, J., Rybář, J. and Špůrek, M. (1977). Systematic registration of slope deformation in Czechosolvakia. Bulletin of the International Association of Engineering Geology, 16; 48-51.

Patton, F.D. (1966). Multiple modes of shear failure in rock. Proceedings of the 1st International Congress on Rock Mechanics, Lisbon, 1; 509-513.

Peltier, L.C. (1950). The geographic cycle in periglacial regions as it is related to climatic geomorphology. Annals of the Association of American Geographers, 40; 214-236.

Pitty, A.F. (1966). Some problems in the location and delimitation of slope profiles. Zeitschrift für Geomorphologie, 10; 454-461.

Pitty, A.F. (1967). Some problems in selecting a ground surface length for slope angle measurement. Revue de Geomorphologie Dynamique, 17; 66-71.

Pitty, A.F. (1968). A simple device for the measurement of hillslopes. Journal of Geology, 76; 717-720.

Pitty, A.F. (1969). A scheme for hillslope analysis. I. Initial considerations and calculations. University of Hull, Occasional Publication, Department of Geography, No. 9. 8pp.

Prentice, J.E. and Morris, P.G. (1959). Cemented screes in the Manifold Valley. East Midland Geographer, 4; 275-280.

Quigley, R.M. and Vogan, R.W. (1970). Black shale heaving at Ottawa, Canada. Canadian Geotechnical Journal, 7; 106-115.

Radbruch-Hall, D.H. (1978). Gravitational creep of rock masses on slopes. In: Rockslides and Avalanches. (Ed. Voight, B.). Developments in Geotechnical Engineering, 14A. Elsevier, Amsterdam. p. 607-654.

Radbruch-Hall, D.G., Varnes, D.J. and Colton, R.B. (1977).
    Gravitational spreadings of steep sided ridges
    ('Sackung') in Colorado. <u>Journal of Research, United
    States Geological Survey</u>, 5; 359-363.

Ramsbottom, W.H.C. (1966). A pictorial diagram of the
    Namurian rocks of the Pennines. <u>Transactions of the
    Leeds Geological Association</u>, 7; 181-184.

Ramsbottom, W.H.C., Rhys, G.H. and Smith, E.G. (1962).
    Boreholes in the Carboniferous rocks of the Ashover
    District Derbyshire. <u>Bulletin of the Geological Survey
    Great Britain</u>, 19; 75-168.

Rapp, A. (1960). Recent development of mountain slopes in
    Karkevagge and surroundings, north Scandinavia.
    <u>Geografisca Annaler</u>, 42; 65-200.

Raynar, D.H. (1953). The Lower Carboniferous Rocks in the
    north of England: a review. <u>Proceedings Yorkshire
    Geological Society</u>, 28; 231-315.

Reading, H.G. (1964). A review of the factors affecting the
    sedimentation of Millstone Grit (Namurian) in the
    Central Pennines. In: <u>Deltaic and Shallow Marine
    Deposits</u> (Ed. Van Straaten, L.). Elsevier, Amsterdam.
    p. 340-346.

Redda, A. (1986). Landform development in the Vale of
    Edale. <u>Unpublished Ph.D. Thesis, University of
    Sheffield</u>.

Rice, R.M., Corbett, E.S. and Bailey, R.G. (1969). Soil
    slips related to vegetation, topography and soil in
    southern California. <u>Water Resources Research</u>, 5;
    647-659.

Rice, R.M. and Foggin, G.T. (1971). Effect of high
    intensity storms on soil slippage on mountainous
    watersheds in Southern California. <u>Water Resources
    Research</u>, 7; 1485-1496.

Robinson, G. (1966). Some residual hillslopes in the Great
    Fish River Basin, South Africa. <u>Geographical Journal</u>,
    132; 386-90.

Rogers, N.W. and Selby, M.J. (1980). Mechanisms of shallow
    translational landsliding during Summer rainstorms:
    North Island, New Zealand. <u>Geografiska Annaler</u>, 62A;
    11-21.

Rouse, W.C. (1969). An investigation of stability and
    frequency distribution of slopes in selected areas of
    West Glamorgan. <u>Unpublished Ph.D. Thesis, University
    of Wales</u>. 274pp.

Rouse, W.C. (1975). Engineering properties and slope form in Granular soil. Engineering Geology, 9; 221-235.

Rouse, W.C. and Farhan, Y.I. (1976). Threshold slopes in South Wales. Quarterly Journal of Engineering Geology, 9; 327-338.

Rutter, A.J. (1955). The composition of wet-heath vegetation in relation to the water table. Journal of Ecology, 43; 507-543.

Rybar, J., Pašek, J. and Repka, L. (1965). Dokumentation der systematischen untersuchung der rutschugsgebiete in der Tschechoslowakei. Engineering Geology, 1; 21-29.

Said, M. (1969). The Pleistocene Geomorphology of the Burbage Basin (Southern Pennines). Unpublished Ph.D. Thesis, University of Sheffield. 246pp.

Savigear, R.A.G. (1956). Technique and terminology in the investigation of slope forms. Union Geographical International; Premier Rapport de la Commission pour l'etude des versants, Rio de Janeiro, 66-75.

Scheidegger, A.E. (1970). The rheology of rock creep. Rock Mechanics, 2; 138-45.

Scheidegger, A.E. (1975). Physical Aspects of Natural Catastrophes. Elsevier, Amsterdam. 289pp.

Selby, M.J. (1976). Slope erosion due to extreme rainfall: a case study from New Zealand. Geografiska Annaler, 58A; 131-8.

Selby, M.J. (1980). A rock mass strength classification for geomorphic purposes, with tests from Antarctica and New Zealand. Zeitschrift für Geomorphologie, 24; 31-51.

Selby, M.J. (1982a). Hillslope Materials and Processes. Oxford University Press, Oxford. 264pp.

Selby, M.J. (1982b). Controls on the stability and inclinations of hillslopes formed on hard rock. Earth Surface Processes and Landforms, 7; 449-469.

Selby, M.J. (1982c). Rock mass strength and the form of some inselbergs in the central Namib Desert. Earth Surface Processes and Landforms, 7; 489-497.

Sheko, A.I. (1977). Theoretical principles of regional temporal prediction of landslide activation. Bulletin of the International Association of Engineering Geology, 16; 67-68.

Sherwood, P.T. (1970). The reproductibility of the results of soil classification and compaction tests. Transport and Road Research Laboratory Report, LR339. Crowthorne, Berks. 33pp.

Sherwood, P.T. and Ryley, M.D. (1970). An investigation of a cone penetrometer method for the determination of the liquid limit. Géotechnique, 20; 203-208.

Simpson, I.M. (1982). The Peak District Rocks and Fossils: A Geological Field Guide. Unwin, London, 120pp.

Sissons, J.B. (1954). Erosion surfaces and drainage systems of south-west Yorkshire. Proceedings of the Yorkshire Geological Society, 29;305-42.

Skempton, A.W. (1964). Long term stability of clay slopes. Géotechnique, 14; 77-101.

Skempton, A.W. (1970). First time slides in over-consolidated clay slopes. Géotechnique, 20; 320-324.

Skempton, A.W. and DeLory, F.A. (1957). Stability of natural slopes in London Clay. Géotechnique, 20; 320-324.

Skempton, A.W. and Hutchinson, J.N. (1969). Stability of natural slopes and embankment foundations. Proceedings of the 7th International Conference on Soil Mechanics and Foundation Engineering, Mexico, 1; 291-340.

Skempton, A.W. and Hutchinson, J.N. (1976). A discussion on valley slopes and cliffs in southern England: morphology, mechanics and Quaternary history. Philosophical Transactions of the Royal Society, London. Series A, 283; 421-635.

Skempton, A.W. and La Rochelle, P. (1965). The Bradwell Slip, a short term failure in London Clay. Géotechnique, 15; 221-242.

Skempton, A.W. and Petley, D.J. (1967). The strength along structural discontinuities. Proceedings of the European Conference on Soil Mechanics and Foundation Engineering, Oslo, 2; 3-20.

Skempton, A.W. and Weeks, A.G. (1976). The Quarternary history of the Lower Greensand escarpment and Weald Clay vale near Sevenoaks, Kent. Philosophical Transactions of the Royal Society, London, Series A, 283; 493-526.

So, C.L. (1971). Mass movements associated with the rainstorm of June 1966 in Hong Kong. Transactions of the Institute of British Geographers, 53; 55-65.

Sowers, G.F. and Royster, D.L. (1978). Field Investigation. In: Landslides: Analysis and Control. (Eds. Schuster, R.L. and Krizek, R.J.). Transportation Research Board, National Academy of Sciences, Washington DC, Special Report, 176; 81-111.

Spears, D.A. and Amin, M.A. (1981). A mineralogical and geochemical study of turbidite sandstones and interbedded shales, Mam Tor, Derbyshire, UK. Clay Minerals, 16; 333-345.

Speight, J.G. (1971). Log normality of slope distributions. Zeitschrift für Geomorphologie, 15; 290-312.

Starkel, L. (1976). The role of extreme (catastrophic) meterological events in contemporary evolution of slopes. In: Geomorphology and Climate. (Ed. Derbyshire, E.). Wiley, London. p. 203-246.

Statham, I. (1975). Some limitations to the applications of the concept of angle of repose to natural hillslopes. Area, 7; 264-8.

Stefanovic, P., Radwan, M.M. and Tempfli, K. (1977). Digital terrain models: data acquisition, processing and applications. Journal of the International Training Centre for Aerial Survey, Delft, 1; 61-76.

Stevenson, I.P. and Gaunt, G.D. (1971). Geology of the country around Chapel-en-le-Frith. Memoirs of the Geological Survey of England and Wales. HMSO, London. pp444.

Steward, H.E. and Cripps, J.C. (1983). Some engineering implications of chemical weathering of pyritic shale. Quarterly Journal of Engineering Geology, 16; 281-289.

Strahler, A.N. (1950). Equilibrium theory of erosional slopes approached by frequency distribution analysis. American Journal of Science, 248; 673-696, 800-814.

Straw, A. (1968). A Pleistocene diversion of drainage in northern Derbyshire. East Midland Geographer, 4; 275-80.

Straw, A. and Lewis, G.M. (1962). Glacial drifts in the area around Bakewell, Derbyshire. East Midland Geographer, 18; 72-80.

Summerfield, M.A. (1976). Slope form and basal stream relationships: a case study in the Derwent Basin of the southern Pennines, England. Earth Surface Processes and Landforms, 1; 89-96.

Sylvester-Bradley, P.C. and Ford, T.D. (1968). The Geology of the East Midlands. Leicester University Press, Leicester. 400pp.

Tallis, J.H. (1964a). Studies on southern Pennine peats: Part I. The general pollen record. Journal of Ecology, 52; 323-331.

Tallis, J.H. (1964b). The pre-peat vegetation of the southern Pennines. New Phytologist, 63; 363-373.

Tallis, J.H. and Switsur, V.R. (1974). Studies on southern Pennine peats VI: a radiocarbon-dated pollen diagram from Featherbed Moss, Derbyshire. Journal of Ecology, 62; 743-51.

Tallis, J.H. and Johnson, R.H. (1980). The dating of landslides in Longdendale, north Derbyshire, using pollen analytical techniques. In: Timescales in Geomorphology. (Ed. Cullingford, R.A., Davidson, D.A. and Lewin, J.), Wiley, Chichester. p. 189-207.

Tallis, J.H. and Switsur, V.R. (1983). Forest and moorland in the South Pennine uplands in the mid-Flandrian period. I. Macro-fossil evidence of the former forest cover. Journal of Ecology, 71; 585-600.

Tanaka, S. (1963). On the forecast of the occurrence sites on mountain-slides. Report of the Construction Engineering Research Institute Foundation, Tokyo, 4; 147-161. (In Japanese, English summary).

Tanaka, S. and Okimura, T. (1972). Research on slope slides caused by heavy rain which hit Banshu area on 18th July 1971. Report of the Construction Engineering Research Institute Foundation, Tokyo, 14; 39-52. (In Japanese, English summary).

Taylor, D.W. (1937). Stability of earth slopes. Journal of the Boston Society of Civil Engineers, 24; 197-246.

Taylor, R.K. and Spears, D.A. (1970). The breakdown of British Coal Measure rocks. International Journal of Rock Mechanics and Mining Science, 7; 481-501.

Terzaghi, K. (1931). Earth slips and subsidences from underground erosion. Engineerings News-Record, 107; 90-92.

Terzaghi, K. (1950). Mechanism of landslides. In: Application of Geology to Engineering Practice (Berkeley Volume, New York). Geological Society of America, p. 83-125.

Terzaghi, K. (1962). Stability of steep slopes on hard weathered rock. Géotechnique, 12; 251-70.

Tennessee Valley Authority (1965). Area-stream factor correlation. Bulletin of the International Association of Scientific Hydrology, 10; 22-37.

Thrower, N.J.W. and Cooke, R.U. (1968). Scales for determining slope from topographic maps. The Professional Geographer, 20; 181-186.

Tilmann, S.E., Upchurch, S.B. and Ryder, G. (1975). Landuse site reconnaissance by computer-assisted derivative

mapping. Bulletin of the Geological Society of America, 86; 23-24.

Van Breeman, N. (1972). Soil forming processses in acid sulphate soils. In: Acid Sulphate Soils. (Ed. Dost, H.). Proceedings of the International Symposium on Acid Sulphate Soils, Wageningen, Netherlands. p. 96-101.

Vargas, M. (1971). Effect of rainfall and groundwater levels. Proceedings of the 4th Pan-American Conference on Soil Mechanics and Foundation Engineering, New York, 1; 138-141.

Vargas, M. and Pichler, E. (1957). Residual soil and rock slides in Santos, Brazil. Proceedings of the 4th International Conference on Soil Mechanics and Foundation Engineering, London, 2; 394-398.

Varnes, D.J. (1958). Landslide types and processes. In: Landslides and Engineering Practice. (Ed. Eckel, E.B.). Highway Research Board, Washington, Special Report, 29; NAS-NRC Publication 544; p. 20-47.

Varnes, D.J. (1978). Slope movements, types and processes. In: Landslides, Analysis and Control. (Eds. Schuster, R.L. and Krizek, R.J.). National Academy of Science, Special Report, 76, Washington, U.S.A., p. 11-33.

Varnes, D.J. and the International Association of Engineering Geologists. Communication on landslides and other mass movements on slopes (1984). Landslide Hazard Zonation: a Review of Principles and Practice, UNESCO. 63pp.

Vaughan, P.R. (1976). The deformation of the Empingham Valley slope. Philosophical Transactions of the Royal Society, London. Series A, 283; 451-462.

Vear, A. and Curtis, C.D. (1981). A quantitative evaluation of pyrite weathering. Earth Surface Processes and Landforms, 6; 191-8.

Vücetic, R. (1958). Determination of shear strength and other characteristics of coarse clayey schist material compacted by a pneumatic wheel roller. Proceedings of the 6th International Congress on Large Dams, Brussels, 4; 465-73.

Waldron, L.J. (1977). The shear resistance of root-permeated homogeneous and stratified soil. Soil Science Society of America Journal, 41; 843-849.

Walker, R.G. (1964). Shale Grit and Grindslow Shales: transition from turbidite to shallow water sediments in the Upper Carboniferous of Northern England. Journal of Sedimentary Petrology, 36; 90-114.

Walker, R.G. (1967). Turbidite sedimentary structures and their relationship to proximal and distal depositional environments. Journal of Sedimentary Petrology, 37; 25-43.

Walters, S.G. and Ineson, P.R. (1981). A review of the distribution and correlation of igneous rocks in Derbyshire, England. Mercian Geologist, 8; 81-132.

Ward, W.H. (1945). The stability of Natural slopes. Geographical Journal, 105; 170-191.

Warwick, G.T. (1964). Dry valleys of the southern Pennines. Erkünde, 18; 116-123.

Waters, R.S. and Johnson, R.H. (1958). The terraces of the Derbyshire Derwent. East Midland Geographer, 2; 3-15.

Weeks, A.G. (1969). The stability of natural slopes in south-east England as affected by periglacial activity. Quarterly Journal of Engineering Geology, 2; 49-61.

Weeks, A.G. (1970). The stability of the Lower Greensand escarpment in Kent. Ph.D. Thesis, University of Surrey.

West, R.G. (1977). Pleistocene Geology and Biology: With Especial Reference to the British Isles. Longman, London. 440 pp.

Weyman, D.R. (1970). Throughflow on hillslopes and its relation to the stream hydrograph. Bulletin of the International Association of Scientific Hydrology, 15; 25-33.

Weyman, D.R. (1973). Measurement of the downslope flow of water in soil. Journal of Hydrology, 20; 267-288.

Weyman, D.R. (1974). Runoff process, contributing area and stream flow in a small upland catchment. Institute of British Geographers Special Publication 6; 33-43.

Whipkey, R.Z. (1965a). Subsurface stormflow from forested slopes. Bulletin of the International Association of Scientific Hydrology, 10; 74-85.

Whipkey, R.Z. (1965b). Theory and Mechanics of Subsurface Stormflow. International Symposium on Forest Hydrology. (Eds. Sopper, W.E. and Lull, H.W.). Pergamon Press. p. 255-259.

Willet, H.C. (1950). The general circulation of the last (Würm) glacial maximum. Geografiska Annaler, 32; 179-187.

Wilson, C.M. (1971). A preliminary investigation into the importance of throughflow as run-off in an upland catchment in Wales. Swansea Geographer, 9; 7-14.

Wilson, P. (1981). Periglacial valley – fill sediments at Edale, north Derbyshire. <u>East Midland Geographer</u>, 7; 263-271.

Young, A. (1961). Characteristics and limiting slope angles. <u>Zeitschrift für Geomorphologie</u>, 5; 126-131.

Young, A. (1964). Slope profiles: a symposium, discussion. <u>Geographical Journal</u>, 130; 80-82.

Young, A. (1971). Slope profiles analysis; the system of best units. <u>Institute of British Geographers Special Publication</u>, 3; 1-13.

Young, A. (1972). <u>Slopes</u>. Oliver and Boyd, Edinburgh. 288pp.

Zaruba, Q. and Mencl, V. (1969). <u>Landslides and their Control</u>. Elsevier, New York and Academia, Prague. 205 pp.

Zeuner, F. (1958). <u>Dating the Past</u>. 4th Editn. Methuen, London. 516pp.

A1.   Landslide Classification Type Code

Landslide No.	Name	Grid Ref.	Landslide Type Code
1	Alport Moor	(123951)	DR
2	Broomhead	(260955)	DTMRFx
3	Spout House	(280950)	DRf
4	Ashton Clough	(080943)	DR
5	Doctors Gate	(080940)	DR
6	Ravens Clough	(131946)	DR
7	Westend	(136947)	DR
8	Ridge Upper Moor	(144944)	DR
9	Ox Hey	(168944)	DR
10	Grindlesgrain 1	(122933)	DR
11	Grindlesgrain 2	(123929)	DRx
12	Banktop Hey	(147935)	DRf
13	Rocher Top	(263934)	DRf
14	Upper Thornseat	(923246)	STFh
15	Bradfield	(269923)	DRF
16	Ferny Side	(134914)	DR
17	Alport Farm	(133912)	DRF
18	Alport Castles	(140910)	DMRTFX
19	Abbey Bank	(171913)	DR
20	Fox Hole Carr	(219910)	DRf
21	Firs Hill	(277914)	DRf
22	Ashop Clough	(095907)	DR
23	Saukin Ridge	(104907)	DRtfx
24	Dinas Sitch Tor	(113905)	DRMFx
25	Cowms Rocks	(125904)	DMRTFx
26	Ashton Tor	(138904)	DRF
27	Hey Ridge	(140899)	DRF
28	Ashop	(155893)	DMRTF
29	Alport Grain	(160905)	DR
30	Gores	(169904)	DR
31	Broad Carr	(224900)	DRf
32	Furnace Hill	(256897)	DRF
33	Low Woodhouse	(274905)	DRF
34	The Wicken	(127889)	DRf
35	Jubilee	(176894)	DR
36	Lanehead	(184891)	DRf
37	Loftshaw	(243897)	DR
38	Royds Clough	(260897)	DRF
39	Dean Hill	(132888)	DR
40	Blackden Edge	(132884)	DRtF
41	Crookstone	(145880)	DRf
42	Blackley	(156884)	DR
43	Haggwater	(158885)	DR
44	Hagglee	(163883)	DR
45	Bridge-End	(184880)	DRf
46	Meadows	(248881)	STFh
47	Hollow Meadows	(260882)	DRf
48	Fox Holes 1	(100872)	DRTFx

49	Grinds	(114875)	DRTFx
50	Grinds Brook 1	(116873)	DR
51	Nether Tor	(121875)	DRFx
52	Golden Clough	(123871)	DRF
53	The Cloughs	(088865)	DR
54	Jacobs Ladder	(088865)	DR
55	Wool Packs	(096868)	DR
56	Crowden Brook 1	(100867)	DR
57	Crowden Brook 2	(102863)	DR
58	Crowden Brook 3	(102863)	DR
59	Crowden Brook 4	(103863)	DR
60	Grindslow 1	(117866)	DR
61	Grindslow 2	(188866)	DR
62	Grinds Brook 2	(119869)	DR
63	Grinds Brook 3	(121868)	DR
64	Lady Booth	(142865)	DRf
65	Clough 1	(144868)	DR
66	Clough 2	(145869)	DR
67	Clough 3	(145868)	DR
68	Noe 1	(147860)	DR
69	Noe 2	(150863)	DMRF
70	Carr House	(154864)	DR
71	Wooler Knoll 1	(168860)	DR
72	Wooler Knoll 2	(169862)	DR
73	Wooler Knoll 3	(169860)	DR
74	Crook Hill	(185866)	DR
75	Ashopton	(196866)	DRf
76	Ladybower	(205866)	DRfx
77	Mouselden	(210868)	DR
78	Horden 1	(213867)	DR
79	Horden 2	(213866)	DR
80	Jarvis Clough	(214863)	DRf
81	Stanage End	(223866)	DTfx
82	Round Hill	(251869)	DR
83	Brown Edge	(255861)	DRf
84	New Hagg	(263870)	DRf
85	Fox Holes 2	(274864)	DRf
86	Rivelin	(277865)	DRF
87	Edale Head 1	(090859)	DR
88	Edale Head 2	(089858)	DR
89	Edale Head 3	(091858)	DR
90	Brown Knoll	(092853)	DRF
91	Horsehill Tor	(097853)	DRF
92	Highfield	(101851)	DRf
93	Upper Booth	(102853)	DR
94	Broadlee Bank Tor	(110856)	DRF
95	Waterside 1	(121850)	DR
96	Waterside 2	(123852)	DR
97	Mill	(136855)	DR
98	Lower Hollins 1	(136851)	DR
99	Lower Hollins 2	(137852)	DR
100	Backtor	(143855)	DMRFx

101	Lose Hill 1	(147855)	DR
102	Lose Hill 2	(151857)	DR
103	Oaker Tor 1	(158853)	DR
104	Ladybrook	(161851)	DR
105	Oaker Tor 2	(163853)	DR
106	Oaker Tor 3	(163854)	DR
107	Oaker Tor 4	(162855)	DR
108	Oaker Tor 5	(163856)	DR
109	Wooler Knoll 4	(168858)	DR
110	Fullwood 1	(174851)	DR
111	High Neb	(225853)	DR
112	Ocean View	(257858)	DR
113	Knoll Top	(279852)	DR
114	Roych 1	(084845)	DR
115	Roych 2	(082843)	DR
116	Roych Tor	(083839)	DR
117	Cartlidge	(098844)	DRf
118	Dalehead	(100839)	DRf
119	Tagsnaze	(101847)	DR
120	Orchard	(101845)	DR
121	Mam Nick	(123830)	DMRF
122	Greenlands	(127845)	DMRF
123	Backtor Nook 1	(139849)	DRf
124	Mam Farm	(133842)	DR
125	Hollins Cross	(135844)	DR
126	Woodseats	(137844)	DR
127	Backtor Nook 2	(141848)	DR
128	Fullwood 2	(174849)	DR
129	Thornhill Carrs	(195845)	DRF
130	Bamford Edge 1	(213845)	DR
131	Bamford Edge 2	(214844)	DR
132	Bamford Edge 3	(215841)	DR
133	Bole Hill 1	(218841)	DR
134	Bole Hill 2	(219842)	DR
135	Hallam Moor	(265845)	DRf
136	Rushup Edge	(116834)	DR
137	Mam Tor	(134837)	DMRFx
138	The Folly	(168831)	DR
139	Laneside 1	(176832)	DR
140	Laneside 2	(177831)	DR
141	Laneside 3	(178831)	DR
142	High Lees	(218837)	DR
143	Bolehill Wood	(222838)	DR
144	Cattis Side	(237832)	DR
145	Outseats	(239835)	DR
146	Stanage 1	(242837)	DR
147	Stanage 2	(243836)	DR
148	Bettfield	(085824)	DR
149	Cave Dale	(148824)	DR
150	Brough	(186824)	DR
151	Overstones 1	(251826)	SThf
152	Overstones 2	(251826)	SThf

153	Callow Bank	(253823)	DMRF
154	Callow	(253820)	STf
155	Higger 1	(258824)	DRf
156	Higger 2	(260825)	SRF
157	Fiddlers Elbow	(262827)	DTx
158	Burbage Brook 1	(263825)	SRh
159	Burbage Brook 2	(261822)	DR
160	Burbage Brook 3	(262823)	DR
161	Grey Ditch	(179816)	DR
162	Bradwell	(178813)	DR
163	Elmore	(187818)	DR
164	The Car 1	(185816)	DR
165	The Car 2	(187817)	DR
166	Rebellion Knoll 1	(185813)	DRf
167	Rebellion Knoll 2	(184812)	DR
168	Overdale 1	(186813)	DR
169	Shatton Moor 1	(189816)	STF
170	Shatton Moor 2	(191815)	STF
171	Shatton 1	(197817)	DR
172	Shatton 2	(197815)	DR
173	Old Lees 1	(202817)	DRf
174	Old Lees 2	(202816)	DR
175	Old Lees 3	(203815)	DR
176	Banktop 1	(209814)	DR
177	Offerton 1	(208813)	DR
178	Banktop 2	(212815)	DR
179	Offerton 2	(218814)	DR
180	Toothill	(244819)	DR
181	Mitchellfield 1	(250817)	STh
182	Higger Tor 1	(253818)	DRx
183	Mitchellfield 2	(253817)	DRF
184	Higger Lodge	(252816)	DR
185	Higger Tor 2	(258818)	DR
186	Earl Wark	(258818)	DR
187	Burbage Brook 4	(264813)	DR
188	Burbage Brook 5	(263810)	STh
189	Burbage Rocks	(266810)	DTx
190	Boltedge	(085800)	DR
191	Bradwell Hills	(177807)	DR
192	Deadmen's Clough 1	(177803)	DRF
193	Deadmen's Clough 2	(177800)	DRF
194	Overdale 2	(184809)	DRF
195	Overdale 3	(185806)	DR
196	Silver Well	(187804)	DR
197	Broadhay	(223809)	DR
198	Mount Pleasant	(226806)	DR
199	Hoghall	(230803)	DR
200	Hathersage Booths	(241807)	DR
201	Burbage Bridge	(264807)	DTRx
202	Durham Edge 1	(177794)	DRf
203	Abney Moor 1	(187796)	STh
204	Abney Moor 2	(191798)	DR

205	Abney Moor 3	(193797)	DR
206	Abney 1	(201798)	DR
207	Abney 2	(203798)	DR
208	Abney 3	(205798)	DR
209	Cup and Ring	(220794)	DRf
210	Eyam Moor	(221790)	DR
211	Leam 1	(238796)	STh
212	Leam 2	(240795)	DR
213	Fallcliff	(241794)	STh
214	Longshaw	(267798)	DR
215	Little John	(266796)	DR
216	Burrs Mount	(176785)	DRF
217	Nether Water 1	(175789)	DR
218	Nether Water 2	(176789)	DR
219	Durham Edge 2	(177789)	DR
220	Bretton	(185784)	DR
221	Bretton Clough	(205787)	DMRTF
222	Nether Padley 1	(254782)	DR
223	Nether Padley 2	(257782)	DR
224	White Edge 1	(258784)	DR
225	White Edge 2	(267787)	DR

Table A2. The Matrix Assessment Approach Computer program used to calculate the landslide susceptibility index.

Jul 31 12:53 1986 crsclass.for Page 1

```
        CHARACTER*1 KAR
        DIMENSION LIST(11520),KOUNT(11520),LANDSL(11520),IVAR(9),NPOW(9)
C===========================================================================
C   MODED CLASS TO AGREE WITH DIAGRAMS IN PAPER FOR S & M
C   BASICALLY TO REDUCE NUMBER OF CLASSES TO 4 OR 5
C===========================================================================
C
C******************** INPUT FILES PROCESS ***********************
C
        OPEN(21,FILE='aspect.dat',STATUS='OLD')
        OPEN(22,FILE='soil.dat',STATUS='OLD')
        OPEN(23,FILE='rock.dat',STATUS='OLD')
        OPEN(24,FILE='relief.dat',STATUS='OLD')
        OPEN(25,FILE='valley.dat',STATUS='OLD')
        OPEN(26,FILE='slope.dat',STATUS='OLD')
        OPEN(27,FILE='alt.dat',STATUS='OLD')
        OPEN(28,FILE='rcomb.dat',STATUS='OLD')
        OPEN(29,FILE='pedol.dat',STATUS='OLD')
        OPEN(30,FILE='SUSCEPT',STATUS='NEW')
        LMAX=11520
        WRITE(*,200)LMAX
200     FORMAT('TOTAL CLASSIFICATION SPACE ALLOCATED: ',I6,' UNITS')
C......SET UP POWERS OF 10 TO ALLOW ALL CLASSES REQUIRED.
        NPOW(1)=1
        NPOW(2)=10
        NPOW(3)=100
        NPOW(4)=1000
        NPOW(5)=10000
        NPOW(6)=100000
        NPOW(7)=1000000
        NPOW(8)=10000000
        NPOW(9)=100000000
C......IDENTIFY ANY UNUSED VARIABLES FOR THIS RUN
        WRITE(*,201)
201     FORMAT('Which variables are being used for this run?')
        DO 102 I=1,9
        WRITE(*,202)I
202     FORMAT('Variable',I2,' (y/n): ',$)
        READ(*,206)KAR
206     FORMAT(A)
        IVAR(I)=0
        IF(KAR.EQ.'Y'.OR.KAR.EQ.'y')IVAR(I)=10*NPOW(I)
102     CONTINUE
C
C******************** CLASSIFICATION PROCESS ********************
C
C......SET NUMBER OF ENTRIES IN LIST TO ZERO
        NMAX=0
C......GO THROUGH THE DATA FILE
        CALL BAR('SET UP CLASSIFICATION SYSTEM',11520,0)
        DO 100 IM=1,11520
        CALL RREAD(IA,IB,IC,ID,IE,IF,IG,IH,IJ,LSL)
C......TEST FOR UNUSEFUL (WATER COVERED) CELL
        IF(IA.EQ.9)GOTO 100
C......ASSEMBLE UNIQUE NUMBER REPRESENTING CELL
```

Jul 31 12:53 1986 crsclass.for Page 2

```
          NUM=IA*IVAR(1)+IB*IVAR(2)+IC*IVAR(3)+ID*IVAR(4)+
     1        IE*IVAR(5)+IF*IVAR(6)+IG*IVAR(7)+IH*IVAR(8)+IJ*IVAR(9)
C......DOES IT EXIST IN THE PRESENT LIST?
          CALL FINDIT(NUM,LIST,LMAX,NMAX,KNOWN,KPOS)
C......IF NONEXISTENT, PUT IT IN THE LIST
          IF(KNOWN.EQ.0)CALL PUTINL(NUM,LIST,KOUNT,LANDSL,LMAX,NMAX,KPOS)
C......IT NOW EXISTS, SO INCREMENT PRESENCE AND LANDSLIDE COUNTERS
          KOUNT(KPOS)=KOUNT(KPOS)+1
          IF(LSL.EQ.1)LANDSL(KPOS)=LANDSL(KPOS)+1
C......UPDATE WORK-BAR MOTION
     100  CALL BAR(' ',11520,IM)
          CALL BAR(' ',11520,-1)
          WRITE(*,203)NMAX
     203  FORMAT('CLASSIFICATION SPACE UNITS USED: ',I6)
C......REWIND DATA FILES
          DO 101 I=21,29
     101  REWIND I
C
C**************** SUSCEPTABILITY IDENTIFICATION PROCESS ******************
C
C......NOW GO THROUGH DATA SET AGAIN, AND DETERMINE FOR EACH CELL IN
C......TURN, THE LANDSLIDE SUSCEPTABILITY INDEX.
          CALL BAR('SUSCEPTABILITY CALCULATION',11520,0)
          DO 103 IM=1,11520
          CALL RREAD(IA,IB,IC,ID,IE,IF,IG,IH,IJ,LSL)
C......TEST FOR UNUSEFUL (WATER COVERED) CELL. IF FOUND, MARK IVAL
          IF(IA.EQ.9) THEN
            IVAL=-1
            GOTO 104
          ENDIF
C......ASSEMBLE UNIQUE NUMBER REPRESENTING CELL
          NUM=IA*IVAR(1)+IB*IVAR(2)+IC*IVAR(3)+ID*IVAR(4)+
     1        IE*IVAR(5)+IF*IVAR(6)+IG*IVAR(7)+IH*IVAR(8)+IJ*IVAR(9)
C......FIND ITS POSITION IN THE LIST (IT CERTAINLY OUGHT TO EXIST!)
          CALL FINDIT(NUM,LIST,LMAX,NMAX,KNOWN,KPOS) '
          IF(KNOWN.EQ.0) THEN
            WRITE(*,204)IM
     204    FORMAT('OH DEAR - CELL ',I5,' UNKNOWN!')
            IVAL=-1
          ELSE
            IVAL=LANDSL(KPOS)*1000./KOUNT(KPOS)
          ENDIF
     104  WRITE(30,205)IVAL
     205  FORMAT(I4)
     103  CALL BAR(' ',11520,IM)
          CALL BAR(' ',11520,0)
          STOP
          END


          SUBROUTINE PUTINL(NUM,LIST,KOUNT,LANDSL,KAX,NMAX,KPOS)
          DIMENSION LIST(KAX),KOUNT(KAX),LANDSL(KAX)
C......PUT NEW MEMBER (NUM) INTO THE LIST HELD IN (LIST), WHICH HAS AT
C......PRESENT NMAX MEMBERS. THE POSITION FOR THE NEW ENTRY (FOUND USING
C......FINDIT) IS KPOS.
C
C......THIS IS DONE AT THE MOMENT BY SIMPLY MOVING THE WHOLE LIST DOWN
```

Jul 31 12:53 1986 crsclass.for Page 3

```
C......TO MAKE AN EXTRA SPACE. OBVIOUSLY A POINTER SYSTEM WOULD BE BETTER!
C
C......DETERMINE WHETHER WE HAVE ENOUGH ROOM FOR THE TASK
       IF(NMAX.EQ.KAX) THEN
          WRITE(*,200)NMAX
  200     FORMAT('PRESENT SPACE ALLOCATION TOO LIMITING AT',I7)
          STOP
       ENDIF
C......CHECK FOR KPOS BEING AT FAR END ANYWAY (IN WHICH CASE IT NEED ONLY
C......BE ADDED, WITHOUT ANY SHIFTING. OTHERWISE SHIFT ALL THE PRESENT
C......CONTENTS FROM KPOS TO NMAX DOWN ONE PLACE
       IF(KPOS.LE.NMAX) THEN
          J=NMAX+1
          L=NMAX
          DO 100 I=KPOS,NMAX
          LIST(J)=LIST(L)
          KOUNT(J)=KOUNT(L)
          LANDSL(J)=LANDSL(L)
          J=J-1
  100     L=L-1
       ENDIF
C......THEN INCREMENT NMAX, INSERT NEW NUMBER (NUM) IN ITS RIGHTFUL
C......POSITION, AND ZERO STORAGE VARIABLES.
       NMAX=NMAX+1
       LIST(KPOS)=NUM
       KOUNT(KPOS)=0
       LANDSL(KPOS)=0
       RETURN
       END

       SUBROUTINE FINDIT(NUM,LIST,KAX,NMAX,KNOWN,KPOS)
       DIMENSION LIST(KAX)
C......FIND, USING BINARY SEARCH, THE POSITION OF NUM IN THE FIRST
C......COLUMN OF THE LIST HELD IN LIST. THERE ARE PRESENTLY NMAX
C......SIGNIFICIANT ITEMS IN LIST. ON EXIT KNOWN IS SET TO 1 (FROM 0)
C......IF A MATCH IS FOUND, AND KPOS TO THE MATCH POSITION. IF KNOWN IS
C......0, THEN KPOS IS THE POSITION THAT THE NEW NUMBER (NUM) NEEDS TO
C......BE INSERTED IN THE LIST.
C
C......SET KNOWN UNKNOWN
       KNOWN=0
C......CHECK FOR NO ENTRIES YET IN LIST, AND RETURN IF NONE FOUND
       IF(NMAX.EQ.0) THEN
          KPOS=1
          RETURN
       ENDIF
C......SOME ENTRIES EXIST, SET TOP AND BOTTOM BOUNDS OF SEARCH
       KTOP=1
       KBOT=NMAX
C......CHOOSE NEXT TEST POSITION AND CONTINUE THE BINARY SEARCH
  100  KPOS=(KBOT+KTOP)/2
       IF(NUM-LIST(KPOS))101,102,103
C......MOVE BOTTOM BOUND UP TO KPOS
  101  KBOT=KPOS
       IF(KBOT.EQ.KTOP) THEN
          RETURN
```
Jul 31 12:53 1986 crsclass.for Page 4

```
          ELSE
            GOTO 100
          ENDIF
C......MOVE TOP BOUND DOWN TO KPOS
   103    KTOP=KPOS
          IF(KBOT.EQ.KTOP) THEN
            IF(KPOS.EQ.NMAX)KPOS=KPOS+1
            RETURN
          ELSE
            IF(KBOT-KTOP.EQ.1)KTOP=KBOT
            GOTO 100
          ENDIF
C......MATCH HAS BEEN FOUND
   102    KNOWN=1
          RETURN
          END


          SUBROUTINE BAR(KARS,LENGTH,NOW)
          CHARACTER*(*) KARS
C......DRAW A LINE OF "->>>" ON THE TERMINAL (TOTAL OF 70) AT
C......TIMES WHEN THE VALUE OF NOW REACHES THE NEXT 70TH OF THE
C......TOTAL GIVEN IN LENGTH. A CALL OF BAR WITH NOW OF ZERO
C......SETS UP THE BAR, AND ONE WITH NOW OF -1 WILL ENSURE MOVING ONTO
C......A NEW LINE.
          IF(NOW)101,102,103
C......FINAL CR
   101    WRITE(*,202)
   202    FORMAT(/)
          RETURN
C......INITIAL OUTPUT LINE
   102    WRITE(*,200)KARS
   200    FORMAT(/,A,/,'-',$)
          RETURN
C......INCREMENTAL ">"
   103    J=FLOAT(NOW)/FLOAT(LENGTH)*70.+0.5
          I=FLOAT(NOW-1)/FLOAT(LENGTH)*70.+0.5
          IF(I.LE.0.OR.I.GE.J)RETURN
          L=J-1
          DO 100 K=I,L
   100    WRITE(*,201)
   201    FORMAT('>',$)
          RETURN
          END


          SUBROUTINE RREAD(IA,IB,IC,ID,IE,IF,IG,IH,IJ,N)
C......MODED CLASS STRUCTURE TO AGREE WITH MAPS IN PAPER
          READ(21,10)IA,N
          IA=MIN0(IA,9)
          IF(IA.EQ.9) THEN
            DO 48 JMP=22,29
   48       READ(JMP,*)JJ
            RETURN
          ELSE
            IA=MAX0(IA,1)
            IA=(IA+1)/2
            READ(22,20)IB
```

```
        IB=MAX0(MIN0(IB,11),1)
        IF(IB.EQ.6)IB=5
        IF(IB.EQ.7)IB=6
        IF(IB.EQ.8)IB=7
        IF(IB.EQ.9)IB=7
        IF(IB.EQ.10)IB=6
        IF(IB.EQ.11)IB=5
        READ(23,20)IC
        IC=MAX0(MIN0(IC,11),1)
        IF(IC.EQ. 1)IC=1
        IF(IC.EQ. 2)IC=2
        IF(IC.EQ. 3)IC=2
        IF(IC.EQ. 4)IC=3
        IF(IC.EQ. 5)IC=4
        IF(IC.EQ. 6)IC=4
        IF(IC.EQ. 7)IC=5
        IF(IC.EQ. 8)IC=5
        IF(IC.EQ. 9)IC=5
        IF(IC.EQ.10)IC=6
        IF(IC.EQ.11)IC=4
        READ(24,30)MU
        IF(MU.GE.0.AND.MU.LE.25) ID=1
        IF(MU.GE.26.AND.MU.LE.75) ID=2
        IF(MU.GE.76.AND.MU.LE.125) ID=3
        IF(MU.GT.125)ID=4
        READ(25,30)MW
        IE=MAX0(MIN0((MW-1)/200+1,4),1)
        READ(26,20)MX
        MX=MAX0(MIN0(MX,120),0)
        IF(MX.GE.0 .AND.MX.LE.15)IF=1
        IF(MX.GE.16.AND.MX.LE.35)IF=2
        IF(MX.GE.36.AND.MX.LE.70)IF=3
        IF(MX.GE.71)IF=4
        READ(27,40)MU
        MU=MAX0(MIN0(MU,3000),0)
        IG=MIN0((MU-1)/500+1,4)
        READ(28,*)MU
        IH=MAX0(MIN0(MU-1,0),9)
        READ(29,*)MZ
        MZ=MAX0(MIN0(MZ,18),1)
        IF(MZ.EQ. 1)IJ=2
        IF(MZ.EQ. 2)IJ=3
        IF(MZ.EQ. 3)IJ=1
        IF(MZ.EQ. 4)IJ=4
        IF(MZ.EQ. 5)IJ=3
        IF(MZ.EQ. 6)IJ=4
        IF(MZ.EQ. 7)IJ=2
        IF(MZ.EQ. 8)IJ=2
        IF(MZ.EQ. 9)IJ=4
        IF(MZ.EQ.10)IJ=4
        IF(MZ.EQ.11)IJ=5
        IF(MZ.EQ.12)IJ=3
        IF(MZ.EQ.13)IJ=4
        IF(MZ.EQ.14)IJ=3
        IF(MZ.EQ.15)IJ=4
        IF(MZ.EQ.16)IJ=4
Jul 31 12:53 1986  crsclass.for Page 6
        IF(MZ.EQ.17)IJ=5
        IF(MZ.EQ.18)IJ=5
        RETURN
      ENDIF
      RETURN
10    FORMAT(2I1)
20    FORMAT(I2)
30    FORMAT(I3)
40    FORMAT(I4)
      END
```

Table A3   Classification of Major Soil Groups
and Subgroups.

3. Lithomorphic (A/C) Soils: Shallow, with distinct, humose or peaty
   topsoil, but no subsurface horizons more than 5cm thick (other than a
   bleached horizon). Normally over bedrock, very stony rock rubble or
   little altered soft unconsolidated deposits within 30cm depth.

3.1 Rankers: Loamy or clayey, with non-calcareous topsoil over bedrock
    (including massive limestone), non-calcareous rock rubble or soft
    non-calcareous deposits.

3.11c (HR) Humic Ranker (with humose or peaty topsoil).
3.13c (BR) Brown Ranker (distinct topsoil and unmottled subsoil if
           present).

5. Brown Soils: With dominantly brownish or reddish subsoils and no
   prominent mottling or greyish colours (gleying) above 40cm depth.
   They are developed mainly on permeable materials at elevations below
   about 300m O.D. Most are in agricultural use.

5.4 Brown Earths: Non-alluvial, with non-calcareous or clayey subsoils
    without significant clay enrichment.

5.41 (BE) Typical Brown Earths (unmottled).

5.6 Brown Alluvial Soils: In non-calcareous loamy or clayey alluvium
    more than 30cm thick.

5.61 (Rt,a) Typical Brown Alluvial Soils (unmottled).

6. Podzolic Soils: with black, dark brown or ochreous humus and iron-
   enriched subsoils formed as a result of acid weathering conditions.
   Under natural or semi-natural vegetation, they have an unincorporated
   acid organic horizon at the surface.

6.1 Brown Podzolic Soils: with a dark brown or ochreous, iron-enriched
    subsoil and no overlying bleached horizon.

6.11a (BP) Typical Brown Podzolic Soils (unmottled with distinct
           topsoil).

6.3 Podzols: well drained, with a bleached subsurface horizon and no
    thin iron-pan.

6.31a (HFP) Humo-Ferric Podzol (with black or dark brown humus and iron
            -enriched layer beneath the bleached horizon).

6.5 Stagnopodzols: with peaty topsoil and periodically wet bleached sub-
    surface horizon over an iron-enriched subsoil, mainly foun in
    uplands.

6.51a (IS) Ironpan Stagnopodzols (with thin iron pan).

7. Surface-Water Gley Soils: Non-alluvial, seasonally waterlogged slowly permeable soils, formed above 3m O.D. and prominently mottled above 40cm depth. They have no relatively permeable material starting within and extending below 1m of the surface.

7.1 Stagnogley Soils: with a distinct topsoil. They are found mainly in lowland Britain.

7.12a (PS) Pelo-Stagnogley Soils (clayey).
7.13b,g (CSG) Cambic Stagnogley Soils (with no clay enriched subsoil).

7.2 Stagnohumic Gley Soils: with a humose or peaty topsoil. They are mainly upland soils, intermediate between Stagnogley soils and Peat soils.

7.21c (CSG) Cambic Stagnogley Soils (with no clay-enriched subsoil).

10. Peat Soils: with more than 40cm of organic material in the upper 800cm or with more than 30cm of organic material over bedrock or very stony rock rubble.

10.1 Raw Peat Soils: In undrained organic material that has remained wet to within 20cm of the surface.

10.11 (HP) Raw Oligo-Fibrous Peat Soils (mainly fibrous or semi-fibrous with pH less than 4.0 throughout).

Table A4 Soil Profile of the Upper Slope Section

Location: Upper Slope section
Slope: 33°
Site: steep scarp slope
Drainage: well drained
Vegetation: Nardus
Geology: Shale Grit (sandstone)

FO	5cm	Dead, undecayed grass roots and leaves.
H	5	Black (N2/), structureless humus with many bleached quartz grains and a very small amount of well-weathered gravel; abundant fibrous roots; clear, smooth boundary.
Ae	15	Very dark grey (5YR 3/1); sand/loamy sand with a small amount of gravel and medium – and coarse-grained sandstone fragments up to 20cm; single grain structure; many fibrous roots; pH 3.8; clear, irregular boundary.
Bh	8	Black (5YR 2/1); loamy sand with coarse-grained sandstone fragments up to 10cm; a few fibrous roots; pH 3.5; clear, irregular boundary.
B21	4	Dark reddish brown (5YR 3/3); loamy sand with much gravel and medium and coarse-grained fragments up to 15cm; weak, medium, sub angular blocky structure; some fine, fibrous roots; pH 3.8; clear, irregular boundary.
B22	12	Strong brown (7.5YR 5/6); loamy sand with much gravel and numerous medium- and coarse-grained sandstone fragments up to 30cm; some fibrous roots; pH 4.3; gradual, irregular boundary.
B23	15	Strong brown (7.5YR 5/8); loamy sand with a moderate amount of gravel and numerous large coarse-grained sandstone fragments up to 30cm; many matted, fibrous roots; pH 4.3; clear, wavy boundary.
C1	25	Yellowish brown (10YR 5/6); loamy sand with a moderate amount of gravel and numerous coarse-grained sandstone fragments up to 30cm; pH 4.3; clear irregular boundary.
C2	23	Very dark brown (10YR 2/2) with large dark brown mottles; loamy sand with a moderate amount of soft sandstone gravel and medium-grained sandstone fragments up to 30cm; pH 4.3; clear, irregular boundary.
C2	23	Very dark brown (10YR 2/2) with large dark brown mottles; loamy sand with a moderate amount of sandstone gravel and medium-grained sandstone fragments up to 10cm; some fibrous roots; pH 4.35; clear, irregular boundary.
C3	23	Yellowish brown (10YR 5/8); loamy sand with a moderate amount of mainly soft sandstone gravel and medium-grained sandstone fragments up to 10cm; occasional roots; pH 4.45; clear smooth boundary.
C4 (z = 158cm)		Dark yellowish brown (10YR 4/4); sandy loam with a moderate amount of very soft sandstone gravel; pH 4.3.

Table A5 Soil Profile of the Middle Slope Section

Location: Middle Slope section
Slope: 24°
Site: convex mid/transportational slope
Drainage: moderately well drained
Vegetation: Molinia with Eriophorum, Deschampsin, funcus and mosses in
            swampy areas
Geology: Shale Grit/shale transition

FO	6cm	Dead, undecayed grass roots and leaves; abrupt, wavy boundary.
F1	8	Partially decayed vegetal matter; clear, wavy boundary.
F21	14	Dark yellowish brown (10YR 3/4) to black (10YR 2/1), partially decayed vegetal matter; clear, wavy boundary.
F22	8	Dark reddish brown (5YR 2/2) partially decayed vegetal matter with lenses of sand; clear, wavy boundary.
A11	7	Dark yellowish brown (10YR 3/4) merging downwards to dark greyish brown (10YR 4/2); sandy loam with a moderate amount of gravel and occasional angular to sub-angular sandstone fragments up to 3cm, many roots; pH 3.6; gradual boundary.
A12	13	As A11, but fragments up to 10cm and gleyed; clear, irregular boundary.
A1/G	12	Olive grey (5YR 5/2); sandy loam with a moderate amount of gravel, many roots; pH 4.5; clear, wavy boundary.
G	21	Grey (NS/) with common, distinct, medium yellowish red (5YR 5/8 and 4/8) mottles, increasing in frequency towards the base; predominantly loam with pockets of sand, and with a moderate amount of gravel and light olive brown sandstone fragments mostly up to 10cm but occasionally reaching 20cm; fibrous roots; iron staining along root channels, pH 4.7; abrupt, smooth boundary.
G/C	33	Grey (NS/) with many prominent, medium yellowish red mottles; loam with much gravel and numerous sandstone fragments stained with iron on the surface; no living roots; ph 4.35; clear, irregular boundary.
C1	18	Predominantly yellowish red; many large sandstone fragments, sub-horizontal in attitude; distinct, irregular boundary.
C2	10	Sandstone-shale transition; strong iron staining.
C3	25	Weathered shale with sandstone bands; shale strong brown (7.5YR 5/8) with yellowish red (5YR 4/6) iron staining along cleavage planes; loam with a moderate amount of gravel; gradual boundary.
R		Shale.
(z = 175cm)		

Table A6 Soil Profile of the Lower Slope Section

Location: Lower Slope section
Slope: 16°
Site: seepage basal slope, slightly concave
Drainage: poor
Vegetation: Deschampsia with Nardus and Molinia, Juncus and sphagnum
Geology: Shale

FO	10cm	Dead, undecayed grass roots and leaves; clear, smooth boundary.
F11	15	Dark brown vegetal matter, structure partially destroyed; clear, smooth boundary.
F12	5	Light brown vegetal matter, structure partially destroyed; clear, smooth boundary.
F21	13	Brown vegetal matter, structure largely destroyed; clear, smooth boundary.
F22	10	Dark brown vegetal matter, structure largely destroyed; clear, smooth boundary.
A1	9	Yellowish brown (10YR 5/4); loam with a very small amount of gravel, and occasional subrounded grit boulders up to 30cm; many roots; pH 4.3; clear, smooth boundary.
A/G	17	Greyish brown (2.5YR 5/2); silty loam with sandy pockets and a very small amount of gravel and occaionnal sub-angular to subrounded grit stones and boulders up to 30cm; many roots; pH 4.65; gradual smooth boundary.
G1	23	Light grey/grey (N6/); sandy clay loam with a small amount of gravel, siltstone fragments up to 10cm and bases of large grit boulders; many roots; pH 4.5; clear, smooth boundary.
G2	20	Light grey/grey (N6/); silt clay with a small amount of gravel; some roots; pH 4.8; clear, smooth boundary.
G3	15	Light grey/grey (N6/); clay silt loam with no gravel; pH 4.75; clear, smooth boundary.
G4	14	Light grey/grey (N6/); grey clay with shale and soft fine sandstone fragments up to 5cm; clear, smooth boundary.
D		Slightly gleyed shale.

(z = 151cm)

Table A7 Properties of soil samples taken from the lower slope section

			Lower Slope Section		
Shear Test Number	Moisture Content (%)	Soil unit weight (γ) kN/m^3	Soil dry unit weight (γd) kN/m^3	Saturated unit weight γs kN/m^3	Plasticity Index PI
1	32.9	18.69	14.06	18.56	11
2	31.5	14.10	10.73	16.49	9
3	32.8	18.52	15.95	18.49	14
4	31.2	20.58	15.68	19.57	10
5	33.2	20.09	15.08	19.20	14
6	33.2	16.55	12.43	17.55	14
7	32.8	15.36	11.56	17.01	13
8	32.0	17.93	12.93	17.86	13
9	32.4	19.34	14.61	18.70	12
10	31.7	18.62	14.14	18.61	14
11	33.3	17.37	13.03	17.92	13
12	31.0	16.49	12.59	17.65	14
13	31.5	19.76	15.02	17.16	12
14	32.4	18.49	13.96	18.31	13
15	31.8	17.57	13.33	18.11	13
Mean	32.3	17.97	13.54	17.74	12.6

Table A8 Properties of soil samples taken from the middle slope section

	Middle Slope Section				
Shear Test Number	Moisture Content (%)	Soil unit weight $(\gamma)\,kN/m^3$	Soil dry weight $(\gamma d)\,kN/m^3$	Saturated unit weight $\gamma s\,kN/m^3$	Plasticity Index PI
1	29.3	16.83	13.01	17.91	9
2	28.2	17.10	13.33	18.11	6
3	26.4	16.88	13.36	18.13	7
4	29.7	14.97	11.54	16.99	9
5	29.7	15.45	11.91	17.22	9
6	25.4	16.87	13.46	17.48	8
7	30.1	14.30	10.99	16.65	9
8	27.4	14.09	11.06	16.69	6
9	28.7	15.55	12.09	17.33	10
10	29.7	17.02	13.12	17.98	9
11	27.5	15.09	11.83	17.18	8
12	28.2	15.49	12.08	17.33	10
13	26.6	15.75	12.44	17.56	8
14	26.8	16.74	13.20	18.03	9
15	27.5	16.04	12.58	17.64	10
Mean	28.1	15.88	12.40	17.48	8.5

Table A9   Properties of soil samples taken from the upper slope section

		Upper Slope Section			
Shear Test Number	Moisture Content (%)	Soil unit weight (γ) kN/m^3	Soil dry unit weight (γd) kN/m^3	Saturated unit weight γs kN/m^3	Plasticity Index PI
1	21.7	14.45	11.87	17.20	5
2	17.3	17.51	14.92	19.10	7
3	24.1	16.92	13.63	18.30	7
4	24.1	16.66	13.42	18.16	7
5	25.3	17.97	14.34	18.74	9
6	23.4	13.98	11.32	16.86	7
7	24.0	15.64	12.61	12.61	9
8	19.5	16.03	13.41	18.16	7
9	18.2	17.55	14.85	19.06	6
10	22.4	16.32	13.33	18.11	7
11	24.6	15.04	12.07	17.33	8
12	33.3	17.89	13.42	18.17	9
13	22.4	16.79	13.72	18.35	7
14	24.4	15.43	12.40	17.53	7
15	23.8	17.21	13.90	18.47	8
Mean	23.2	16.36	13.28	17.74	7.3